



University
of Glasgow

Costantini, Rosa (2021) *Strain across historic tapestries: a multi-analytical investigation on damage mechanisms and conservation strategies*. PhD thesis.

<http://theses.gla.ac.uk/82286/>

-

Copyright and moral rights for this work are retained by the author

A copy can be downloaded for personal non-commercial research or study, without prior permission or charge

This work cannot be reproduced or quoted extensively from without first obtaining permission in writing from the author

The content must not be changed in any way or sold commercially in any format or medium without the formal permission of the author

When referring to this work, full bibliographic details including the author, title, awarding institution and date of the thesis must be given

Enlighten: Theses

<https://theses.gla.ac.uk/>
research-enlighten@glasgow.ac.uk

Strain across historic tapestries: a multi-analytical
investigation on damage mechanisms
and conservation strategies

Rosa Costantini

Submitted in fulfilment of the requirement for the degree of
Doctor of Philosophy

School of Culture and Creative Arts

College of Arts

University of Glasgow

February 2021

A Saverio

Abstract

This cross-disciplinary work improves the understanding on the mechanical degradation mechanisms occurring in tapestries, and how they can be prevented through conservation. Moreover, the research in this thesis offers new insights on the usefulness of 2D DIC as a diagnostic tool for monitoring strain across historic textiles.

First, through a literature review, the cultural relevance of tapestries was highlighted, demonstrating the importance of preserving these artworks (Chapter 1). Chemical and physical properties of the main constituent materials in tapestries, wool and silk, were discussed, together with past studies focusing on tracking degradation (Chapter 2). Through this, the multi-analytical approach to be employed in the experimental parts was delineated.

The mechanical (uniaxial tensile testing) and chemical properties (FTIR-ATR, UHPLC-PDA) of samples from different historic tapestries were investigated. The reciprocal influence of variables, e.g. stress at failure, level of cystine oxidation (in wool), dyes, and weave features, was discussed. The outcomes demonstrate the complexity of the mechanical behaviour when considering small-scale fragments, and so the need of combining chemical and physical testing for properly establishing the condition of tapestries (Chapter 3).

Moving to the study of tapestries from a macroscopic perspective and while on display, the feasibility of 2D DIC for strain monitoring was proved. Among the mechanical mechanisms observed, fatigue showed to have the most influence on overall strains, while creep affected damaged areas like slits (Chapter 4). 2D DIC was also employed for evaluating the efficiency of sloping boards (Chapter 5), support and stitching methods (Chapter 6). In addition to the strain monitoring of (mainly) bespoke mock-ups, friction measurements and tensile testing were conducted to further validate display and conservation approaches. The outcomes suggested that the high friction promoted by covering fabrics is essential for the efficacy of sloping boards, while inclination alone may have only a marginal role (Chapter 5). The effectiveness of couching can be affected by spacing, while support techniques should be selected depending on the extension of structural weaknesses (Chapter 6).

Table of contents

Abstract	3
Table of contents.....	4
List of tables	8
List of figures	10
Preface.....	18
Acknowledgments	21
Author's declaration	23
Abbreviations	24
1 Introduction to tapestries: why and how to conserve them	25
1.1 Tapestries: the background	25
1.1.1 The historical context and the cultural value	25
1.1.2 The making of tapestry	30
1.1.3 The materials	33
1.2 Conservation practices	34
1.2.1 The approach over the time	35
1.2.2 Current conservation practices.....	40
References.....	46
2 Introduction to the degradation of tapestries: why it happens and how to monitor it.....	51
2.1 The degradation of tapestries: from the perspective of fibres.....	51
2.1.1 Wool	52
2.1.1.1 Chemical and physical structure	52
2.1.1.2 Key mechanical behaviour	54
2.1.1.3 Degradation	56
2.1.2 Silk.....	59
2.1.2.1 Chemical and physical structure	59
2.1.2.2 Key mechanical behaviour	60
2.1.2.3 Degradation	61
2.2 Evaluating the physical degradation of tapestries and the related effectiveness of conservation practices: state of the art	65
2.2.1 The basis of the current research: the previous project at the University of Southampton (2007-2010)	65
2.2.1.1 The project: main aims and outcomes	65
2.2.1.2 Critical evaluation of the research	69
2.2.1.3 Future work suggested by the research	70
2.2.2 Other works	71
2.2.2.1 Researching the mechanical behaviour and degradation of tapestries..	71

2.2.2.2	Testing the efficacy of conservation techniques for tapestries	73
2.3	Relating the physical and chemical degradation of tapestries: state of the art	76
2.3.1	Tracking chemical degradation in historic wool	77
2.3.2	Tracking chemical degradation in historic silk	79
2.4	Conclusions: objectives and analytical approach of the current study ..	81
	References.....	84
3	Characterisation of physical and chemical properties of historic tapestries	89
3.1	Materials and methods.....	91
3.1.1	Historic tapestry fragments	91
3.1.2	Newly woven wool rep fabric	92
3.1.3	Uniaxial tensile testing	95
3.1.4	ATR-FTIR	97
3.1.5	UHPLC-PDA	98
3.1.5.1	Extraction method	100
3.2	Results and discussion	100
3.2.1	Uniaxial tensile testing	100
3.2.1.1	Samples from historic tapestry fragments	100
3.2.1.2	Newly woven wool rep fabric	108
3.2.2	ATR-FTIR	111
3.2.3	UHPLC-PDA	120
3.2.4	Connecting the data from the multi-analytical investigation of historic samples	134
3.3	Conclusions	136
	References.....	138
4	2D DIC for investigating mechanical damage mechanisms in tapestries	144
4.1	Introduction	144
4.1.1	2D DIC: basic principles of the technique and common sources of errors	144
4.1.1.1	Theoretical foundation and sources of error related to the correlation algorithm	145
4.1.1.2	Experimental sources of errors	148
4.1.2	Evaluating the usefulness of DIC as a tool to measure strain across historic hangings through synthetic deformation fields	152
4.2	Materials and methods.....	153
4.2.1	Case studies	154
4.2.1.1	Wool rep sample	154
4.2.1.2	Tapestries	155
4.2.2	Monitoring set-up and strain calculation	165
4.3	Results and discussion	168

4.3.1	Wool rep sample	168
4.3.1.1	Causes of strain.....	168
4.3.1.2	Evaluation of artificial speckle patterns as correlation devices.....	171
4.3.1.3	Evaluation of DIC parameters: subset size, step size	174
4.3.2	Tapestries.....	176
4.3.2.1	TapestryFragment_1	177
4.3.2.2	TapestryFragment_2	183
4.3.2.3	<i>Kesi</i>	187
4.3.2.4	Historic tapestry conserved with full support.....	189
4.3.2.5	Contemporary tapestry at Stirling Castle	193
4.3.2.6	Evaluation of DIC parameters when monitoring historic tapestries: step size, subset size	200
4.3.2.7	Notes on the mathematical relationship between strain and RH.....	206
4.4	Conclusions	207
4.4.1	Parameters affecting 2D DIC analysis.....	207
4.4.2	Mechanical damage mechanisms affecting tapestries when on display	208
	References.....	210
5	Evaluation of sloping boards as a display method.....	214
5.1	Introduction	215
5.1.1	Origins and current diffusion of sloping boards for displaying tapestries.....	215
5.1.2	Previous studies on the efficacy of sloping boards	218
5.1.3	Fabric on fabric friction: definition, how to measure it and what factors may influence it.....	221
5.1.4	Theoretical analysis of the role of inclination and friction	224
5.2	Materials and Methods	227
5.2.1	Friction measurements	227
5.2.2	2D DIC strain monitoring: fixed-load experiments with non-historic samples on uncovered board slanted at different angles	230
5.2.3	2D DIC strain monitoring of a historic tapestry fragment displayed on a half covered and half uncovered vertical board	231
5.3	Results and discussion	232
5.3.1	The role of friction	232
5.3.1.1	Friction measurements: weighted specimens	233
5.3.1.2	Friction measurements: unweighted specimens	233
5.3.2	The role of inclination: fixed-load experiments with non-historic samples (uncovered board)	236
5.3.2.1	Display at 0° from the vertical	236
5.3.2.2	Display at 5° from the vertical	239
5.3.2.3	Display at 45° from the vertical.....	241

5.3.2.4	Discussion: comparison between the tests at different inclinations....	242
5.3.3	2D DIC strain monitoring of a historic tapestry fragment displayed on a half covered and half uncovered vertical board	244
5.4	Conclusions	247
6	Evaluation of stitching and support methods	251
6.1	Materials and methods.....	252
6.1.1	2D DIC monitoring of newly woven conserved samples	252
6.1.2	2D DIC monitoring of a historic tapestry fragment after conservation	259
6.1.3	Uniaxial tensile testing	261
6.1.3.1	Fabrics for support treatments.....	261
6.1.3.2	Newly woven conserved samples.....	263
6.2	Results and discussion	264
6.2.1	2D DIC monitoring of newly woven conserved samples	264
6.2.1.1	Full support vs patch support, brick vs laid couching (test 6.1).....	264
6.2.1.2	Full support with vs without grid lines, brick vs laid couching (test 6.2) ..	268
6.2.1.3	Full support with grid lines across vs distant from damaged areas (test 6.3)	271
6.2.1.4	Full support vs brick/laid couching (test 6.4).....	274
6.2.1.5	Full support vs patch support in highly damaged samples (test 6.5) ...	277
6.2.1.6	Different spacing (test 6.6)	281
6.2.1.7	Summary and discussion.....	285
6.2.2	2D DIC monitoring of a historic tapestry fragment after conservation	287
6.2.3	Uniaxial tensile testing: fabrics for support treatments.....	293
6.2.3.1	Linen fabrics	293
6.2.3.2	Polyester Stabiltex™	298
6.2.3.3	Discussion: comparison between the tensile properties of fabrics for support treatments and historic tapestries	299
6.2.4	Uniaxial tensile testing: newly woven conserved samples	302
6.3	Conclusions	307
	References.....	309
7	Conclusions and future research.....	311
7.1	Future research.....	314
	Complete bibliography.....	316
	Publications and presentations.....	337

List of tables

Table 1.1. Dyes commonly employed in historic European tapestries. Data taken from Quye et al., 2009 [14].	34
Table 3.1 Experimental design of Chapter 3.	90
Table 3.2. Historic tapestries tested.	91
Table 3.3. Specimens from the historic fragments characterised through uniaxial tensile testing.	96
Table 3.4. Samples from the historic fragments analysed through ATR-FTIR. As indicated, some of the samples were also analysed through UHPLC-PDA.	98
Table 3.5. Uniaxial tensile properties of the samples from historic tapestries.	104
Table 3.6. Uniaxial tensile properties of the wool rep fabric (average of five measurements per direction, the standard deviation, SD, is also indicated to show the variation of the data).	110
Table 3.7. Classification of wool samples from the different tapestry fragments based on the intensity of peaks related to cystine oxidation products.	118
Table 3.8. Main compounds, and related dye sources, revealed in the wool samples from historic tapestry fragments.	121
Table 4.1. Details of <i>Florence</i> tapestry.	163
Table 4.2. Details of monitoring tests and of the experimental design.	167
Table 4.3. R^2 from the linear fitting of ε_{yy} [%] calculated from the DIC analysis of the wool rep sample (dotted pattern) with different parameters.	176
Table 4.4. Slope from the linear fitting, ε_{yy} [%] versus RH [%], from the monitoring tests of the different artworks.	206
Table 5.1. Experimental design of Chapter 5.	215
Table 5.2. Details of the board-covering fabrics tested.	227
Table 5.3. Details of the historic tapestry fragments, wool rep, linen and cotton fabrics tested against the board-covering fabrics to measure μ_s .	228
Table 5.4. Angle [°] at which the weighted fabric samples (i.e. wrapped around a glass plate) started to slip from the board covered with cotton molton. The SD is also indicated (15 measurements per sample).	233
Table 5.5. Coefficient of static friction between the weighted fabric samples and cotton molton.	233
Table 5.6. Angle [°] at which the unweighted tapestry samples started to slip from the board covered with different textiles. The SD is also indicated (15 measurements per sample/covering fabric).	234
Table 5.7. Coefficient of static friction between the unweighted tapestry samples and the board-covering fabrics. Whenever the sign - is used, it indicates that the coefficient could not be calculated, as $\theta \geq 90^\circ$.	235
Table 6.1. Experimental design of Chapter 6.	252
Table 6.2. Wool rep mock-ups used for testing the efficacy of support and stitching techniques. Samples AI-F are described by Figure 6.1a, samples G-I by Figure 6.1c (before conservation). Mock-ups DI/DII and G were left untreated and used as control samples. This aimed to highlight the impact of conservation strategies from the comparison with conserved samples.	255
Table 6.3. Wool rep mock-ups used for testing the influence of spacing in brick and laid couching. The samples are described by Figure 1b (before conservation). Da. was left untreated (control sample).	256
Table 6.4. Grid lines systems used for attaching full supports to the samples.	257
Table 6.5. Codes, objectives, and wool rep samples used in the experiments on the efficacy of stitching and support techniques.	258
Table 6.6. Materials used for conserving the wool rep samples.	258

Table 6.7. Details of support fabrics.	262
Table 6.8. Conserved wool rep specimens uniaxially tensile tested.	264
Table 6.9. Uniaxial tensile properties of the two linen fabrics (the SD is also indicated, average of five measurements per direction).	295
Table 6.10. Uniaxial tensile properties of the polyester Stabiltex™ (the SD is also indicated, average of five measurements per direction).	299
Table 6.11. Uniaxial tensile properties of specimens conserved with different support and stitching techniques.	306

List of figures

Figure 1.1. Detail of a <i>kesi</i> , Karen Finch Reference Collection, CTCTAH.	26
Figure 1.2. <i>The Unicorn Rests in a Garden</i> (from the <i>Unicorn Tapestries</i> set). Woven in South Netherlandish between 1495-1505. Accession number: 37.80.6. © The Metropolitan Museum of Art.	27
Figure 1.3. Cartoon for a tapestry, <i>The Miraculous Draught of Fishes</i> . Raphael, Italy, about 1515-1516. Bodycolour on paper laid onto canvas. Museum number: ROYAL LOANS.2. © Victoria & Albert Museum.	28
Figure 1.4. Tapestry weave structure, in the hanging direction, with two differently coloured sets of weft threads [12].	30
Figure 2.1. Chemical structure of: a) cysteine; b) cystine.	52
Figure 2.2. Structure of a merino wool fibre. © CSIRO.	53
Figure 2.3. Generic stress-strain curve for wool (the x-axes is out of scale to better show the Hookean region). Taken from Huson, 2018 [3].	55
Figure 2.4. Sorption isotherms for degummed silk. The difference in the moisture content between the two curves indicates the hysteresis. Plotted data from Hutton and Gartside, 1949 [31].	61
Figure 2.5. Cysteic acid.	78
Figure 3.1. Weave structure of the wool rep fabric (59x magnification).	93
Figure 3.2. Detail of the weave structure of the historic tapestry fragment T6 (a) and the wool rep fabric (b). In both figures, the red arrows indicate weft direction, while the blue arrows warp direction. Historic tapestries are hung in the weft direction.	94
Figure 3.3. Stress-strain curves of sample T1_Wa1 (warp direction) and T1_We1 (weft direction). The dotted lines highlight the elastic region, while the brackets the de-crimping one.	102
Figure 3.4. Stress-strain curves of sample T1_We4, T2_We3, T6_We1 (weft direction).	103
Figure 3.5. Young's moduli of specimens from historic tapestry fragments, tensioned in the warp direction. The bar indicates the SE, whenever it was possible to test more samples with uniform or heterogeneous weave structure.	105
Figure 3.6. Young's moduli of specimens from historic tapestry fragments, tensioned in the weft direction. The bar indicates the SE, whenever it was possible to test more samples with uniform or heterogeneous weave structure.	106
Figure 3.7. Breaking stress of specimens from historic tapestry fragments, tensioned in the warp direction. The bar indicates the SE, whenever it was possible to test more samples with uniform or heterogeneous weave structure.	107
Figure 3.8. Breaking stress of specimens from historic tapestry fragments, tensioned in the weft direction. The bar indicates the SE, whenever it was possible to test more samples with uniform or heterogeneous weave structure.	107
Figure 3.9. Sample T1_We3 at the end of the uniaxial tensile testing.	108
Figure 3.10. Stress-strain curves of samples of the warp-faced wool rep fabric in both weft (orange line) and warp direction (blue line).	109
Figure 3.11. Stress-strain curves of samples from the warp-faced wool rep fabric and historic tapestry fragment T1.	110
Figure 3.12. ATR-FTIR spectrum of sample T1_We.Red (average, baseline- corrected).	111

Figure 3.13. ATR-FTIR spectrum of sample T1_We.WhiteS (average, baseline-corrected).	112
Figure 3.14. ATR-FTIR averaged spectra of wool warp samples from fragment T1, T5, and T7 (after baseline correction). Spectral differences in the intensity of peaks at around 1075 cm ⁻¹ (CM), 1040 cm ⁻¹ (CA), and 1022 cm ⁻¹ (B-salt) allow to differentiate three groups.	113
Figure 3.15. ATR-FTIR averaged spectra of wool reference samples prepared for the MODHT project and mordanted respectively with alum (Ref_LogAl) and iron salt (Re_LogFe). In addition, the spectrum of an undyed wool sample from the rep fabric is shown (green line).	116
Figure 3.16. Second derivate ATR-FTIR spectra of warp samples from T1, T5, T7 (after average, baseline correction, normalisation, but no further processing/smoothing).	116
Figure 3.17. CA/AmideIII ratio from the analysis of the second derivate ATR-FTIR spectra of warp threads from historic samples.	117
Figure 3.18. ATR-FTIR averaged spectra of wool weft samples from fragment T1, T5, and T4 (after baseline correction). All the specimens here presented were dyed with a luteolin-based source (Section 3.2.3).	118
Figure 3.19. CA/AmideIII ratio from the analysis of the second derivate ATR-FTIR spectra of weft threads from historic samples.	118
Figure 3.20. ATR-FTIR averaged spectrum of sample T3_We.Black: the peak at 1320 cm ⁻¹ can be linked to the presence of calcium oxalate salts.	120
Figure 3.21. Chromatogram, acquired at 350 nm, from the analysis of sample T4_We.Beige.	123
Figure 3.22. UV-Vis abs spectra of: a) luteolin; b) chrysoeriol; c) apigenin.	123
Figure 3.23. UV-Vis abs spectrum of sulfuretin.	124
Figure 3.24. Chromatogram, acquired at 255 nm, from the analysis of sample T3_We.Brown.	125
Figure 3.25. UV-Vis abs spectrum of urolithin C.	126
Figure 3.26. Chromatogram, acquired at 450 nm, from the analysis of sample T2_We.DBrown.	127
Figure 3.27. UV-Vis abs spectra of alizarin (a) and purpurin (b).	127
Figure 3.28. Chromatogram, acquired at 255 nm, from the analysis of sample T2_We.Red.	129
Figure 3.29. UV-Vis abs spectra of dcll (a) and carminic acid (b).	129
Figure 3.30. Chromatogram, acquired at 255 nm, from the analysis of sample T1_We.DBrown.	130
Figure 3.31. UV-Vis abs spectra of gallic acid (a) and ellagic acid (b).	131
Figure 3.32. UV-Vis abs spectrum of unknown compound detected in T1_We.DBrown, possibly associated to logwood.	132
Figure 3.33. Chromatogram, acquired at 255 nm, from the analysis of sample T5_We.Blue.	133
Figure 3.34. UV-Vis abs spectrum of indigotin.	134
Figure 3.35. CA/AmideIII ratio and dye sources of weft threads from historic samples.	135
Figure 4.1. Example of defining features in the DIC analysis: the ROI is the area indicated in red, the subset is marked by the blue line, and the point of interest corresponds to the green dot.	146
Figure 4.2. Scheme of a subset before and after deformation.	147
Figure 4.3. Effect of out-of-plane movement of the specimen (translation towards the lens) on the in-plane displacements calculated by DIC.	151

Figure 4.4. Monitoring set-up of the wool rep sample with two speckle patterns applied: spray (left side), and dots (right side).	155
Figure 4.5. TapestryFragment_1, Karen Finch Reference Collection, CTCTAH. Two open slits are highlighted in red.	156
Figure 4.6. Detail of the back of TapestryFragment_1.	157
Figure 4.7. Weave structure of TapestryFragment_1 showing horizontal warps and vertical wefts, as it would hang (55x magnification).	157
Figure 4.8. TapestryFragment_2, Karen Finch Reference Collection, CTCTAH.	158
Figure 4.9. Detail of the front of TapestryFragment_2 showing an open slit. ..	158
Figure 4.10. Weave structure of TapestryFragment_2 showing horizontal warps and vertical wefts, as it would hang (57x magnification).	159
Figure 4.11. <i>Kesi</i> , Karen Finch Reference Collection, CTCTAH.	160
Figure 4.12. Details of weave structure of <i>kesi</i> (58x magnification): a) area with metal threads; b) painted decoration and metal threads.	161
Figure 4.13. <i>Florence</i> tapestry: a) direct light; b) transmitted light. Registration number: 46.93. © CSG CIC Glasgow Museums Collection.	162
Figure 4.14. Details of <i>Unicorn tapestry</i> . The figurative design of the contemporary piece was greatly inspired by that of <i>The Unicorn Surrenders to a Maiden</i> belonging to the Metropolitan Museum of Art (accession number: 38.51.2).	164
Figure 4.15. Mean ϵ_{xx} and ϵ_{yy} [%] of the wool rep sample with two speckle patterns during the 48-hour monitoring. RH [%] is indicated by the dotted line.	169
Figure 4.16. Mean strain [%], longitudinal (a) and horizontal (b), during the 48-hour monitoring of the wool rep sample plotted against RH [%].	170
Figure 4.17. Strain maps, ϵ_{xx} and ϵ_{yy} [%], of the wool rep sample with two speckle patterns (spray pattern on the left side, dotted pattern on the right side) at the end of the 48-hour monitoring.	171
Figure 4.18. Error map expressed in sigma [pixel] of the wool rep sample with two speckle patterns (spray pattern on the left side, dotted pattern on the right side) at the end of the 48-hour monitoring.	172
Figure 4.19. Mean longitudinal strain calculated across the area with dotted pattern (green) and sprayed pattern (purple) against RH [%].	173
Figure 4.20. Mean ϵ_{yy} [%] calculated across the area with dotted pattern using different DIC parameters: 31 as subset size, 5 as step size (green line); 61 as subset size, 5 as step size (orange line); 61 as subset size, 3 as step size (blue line).	175
Figure 4.21. Mean ϵ_{yy} [%] calculated across the area with sprayed pattern using different DIC parameters: 31 as subset size, 5 as step size (green line); 61 as subset size, 5 as step size (orange line); 61 as subset size, 3 as step size (blue line).	175
Figure 4.22. Mean ϵ_{yy} [%] calculated across the area with dotted pattern using different DIC parameters.	176
Figure 4.23. Mean ϵ_{yy} [%] calculated across the entire surface of TapestryFragment_1 against time. RH [%] fluctuations are indicated by the dotted line.	178
Figure 4.24. Mean ϵ_{xx} [%] calculated across the entire surface of TapestryFragment_1 against time. RH [%] fluctuations are indicated by the dotted line.	178
Figure 4.25. Mean ϵ_{yy} [%] across TapestryFragment_1 plotted against the changes in RH [%].	179

Figure 4.26. Mean ϵ_{xx} [%] across TapestryFragment_1 plotted against the changes in RH [%].	179
Figure 4.27. Error map expressed in sigma [pixel] of TapestryFragment_1 at the end of the 200-hour monitoring.	180
Figure 4.28. Longitudinal strain map of TapestryFragment_1 at the end of the 200-hour monitoring.	181
Figure 4.29. Pseudo ϵ_{yy} [%] acting across the slits versus time. RH [%] fluctuations are indicated by the dotted line.	182
Figure 4.30. Error map expressed in sigma [pixel] of TapestryFragment_2 at the end of the 168-hour monitoring.	184
Figure 4.31. Longitudinal strain map of TapestryFragment_2 at the end of the 168-hour monitoring. The area delineated by the dotted line refers to an open slit.	185
Figure 4.32. Mean ϵ_{yy} [%] calculated across TapestryFragment_2 against time. RH [%] fluctuations are indicated by the dotted line.	186
Figure 4.33. Pseudo ϵ_{yy} [%] calculated across the slit in TapestryFragment_2 against time. RH [%] fluctuations are indicated by the dotted line.....	186
Figure 4.34. Error map expressed in sigma [pixel] of the <i>kesi</i> at the end of the 68-hour monitoring (61 subset size, 5 step size).....	187
Figure 4.35. Longitudinal strain map of the <i>kesi</i> at the end of the 68-hour monitoring (61 subset size, 5 step size).....	188
Figure 4.36. Mean ϵ_{yy} [%] calculated across the <i>kesi</i> against time. RH [%] fluctuations are indicated by the dotted line.	189
Figure 4.37. Mean ϵ_{xx} [%] calculated across the <i>kesi</i> against time. RH [%] fluctuations are indicated by the dotted line.	189
Figure 4.38. Error map expressed in sigma [pixel] of <i>Florence</i> at the end of the 100-hour monitoring (61 subset size, 5 step size).	190
Figure 4.39. Longitudinal strain map of <i>Florence</i> at the end of the 100-hour monitoring (61 subset size, 5 step size).....	191
Figure 4.40. Mean ϵ_{yy} [%] during the 100-hour monitoring of <i>Florence</i> tapestry. RH [%] fluctuations are indicated by the dotted line.	192
Figure 4.41. Mean ϵ_{yy} [%] across <i>Florence</i> tapestry against RH [%] (25-100 hours).	193
Figure 4.42. Picture from the monitoring of the <i>Unicorn tapestry</i> . The photo, taken at 10:30 pm on the 23/07/2015, was not suitable for 2D DIC analysis. ..	194
Figure 4.43. Picture from the monitoring of the <i>Unicorn tapestry</i> . The photo, taken at 10:30 am on the 23/07/2015, was used for 2D DIC analysis.	195
Figure 4.44. Error map expressed in sigma [pixel] of <i>Unicorn tapestry</i> at the end of the 30-day monitoring when first hung (23/07/2015).	196
Figure 4.45. Longitudinal strain map of <i>Unicorn tapestry</i> at the end of the 30-day monitoring when first hung (23/07/2015).	196
Figure 4.46. Mean ϵ_{yy} [%] during the first month of monitoring of <i>Unicorn tapestry</i> . RH [%] fluctuations are indicated by the dotted line (23/06/2015 - 23/07/2015).	197
Figure 4.47. Mean ϵ_{yy} [%] during the ten days of monitoring of <i>Unicorn tapestry</i> , after around a year of it being on display (31/05/2016 - 09/06/2016). RH [%] fluctuations are indicated by the dotted line.	198
Figure 4.48. Longitudinal strain map of <i>Unicorn tapestry</i> at the end of 10-day monitoring after a year since first hung (09/06/2016).	199
Figure 4.49. Error maps expressed in sigma [pixel] of the <i>kesi</i> at the end of the 68-hour monitoring: a) 31 subset size, 5 step size; b) 61 subset size, 3 step size.	201

Figure 4.50. Error maps expressed in sigma [pixel] of the <i>Florence</i> tapestry at the end of the 100-hour monitoring: a) 31 subset size, 5 step size; b) 61 subset size, 3 step size.	202
Figure 4.51. ε_{yy} [%] map of the <i>kesi</i> at the end of the 68-hour monitoring: a) 31 subset size, 5 step size; b) 61 subset size, 3 step size.	203
Figure 4.52. ε_{yy} [%] map of <i>Florence</i> tapestry at the end of the 100-hour monitoring: a) 31 subset size, 5 step size; b) 61 subset size, 3 step size.	204
Figure 4.53. Mean ε_{yy} [%] calculated across the <i>kesi</i> when using different subset and step size.	205
Figure 4.54. Mean ε_{yy} [%] calculated across <i>Florence</i> tapestry when using different subset and step size.	205
Figure 5.1. Sloping boards at the: a) Cluny Museum in Paris; b) Designmuseum Denmark in Copenhagen (profile).	217
Figure 5.2. Forces acting on a tapestry displayed on a fabric-covered board. Reproduced from Barker [1].	219
Figure 5.3. Object on an inclined plane and related applied forces.	222
Figure 5.4. Line force per unit length acting along the top of the tapestry versus inclination angle of the display board with different coefficients of friction, normalised by the load at 0° of inclination.	226
Figure 5.5. Strain versus height of the tapestry when displayed 5° from the vertical at different coefficient of friction: 0; 0.5; 1.5; 20.	226
Figure 5.6. Set-up of wool rep specimens for the tests studying the effects of inclination. The open slits in the artificially damaged samples are indicated within the red dotted lines.	231
Figure 5.7. Monitoring set-up of the historic tapestry fragment displayed on a vertical wooden board, half uncovered, and half covered with cotton molton.	232
Figure 5.8. Longitudinal strain map of samples displayed at 0° from the vertical at the end of the 168-hour monitoring. Samples A, B, C have one central slit 50 mm wide, while sample D is undamaged.	237
Figure 5.9. Overall ε_{yy} [%] of the damaged sample A, B and C and undamaged sample D during the 168-hour monitoring. RH [%] is indicated by the dotted line.	238
Figure 5.10. Pseudo ε_{yy} [%] across the damaged areas (open slits) of sample A, B and C. RH [%] is indicated by the dotted line.	239
Figure 5.11. Overall ε_{yy} [%] of the damaged sample AI and BI during the 168-hour monitoring. RH [%] is indicated by the dotted line.	240
Figure 5.12. Pseudo ε_{yy} [%] across the damaged areas (open slits) of sample AI and BI. RH [%] is indicated by the dotted line.	240
Figure 5.13. Overall ε_{yy} [%] of the damaged sample AII, BII and CII during the 168-hour monitoring. RH [%] is indicated by the dotted line.	241
Figure 5.14. Pseudo ε_{yy} [%] across the damaged areas (open slits) of sample AII, BI and CII. RH [%] is indicated by the dotted line.	242
Figure 5.15. Maximum values of mean pseudo ε_{yy} [%] registered across the slits of the samples displayed at 0, 5, 45 degrees from the vertical for one week. The error bars indicate the SD, as three damaged replicas were tested for each inclination.	243
Figure 5.16. Pseudo ε_{yy} across the damaged areas of samples displayed at 5 and 45 degrees from the vertical (solid blue and green line) during the 168-hour monitoring tests. RH [%] variations are indicated by the dotted lines.	244
Figure 5.17. Longitudinal strain map of TapestryFragment_1 at the end of the 300-hour monitoring displayed on a vertical wooden board half uncovered and half covered with cotton molton. The arrows indicate open slits.	245

Figure 5.18. Mean ε_{yy} [%] across the area of the historic fragment in contact with the cotton molton (orange line), and the area in contact with the wooden surface of the board (blue line). RH [%] is indicated by the dotted line.	246
Figure 6.1. Wool rep mock-ups with artificial damage.	254
Figure 6.2. Damaged area on a wool rep sample conserved with brick couching, 4-mm spacing: a) front; b) back.	254
Figure 6.3. Damaged area on a wool rep sample conserved with laid couching, 4-mm spacing: a) front; b) back.	255
Figure 6.4. Back of wool rep mock-ups treated with: a) full support; b) patch support.	255
Figure 6.5. Wool rep mock-ups with full support applied on the back through scrim lines (at the edges of the samples) and grid lines (in the centre): a) grid lines far from the areas of damage (samples AI, All, E, I); b) grid lines across the areas of damage.	257
Figure 6.6. Detail of the back of TapestryFragment_1 after the first conservation treatment consisting of the application of three linen patches through brick couching in correspondence to weak areas. Brick couching was carried out at the following spacing: 3 mm (areas within yellow dotted line); 6 mm (areas within purple dotted line), 8 mm (area within brown dotted line).	260
Figure 6.7. Back of TapestryFragment_1 after the second conservation treatment consisting of the application of a linen full support.	261
Figure 6.8. Weave structure (59x magnification) of: a) linen A; Stabiltex TM (annotated); linen B unwashed; linen B washed.	262
Figure 6.9. Specimen cut from sample AI.	263
Figure 6.10. Strain map, ε_{yy} [%], of sample AI (full support, brick and laid couching) and sample B (patch support, brick and laid couching) at the end of the 168-hour monitoring.	265
Figure 6.11. Mean ε_{yy} [%] of sample AI and sample B during the 168-hour monitoring. RH [%] is indicated by the dotted line.	266
Figure 6.12. Pseudo ε_{yy} [%] across the damaged but conserved areas of sample AI.	267
Figure 6.13. Maximum pseudo ε_{yy} [%] across areas of sample AI and B conserved with brick and laid couching.	267
Figure 6.14. Strain map, ε_{yy} [%], of sample DI (no conservation), All (full support with grid lines, brick and laid couching) and sample C (full support without grid lines, brick and laid couching) at the end of the 168-hour monitoring.	268
Figure 6.15. Mean ε_{yy} [%] of sample DI, All, and C during the 168-hour monitoring. RH [%] is indicated by the dotted line.	269
Figure 6.16. Pseudo ε_{yy} [%] across the damaged areas of sample D, and conserved areas of sample All.	270
Figure 6.17. Maximum pseudo ε_{yy} [%] across the damaged/untreated areas of sample DI and the damaged/conserved areas of sample All and C.	270
Figure 6.18. Strain map, ε_{yy} [%], of sample DII (no conservation), E (full support with grid lines at a distance from the damaged area) and sample F (full support with grid lines across the damaged area) at the end of the 168-hour monitoring.	272
Figure 6.19. Mean ε_{yy} [%] of sample DII, E, and F during the 168-hour monitoring. RH [%] is indicated by the dotted line.	273
Figure 6.20. Pseudo ε_{yy} [%] across damaged areas of sample DII, E, and F during the 168 hours of monitoring.	274
Figure 6.21. Maximum pseudo ε_{yy} [%] across the damaged areas of sample DII, E and F.	274

Figure 6.22. Strain map, ϵ_{yy} [%], of sample AI (full support, brick and laid couching), F (full support with grid lines across the damaged areas), E (full support with scrim lines distant from the damaged areas) at the end of the 168-hour monitoring.	275
Figure 6.23. Mean ϵ_{yy} [%] of sample AI, F, and E during the 168-hour monitoring. RH [%] is indicated by the dotted line.	276
Figure 6.24. Pseudo ϵ_{yy} [%] across damaged areas of sample AI (blue line, brick couching; red line, laid couching), F (grey line), E (yellow line) during the 168 hours of monitoring.	277
Figure 6.25. Maximum pseudo ϵ_{yy} [%] across the damaged areas of sample AI (conserved with brick and laid couching), E and F.	277
Figure 6.26. Strain map, ϵ_{yy} [%], of sample G (no conservation), H (patch support) and sample I (full support) after 160 hours of monitoring. The locations of particularly weak areas are marked within dotted lines.	278
Figure 6.27. Mean ϵ_{yy} [%] of sample G, H, and I during the 160-hour monitoring. RH [%] is indicated by the dotted line.	279
Figure 6.28. Pseudo ϵ_{yy} [%] across damaged areas (12 bare warps) of sample G, H, and I during the 160 hours of monitoring.	280
Figure 6.29. Maximum pseudo ϵ_{yy} [%] across the damaged areas (12 bare warps) of sample G, H and I.	280
Figure 6.30. Maximum pseudo ϵ_{yy} [%] across the particularly damaged areas of sample G, H and I.	281
Figure 6.31. Strain map, ϵ_{yy} [%], after 168 hours of monitoring of sample: Br.1, Br.2, Br.3 (brick couching); La.1, La.2 (laid couching); Da. (no conservation).	282
Figure 6.32. Mean ϵ_{yy} [%] during the 168-hour monitoring of sample: Br.1, Br.2, Br.3 (brick couching); La.1, La.2 (laid couching); Da. (no conservation). RH [%] is indicated by the dotted line.	283
Figure 6.33. Pseudo ϵ_{yy} [%] across damaged areas of sample Br.1, Br.2, Br.3, La.1, La.2, Da. during the 168 hours of monitoring.	284
Figure 6.34. Maximum pseudo ϵ_{yy} [%] across the damaged areas of sample Br.2, Br.3, La.1, La.2, Da.	284
Figure 6.35. Mean and pseudo ϵ_{yy} [%] of sample Br.1 (15-mm spacing) and Br.2 (8-mm spacing) during the 168 hours of monitoring.	285
Figure 6.36. Strain map, ϵ_{yy} [%], of TapestryFragment_1 at the end of the 200-hour monitoring after the first conservation treatment (application of patches through couching). The conserved areas are highlighted in yellow, while those left untreated in blue. The location of the patches is indicated by the thick black dotted line, while that of brick couching by the fine black dotted line.	288
Figure 6.37. Pseudo ϵ_{yy} [%] across damaged areas of TapestryFragment_1 during the 200-hour monitoring after the first conservation treatment (application of patches though couching).	290
Figure 6.38. Mean ϵ_{yy} [%] during the 200-hour monitoring TapestryFragment_1 after the first conservation treatment. RH [%] is indicated by the dotted line.	290
Figure 6.39. Strain map ϵ_{yy} [%] of TapestryFragment_1 at the end of the 200-hour monitoring of TapestryFragment_1 after the second conservation treatment (application of full support). The area treated with full support is indicated by the horizontal black lines.	291
Figure 6.40. Pseudo ϵ_{yy} [%] across damaged areas of TapestryFragment_1 during the 200 hours of monitoring after the first conservation treatment (application of full support).	292

Figure 6.41. Mean ϵ_{yy} [%] during the 200-hour monitoring TapestryFragment_1 after the second conservation treatment. RH [%] is indicated by the dotted line.	292
Figure 6.42. Stress-strain curves of specimens from washed Linen A (blue line) and washed Linen B (yellow line) tested in the weft direction.	293
Figure 6.43. Stress-strain curves of specimens from washed Linen A (blue line) and washed Linen B (yellow line) tested in the warp direction.	294
Figure 6.44. Stress-strain curve of specimen from unwashed Linen B in the weft direction.	294
Figure 6.45. Stress-strain curve of specimen from unwashed Linen B in the warp direction.	295
Figure 6.46. Young's modulus of the washed Linen A, washed Linen B, unwashed Linen B.	296
Figure 6.47. Breaking stress of washed Linen A, washed Linen B, unwashed Linen B.	297
Figure 6.48. Breaking strain of washed Linen A, washed Linen B, unwashed Linen B.	298
Figure 6.49. Stress-strain curves of polyester Stabiltex™ in the weft and warp direction.	299
Figure 6.50. Stress-strain curve of specimen Al_B2 (full support, grid lines far from areas of damage, 4-mm brick couching) and C_B1 (full support, no grid lines, 4-mm brick couching).	303
Figure 6.51. Stress-strain curve of specimen Al_L1 (full support, grid lines far from areas of damage, 4-mm laid couching) and C_L1 (full support, no grid lines, 4-mm laid couching).	303
Figure 6.52. Specimen Al_B2 (a) and C_L1 (b) during the uniaxial tensile testing.	304
Figure 6.53. Stress-strain curves of specimen B_B1 (patch support, 4-mm brick couching), Br.2 (patch support, 8-mm brick couching).	305
Figure 6.54. Stress-strain curves of specimen B_L1 (patch support, 4-mm laid couching), La.1 (patch support, 15-mm laid couching).	305

Preface

The appreciation of tapestries in Europe has fluctuated over centuries, inevitably influencing conservation. Despite being regarded as one of the most precious forms of art in the 16th century, from the late 18th century tapestries had been declassified and considered more as interior decorative elements. Nowadays, the symbolic and material value of tapestries is recognised, making these artworks a fundamental part of many historic collections. Nevertheless, in many cases the exposure to environmental factors and the long-lasting displays, during which the (heavy and large) objects are hung, have already being responsible for the loss of organic components, like fibres and dyes. Unfortunately, difficult conservation histories determined that only a relatively small number of tapestries has survived until today.

In recent decades, the re-born interest for historic hangings has encouraged the development of related projects in the field of art history and conservation, but also in cultural heritage science. Up to now, the scientific studies have mainly considered how organic materials in tapestries, wool, silk, and dyes, may undergo chemical deterioration. On the other hand, the mechanical behaviour has only interested few studies and so it requires further investigation. Understanding the physical response of tapestries while on display, especially from a macroscopic perspective, is crucial; this would benefit textile conservators, who are still debating on the effectiveness of approaches. It is important to note that tapestries are weft-faced textile and displayed hanging in the weft direction. Therefore, weft yarns are easily exposed to degradation, and this represents both a structural issue and a problem for the preservation of the figurative design. Acknowledging the processes that determine weft loss is essential for ensuring the future display, as well as the future appreciation of the pictorial motif.

The study presented in this thesis aimed to enrich the knowledge on the degradation and preservation of tapestries by answering the main following questions:

- 1) Which factors affect the structural stability of tapestries and how successfully can they be investigated by using analytical tools?

- 2) What are the mechanical degradation processes affecting tapestries while hung for their display?
- 3) How effectively can the structural stability of tapestries be improved by using different display methods and conservation strategies?

To answer these research questions, a multi-disciplinary approach was employed, combining textile conservation, analytical chemistry, and mechanical engineering. It is underlined that this thesis was carried out within the context of a broader project at the University of Glasgow, financially supported by the Leverhulme Trust. The project, entitled *From the Golden Age to the Digital Age: Modelling and Monitoring Historic Tapestries*, involved the Centre for Textile Conservation and Technical Art History (CTCTAH) and the School of Engineering.

The thesis is structured as follows:

Chapter 1 presents a literature review on tapestry making, the evolution over centuries, the materials involved and conservation strategies. Special emphasis was given to treatments in use today for improving structural stability and for preventing the propagation of mechanical damage. The variety of approaches discussed in the chapter highlights how tapestry conservation is still largely influenced by subjective factors, and so the great need for a scientific investigation.

Properties and degradation of wool and silk, main materials within tapestries, are summarised in Chapter 2. Furthermore, past works aiming to define and track (chemical and physical) processes occurring in historic tapestries were revised. Among the works discussed, outcomes from a previous three-year research carried out at the University of Southampton and from the Monitoring of Damage in Historic Tapestries (MODHT) project were described in detail. Both previous studies were central in selecting the analytical approach employed in the following experimental part.

In Chapter 3 samples from different historic hangings (Karen Finch Reference Collection at the CTCTAH) were investigated using: uniaxial tensile testing, attenuated total reflectance Fourier transform infrared spectroscopy (ATR-FTIR),

ultra high performance liquid chromatography with photodiode array detector (UHPLC-PDA). The multi-analytical approach pointed to define the stress-strain response of historic textiles and how the tensile properties may vary depending on the level of chemical degradation of the fibrous material (wool) and on weave features. Moreover, the identification of dye sources through UHPLC-PDA helped in recognising the partial contribution of fibres treatments in promoting chemical deterioration.

The tests in Chapter 4 validated the use of the contactless optical technique 2D digital image correlation, DIC, for monitoring strain across tapestries. Differently from the approaches employed in Chapter 3, 2D DIC was trialled as a full-field diagnostic tool for examining the mechanical behaviour of woven hangings when on display. Six case studies, with various sizes and features, were monitored; through this, the impact of experimental variables in the feasibility of DIC was assessed.

For the first time, the usefulness of sloping boards, an untraditional display method for tapestries, in preventing weft elongation was systematically examined. The experiments, presented in Chapter 5, considered the separate influence of friction and inclination. While the role of fabric/fabric friction was studied through measurements of the coefficient of static friction, the role of inclination was examined through the 2D DIC monitoring of mock-ups displayed at different angles.

Finally, the experiments in Chapter 6 were designed to define the efficacy of various conservation treatments. Namely, support and couching methods were evaluated by monitoring strain across textile objects (mainly bespoke mock-ups) differently conserved. The data gathered from the 2D DIC analysis were compared and enriched with those from the characterisation of the uniaxial tensile properties of treated samples and conservation materials.

Acknowledgments

This work was supported by the Leverhulme Trust, grant number RPG-2015-179. I am extremely grateful to my principal supervisor, Prof Frances Lennard, for her support, guidance, and to keep on reminding me the relevance of this project from conservators' perspective. Her contribution was fundamental in designing the project and in defining which practical aspects to look at when investigating conservation strategies. I am very thankful to Prof Lennard also for conserving the mock-ups in this thesis. I would like to thank my co-supervisor, Dr Philip Harrison, for offering me a different perspective on the work undertaken and for his theoretical analysis on the efficacy of sloping boards. I am also grateful to Dr Jafar Alsayednoor, post-doctoral researcher within the project, for training and supporting me from the beginning.

My deepest thanks to conservators at Glasgow Museums, Maggie Dobbie, Helen Hughes, Harriet Woolmore, who played a fundamental role in the project; thank you very much for the constructive discussions and suggestions. I would like to acknowledge Lynsey Haworth (Historic Environment Scotland) for arranging the monitoring of the tapestry in Stirling Castle. I am grateful to the lecturers of the Textile Conservation course, Sarah Foscett, Karen Thomson, and Dr Margaret Smith, as well as all CTC students, for the helpful suggestions and so kindly allowing me to use spaces and materials. In particular, many thanks to Dr Anita Quye for the access to the UHPLC and the materials for the dye analysis, and to Dr Julie Wertz for training me using the equipment. I would like to thank Prof Christina Young and the Technical Art History group who provided access to ConsLab2 and to the tensile testing machine. A huge thank to Dr Cecilia Gauvin who greatly assisted me during the mechanical characterisation of the samples. I am grateful to Iona Shepherd (Glasgow Life), Stephen McCann, and Sam Dyer (University of Glasgow) for their advices regarding camera settings.

Thanks to all the researchers and conservators, from the advisory panel and more, who got involved and interested in the study; in particular, Susanne Bouret for her contribution to the discussion on sloping boards. I am extremely grateful to Dr Mohamed Dallel (Laboratoire de Recherche des Monuments Historiques) for his interest and willingness in trying to develop the project, despite the difficult current worldwide situation.

I'm grateful to my previous supervisors, Dr Francesca Caterina Izzo, Ina Vanden Berghe, Dr Nobuko Shibayama, Dr Federica Pozzi, for the past encouragement, essential also for undertaking this work.

Many thanks to my "Glaswegian" colleague, but mainly friend, Daniel for always being there during grey and cold Scottish days.

Lastly, I'd like to thank Tom, friends, family, but especially my grandparents, Adriana, Silvana, and Aldo, for being such unconventional models.

Author's declaration

I declare that, except where explicit reference is made to the contribution of others, that this dissertation is the result of my own work and has not been submitted for any other degree at the University of Glasgow or any other institution.

Rosa Costantini

Abbreviations

abs	Absorbance
ATR	Attenuated total reflectance
CA	Cysteic acid
CTCTAH	Centre for textile conservation and technical art history
DIC	Digital image correlation
DMSO	Dimethyl sulfoxide
FEA	Finite element analysis
FTIR	Fourier transform infrared spectroscopy
PDA	Photodiode array
UHPLC	Ultra high performance liquid chromatography
UV-Vis	Ultraviolet-visible
RH	Relative humidity
SD	Standard deviation
SE	Standard error

1 Introduction to tapestries: why and how to conserve them

Chapter 1 discusses the importance of tapestries from a historical and cultural perspective, as well as the conservation practices currently in use to ensure their preservation. The elaborate manufacturing process, the richness of the materials, and the high cultural value are fundamental factors to consider when approaching the field of tapestry conservation. Indeed, often times preserving historic hangings is very challenging, time-consuming and highly costly; therefore, it is important to underline why this activity is so crucial.

The first part of this chapter describes how tapestry making developed and changed over centuries in Europe and how this art form went through period of great appreciation to less fortunate time. The historical manufacturing technique, with all its stages, is delineated, together with the materials usually employed.

The second part of Chapter 1 deals with practices in tapestry conservation: how they evolved over time, especially in the 20th century, and what treatments are preferred today. In particular, on the basis of the objective of the thesis, the chapter focuses on the approaches aiming to provide structural support and to avoid the propagation of mechanical damage, including also display methods.

1.1 Tapestries: the background

1.1.1 The historical context and the cultural value

Tapestry making is a craft with ancient roots, well-known and developed in many different cultures worldwide. Although in the European tradition the word tapestry is commonly used just for indicating figurative woven hangings, the term actually refers more broadly to textiles made with a specific weaving technique. In Asia, for instance, this technique was called *kesi* and it was employed to create, in addition to pictorial hangings, clothes and furnishing fabrics. Differently from European tapestries, Chinese *kesi* were usually made exclusively in silk; an example from the Karen Finch Refence Collection is

provided in Figure 1.1. The Inca version of the craft was instead known as *cumbi* and used for making precious costumes [1].



Figure 1.1. Detail of a *kesi*, Karen Finch Reference Collection, CTCTAH.

The most ancient surviving examples of tapestry are reported to be three fragments conserved at the Cairo Museum dated from 1440 B.C. [2]. In Europe, the art of tapestry making started during the early middle ages. However, it is difficult to clearly define when the craft appeared: some documents reported the presence and manufacture of hanging textiles in France since the 7th century, although, as no examples survived, they might not have been actual tapestries but perhaps other types of woven textiles, such as embroideries [3, 4]. Nevertheless, it can be said that between the 11th and 12th century, some first workshops were established. These studios specialised in the creation of small tapestries of a medium quality. Some of the first European examples testifying to this are the German *Cloth of St. Gereon* (11th century) and the Norwegian *Baldishol* (11th - 13th century) [5, 6].

By the end of the 14th century, the art was eventually refined and so tapestries of great dimensions and quality began to appear for covering, insulating and embellishing the stony and dark walls of medieval buildings, such as palaces and churches, throughout Europe. Tapestries were regarded as both functional and decorative elements, as well as a clear symbol of power and richness. Besides,

tapestries showed the further advantage of being transportable over the different properties of the wealthy patrons. During the 14th century, renewed workshops were based in towns like Arras, Tournai and Paris, where in the meantime corporations of tapestry weavers (e.g. the Parisian *Tapissiers de la haute lisse*) flourished to protect the craftsmen and so the craftsmanship. A century later, Brussels' workshops became the most important ones in the European production. It is interesting to underline that in 1476 the guild rules prevented any other artists than the ones of the Guild of Saint Luke of Brussels to be involved in the creation of the design. Therefore, the manufacture was entirely Flemish, at least until the beginning of the 16th century [5, 6]. An example of 16th-century Flemish manufacture is shown in Figure 1.2, where one of the tapestries from the *Unicorn* set is depicted. Now the historic hanging is on display at the Metropolitan Museum of Art (the Cloisters) in New York.



Figure 1.2. *The Unicorn Rests in a Garden* (from the *Unicorn Tapestries* set). Woven in South Netherlandish between 1495–1505. Accession number: 37.80.6. © The Metropolitan Museum of Art.

As just said, the Flemish hegemony began to be contained from the 16th century. Indeed, in 1515 Pope Leo X asked Raphael to prepare the figurative design (the cartoons) of a set of tapestries, the *Acts of the Apostles* [5, 6]. These cartoons are now conserved at the Victoria and Albert Museum (Figure 1.3). Although the hangings were still woven in Brussels, this episode was important since it renewed the pictorial style, which became greatly influenced by the Italian Renaissance taste. The new style was characterised by scenes (now including more secular themes) framed by complex borders and focused on few full-size characters and patterns, breaking with the former Medieval and Gothic tradition rich in decorative motifs and figures [5-7].



Figure 1.3. Cartoon for a tapestry, *The Miraculous Draught of Fishes*. Raphael, Italy, about 1515-1516. Bodycolour on paper laid onto canvas. Museum number: ROYAL LOANS.2. © Victoria & Albert Museum.

During the first half of the 16th century, Brussels was regarded as the most prestigious centre for the *weaving* of tapestries, reaching the highest level of quality in history, from both the technical and artistic point of view. For these reasons, the second third of the 16th century is described as the “Golden Age of the Netherlandish tapestry weaving” [8]. To protect this esteemed status, from 1528, Brussels’ tapestries were marked with an official sign, to avoid forgery.

Nevertheless, there was a fraudulent market involving other centres, such as Antwerp, that copied the mark on their pieces. A limited number of workshops was also established in Italian towns, like Mantua and Ferrara. These ateliers were founded by Italian patrons (namely Este and Gonzaga) that brought Flemish and French weavers to their own courts [5, 6]. From the 1560s, civil wars and religious persecutions drastically affected the southern Netherlandish industry, forcing many weavers to migrate towards Italy, Germany, Holland, England and France [3, 6, 8].

In the 17th century, France substituted the Low Countries in their leading role in tapestry production. French kings, like Henry IV and later Louis XIV, greatly promoted this shift, encouraging the flourishing of ateliers such as the well-known and enduring *Manufacture des Gobelins* [6, 8, 9].

During the second third of the 18th century, together with the development of the decorative Rococo style, tapestries started to be requested as interior design objects. This was the last significant period for the art of tapestry making in Europe, as from that moment onwards the appreciation of hangings began to decline, in favour of an increasing positive perception of paintings. By the end of the 18th century, precious historic tapestries were cut and many of them (such as those of the English royal collection) started to be displayed permanently, while traditionally they were only installed on specific occasions. These factors markedly affected the preservation of woven hangings, as well as how they have been perceived, restored and conserved later on [5, 8, 10].

The extreme high value of historic tapestries should be therefore remembered, underlining how, especially between the 14th and the 16th century, they were considered as the most widespread and explicit artistic devices to show off wealth and power by both religious and lay figures in all Europe. It is emblematic how Henry VIII in 1530s chose to commission tapestries as artistic tools to proclaim himself as the head of the newly born Church of England, while affirming his religious beliefs. Similarly, in 1520s Pope Leo X requested tapestries to demonstrate the greatness of the papacy against the threats of rising Lutheranism. Nonetheless, the high value of woven hangings was not only symbolic: historical sources proved that they were extremely expensive compared to any other art, including painting. A set of tapestries bought by

Henry VIII in 1528 (*Story of David*) cost over 1500 pounds (the price of a battleship), while, at that period, the royal artists Horenbout and Holbein received an annual stipend of between 30 and 33 pounds. Moreover, those same tapestries were carefully restored by appointed skilful professionals in the Standing Wardrobe at Hampton Court, and only occasionally displayed for ceremonies [8].

Today tapestries represent a precious part of the cultural heritage, also considering that only a restricted percentage of the original amount of historic hangings survived over the centuries (e.g. the English royal collection was estimated to have over 2450 tapestries at the moment of Henry VIII's death, while nowadays only around 100 tapestries can be found in the inventory of Hampton Court Palace [11]). All these data are significant to recognise the cultural value of tapestries and so the need of conserving them in the best way possible.

1.1.2 The making of tapestry

From a technical point of view, a tapestry can be defined as a discontinuous weft-faced plain weave. The term weft-faced refers to the fact that the design of tapestries is created by multi-coloured and closely packed weft yarns, which cover completely the structural undyed and widely spaced warp threads. Another technical characteristic of tapestries is that the weft is discontinuous, as the threads are changed according to the colour pattern [1, 5]. A scheme of tapestry weave structure is illustrated in Figure 1.4.

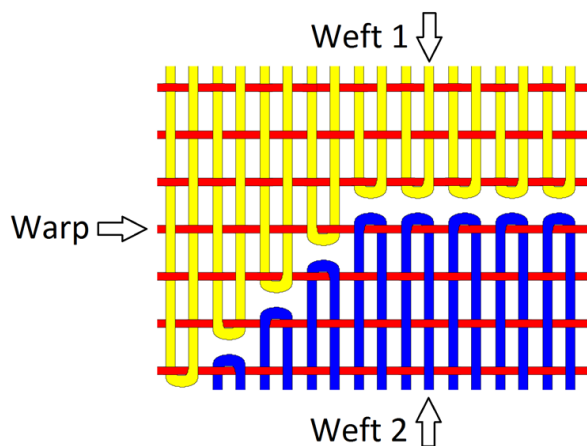


Figure 1.4. Tapestry weave structure, in the hanging direction, with two differently coloured sets of weft threads [12].

Historically, different methods were employed to obtain a change in colour but in the European countries between the 14th and the 18th century the three most popular techniques were: slits, dovetail, and interlock.

Slits occur whenever the weft turns around the warp yarn creating an opening, as shown in Figure 1.4. As slits affect the stability of the woven structure, historically they were usually sewn up after the weaving was completed. Nevertheless, in some other cases, slits were deliberately left open to better delineate specific shapes such as the ones of human faces or hands. Dovetail joints are obtained from turning weft threads of different colours over the same warp yarn, creating a zig-zag motif structurally reinforced. However, interlocking is the most efficient technique to produce a strong tapestry while avoiding the formation of holes in the weave. The method consists in interlacing on the back weft threads of adjacent colours through passing them around or between the same warp once or twice (single or double interlock joints). Although interlocking ensures a resistant structure, it is also highly time-consuming.

In addition, traditionally some other techniques were employed to enrich the woven design with characteristic effects. For instance, hatching was used to form shades through placing near lines of differently coloured weft threads. Besides, hachures (coloured triangular patterns) were created to obtain a similar blending effect, particularly in Flemish tapestries from the 15th and early 16th century [1, 5, 13, 14].

Tapestry making has always been a long process, including many stages and involving different professionals. Before the actual weaving, the design of a tapestry is first made as a drawing or painting (*petit patron*) [10], then translated into a cartoon, a full-scale coloured representation of the tapestry pattern, used as the final template by the weavers. Historically, often times the first version of the design was commissioned by wealthy patrons from a qualified painter (e.g. Figure 1.3) [5, 6, 14].

The potentially difficult process of translating a painting into a tapestry was usually accomplished by skilful professionals, the *Kartonniers*. These cartoon designers had the tasks of correcting the sizes of the painter's draft and of

modifying it according to the specific technical requirements of tapestry weaving [5, 6, 14]. When the cartoon, which was often made of linen sheets or paper [10] (the latter only from the beginning of the 16th century [8]), finally arrived with the weavers, the master of the workshop became the owner and the design was usually replicated for making other pieces. To avoid this, sometimes the patron decided to acquire the original cartoons and even to display them; this also allowed to better preserve the tapestries and to hang them only on special occasions [13].

In the weaving workshop, tapestries were then woven by hand using a loom. Through this instrument, warp yarns are straight so that the weft threads are inserted between the openings (sheds) created by raising or lowering a selected set of warps. Although there are different types of looms, the two most popular ones employed by European weavers were the high-warp (*haute lisse*) and low-warp loom (*basse lisse*). Both of them consist of two bars stretching the warps, though in different directions: in the *haute lisse* the warps are arranged upright, while in the *basse lisse* horizontally.

According to the type of loom, historically the cartoon was placed differently to enable the weavers to copy the design: with the *haute lisse*, the template was positioned behind the warps while, with the *basse lisse*, it was put underneath them. Since with the low-warp loom the cartoon was nearer to the weavers, it was easier for them to follow the pattern. The final product of both types of loom is structurally almost the same, although they have been differently employed depending on the historical period (e.g. the *basse lisse* was preferred during the Renaissance period) [1, 5, 6]. Furthermore, another important and common aspect is that with two types of loom, the pattern was traditionally woven sideways so that, when the work was completed, the tapestry was turned 90 degrees. This was made for both practical and aesthetic reasons. As the size of the loom dictates the proportion of one side of the tapestries, from a practical point of view, this technique enabled to create much larger pieces with dimensions suitable for the walls of castles or cathedrals. Besides that, the motif was woven perpendicular to the warps to prevent the formation of long non-aesthetic series of slits while creating frequent vertical features like trees [6].

1.1.3 The materials

Materials greatly defined the value of a tapestry. In fact, quality and cost of the artwork could vary significantly depending on that, together with other factors such as the cartoon, the skilfulness and the quantity of the manufacture, as well as the warp and weft count (the fineness/density of the weave) [4].

Traditionally, the fibres used in European tapestries were wool (especially from England and Spain) and silk (Italian or Spanish). Undyed wool was used for the structural warp yarns while dyed wool for a large part of the decorative weft. In addition, silk can be found in the weft and, more rarely, also linen (in particular, the use is reported in Swiss and German 16th-century hangings). Besides that, precious pieces featured metal threads made of a yellow dyed or white silk core wrapped by a gold, silver, or silver gilt strip, usually from Venice or Cyprus. Because of their excessive prices, both silk and metal threads were only present in high quality tapestries [5].

Natural dyes and related mordants define the colour palette of historic tapestries. Dyes are described as materials characterised by the presence of a colour, but without any thickness, as opposed to pigments that have both properties [15]. They are organic and they can be applied in a solution for dyeing textiles thanks to the formation of chemical and/or physical bonds (while pigments are mechanically applied in a solid form through the help of an appropriate binding medium). Colorants can be grouped according to their origin (vegetal, animal, synthetic), the chemical class or the principle of the dyeing process. Before the second half of the 19th century dyes were obtained from natural sources (both vegetal and animal) [16], therefore in historic hangings only natural colorants can be found, at least in the original woven parts. The most common dyes in European tapestries are listed in Table 1.1 [14]. In addition to the colorants reported in Table 1.1, other dye sources have been previously detected in European tapestries, namely: logwood [16]; safflower [17-19]; orchil [18, 20, 21]; kermes [22]; Polish cochineal [17].

As shown by the brief descriptions in Table 1.1, the final colour of the dyeing can be affected by the type of mordant employed. Mordants are coordination metals that act as a bridge between the colorant and the fibres, forming a dye-metal-fibre complex. Traditionally, the principal mordant was aluminium ion,

mostly from $\text{AlK}(\text{SO}_4)_2 \cdot 12\text{H}_2\text{O}$ (also known as potash alum or potassium alum). Other mordants were: salts from iron, tin (from the 17th century), chromium (from the 19th century), and copper (even if more rarely). As indicated in Table 1.1, not all dyes required the use of mordant; it depended on their chemical properties and so on the dye class [16].

Table 1.1. Dyes commonly employed in historic European tapestries. Data taken from Quye et al., 2009 [14].

Natural source of dye	Chemical class of the main compounds	Dye class	Colour obtained
Mexican cochineal	Anthraquinone	Mordant	Red (alum), pink (tin chloride)
Madder, wild madder, bedstraws	Anthraquinone	Mordant	Red (alum), purple and brown (iron sulphate)
Soluble redwoods	Homoisoflavonoid	Mordant	Red, brown (alum)
Weld	Flavonoid	Mordant	Yellow (alum), green (iron sulphate or copper sulphate)
Dyer's broom	Flavonoid	Mordant	Yellow (alum), green (iron sulphate or copper sulphate)
Sawwort	Flavonoid	Mordant	Yellow (alum), green (iron sulphate or copper sulphate)
Young fustic	Flavonoid	Mordant	Yellow (alum)
Woad, indigotin-based source	Indigoid	Vat	Blue
Galls	Tannin	Direct or mordant	Brown, black

Considering the final purposes of the current project, it is very important to remark the broad variety of materials involved in tapestries making, as material heterogeneity affects the complex degradation processes of the artefact and therefore its conservation needs.

1.2 Conservation practices

Tapestries are extremely complex objects, with complex deterioration problems and so conservation needs. Considering the manufacturing process, this complexity is linked to several factors, such as the presence of structural heterogeneities and the use of various materials that would eventually undergo a broad range of ageing conditions. This large number of variables over time can be responsible for an intricate mix of physical and chemical degradation processes, difficult to predict. Therefore, tapestry conservation techniques face

various issues that may concern both the physical stability and pictorial integrity of the historic object. This is especially true if weft threads are deteriorated, as they are responsible for both the design and the structure.

Frequent damage of weft threads is due to their over exposure to environmental factors, such as light, which may lead to different degrees of degradation according to the type of fibrous material and its processing technique (e.g. dyeing method, bleaching). For instance, silk wefts are weaker than woollen ones, especially if the former were bleached. In addition, insects may be responsible for fibres loss, while open slits, a typical feature of tapestry weaving, may lead to the propagation of structural problems [23]. In Chapter 2, the degradation paths of wool and silk, main components of historic hangings, are discussed more in detail. Further study on variables affecting structural stability and mechanical damage mechanisms is described in Chapter 3 and Chapter 4.

Because of the fragility of tapestries, as well as of their high cost, their restoration started together with the development of the medieval production itself [23, 24]. Therefore, the maintenance of historic hangings has passed through many centuries and it has evolved along with the principles of restoration and the perception of this art. Nowadays, approaches and practices may vary significantly from country to country, as well as even from conservator to conservator within the same workshop. The difficulty of establishing a common trend in tapestry care may be due, partly, to the lack of a scientific approach in evaluating different techniques. Indeed, science could help providing reliable data that would make conservation less subjective and more objective. To understand this complex topic, first the evolution over time of tapestry restoration and conservation is discussed, followed by a technical description of approaches in use today.

1.2.1 The approach over the time

Among publications that trace back the history of tapestry repair from a general perspective [23-27], Lennard recognises three main stages: I) the reweaving by skilled professionals during the golden age of the manufacture; II) the unconscious and crude approach when the production declined (late 19th and

early 20th centuries); III) the conservative attitude developed from the second half of the 20th century [23].

During the first phase, the maintenance of tapestries was enabled by both the careful reweaving and the fact that the objects were only displayed in specific occasions, allowing their preservation. Some references, collected by Fiette, record the activity of French skilled repairers from the last quarter of the 14th century [25]. On the same hand, different publications give information about the care of the British royal collection [4, 28-30]. Campbell describes the use of reweaving, lining with canvas and cleaning during the reign of Henry VII and Henry VIII. At the same time, Campbell stresses the importance of the Great Wardrobe, the site where, until 1782, the royal collection was safely stored and restored by selected staff [4]. Other European royal courts did the same [31]. The widespread 16th-century custom of lining British tapestries is also indicated by Band [29]. She describes how blue- or black-dyed linings (usually made of linen) were added and renewed to protect the objects from the wall humidity, the handling and the weakness of the woven structure [29]. Regarding the cleaning of hangings, interestingly, Hefford portrays the 17th- and 18th-century use (perhaps also earlier [4] and later [25]) of brushing with crumbled bread in the Wardrobe [27]. In the same article, it is recalled the controversial painting method to cover areas of loss while avoiding reweaving. The habit of painting or chalking was very widespread at the beginning of the 16th century, though tentatively contained by regulations from the second quarter of the same century [27]. Because of the high-quality techniques and the use of appropriate and coherent materials, now it can be challenging to distinguish historical repairs from the original weaving. Usually, today these repairs are kept during the conservation treatment, since they are regarded as part of the historical evolution of the tapestry [23].

The decreasing interest and appreciation of tapestries from the early 19th century, affected the quality and quantity of manufacture, as well as the general care. During this second phase, tapestries were displayed permanently, overhung by paintings, and even cut [24, 29, 30]. The case of *The Lady and the Unicorn* set (the masterpieces of the Cluny Museum in Paris) is emblematic though particularly drastic: the hangings were used to cover greenhouses [31].

Reweaving was still a widespread method to fill areas of loss, but this carried out by a restricted number of unskilled professionals [32]. It is reported that, at the beginning of the 20th century, tapestries repairers were lacking especially in England although they could still be found in France [24, 32]. Besides that, the repairs often involved cheap and low-quality materials, such as newly synthesised unstable dyes. Industrial cotton was employed for reweaving, although it showed a totally different mechanical behaviour from the wool used to weave the original piece [33]. All these factors eventually led to further distortion and damage of the design [34].

However, before the actual start of the third phase, different sources recognise an *ante litteram* conservative attitude towards pictorial hangings. This new approach was born in Sweden in the early 20th century, mainly thanks to the activity of John Böttinger [23-25]. Böttinger worked from 1915 as conservator for the Swedish Guard-Meuble Royal and for the Royal Castles [23]. He stated, also through a written publication dated 1937 [35], the importance of documenting the conditions of the object before and after treatment, as well as the potential damaging effects caused by wet cleaning. As an alternative to this practice, Böttinger promoted the use of vacuum suction, specifying that it should be carried out biannually through a gauze in order to ensure proper care. The safety of the method for the fibres was tested by an appointed scientist [24]. Interestingly, the value of this new collaborative approach between science and textile conservation was also stressed a few decades later, in 1961, by another Swedish textile conservator, Agnes Geijer. In her brief publication, Geijer argued for better cooperation between curators, scientists, and “manual workers” [36]. Böttinger innovative approach included also the use of dyed patches and stitching for the repair of areas of loss [35].

Despite these developments, until at least the second half of the 20th century, tapestries were more often *restored* rather than *conserved* [23]. Restoration usually involved reweaving, which was seen as a tool to recreate the integrity of the figurative design [33, 37], the element that dictated the economic value of the object [34].

From the 1950s, conservation principles started to be widespread, generating debates among professionals and new techniques to conform to the modern

ethic [23, 24]. For instance, adhesives were introduced in the 1960s, especially in the UK and in the Netherlands, to provide stability to the fibres and to attach supports [38-40]. Soon, different conservators faced the damaging effects caused by these synthetic materials and their use was therefore abandoned quickly [41-43]. This experimental attitude affected also traditional reweaving and, especially in the UK, alternative techniques were developed [23, 24, 26]. The work of Karen Finch is regarded as fundamental for this development. Finch started working as a weaver in Denmark, while in 1946 she moved to England where she began her career as a textile conservator, and later as a teacher. Eventually, in 1975, Finch founded the Textile Conservation Centre (now CTCTAH). Some of Finch's articles, published during her long career, aimed to show the path towards innovative practices [32, 34, 43], that can be seen as a further evolution of Böttinger's [24]. Indeed, one her main contribution is related to the introduction of patches or full support linen fabrics stitched on the back of the tapestries (the latter also known as "the English method") [24]. As Finch stated, these methods take into account and overcome relevant issues: the preservation of the original design and materials; the reversibility of the treatment; the need of providing a safe support for display [34].

From the 1960s onwards, all these new methods were subjects of discussion during the increasing number of conferences on textiles and tapestries conservation [23, 24]. Important meetings regarding tapestries took place in: 1964 in Delf (The Netherlands) [44]; 1976 in San Francisco (USA) [45]; 1980 in Como (Italy) [46]; 1981 in Florence (Italy) [47]; 1984 in Paris (France) [48]; 1987 in Brussels (Belgium) [49]; 1994 in Amsterdam (The Netherlands) [50]; 1995 in Norfolk (UK) [51]; 2009 in New York (USA). The published volumes resulting from these symposiums document several case studies, able to demonstrate the evolution of approaches and practices, as well as how they differed between countries [44-51].

Regarding image reintegration, some case studies, from the cited volumes and others, show a mixed use of methods: they involved traditional reweaving but also emerging stitching techniques. This trend could be observed in both American [52-54] and European laboratories [55, 56]. In 1995, Marko described this uncertain approach as "a confusion of ideas" [57]. This confused situation

lasted principally until the end of 1980s [26]. It should be noted that reweaving has been employed also later on: one well-known example is the Textile Conservation Department of the Metropolitan Museum of Art, where the pictorial integrity of hangings is still recognised as a crucial factor [58]. However, different methods, such as inpainted support patches, have been proposed during the last decades [59-61]. In general, the recent need of finding an alternative to reweaving has been spreading more insistently, not only to conform to conservation ethics, but also to try reducing the high cost and time of the intervention [62, 63].

Besides image reintegration, the same conferences depicted heterogeneities also on the approach concerning support methods and the materials involved. Regarding the type of support, the choice could be made among full support [41, 42, 61, 64, 65], patches [41, 53, 55, 63] and strips of fabric (straps) [53, 54, 66]. The cited publications prove that full support has been widely used in Europe, especially in the UK, while straps have been traditionally chosen by American workshops (also more recently [58, 67]). Sometimes patches are reported to be employed together with a full support fabric [41] (or even straps [53]), as they may be used not exclusively to reinforce weak areas but also for the image reintegration. The conservators' vocabulary on structural treatments may vary significantly from paper to paper, so it may be difficult to discriminate the methods presented. One issue concerns the contradictory use of the term *lining*. In some publications, it clearly indicates an additional fabric (usually in cotton) stitched to the back as a protection from dust and wall humidity [42, 54, 61, 66], while in others the word is more ambiguous and may refer to a support technique [24, 63].

Regarding display and hanging methods, historically tapestries were hung loose from the top. The traditional system implies the use of damaging nails fixed to the wall [68]. From the 1970s, Velcro™ was introduced and, since then, it has been widely employed (e.g. [36, 40, 51-53, 59, 61, 69]). Nowadays, some museums choose to display tapestries using sloping boards [69, 70], as discussed in detail in Chapter 5.

In general, from the 1980s, a more scientific approach started to affect the field of tapestry conservation. Materials and manufacture of historical tapestries have

been studied, leading to a better understanding of the related degradation processes and conservation needs [23]. Importantly, in 2002 the three-year project Monitoring of Damage to Historic Tapestries (MODHT) started, bringing together many professionals from all over Europe to investigate causes behind the degradation of hangings, mostly from a chemical perspective [14]. Besides, fewer studies focused on the mechanical behaviour and physical degradation of tapestries [71-73]. Projects within the field of heritage science and addressed to the study of tapestries are reviewed in Chapter 2.

1.2.2 Current conservation practices

During the last three decades, three surveys were carried out on the current methods employed in tapestry conservation, and especially on support treatments. The questionnaires are by: Hofenk de Graaff (1997) [26]; Breeze (2000) [24]; Duffus (2013) [74]. The three studies investigated the techniques and materials employed by conservators from the USA [24] and worldwide [26, 74], giving an overview of the practices and materials used nowadays. More recently (2019), another questionnaire was carried out by Catic for her masters dissertation on stitching methods for treating weak areas in tapestries. The questionnaire was addressed to conservators working in some European countries, and it asked questions related to both stitching and display approaches [75]. Besides, *Tapestry Conservation: Principles and Practices* edited by Lennard and Hayward (2006) still represents a key publication, providing examples of current trends [76]. It is worth noting that in 2020 another comprehensive book on tapestry conservation by Marko was published [77].

The techniques listed below all aim to improve structural stability, in some cases, together with providing pictorial continuity. Indeed, structural stability is the topic of the current study. For the same reason, treatments such as cleaning are not reported.

Image reintegration

- *Re-warping*: this method can be used to replace missing or weak warp yarns. Re-warping is carried out through knotting and channelling new wool warp threads in a sound part of the weave structure, restoring the

internal structure while providing the needed tension to the weave [26, 31]. Re-warping can be made on the support fabric instead of the actual tapestry, in order to prevent damaging original wefts near the hole. This technique is usually the first step of the treatment, as it is often followed by brick couching or reweaving for replacing the missing weft threads [26]. Wool or cotton are usually employed [24, 26].

- *Reweaving*: this method is the one that has been traditionally used for the repair of areas of loss in tapestries. The technique can still be found in some workshops, although in the last decades it has been progressively abandoned as it does not conform to conservation ethics [23]. Before the treatment, original wefts can be removed, and this opposes the preservation of historical materials. Moreover, if no proper references are available (i.e. the original cartoon, old pictures) imaginative obtrusive interventions may be created [34]. Another drawback of reweaving is the fact that it is highly time-consuming and expensive [62, 63].
- *Needle weaving*: this type of treatment is comparable to reweaving, though it is usually carried out in areas of missing wefts where warp yarns are still present. The technique involves an *in situ* re-wefting using a needle, differently from traditional reweaving where looms and bobbins are employed [31].
- *Laid couching*: this treatment is commonly employed in textile conservation to stitch the damaged fabric to a stronger one used as support [78]. Laid couching is obtained first by inserting a long stitch along the weft direction (in the case of tapestries), and then securing it by adding smaller stitches perpendicular to the long one [79]. The stitches can be placed at different distances, possibly influencing the final strength of the textile object [75, 78]. According to the responses to Catic's questionnaire, laid couching is especially used by textile conservators in Germany (11 out of 11 German respondents) [75].
- *Couching stitching*: this technique, also known as *brick couching*, is used for providing both structural support and figurative infilling in areas of damage. The method consists of placing lines of running stitches in the

weft direction through the support fabric: the stitches go over one warp on the front and under the next, in an alternate pattern. The spacing and distribution of stitches may vary depending on the damage (i.e. if there is still a good amount of original wefts, the stitching can go over one warp on the front and under three-five warps on the back) [31, 80]. Breeze and Hofenk de Graaff's surveys indicate that brick couching is the current preferred method for conserving areas of weft loss [24, 26], with the exception of German workshops, as specified by Catic's study [75]. Questionnaires report that, for replacing wool threads, wool or cotton yarns are usually selected, while for missing silk, (stranded) cotton is often employed, though a few conservators may opt for silk [24, 26, 75]. Sometimes, also polyester is used for stitching across areas of missing wool and silk wefts [75].

- *Dyed fabric infills*: this method is usually preferred for integrating while supporting large areas of loss or missing parts whose design cannot be reproduced [80].

Support methods

- *Slits re-stitching*: this technique can be used for damaged and weak slits. The decision of whether to stitch damaged slits or not may depend on several factors, such as time and money available for the intervention, length and location of the holes, the overall condition of the tapestry, and the original intentions of the weaver (some slits were indeed deliberately left open, as discussed in Section 1.1.2). Cotton and polyester are often used for stitching. The treatment can be carried out both directly on the hanging or through a support fabric [24, 26].
- *Full support*: this technique consists in stitching a fabric on the entire back of the tapestry. Full supports are especially used when the object needs an extensive intervention as its overall structural conditions are not good. Usually, a certain excess of fabric (also called "bag") is added while applying the support, to allow ease. In order to attach the support to the tapestry, various stitching techniques can be used (mainly running stitches) and distributed in different ways [24, 26, 74].

- *Patch support*: patches can be applied to tapestries as a support and a figurative infilling treatment. In particular, patches are selected when the overall structure of the hanging is sound and it only shows some weak areas [24, 26, 74].
- *Strap support*: the use of textile (usually cotton or linen) straps is sometimes seen as a way of carrying the weight of the hanging without adding any extra load, like in the case of a full support. As no repairs are done in the strips, that are always distributed alongside the weft direction of the tapestry, they can be removed easily. Importantly, straps allow to leave part of the original back always available for observations [57]. Through this system, the weave structure is allowed to fluctuate accordingly to the environmental conditions [53]. Nevertheless, for some conservators these movements may lead to an irregular tension distribution, eventually causing the so-called swag [53] or festooned effect [57]. Another objection against straps is the possible formation of darker bands on the front, because of the uneven dust filtration (perhaps overcome through adding a dust cover) [53]. The spacing of straps, and so the percentage of covered area, may vary [24, 26]. Strap support is mainly popular in the USA [24, 26, 74].

In addition to the choice on the type of support, other variables need to be selected, such as: the fabric for the treatment (and if/how it is pre-treated); the stitching technique (and materials) for securing the systems; the spacing and distribution of stitches. A more detailed overview of practice today can be drawn from previously cited surveys [24, 26, 74]. For instance, regarding the materials employed, for full supports, cotton and linen are the most widespread, though also synthetic ones have been rarely suggested. Duffus' survey [74] shows that conservators still do not agree about the reasons behind the fabric choice. Some think that the fabric should respond to the environmental changes in a comparable way of the tapestry in order to enable its fluctuations, while others say that the material has to be selected for its ability to restrict the movement. These contrasting answers, similar to the ones previously collected by Hofenk de Graaff [26], prove that there is still uncertainty and misunderstanding on the (desirable) qualities of support fabrics. In the case of straps and patches,

Breeze's questionnaire [24] shows that cotton is the most selected textile for both types of support in the USA.

Additional protection

- *Lining*: this term usually (though not always, leading to misunderstanding) indicates an additional fabric that covers entirely the tapestry on the back for protecting it from dust, abrasion and humidity of the wall. The most common material for linings is cotton, especially plain weave or sateen fabrics, while more rarely linen can be chosen [24, 26]. Many conservators opt for cotton because of the high density of its weave, allowing the textile to act as a dust protection [26]. Linings, like supports, can be attached using different stitching techniques (i.e. locking stitches, running stitches) and thread types (i.e. cotton, polyester) [24, 26].

Display methods

- *Vertical hanging*: historically tapestries were hung vertically. This approach is the most widespread also nowadays, in agreement with the tradition.
- *Sloping boards*: in recent years, tapestries have started to be displayed at different angles through slanted boards. This approach is especially widespread in central Europe (Germany and France), and André Brutillot is regarded as one of the experts who greatly promoted this technique [69, 70, 81]. According to Brutillot, some of the advantages of sloping boards are: the retarded elongation of the weft threads; the lack of undulations (as the object lies flat on the board); the contained accumulation of dust; the reduced need of conservation treatments [81]. However, not all conservators think that sloping boards are a valuable solution since they alter both the historical presentation and the viewing perspective. Moreover, in opposition to Brutillot's idea, it is often thought that the angled disposition may actually promote dust accumulation [81]. Another drawback is that usually boards are only tilted by a few degrees, such as 5° from the vertical, perhaps not enough to produce a significant ease from strain [82]. It should be noted that no studies have been

published so far to clarify the role of friction in this type of system, although the boards are usually covered by fabrics that aim at promoting this (e.g. cotton molton and polyester felt [75, 83]). The use, and the actual efficacy, of sloping boards is discussed in Chapter 5.

- *Velcro*[™]: has been the most common tool to hang tapestries from the 1970s. This hook-and-loop fastener represents a good advantage in case of emergency procedures, in opposition to the historical hanging systems that involved the use of hooks, rings and nails [23]. However, Marko underlines the importance of considering the context, as in some cases keeping the original hanging systems (though including also the *Velcro*[™]) may be significant to show the historical techniques [61]. *Velcro*[™] can be fixed in different ways, either directly to the tapestry or through a fabric extension.

References

1. Phipps, E., *Looking at textiles: a guide to technical terms*. 2011, Los Angeles: J. Paul Getty Museum. 94 p.
2. Franses, J., *Tapestries and their mythology*. 1973, London: John Gifford Ltd. 160 p., 18 p. of plates.
3. Thomson, W.G., *A history of tapestry from the earliest times until the present day*. 1906, London: Hodder and Stoughton. xvi, 506 p.
4. Campbell, T.P., *Henry VIII and the art of majesty: tapestries at the Tudor Court*. 2007, New Haven; London: Yale University Press. xviii, 419 p.
5. Campbell, T.P., M.W. Ainsworth, and B. White, *Tapestry in the Renaissance: art and magnificence*. 2002, London; New York; New Haven: Metropolitan Museum of Art. 594 p.
6. *Five centuries of tapestry from the Fine Arts Museums of San Francisco*, ed. A.G. Bennett. 1992, San Francisco: Fine Arts Museums of San Francisco. 329 p.
7. Thomson, F.P., *Tapestry: mirror of history*. 1980, Newton Abbot: David & Charles. 224 p.
8. *Tapestry in the Baroque: threads of splendor*, ed. T.P. Campbell. 2007, New York: Metropolitan Museum of Art. 563 p.
9. Hunter, G.L., *The practical book of tapestries*. 1925, Philadelphia: J. B. Lippincott Company. 302 p.
10. Thurman, C.M., *Tapestry: the purposes, form, and function of the medium from its inception until today*, in *Acts of the Tapestry Symposium*, A. Bennett, Editor. 1979, Fine Arts Museums of San Francisco: San Francisco. p. 5-19.
11. www.royalcollection.org.uk
12. Alsayednoor, J., et al., *Evaluating the use of digital image correlation for strain measurement in historic tapestries using representative deformation fields*. Strain, 2019. **55**(2): p. e12308.
13. Freeman, M.B., *The Unicorn Tapestries*. 1983, Lausanne: The Metropolitan Museum of Art. 244 p.
14. Quye, A., et al., *'Wroughte in gold and silk' : preserving the art of historic tapestries*. 2009, Edinburgh: NMS Enterprises Limited-Publishing. viii, 134 p.
15. Campanella, L., et al., *Chimica per l'arte*. 2007, Ozzano Emilia: Zanichelli. 490 p.
16. Kirby, J., et al., *Natural colorants for dyeing and lake pigments: practical recipes and their historical sources*. 2014, London: Archetype Publications Ltd in association with CHARISMA. 114 p.
17. Degano, I., J.J. Łucejko, and M.P. Colombini, *The unprecedented identification of Safflower dyestuff in a 16th century tapestry through the application of a new reliable diagnostic procedure*. Journal of Cultural Heritage, 2011. **12**(3): p. 295-299.
18. Troalen, L.G., *Historic Dye Analysis: Method Development And New Applications In Cultural Heritage*, in *School Of Chemistry*. 2013, University Of Edinburgh.
19. Halpine, S.M., *An Improved Dye and Lake Pigment Analysis Method for High-Performance Liquid Chromatography and Diode-Array Detector*. Studies in Conservation, 1996. **41**(2): p. 76-94.
20. Clementi, C., et al., *In-situ fluorimetry: a powerful non-invasive diagnostic technique for natural dyes used in artefacts. Part II*.

- Identification of orcein and indigo in Renaissance tapestries.* Spectrochimica Acta Part A: Molecular and Biomolecular Spectroscopy, 2009. **71**(5): p. 2057-62.
21. Carò, F., et al., *Redeeming Pieter Coecke van Aelst's Gluttony Tapestry: Learning from Scientific Analysis.* Metropolitan Museum Journal, 2014. **49**: p. 151-164.
 22. Zaffino, C., et al., *In-situ spectrofluorimetric identification of natural red dyestuffs in ancient tapestries.* Microchemical Journal, 2017. **132**: p. 77-82.
 23. Lennard, F., *Preserving image and structure: tapestry conservation in Europe and the United States.* Studies in Conservation, 2013. **51**(sup1): p. 43-53.
 24. Breeze, C.M., *A Survey of American Tapestry Conservation Techniques.* 2000: American Textile History Museum.
 25. Fiette, A., *Tapestry restoration: An historical and technical survey.* The Conservator, 1997. **21**(1): p. 28-36.
 26. Hofenk de Graaff, J.H., *Tapestry Conservation: Support Methods and Fabrics.* 1997.
 27. Hefford, W., *Bread, brushes and broom: aspects of tapestry restoration in England, 1660-1760*, in *Acts of the Tapestry Symposium*, A. Bennett, Editor. 1979, Fine Arts Museums of San Francisco: San Francisco p. 65-75.
 28. Hayward, M., *Fit for a king? Maintaining the early Tudor tapestry collection*, in *Tapestry Conservation: Principles and Practice*, F. Lennard and M. Hayward, Editors. 2006, Butterworth-Heinemann: Oxford. p. 13-19.
 29. Band, J., *The survival of Henry VIII's History of Abraham tapestries: an account of how they were perceived, used and treated over the centuries*, in *Tapestry Conservation: Principles and Practice*, F. Lennard and M. Hayward, Editors. 2006, Butterworth-Heinemann: Oxford. p. 20-27.
 30. Shepard, L., *Changing approaches to tapestry conservation: the conservation of a set of seven eighteenth-century tapestries*, in *Tapestry Conservation: Principles and Practice*, F. Lennard and M. Hayward, Editors. 2006, Butterworth-Heinemann: Oxford. p. 28-36.
 31. Foskett, S., *A Brief History of the Maintenance and Care of Tapestries*, in *Tapestries from the Burrell Collection*, E. Cleland and L. Karafel, Editors. 2017, Philip Wilson Publishers: London. p. 27-33.
 32. Finch, K., *Evolution of tapestry repairs: a personal experience*, in *Seminaire international la restauration et la conservation des tapisseries.* 1984, IFROA: Paris. p. 125-132.
 33. Fusek, J., *An attempt to regain the original colour and structure of an old tapestry.* Studies in Conservation, 1964. **9**(sup1): p. 109-112.
 34. Finch, K., *Tapestries: conservation and original design*, in *The Conservation of Tapestries and Embroideries*, K. Grimstad, Editor. 1989, The Getty Conservation Institute: Marina del Rey. p. 67-74.
 35. Böttiger, J., *Les tapisseries des châteaux royaux de Suède: expériences et conseils.* 1937, Uppsala: Almqvist & Wiksells Boktryckeri.
 36. Geijer, A., *Treatment and Repair of Textiles and Tapestries.* Studies in Conservation, 1961. **6**(4): p. 144-147.
 37. Diehl, J.M., *The workshop for the restoration of ancient textiles, Haarlem*, in *Delft Conference on the Conservation of Textiles.* 1964, IIC: London. p. 105-108.

38. Pow, C.V., *The Conservation of Tapestries for Museum Display*. Studies in Conservation, 1970. 15(2): p. 134-153.
39. Marko, K., *Experiments in Supporting a Tapestry Using the Adhesive Method*. The Conservator, 1978. 2(1): p. 26-29.
40. Lodewijks, J., *The Use of Synthetic Material for the Conservation and Restoration of Ancient Textiles*. Studies in Conservation, 2014. 9(sup1): p. 79-85.
41. Marko, K., *Two case histories: a seventeenth-century Antwerp tapestry and an eighteenth-century English Soho tapestry*, in *The Conservation of Tapestries and Embroideries*, K. Grimstad, Editor. 1989, The Getty Conservation Institute: Marina del Rey. p. 95-101.
42. Molfinio, A.M. and F. Pertegato, *L'arazzo di Ester e Assuero le ragioni e i problemi di un restauro in Museo (Poldi Pezzoli)*, in *Tecniche di conservazione degli arazzi: tre giornate di studio Firenze 18-20 Settembre 1981*. 1986, Leo S. Olschki: Firenze. p. 87-91.
43. Finch, K., *Problems of tapestry preservation*, in *Tecniche di conservazione degli arazzi: tre giornate di studio Firenze 18-20 Settembre 1981*. 1986, Leo S. Olschki: Firenze. p. 39-45.
44. *1964 Delft conference on the conservation of textiles: collected preprints*. 1964, London: IIC. 153 p.
45. *Acts of the Tapestry Symposium, November 1976*. 1979, San Francisco: Fine Arts Museums of San Francisco. 223 p.
46. *Conservazione e restauro dei tessuti: Convegno internazionale. Como 1980*. 1980. Como: Edizioni C.I.S.S.T.
47. *Tecniche di conservazione degli arazzi: tre giornate di studio Firenze 18-20 Settembre 1981*. in *Convegno Internazionale di Studi sull'Ars Nova Italiana del Trecento*. 1986. Firenze: Leo S. Olschki.
48. *Seminaire international la restauration et la conservation des tapisseries, Paris 18, 19, 20 juin 1984*. 1984, Paris: Centre national des arts plastiques. 162 p.
49. *The Conservation of Tapestries and Embroideries: Proceedings of Meetings at the Institut Royal du Patrimoine Artistique Brussels, Belgium September 21-24, 1987*, ed. K. Grimstad. 1989, Marina del Rey: The Getty Conservation Institute. 117 p.
50. *'The Misled Eye...' Reconstruction and Camouflage Techniques in Tapestry Conservation*, ed. J. Barnett and S. Cok. 1996, Amsterdam: Textiel Restauratoren Overleg Nederland (TRON). 142 p.
51. Marko, K., *Textiles in trust*. 1997, London: Archetype Publications in association with the National Trust. xiii, 199 p., 24 p. of plates.
52. Kajitani, N., *Conservation maintenance of tapestries at the Metropolitan Museum of Art*, in *The Conservation of Tapestries and Embroideries*, K. Grimstad, Editor. 1989, The Getty Conservation Institute: Marina del Rey. p. 53-66.
53. Hutchison, R.B., *Gluttony and Avarice: two different approaches*, in *The Conservation of Tapestries and Embroideries*, K. Grimstad, Editor. 1989, The Getty Conservation Institute: Marina del Rey. p. 89-94.
54. Ward, S. and P. Ewer, *Tapestry Conservation at Biltmore House*. The International Journal of Museum Management and Curatorship 1988. 7: p. 381-388.
55. De Boeck, J., et al., *The treatment of two sixteenth-century tapestries at the Institut Royal du Patrimoine Artistique*, in *The Conservation of*

- Tapestries and Embroideries*, K. Grimstad, Editor. 1989, The Getty Conservation Institute: Marina del Rey. p. 113-117.
56. Dolcini, L., *The tapestries of the Sala dei Duecento in the Palazzo Vecchio*, in *The Conservation of Tapestries and Embroideries*, K. Grimstad, Editor. 1989, The Getty Conservation Institute: Marina del Rey. p. 81-87.
 57. Marko, K., *Tapestry conservation - a confusion of ideas*, in *Lining and Backing: the Support of Paintings, Paper and Textiles*. 1995, UKIC: London. p. i-iv.
 58. Barnett, R., et al., *Tapestry conservation at the Metropolitan Museum of Art*, in *Tapestry Conservation: Principles and Practice*, F. Lennard and M. Hayward, Editors. 2006, Butterworth-Heinemann: Oxford. p. 155-162.
 59. Pertegato, F., *Painting in tapestry conservation: is it heresy?*, in *'The Misled Eye...' Reconstruction and Camouflage Techniques in Tapestry Conservation*, J. Barnett and S. Cok, Editors. 1996, TRON: Amsterdam. p. 97-109.
 60. Cussell, S., *Tapestry conservation techniques at Chevalier Conservation*, in *Tapestry Conservation: Principles and Practice*, F. Lennard and M. Hayward, Editors. 2006, Butterworth-Heinemann: Oxford. p. 145-152.
 61. Lion, V. and S. Cussell, *The tapestry imposes its own treatment*, in *'The Misled Eye...' Reconstruction and Camouflage Techniques in Tapestry Conservation*, J. Barnett and S. Cok, Editors. 1996, TRON: Amsterdam. p. 81-90.
 62. Clarke, A. and F. Hartog, *The cost of tapestry conservation*, in *'The Misled Eye...' Reconstruction and Camouflage Techniques in Tapestry Conservation*, J. Barnett and S. Cok, Editors. 1996, TRON: Amsterdam. p. 69-72.
 63. Maes, Y., *The conservation/restoration of the sixteenth-century tapestry The Gathering of the Manna*, in *The Conservation of Tapestries and Embroideries*, K. Grimstad, Editor. 1989, The Getty Conservation Institute: Marina del Rey. p. 103-112.
 64. Lugtigheid, R., *The eye deceived: camouflage techniques used at the Werkplaats tot Herstel van Antiek Textiel in Haarlem*, in *'The Misled Eye...' Reconstruction and Camouflage Techniques in Tapestry Conservation*, J. Barnett and S. Cok, Editors. 1996, TRON: Amsterdam. p. 59-67.
 65. Cousens, S., *The Conservation Treatment of a Heavily Restored Fragment of a Hercules Tapestry: a Method of Approach*, in *'The Misled Eye...' Reconstruction and Camouflage Techniques in Tapestry Conservation*, J. Barnett and S. Cok, Editors. 1996, TRON: Amsterdam. p. 132-135.
 66. Mathisen, S.A., *An Excess of Metal Threads: the Techniques Used in Conservation of the Tapestry Entitled 'The Bridal Chamber of Herse'*, in *'The Misled Eye...' Reconstruction and Camouflage Techniques in Tapestry Conservation*, J. Barnett and S. Cok, Editors. 1996, TRON: Amsterdam. p. 73-80.
 67. Francis, K., et al., *Tapestries on long-term view at the Isabella Stewart Gardner Museum: a synthesis of treatment options*, in *Tapestry Conservation: Principles and Practice*, F. Lennard and M. Hayward, Editors. 2006, Butterworth-Heinemann: Oxford. p. 163-170.
 68. Reeves, P., *Alternate Methods of Hanging Tapestries*. Bulletin of the American Institute for Conservation of Historic and Artistic Works, 1973. 13(2): p. 83-98.

69. Wild, C. and A. Brutillot, *The conservation of tapestries in Bavaria*, in *Tapestry Conservation: Principles and Practice*, F. Lennard and M. Hayward, Editors. 2006, Butterworth-Heinemann: Oxford. p. 177-184.
70. Brutillot, A., *Conservation of a fifteenth-century tapestry from Franconia*, in *The Conservation of Tapestries and Embroideries*, K. Grimstad, Editor. 1989, The Getty Conservation Institute: Marina del Rey. p. 75-79.
71. Howell, D., *Some Mechanical Effects of Inappropriate Humidity on Textiles*, in *ICOM committee for conservation, 11th triennial meeting in Edinburgh, Scotland, 1996: Preprints*, J. Bridgland, Editor. 1996, James & James: London. p. 692-697.
72. Ballard, M.W., *Hanging Out Strength, Elongation and Relative Humidity: Some Physical Properties of Textile Fibers*, in *ICOM committee for conservation, 11th triennial meeting in Edinburgh, Scotland, 1996: Preprints*, J. Bridgland, Editor. 1996, James & James: London. p. 665-669.
73. Lennard, F., et al., *Strain monitoring of tapestries: results of a three-year research project*, in *ICOM-CC 16th Triennial Conference, Lisbon, 2011: Preprints*, J. Bridgland, Editor. 2012, International Council of Museums: Paris. p. 1-8.
74. Duffus, P., *Manufacture, analysis and conservation strategies for historic tapestries*, in *Faculty of Engineering and Physical Sciences*. 2013, University of Manchester.
75. Catic, E.M., *A Research Project to Measure the Effectiveness of Stitching Methods when Stabilizing Weak Areas in Tapestries*. 2019, University of Glasgow.
76. *Tapestry Conservation: Principles and Practice*. Butterworth-Heinemann series in conservation and museology, ed. F. Lennard and M. Hayward. 2006, Oxford: Butterworth-Heinemann. xxv, 247 p.
77. Marko, K., *Woven Tapestry: Guidelines for Conservation*. 2020: Archetype Publications Limited.
78. Sutherland, H. and F. Lennard, "Each to their own"? *An investigation into the spacing of laid-thread couching as used in textile conservation*. Newsletter of the ICOM Committee for Conservation, Working Group of Textiles, 2017. 39.
79. Schön, M., *The Mechanical and Supporting effect of stitches in Textile Conservation*. 2017, Göteborgs Universitet.
80. Lennard, F., *Methods of infilling areas of loss*, in *Tapestry Conservation: Principles and Practice*, F. Lennard and M. Hayward, Editors. 2006, Butterworth-Heinemann: Oxford. p. 138-144.
81. <https://www.youtube.com/watch?v=uDQSI1yJEs0>.
82. Barker, K., *Reducing the Strain: Is it worth displaying a large fragile textile at a slight angle?* Conservation news, 2002: p. 30.
83. Trosbach, G., *Physikalische Untersuchungen an historischen Tapisserien*, in *Fakultat für Architektur*. 2002, Technische Universität München.

2 Introduction to the degradation of tapestries: why it happens and how to monitor it

Chapter 2 presents a literature review on the chemical and physical properties of wool and silk, main materials within historic European tapestries. In particular, the first part of the chapter gives an overview on the degradation processes that may alter the mechanical behaviour of the two natural fibres.

The second section of the chapter focuses on past works aiming to characterise physical and chemical properties of textiles made of wool and silk, and more specifically historic hangings. Moreover, studies evaluating the efficacy of structural conservation practices for textile artworks are discussed. Particular attention is given to the outcomes from a research carried out at the University of Southampton between 2007 and 2010. The previous work was central for the development of the current project, especially for defining the analytical approach to use for studying mechanical damage mechanisms while a tapestry is hanging. In addition, works from the Monitoring of Damage in Historic Tapestries project (MODHT) were reviewed, for delineating methodologies helpful for the investigation of degradation processes affecting mechanical and chemical properties of historic hangings.

2.1 The degradation of tapestries: from the perspective of fibres

Tapestries are complex heterogeneous systems, because of the discontinuous weave structure but also because of the large number of materials involved. Therefore, predicting the behaviour over time of these works of art is very challenging.

As described in Chapter 1, historic hangings are principally made of wool and silk in the load-bearing weft direction, while wool is mostly used for the warp. Hence, the degradation of a hanging tapestry would be greatly determined by the characteristic response of wool and silk to the environment and to other ageing conditions the object would be exposed to. In the following sections the chemical and physical properties of wool and silk are discussed, highlighting factors that may affect them.

2.1.1 Wool

2.1.1.1 Chemical and physical structure

Wool is an animal hair from sheep [1]. Chemically wool can be defined as a proteinaceous polymer, as primarily made of proteins, which are natural macromolecules of high relative molecular mass (polymers). Proteins are the results of a sequence of condensed amino acids, or peptides: the general structure of proteins can be described as $-(\text{NHCHRCO})_n-$, while an amino acid is defined as $\text{H}_2\text{N}-\text{CH}(\text{R})-\text{COOH}$, where R represents the side group.

Within wool, up to 170 proteins can be found [2, 3], formed by the different sequence and relative amount of the 20 amino acids present in this material [2]. The side groups of amino acids greatly affect the physical and chemical properties of the fibres since they establish the type of links between adjacent polypeptide chains. Among amino acids in wool, cysteine (Figure 2.1a), whose side group is a thiol ($\text{R}-\text{SH}$), plays a very important role as it is predominant [2, 3]. Around 82% of the proteins within clean wool are indeed keratinous, meaning that they contain a high amount of cysteine. The reaction (oxidation) between thiols in neighbouring cysteine residues lead to the formation of covalent disulphide cross-links. Through such reaction between two cysteine molecules, cystine is formed (Figure 2.1b). The presence of cystine ultimately stabilises the matrix structure and it influences physical properties, especially in wet wool. Besides disulphide bonds, there are other chemical crosslinks, some covalent (i.e. isopeptide crosslinking) while others are non-covalent (i.e. hydrophobic interactions, ionic bonds, hydrogen bonds). All these combined interactions contribute to define the specific properties of wool [2].

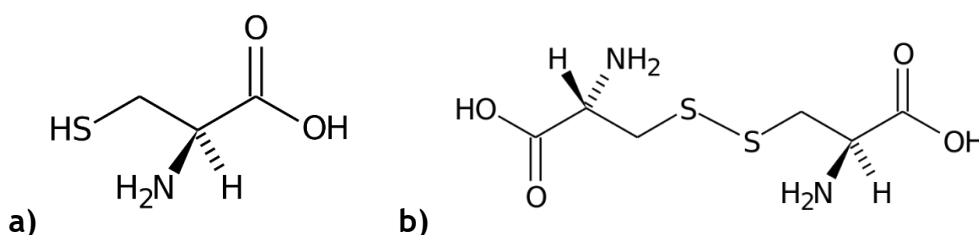


Figure 2.1. Chemical structure of: a) cysteine; b) cystine.

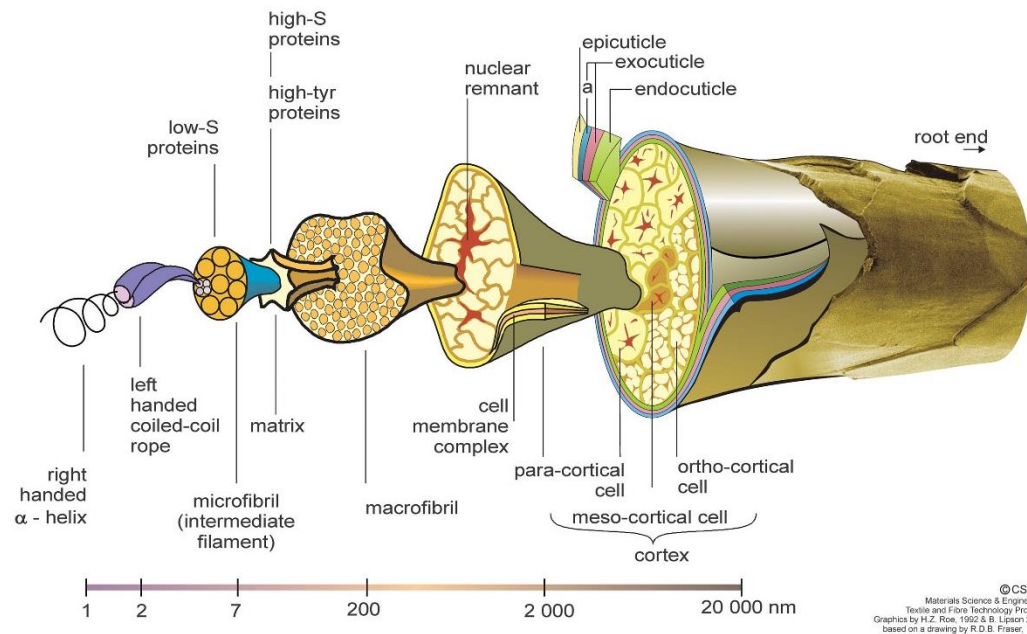


Figure 2.2. Structure of a merino wool fibre. © CSIRO.

Morphologically, wool fibres have a complex structure, as illustrated in Figure 2.2, containing principally two types of cells: the cortical (in the bulk) and the cuticle (in the external layer). In addition, specialised cells called medulla can be found in the middle of coarse wool [2, 3].

Cuticles are distributed on the surface of wool. As the cells overlap, this imparts the scale-like characteristic superficial appearance of this type of fibres. Cuticles are cystine-rich cells with a layered structure, where each layer is characterised by a different cystine content. Namely, the layers are called: epicuticle (whose nature and existence are still debated [3, 4]), exocuticle-A, exocuticle-B, endocuticle [3]. Closest to the surface, there is also a lipid layer of 18-methyleicosanoic acid (18-MEA), which makes the surface hydrophobic, affecting the wettability and consequently the dyeability of wool [3, 5].

Protected by the cuticles, there is the bulk or cortex, the inner part that composes around of the 90% of the fibre and greatly influences its mechanical properties. The cortex is constituted by cortical cells that can be divided into ortho-, para- and meso-cortical cells (the latter only present in coarse fibres). Each cortical cell consists of several macrofibrils, differently distributed according to the type of cells. Macrofibrils are cylindrical aggregations of many

crystalline microfibrils or intermediate filaments (IF). Microfibrils are rod-like filaments of α -helical low-sulfuric proteinaceous formations grouped and embedded in a relative amorphous matrix to constitute macrofibrils [3].

Another important component within wool's morphology is the cell membrane complex (CMC), that divides the cuticle cells from the bulk as well as the different macrofibrils from each other. The CMC represents only a small fraction of the total weight of the fibre (around up to 6%), however it has been of great interest because of its potential role in defining mechanical and chemical properties. The fundamental characteristic of the CMC is that it represents the only continuous phase in the fibre. The CMC is a multi-layered system whose chemical composition has not yet been clearly defined, but that perhaps includes: non-keratinous proteins, lipids, a chemically resistant membrane [3, 6, 7].

2.1.1.2 Key mechanical behaviour

From a general point of view, fibres, including wool, can be described as visco-elastic materials [8]. The strain response of visco-elastic materials to stress (where strain is the change in length, and stress the force applied per unit area or per linear density [9]) shows two time-dependent types of deformation: primary creep and secondary creep. Primary creep represents a recoverable deformation that occurs when fibres stretch and return to their original length once the force is removed (elastic region, 100% elastic recovery). After that, secondary creep takes place and the material will no longer recover completely, thus showing a viscous behaviour. The yield point marks the moment in the strain-stress curve when the behaviour switches from elastic to non-elastic [8, 9].

Among natural fibres, wool is characterised by an uncommonly high elastic recovery. As depicted in Figure 2.3, wool recovers completely at maximum 2% elongation (Hookean region), but then, after the yield point and until 30% elongation (at 57% RH) it keeps on exhibiting some elasticity [3, 10] (e.g. 63% elastic recovery at 20% elongation [11]). This unusual region between 2% and 30% elongation is sometimes called yield region [3, 10].

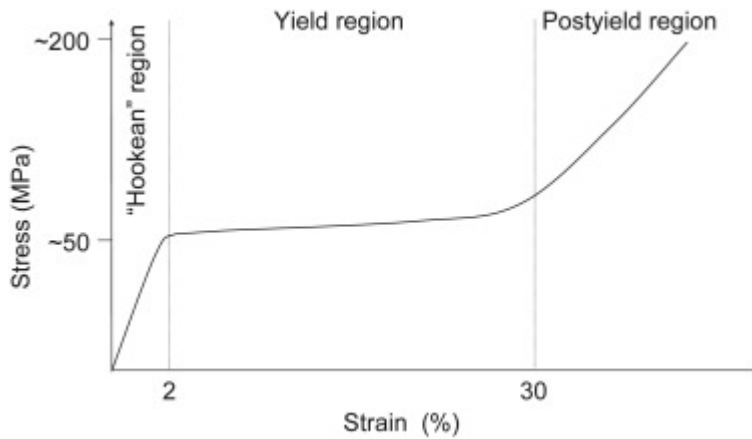


Figure 2.3. Generic stress-strain curve for wool (the x-axes is out of scale to better show the Hookean region). Taken from Huson, 2018 [3].

Besides its high elasticity, wool has a low tensile strength (when dry, the tenacity is around 1.0/1.7 gr/den [11]), especially if compared to other fibres such as silk [8, 11].

Since natural fibres are hygroscopic material, their physical behaviour (including ultimate tensile strength, but also the elastic recovery [12]) can be affected by the amount of water absorbed and so by relative humidity (RH). Therefore, it should be underlined that the water uptake is not directly proportional to RH, as the relationship between the two (illustrated by the absorption and desorption isotherms) is sigmoidal. In addition, the water content within fibres also depends on whether they experience a decrease or an increase in RH. This leads to the so-called hysteresis phenomenon, which is depicted as a divergency between the absorption and desorption isotherm [9, 13]. Finally, it should be considered that textiles may take time to reach an equilibrium with the environment [13]. Hence, the moisture content may also depend on the specific rates of absorption and desorption at different levels of RH [12].

In the case of wool, the sigmoidal relationship of the absorption isotherm means that the fibres will bind the same amount of water when the RH varies from 30% to 60% (+30% RH) as when the RH fluctuates from 82% to 92% (+10% RH) [13]. At the same time, because of hysteresis, at 65% RH (21 °C) moisture content within wool will be: 13.01% in case of absorption from dry condition, while 16.90% in case of desorption from saturation. In addition, while 2.5 hours will be needed to reach equilibrium from the absorption, the desorption will take place more slowly, precisely in 103 days [12].

Howell, in his paper dated 1996, emphasised that, also in the case of textile conservation research, great attention should be paid to the actual amount of time needed to reach the equilibrium in the moisture regain. This was confirmed by weighting for a period of six months a tapestry (supposedly made of wool) displayed in a historic house, while monitoring RH and temperature. The results demonstrated that the high fluctuations in the RH values (30-70%) caused less remarkable changes in weight (between 2-4%) than the ones expected by the literature for wool (8%). According to the author, this could have happened since the variations in RH were too rapid to actually allow the moisture content within the fibres to reach equilibrium [13].

2.1.1.3 Degradation

The effects of humidity and temperature

As just underlined, wool is a highly hygroscopic type of fibre [8, 11]. Water acts as a plasticizer for wool, promoting the mobility of molecules and therefore affecting the mechanical behaviour of the material [3]. Soaking wool can absorb an amount of water up to 200% of its dry weight, causing damaging swelling and making the material more vulnerable to mechanical changes [14].

In her PhD work, Duffus [15] attempted to better establish the effects of cycles of humidity and temperature on the mechanical strength of tapestries. To do so, the tensile strength of historic samples was evaluated and compared to that of artificially aged woollen tapestry-like mock-ups. In the case of humidity and temperature, their effects were investigated simultaneously. Indeed, the artificial ageing consisted of treating the samples at a constant temperature of 80 °C while going from 20% to 80% RH for up to 240 times. The treatment proved to negatively affect the elasticity and strength of the wool samples, though the results were not discussed extensively from a quantitative point of view. Overall, it was underlined that the historic samples were weaker than the replica [15].

As mentioned in the previous paragraph, for historic hangings made of wool fluctuations in RH values may cause changes in weight. Therefore, increases and decreases in RH (as well as the rate of these variations) should be considered

when evaluating mechanical damage, since the load experienced by displayed artworks, as well as threads sizes (swelling), may vary. Damaging mechanisms linked to RH are further discussed in Section 2.2.2.1 and in Chapter 4.

The effects of dyeing

During the dyeing process (in the case of historic tapestries, originally with natural sources) wool may undergo the damaging effects of different factors: high water uptake, high temperature, extreme and/or ranging pH, chemical reagents.

In general, dyeing usually involves treating the fibres for different hours with boiling or very hot water, decreasing already the material strength [3, 8, 11]. When the dye bath has a pH higher than 5 or lower than 4, where pH 4-5 represents the isoelectric region of wool, the mechanical strength of fibres is even more compromised [3]. From a chemical level, the degradation is caused by the breakdown of disulphide bonds in cystine ($\text{pH} > 3$) and hydrolysis of peptides amide links in both acidic ($\text{pH} 1.8-3$) and alkaline environments [16]. The damaging impact of extreme pH environments when natural dyes are used was described also by Hacke et al. [17, 18]. They analysed, by time-of-flight secondary ion mass spectrometry (ToF-SIMS) and tensile testing, the chemical (surface composition) and physical (tensile strength) properties of woollen tapestry-like samples dyed with different natural colourants. The results showed that, before ageing, very alkaline or acid baths negatively affected the samples [17, 18].

In addition, the use of certain dyes, as well as mordants, may contribute to the modification of the physical properties and rate of deterioration of wool fibres. Indeed, both dyes and mordants may lead to phototendering reactions, affecting especially elasticity and tensile strength [19]. The relationship between dyeing process and tensile properties of wool (and silk), as single fibre, yarn, and fabric, was investigated during the MODHT project [17, 18, 20, 21]. The results, summarised by Quye et al. in [20], confirmed that, also in the case of woollen tapestry-like aged and unaged samples, the tensile strength can be affected by the colourant, mordant and dyeing conditions (pH and temperature). Among all, the outcomes underlined that different mordants may have various and even

opposite effects on wool strength: while alum was found to increase the strength of the samples, oak gall mordant decreased it. The beneficial effects of alum mordant on wool was further studied and stated by Smith et al., who also showed the negative impact of other metal ion mordants [19].

Photodegradation

UV and longer wavelength radiations may cause the photodegradation of wool. Indeed, light does not only promote dye fading but more physical and chemical properties can also be affected by the exposure to it [22]. In general, depending on the wavelength distribution, the degradation process induced by electromagnetic radiation can be categorised as: photoyellowing, phototendering, and photobleaching [23-25]. Besides wavelength distribution, other factors such as temperature, humidity, pollutants, and chromophores within the fibres, influence the reaction path of the degradation process [24, 25].

Chromophores are chemical groups responsible for the photodegradation taking place in the first place, as they absorb light [24]. The radiation absorbed by chromophores promotes the excitation of the same molecules to a higher energy level. While returning to the initial ground state, the molecules release the excess energy in several ways, which may lead to chemical alteration. Indeed, the energy transfer may result in the formation of free radicals, electronically excited species or isomerisation, all eventually leading to photodegradation processes in keratin proteins such as wool [24, 26]. In the case of wool, various compounds have been recognised as responsible for the absorption of light at different wavelengths, including some constituting amino acids (e.g. tyrosine, tryptophan and cysteine [22, 23]), photodecomposition products and natural pigments [22].

Photoyellowing refers to the change in colour of wool fibres due to exposure to UV radiation (280-380 nm) [24]. This light-induced process, whose clear reaction path is still debated [27], is mainly associated with the degradation of tryptophan that reacts with the presence of atmospheric oxygen, eventually forming the yellow product kynurenine and other coloured derivatives [28].

Similarly, tyrosine also contributes to the formation of photoproducts and so to photoyellowing of wool [29].

The exposure of wool fibre to the near blue range of sunlight (mainly 400-450 nm) leads to the photobleaching effect. Yellow chromophores are responsible for the absorption of blue light that causes their degradation and conversion to uncoloured compounds. This process may affect woollen objects exposed to the daylight radiation filtered by glass windows since, while the UV radiation would be mitigated by the glass, the transmission of the blue light would be promoted [24].

Phototendering indicates the modifications of wool mechanical properties (i.e. elasticity, abrasion resistance, tensile strength) produced by light exposure [24], especially by UV wavelengths between 290-320 nm [25]. The chromophores behind this degradation process are the disulphide bond in cystine, aromatic amino acids, their yellow oxidation products, constituent dyes within undyed wool, and added dyes in artificially coloured fibres [19, 24].

2.1.2 Silk

2.1.2.1 Chemical and physical structure

Silk is a proteinaceous fibre produced by the larval form of different insect species. However, commercial silk is made from secretions of one specific species, the domesticated *Bombyx mori*, a moth originally native of China that eats exclusively mulberry [1, 8] and that has been reared since the Neolithic era [1].

Caterpillars produce silk to make their cocoon: to do so, the silkworms first secrete a liquid substance from two glands, creating two fibroin filaments that are then cemented with sericin. Both fibroin and sericin are proteins, though with a very different aminoacidic composition. When used for weaving, silk is degummed, a process that aims to clean the fibres from sericin, which would make the material stiffer and less prone to dyeing [1, 8]. In addition, silk fibres also contain a very low amount ($\approx 1\%$ respectively) of organic material (fat and wax) and colouring matter and ashes [30].

Fibroin, which makes up to 81% of silk [30], is mainly composed of three small amino acids: glycine (side group -H), alanine (side group -CH₃) and serine (side group -OH). Sequences of these three condensed amino acids result in peptides characterised by small side chains, which eventually form the crystalline regions of fibroin [8]. In these regions, polypeptide chains, linked by hydrogen bonds, have a so-called anti-parallel β -pleated sheet secondary structure (3D arrangement) [14, 30]. The sheets are then bonded together by electrostatic, hydrogen, non-polar links and van der Waals forces, creating protein molecules (tertiary structure) [30]. Each unit cell of fibroin is composed of four polypeptide chains which are aligned to the fibre axis.

Although within fibroin there are also amorphous regions made of amino acids with bulkier side groups (e.g. arginine, threonine, tyrosine), its high crystallinity and tertiary structure strongly define some properties of silk, namely: poor elongation, poor reactivity to chemicals, high tensile and tearing strength [8, 14].

2.1.2.2 Key mechanical behaviour

Like wool, silk exhibits a visco-elastic behaviour [30]. However, silk elastic recovery (after spinning) is quite low compared to that of wool: after 2% elongation, unrecoverable deformation can take place, meaning that the material will remain stretched even after stress release. Besides, the non-full elastic recovery will occur slowly [8, 11].

Just as other natural fibres, silk exhibits a sigmoidal relationship between moisture content and RH, as well as hysteresis and a different rate between the absorption and desorption processes. The sigmoidal trend of moisture regain at different levels of RH is depicted in Figure 2.4, where the hysteresis effect (divergency between absorption and desorption curve) is also evident. In comparison to wool, silk is less hygroscopic and thus it manifests a lower moisture regain [9, 13, 31, 32]. For example, silk fibres at $\approx 60\%$ RH (25 °C [31] and 35 °C [32]) will have a moisture content of around 9% because of absorption from dry condition, while up to around 10.5% due to desorption from saturation [13, 31, 32]. It should be underlined that absorption and desorption

curves may vary also depending on the type of silk, finishing processes (e.g. degumming) [31], and ageing conditions [13].

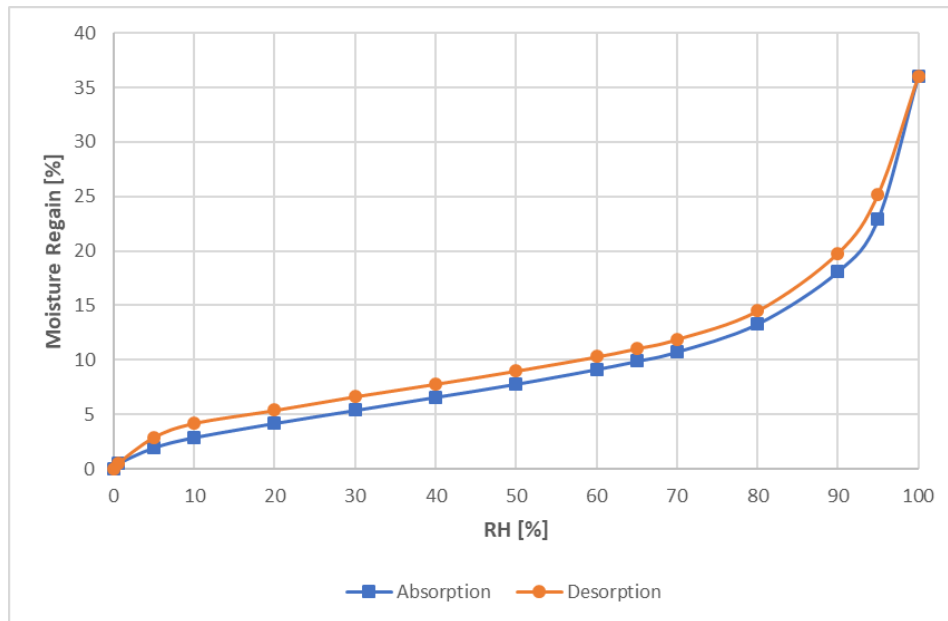


Figure 2.4. Sorption isotherms for degummed silk. The difference in the moisture content between the two curves indicates the hysteresis. Plotted data from Hutton and Gartside, 1949 [31].

Silk is a mechanically strong fibre and, as already mentioned, it exhibits both high tearing and tensile strength [8]. Indeed, tenacity is usually around 3.5-5.0 gr/den [11]. On the other hand, because of the limited elasticity, elongation at break of mulberry silk may vary between 19% to 24% in normal condition [30], and up to 33% at 100% RH [11].

2.1.2.3 Degradation

The effects of humidity and temperature

Even if silk is less hygroscopic than wool, moisture content and thus RH still play an important role in defining its condition. First of all, it should be underlined that, within the fibres, two main types of water can be distinguished depending on the interactions with silk molecules: free water (loosely bonded, e.g. by hydrogen bonds) and bound or structural water (firmly linked to the several polar groups present especially in the amorphous regions) [8, 14, 33]. The ability of silk to bond firmly to water affects its flexibility which indeed persists at 40%

RH. On the other hand, at lower values of relative humidity, silk desiccates making the material more brittle and rigid (this can also be promoted by high temperature) [8, 14]. At the same time, high levels of RH are also known to pose a threat to silk since this may lead to hydrolysis degradation processes [34].

During the last few decades, in the cultural heritage field there has been an increasing awareness that other environmental factors than light, like humidity and heat, may contribute to the high deterioration rate of silk artefacts [13, 35-37]. In the case of RH, since both high and low levels can be dangerous for silk objects, studies have been carried out to try to identify the most appropriate range for their preservation.

As for wool, Howell verified that an issue for silk is not only represented by the % of RH, but also by for how long the textile object is subjected to it. By combining accelerated ageing and mechanical testing, it was suggested that fluctuations between 30 and 60% would only lead to non-remarkable changes in silk artefacts. Contrarily, a greater reduction in the tensile strength was caused by the exposure of samples at 85% RH for six months [13]. In agreement to this, Luxford showed that high RH levels can lead to significant variations in the mechanical properties of silk. Because of this, Luxford suggested to display silk artefacts between 30 and 50% RH [36]. In partial opposition, Nilsson et al. reported that minimal mechanical modifications occurred in silk samples artificially aged at various RH levels (at 25 °C and 60 °C) for 28 days [38, 39]. In the same articles, the authors indicated that thermo-oxidation ageing for up to 56 days (125 °C, 0% RH) caused greater damage than humidity in the mock-ups (also just after 28 days). Overall, thermo-oxidation ageing promoted a level of chemical and physical degradation comparable to that of historic samples tested [38, 39].

In general, it should be underlined that heat and high temperature can lead to oxidation processes which are responsible for the formation of active free-radicals, especially from amino acids residues with hydrogen loosely bonded [14]. This thermo-oxidation process (potentially tracked by the tyrosine content) may then cause loss in tensile strength [40].

Interestingly, in the case of tapestries displayed in historic houses, where the environmental conditions may fluctuate drastically, Luxford et al. [36] reported that the RH behind the artworks and in the room might differ. In particular, the case studies showed that the RH behind the historic hangings were higher than in the rest of the room, perhaps leading to a greater damaging action to the silk fibres on the back [36].

The effects of dyeing and other related finishing treatments

Like wool, during the dyeing process, silk can experience modifications regarding both the mechanical behaviour and the chemical properties. Furthermore, in preparation for the dyeing process, silk may undergo other damaging treatments, namely degumming and the addition of weighting agents.

Degumming is the process through which sericin is removed from silk fibres, with the aim of improving texture (smoother surface) and lustre [14]. To do so, silk can be chemically treated in different ways, such as with enzymes, with boiling and soaping water, with acidic or alkaline solutions [30]. Degumming can result in a loss of mechanical strength as well as water absorption capability [14].

Due to the degumming process, silk weight can decrease up to 25%. To counterbalance this loss and so to increase the stiffness of the material, silk is often treated with weighting agents. Historically different inorganic and organic materials have been employed for weighting, such as: gum Arabic, tannins, sugar, animal glues, waxes, and metal salts [8, 14]. Sometimes weighting treatments overly augmented the original mass of silk, so that the material was unlawfully sold at a higher price [14, 41].

Tannins in combination with iron salts were commonly used, also in historic hangings [20], as weighting agents but also to dye dark shades [34]. As often reported by textile conservators, black and brown silk areas in tapestries appear to be the weakest and most degraded ones [42]: acidity and metal ions of iron-tannate dyes may indeed promote damaging acid hydrolysis and oxidation reactions. As a result of this, tensile strength may decrease and the fibres may become more brittle [43]. However, the effects of weighting on the mechanical properties may vary depending on the environmental conditions experienced

(e.g. exposure to light), the type and amount of weighting and other finishing materials present [41, 44-46].

The MODHT project investigated the effects of the dyeing process on the properties of silk, as done for the wool. The outcomes reported that, in the case of tapestry-like models made of silk, those dyed with cochineal, copper turnings and oak gall (tannins) had a lower tensile strength and stiffness compared to the undyed samples [20, 47]. It was suggested that possibly both the metal and the tannins might have contributed to make the material more vulnerable [20].

López et al. also carried out some experiments to better understand how the mechanical behaviour of cochineal-dyed silk may vary depending on the mordant and dyeing conditions used, however no precise conclusions were drawn [48]. In addition to the negative impact of the previously cited dyes, the outcomes of the MODHT project showed that silk (as well as wool) replicas dyed with woad deteriorated at a relative low rate [20]. In general, it should be noted that when silk is treated with boiling water (as historically required in some dyeing processes), damaging hydrolysis and hence rupture of the main polypeptide chain can take place, regardless of the dye [34].

Photodegradation

Among natural fibres, silk is said to be the most sensitive to light. As for wool, depending on the wavelength of the radiation silk may undergo various degradation paths [8].

UV radiation is thought to cause the greatest damage to silk, namely: yellowing, embrittlement, loss of mechanical strength. The degradation process first starts thanks to the reaction between the electromagnetic radiation and aromatic residues, which indeed absorb in the UV region (especially between 250-300 nm). Aromatic residues within silk are due to the presence of amino acids like tryptophan and tyrosine [8, 14], which also cause the photoyellowing of wool [29]. Studies on artificially aged and historic silk prove that tyrosine is particularly affected by photo-oxidation, even just considering the exposure to visible light [20, 49, 50]. The decrease in the amount of tyrosine is demonstrated to be correlated also to the loss in tensile strength in aged samples [50]. The embrittlement and loss of elasticity (phototendering) are consequences of

crosslinking reactions in the amorphous regions between activated tyrosine residues or lysine [8, 14].

As discussed in the previous section, the role of light on silk degradation was delineated and partly re-evaluated by both Luxford and Nilsson [35, 37]. Their two PhD works included accelerated ageing of silk samples exposed to different environments, to establish which factors may pose the greatest threat to historic artefacts. In both studies, photodegradation turned out to cause less remarkable chemical and physical changes than other variables, like temperature. Importantly, both UV (Nilsson's work) and visible light (Luxford's research) was observed to be less of a threat for silk than temperature [35, 37].

2.2 Evaluating the physical degradation of tapestries and the related effectiveness of conservation practices: state of the art

As introduced in Chapter 1, textile conservators still debate on the best approach to employ when preserving tapestries. Often, decisions are based on subjective ideas, perhaps influenced by the personal background, training and tradition. Therefore, the current project aims to provide objective data on the efficacy of conservation approaches for tapestries, to test how various methods may contribute to preventing mechanical degradation occurring while these artworks are on display. In this section, previous studies on methods for monitoring the physical changes (strain) in tapestries and historic textiles are presented. In particular, a previous project on tapestries conducted at the University of Southampton is described in detail, since it greatly contributed to shape the current work. Furthermore, studies focusing on the mechanical characterisation of woven hangings and on the evaluation of textile conservation treatments are also discussed.

2.2.1 The basis of the current research: the previous project at the University of Southampton (2007-2010)

2.2.1.1 The project: main aims and outcomes

The current work is based on a previous three-year study (2007-2010) carried out at the University of Southampton, led by Frances Lennard, and involving

conservators and engineers. The past research aimed to investigate whether tapestries are pulled apart by their weight and whether it would be possible to quantify the resulting strain by using engineering techniques, possibly able to detect non-visible structural damage. From the project, various articles [51-56] and conference papers [57-61] have been published, covering challenges and outcomes which arose during the work.

To start, in a pilot study the research group reviewed the available engineering methods potentially useful for monitoring displacements across historic tapestries, underlining their previous application in the cultural heritage sector [51]. Namely, the authors focused on two kinds of point strain measurements: resistance strain gauges (RSG) and optical fibre sensors (OFS). Moreover, they also considered three types of full-field measurements: photogrammetry (e.g. digital image correlation, DIC), photoelasticity, holographic/electronic speckle pattern interferometry (ESPI). Point strain measurements require sensors to be applied to the object under investigation, perhaps causing some damage or modifying the mechanical properties of the local bonded area. Because of that, Dulieu-Barton et al. concluded that whole-field measurements, which consisted of optical-based contactless systems, would be a better option for monitoring artworks. In particular, photogrammetry was reported as a promising method for the objectives of the project, as well as photoelasticity, although the latter had not been tested in conservation science at the time. On the other hand, the more widely employed ESPI was defined as likely not suitable, as it only gives qualitative data and it is too sensitive to environmental changes and vibrations [51].

The unsuitability of ESPI for the project purposes was later studied and confirmed [52]. At the same time, the feasibility of OFS, 3D DIC and thermography for the condition monitoring of tapestries was further discussed. It was then concluded that a hybrid approach, involving both photogrammetry and OFS, would be the most ideal [52, 59]. However, both OFS and DIC needed more extensive tests to demonstrate their actual reliability.

The viability of OFS (fibre Bragg grating, FBG) was studied and discussed, focusing especially on: the type of fibres (i.e. silica optical and polymer optical); how to bond the sensors to the textile; how much the bonding might modify the

properties of the fabric [52-54, 58]. Among the application methods researched (stitching, weaving through a patch, using a conservation adhesive containing PVA) at first the adhesive appeared to be the one giving a better response [52]. However, different types of conservation adhesive were used on silica based FBG and proved to significantly reinforce the fabric, indicating their unfeasibility for quantitative measurements [58].

Also in the case of DIC, more extensive testing was needed to establish if it could be used for monitoring tapestries. One of the main challenges consisted of the fact that the image-processing algorithm of the technique requires a greyscale random pattern on the surface of the object as device of correlation to track the displacement. Because of that, engineers usually artificially apply a speckle pattern (e.g. through a spray) on the surface to be monitored. As this is not possible for tapestries, DIC could only rely on the woven pattern or on the figurative design for correlation. However, tests were needed to verify that the weave gives enough contrast. Khenouf et al in [55] validated this by conducting 3D DIC analysis on four specimens (150 x 50 mm) made of a woollen representative fabric. The DIC monitoring was carried out while the samples underwent quasi-static tensile testing to then calculate longitudinal strain. On the surface of three of the specimens a different random speckle pattern was applied, while one was left without any pattern other than the inherent textile weave. The stress-strain curves of the four specimens were all shown to match, proving that the weave pattern can also be used as a device for correlation in DIC analysis, thanks to the inherent irregularities of the hand-woven structure [55].

In addition, in the initial stages of the study the DIC strain data were validated by using OFS, as the latter technique is more established and the results were considered more reliable [62]. Tests using both methods were carried out on traditional engineering materials (i.e. steel and single ply woven glass composite) and the representative textile. The results obtained were considered similar enough to demonstrate the DIC measurements can be accurate and reliable, and therefore that the contactless technique can be used alone [62].

Williams et al. in [62] also claimed the efficacy of DIC for identifying weak areas not evident to the naked eye and prone to degradation. This was proved by

simulating the effects of self-loading by using a laboratory-prepared loading frame on bespoke wool tapestry strips, woven for the project and containing structural weaknesses such as slits. Because DIC results showed areas of high strain corresponding to the structural discontinuities, the authors confirmed the ability of the technique in detecting the presence of damage even before it being visible [62].

Once the technique was better validated and the textile pattern was established to be good enough for the analysis, 3D DIC was employed to carry out more long-term monitoring tests (minimum 48 hours). As summarised in [56], monitoring tests were performed on both the representative textile [55, 62] and actual tapestries (some newly woven, while others historic) [55, 60, 61], also *in situ* [61]. Among the main outcomes, the experiments revealed a clear linear relationship between strain and RH. This demonstrated how greatly tapestries may experience fatigue due to RH fluctuations, together with “creep strain” perhaps due to self-loading [56]. It should be noted that the authors used the term *creep* to specifically define a permanent deformation, even the expression refers to a time-dependent deformation that can also be recoverable [9].

The research group used the direct proportionality between strain and RH to first attempt defining a mathematical model able to predict the strain response of a given tapestry to the humidity fluctuations. Indeed, it is important to underline that the results of the monitoring showed that each test had a different equation stating the linearity between strain and RH. According to the research group, perhaps this was due to differences in the storage/display conditions, and so to the RH range experienced in the past, as well as to the characteristic features of each tapestry [60]. Considering all these variables, the empirical model was built on the simple equation:

$$\xi_{x,y} = k_{x,y} \text{ RH}$$

where ξ is the strain, RH the relative humidity, and k a constant calculated from the experimental data. K values differed from test to test according to the properties of the monitored tapestry (e.g. mass, materials), although in an unclarified way [60, 61].

At the end of the project, the research questions were considered answered, at least partially. The initial research question wondered whether tapestries are pulled apart by their own weight and the results demonstrated that they are strained by a complex mix of creep (responsible for permanent deformations) and fatigue due to RH fluctuations (reversible deformations) [61]. Besides, the project aimed to define whether it would be possible to quantify strain across tapestries using an engineering technique, and the outcomes determined that DIC can be employed. Furthermore, DIC was found to be able to provide quantitative measurements, at least when analysing small areas [61].

2.2.1.2 Critical evaluation of the research

Despite the project showing through extensive work that great confidence can be put on the 3D DIC strain monitoring of tapestries, some characteristic experimental conditions employed by the research group prevented to generally state the viability of the method. In addition, some of the testing conditions are not fully described in the published works, jeopardising the repeatability of the experiments.

For instance, before moving to actual tapestries, the monitoring techniques were tested on a representative fabric, which was reported to have a tapestry-like weave structure [52]. The fabric was shown to have similar mechanical behaviour of that of woven hangings, although this was demonstrated by comparing the textile with newly woven tapestry samples, and not with historic ones [55]. The fabric was employed in different tests with various objectives, including confirming the viability of the weave pattern as a device for correlation in DIC analysis [55]. However, in the published works the authors failed to specify in detail the fabric used, preventing adequate repeatability of the tests: the manufacturer is never reported and it is unclear whether the fabric is weft-faced (as implied by the results in [52, 55, 56]) or warp-faced (as described in [54]). The latter feature is particularly important for the comparison with historic tapestries as they are weft-faced and hung in the weft direction, meaning that, when on display, strain affects mainly the threads responsible for the figurative pattern.

Besides, regarding the long-term monitoring tests conducted on actual tapestries, the research group considered only an individual and small area of the object (around 10 cm² [55, 60], although the dimensions are not reported for all the experiments). Therefore, the full-field application of the DIC technique was never evaluated by the previous study. It is important to underline this as the size of the monitored area affects the resolution of the images and so the contrast essential for the DIC to operate (see Chapter 4). This means that monitoring a tapestry in its entirety may involve more methodological challenges than in the case studies reported.

Regarding the described linear relationship between RH and strain data, the authors did not properly report and/or consider some important features of wool (and perhaps silk) fibres, of which the monitored objects were made. Indeed, as already discussed, natural fibres, thus including wool, exhibit a sigmoidal and not linear relationship between moisture regain % and RH. Moreover, moisture desorption and adsorption rate may differ, making the increase in weight due to water uptake, and so strain variation, even more difficult to predict [9]. Therefore, it should have been better specified that a linear relationship between RH and strain could only take place between certain ranges of RH (perhaps the ones experienced in the tests). Considering this, the mathematical model proposed by the research group to predict the behaviour of historic hangings at different humidity levels would probably be inaccurate and not properly representative [60]. In general, the pieces of information gathered on the strain response to RH variations seem unable to build a model, as suggested by the same authors [61].

2.2.1.3 Future work suggested by the research

Considering the further work welcomed and suggested by the research team, they underlined the need to investigate more in depth the impact of the cycling in RH on the materials degradation. Eventually, this would enable to better distinguish the effects of creep from those caused by changes in environmental conditions [55]. Therefore, enriching the knowledge on the mechanical degradation processes affecting tapestries while on display is considered fundamental.

Another main aspect that needs to be more extensively researched is how to use DIC to efficiently monitor strain across the entire surface of full-size tapestries, and not only on a small area [56, 61]. Furthermore, when moving to the *in situ* monitoring, other practical challenges should be addressed. For instance: would it be possible to only use one camera instead of two, thus conducting a 2D DIC analysis instead of a 3D one?

In addition, one of the main objectives of the past project was to establish whether, through the selected engineering technique, it would have been possible to identify “invisible” weak areas, before the appearance of actual damage. Although eventually DIC was stated to be able to accomplish that, it was proved only for structural discontinuities, such as slits, that are actually evident [61]. Therefore, it would be interesting to challenge and evaluate more extensively the potentiality of DIC, by testing whether also actual invisible weak areas can be located.

Importantly, by validating DIC as a non-invasive tool for strain monitoring across textiles, it was assessed that the technique can be useful for comparing the effectiveness of different conservation treatments [56]. This entire field of research was therefore welcomed by the research group in Southampton, but left untried.

2.2.2 Other works

2.2.2.1 Researching the mechanical behaviour and degradation of tapestries

Different publications deal with the characterisation of the mechanical behaviour of historic tapestries, some focusing on the effects of the heterogeneities in the structure [63, 64] (also from a chemical point of view [20]), some studying in particular the impact of RH [13, 15, 65].

The most extensive work researching many of these aspects is represented by Duffus’ PhD thesis, *Manufacture, Analysis and Conservation Strategies for Historic Tapestries*, submitted in 2013 at the University of Manchester [15]. Through her work, Duffus carried out a comparison between accelerated and natural ageing on the properties (physical and chemical) of tapestries and tapestry-like woven samples. Duffus’ research evaluated the damaging impact of

the selected factors (light, temperature, RH, strain) both on fibres and small-scale textile samples. The results indicated the difficulty in simulating through artificial ageing the condition of the naturally aged objects: the samples from actual tapestries proved to be always in a weaker state than the mock-ups. This demonstrated that an intricate mix of factors (including RH and temperature) contribute over time to the material degradation. Finite element analysis (FEA) was employed to create a macro-model able to estimate stress concentration across a hanging tapestry, also when some structural heterogeneities such as slits are present. The FEA model presented does not describe extensively the mechanical behaviour of tapestries as it is too simple, however it is reported as a useful first trial to develop. Considering the initial objectives of the thesis, the work wanted also to investigate the effects of different conservation practices, especially support methods. To gather information on the common trends spread worldwide, a questionnaire was sent to 116 workshops (receiving back 28 completed forms). Although the questionnaire was useful in illustrating various common approaches, their efficacy was not further tested [15].

The tensile mechanical behaviour of samples from actual historic tapestries was investigated by Máximo Rocha et al. in 2018, who combined tensile testing with 2D DIC strain monitoring [64]. The samples presented some structural differences, including thickness, thread counts, presence/lack of slits, type and distribution of fibre materials. The physical properties of the historic samples proved to be affected by all these factors. In addition, a good correlation was observed between the results from DIC and tensile testing, validating the monitoring technique, at least in the studied experimental approach [64].

In a similar way to Máximo Rocha et al. (though without including DIC), already in 1997 Bilson et al. carried out tensile testing on samples taken from five actual historic tapestries with different features. The results confirmed that structural heterogeneities, such as the presence of open slits, may reduce significantly the tensile strength (if the slits are stitched, the effects are less dramatic) [63]. Besides, indirectly the tensile testing also showed the influence of the dye on the mechanical behaviour of the tapestry samples: blue wool specimens were found to be remarkably stronger than yellow ones [63]. As better discussed in

Chapter 3, the impact of the dyeing process on the physical properties of tapestries was later studied more extensively through the MODHT project [20].

Physical properties and the effects of changes in RH on historic textiles, including tapestries, were also researched by Bratasz et al. [65], Howell [13] and Ballard [9, 12]. Ballard in 1996 provided a glossary and literature review on the topic, underlining the need of increasing the knowledge on the mechanical behaviour of textiles among conservators [9, 12]. On the other hand, experiments to verify the actual implications of moisture content fluctuations on tapestries are reported by Bratasz et al. [65] and Howell [13]. In both works, tests were carried out to establish the moisture content and changes in size (expansion and shrinkage) caused by climate fluctuations on different fabric samples. The two articles demonstrated the non-linear but sigmoidal relationship between RH and moisture content in the fibres (and so strain) and the influence of the hysteresis effect [13, 65]. In addition, Howell, also after monitoring a woollen tapestry for six months, stressed the importance of always considering the time needed for the moisture content to reach equilibrium. Indeed, potentially dangerous fluctuations in weight may also depend on this, rather than just on the humidity conditions [13]. Similarly, also Bratasz et al. aimed to investigate how the mechanical properties of textiles can be affected by humidity fluctuations. To do this, specimens from various textiles, including tapestries, were subjected to cycles of strain by mechanical stretching. This sought to simulate the impact of humidity cycles on the fabrics, potentially responsible for friction between adjacent threads (fretting fatigue). The outcomes established that the (simulated) fretting fatigue does not cause a significant mechanical degradation. In the same article, this was also confirmed by the contained expansion (0.05%) registered after monitoring strain across an historic tapestry for a year by using silica FBG with ceramic coating [65]. It should be noted that no details are reported in the article on the sizes of the historic hanging [65], so it is not possible to quantify the actual dimensional changes.

2.2.2.2 Testing the efficacy of conservation techniques for tapestries

A small number of works focused on the evaluation of tapestry conservation practices, at least from the perspective of the mechanical properties [63, 66-

68]. Bilson et al., in their paper dated 1997, focused on the effects of linings (meaning support fabrics) on hanging textiles such as tapestries [63]. In the first part of the publication, the approach used is theoretical and based on a simplified mathematical model of a tapestry. The calculations made from the model suggested that tapestries in good condition should experience an amount of stress too low to cause any significant damage, as also confirmed by the tensile tests on historic samples reported in the second part of the publication. This implies that full support treatments may not be needed, while instead patches can be used to support only weak areas (e.g. open slits or areas made of silk) [63].

Asai et al. in [66] assessed the efficacy of different conservation stitching systems for attaching full support fabrics to tapestries. To do so, the tensile strength of unaged tapestry samples with slits and/or conservation treatments was evaluated and compared. The outcomes outlined that full interventive conservation (linen full support, stabilising lines, and close couching on the slit) was the most effective treatment, as it decreased the most the elongation near the slit. However, other less interventive approaches also seemed to make the samples stronger. As underlined by the authors, the experiments were only carried out on newly unaged woven tapestry samples, so they cannot directly prove the efficacy of the methods on historic weak objects [66].

Hofenk de Graaff et al., besides conducting a questionnaire on conservation approaches for tapestries [69], carried out some experiments aiming to compare the mechanical behaviour of the two most widespread fabrics used for support treatments, i.e. linen and cotton [67]. Prior to the mechanical characterisation, some of the textile samples were pre-treated (cleaned) as usually done by textile conservators. After this, some of both untreated and treated specimens were artificially aged at different ranges of temperature and humidity. Eventually, the textile samples were uniaxially tensile tested. The results underlined that the mechanical response of both cotton and linen were similarly affected by the ageing (comparable loss of ultimate tensile strength and elongation at break). When considering the effects of pre-treatment, linen became weaker than cotton, while, for both, an increase in the elongation at break was recorded [67].

Catic's masters dissertation from 2019 focused on the evaluating of brick and laid couching when used to treat weak areas in tapestries [68]. To do so, unaged wool rep samples, with some artificially made weak areas, were conserved using both techniques, at different spacing. To compare the efficacy of the stitching in preventing the propagation of mechanical damage, 2D DIC was used to monitor strain across the mock-ups, to which an extra load was added at the bottom. Some of the outcomes were difficult to interpret as the monitoring set-up likely affected the accuracy of the analysis. However, in general it was observed that laid couching seemed to provide the most support, and that the spacing of the stitches influenced the level of strain reduction [68].

From a broader perspective, in the textile conservation field, tensile testing was employed by Nilsson for the evaluation of support methods, although applied to silk historic costumes [37, 70]. In addition, some studies focused on testing the supporting effects of different stitching techniques, always from a general point of view, not limited to tapestries [71-73]. Benson et al. in [71] researched the influence of thread types, synthetic and natural, when used for laid couching on fabrics (made of different natural fibres) through both tensile testing and fixed-load experiment. The results showed that the strength of the treated specimens depended more on the physical structure than on the chemical composition of the threads [71]. Following Benson's research, Sutherland and Lennard [72] investigated the impact of spacing on laid couching, namely when applied on a cotton fabric. They employed fixed-load experiments and DIC to quantify the relative increase/decrease in strength due to different spacing. DIC was only used for few specimens and, although described as promising, no details are reported on the measured strains and on the experimental conditions, at least in the published work [72]. Similar fixed-load experiments to test the consolidating effects (measured as dimensional variations) of brick and laid couching on damaged silk specimens were carried out by Schön [73]. In general, the cited studies described fixed-load testing as a potential accelerated ageing tool to simulate the effects of self-weight loading.

2.3 Relating the physical and chemical degradation of tapestries: state of the art

As described in the previous paragraphs, the mechanical behaviour of natural fibres is strictly related to their chemical composition. Indeed, physical degradation is often linked, or at least promoted, by reactions that occur on a molecular level.

Considering tapestries, as already mentioned, the Monitoring of Damage in Historic Tapestries (MODHT) project greatly contributed to understand which factors may promote the strength loss of wool and silk in historic hangings. The project, which ran between 2002 and 2005, involved conservation scientists and curators from seven European institutions. The different research groups focused on the viability of various analytical techniques for identifying markers of physical and chemical change in wool and silk fibres, so as to track their degradation. To do so, the different methods were first tested on bespoke small-scale models, woven and dyed using methods deriving from traditional ones. The response of the models to accelerated light ageing (no other parameters were considered) was assessed by the selected techniques, while markers able to illustrate the degradation of the proteinaceous fibres were identified. Tensile testing was carried out alongside the different chemical analyses to prove that the deterioration on a molecular level can be associated to tensile properties. After the inspection of the replicas, samples taken from historic tapestries from European collections (English, Spanish and Belgian) were similarly inspected and so the results compared. It is important to underline that only historic threads, and not fragments, were mechanically characterised; this prevented to evaluate, alongside chemical degradation, the influence of structural features in the weave. From a general perspective, at the end of the project it was observed that: I) the data gathered from (the majority of) the different types of analysis showed good correlation, stating the reliability of the analytical methods tested and of the degradation markers; II) the models, even after light ageing, were in better conditions than the historic samples. Furthermore, the influence of the dyeing process on the physical and chemical properties of wool and silk samples was assessed [20].

In the following paragraphs, the successful analytical techniques employed during the MODHT project are presented, together with their main results. In addition, other methods used in other studies with similar objectives (connecting the physical properties of fibres to chemical markers) are also illustrated. It should be noted that the techniques described are all invasive, at least within the context of the considered studies, meaning that they require a sample to be analysed.

2.3.1 Tracking chemical degradation in historic wool

X-ray photoelectron spectroscopy (XPS)

During the MODHT project XPS was employed for the investigation of wool surface of model/historic aged/unaged samples. XPS allows to gather information on both elements and functional groups present on the surface of fibres (quantitative data and distribution). In the context of the MODHT project, this method was found to be able to trace wool degradation by considering as a marker the relative increase in ratio of oxidised surface sulphur. Indeed, oxidation causes the break of disulphide bonds of cystine, leading to the drop of the non-oxidised sulphur content and the growth of oxidised forms [17, 21].

Attenuated total reflectance Fourier transform infrared spectroscopy (ATR-FTIR)

ATR-FTIR was employed during the MODHT project to identify markers of chemical degradation in keratinaceous fibres. Since thread samples were needed to be collected to allow the analysis, in this case, the approach used can be defined as micro-invasive. Like for the other analytical approaches tested, the study, carried out by Odlyha et al., combined the characterisation of weft samples from actual hangings as well as unaged/aged, dyed/undyed models. Through the research, the peak of cysteic acid (chemical structure in Figure 2.5) was found to be a suitable marker to establish the level of chemical degradation in wool. Indeed, due to oxidation processes, cystine was shown to be greatly converted into cysteic acid, whose characteristic ATR-FTIR peak (at 1040 cm^{-1}) increased during the ageing, proving its viability as marker. Among the outcomes, the influence of different dyeing processes and materials on wool degradation was observed [74]. The outcomes agreed with the data gathered

from the analysis with other methods employed during the MODHT project [20]. It should be underlined that a similar approach to that proposed by Odlyha et al. [74] had been employed before by other researchers aiming to study wool degradation, but not for investigating textile artworks [75, 76].

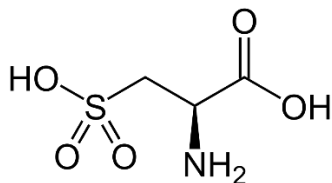


Figure 2.5. Cysteic acid.

More recently, ATR-FTIR analysis was employed by Kissi et al. for validating non-invasive near infrared spectroscopy (NIR) as a tool to define the oxidation level of wool in historic tapestries. From the outcomes gathered, it was concluded that the approach proposed was not fully successful in predicting the level of chemical degradation on actual historic hangings when conducting the analysis *in situ* [77].

Time-of-flight secondary ion mass spectrometry (ToF-SIMS)

ToF-SIMS can be used for investigating chemical features of fibre surface, offering elemental data alongside a mass spectral analysis. When employed during the MODHT project for investigating chemical modifications in wool, the outcomes demonstrated that the technique could track some superficial changes due to the effects of both natural and artificial ageing. Namely, ToF-SIMS was observed to give an indication of the condition of wool fibres based on the detected amount of surface lipid (in wool, mainly represented by 18-MEA), since degradation processes can cause a drop in the lipid content on the surface. Through the study of mock-ups and historic tapestries, it was observed that the 18-MEA content can decrease because of light exposure as well as because of damaging initial treatments of the fibres (i.e. dyeing processes involving extreme pH) [17, 18].

Amino acid analysis

Within the context of the MODHT project, Vanden Berghe studied the efficacy of calibrated amino acid analysis as a tool for detecting degradation of wool (and silk) fibres at molecular level due to oxidation reactions [49, 50]. To do so, high performance liquid chromatography with fluorescence detection was employed on historic/model samples. The micro-invasive technique was selected as it enables the identification of composition of proteins on a sub-microgram level. The method demonstrated that it was useful for tracking changes in wool and so to define degradation markers [50]. In the case of wool, the oxidation of keratin showed to impact especially the amount of tyrosine and cysteine (decrease). Besides these two amino acids, the so-called “Keratin Oxidation Factor” (KOF) was found to be a useful indicator of the oxidation level of wool. KOF is calculated as the ratio between the molar fractions of amino acids that, during ageing, tend to lower (i.e. lysine, histidine, tyrosine, methionine) over the ones that generally augment (i.e. aspartic, glutamic and cysteic acids). Interestingly, the discovered markers highlighted that iron and copper salts used as mordants may promote degradation. The outcomes from the amino acid analysis agreed with the data gathered from the tensile testing, proving the correlation between chemical and mechanical degradation [50].

2.3.2 Tracking chemical degradation in historic silk

ATR-FTIR

Different studies employed ATR-FTIR (and more broadly FTIR) for investigating chemical degradation in historic silk artworks [38, 39, 78-81]. In general, past works pinpoint that the band between 1700-1775 cm^{-1} should be monitored when evaluating the level of degradation in silk. This band corresponds to the vibration of C=O group and it increases with degradation (oxidation). In addition, peaks related to tyrosine (at 828 and 850 cm^{-1}) were found to give some insights on the degradation process, as they are expected to decrease with natural ageing [38, 39].

Amino acid analysis

As done for wool, Vanden Berghe studied the changes in the aminoacidic composition of silk tapestry models and historic samples to detect potential markers indicating the damaging oxidative breakdown process. In the case of silk fibres, tyrosine was found to be the only amino acid useful as an early indicator of chemical degradation. Indeed, the content of tyrosine was found to decrease during the ageing treatments and it was shown to be correlated, on a macroscopic level, to the loss in tensile strength of aged samples [50]. Vilaplana et al. similarly carried out amino acid analysis on unaged/aged models of silk and historic silk pieces, though not tapestries [38]. They also reported that tyrosine content dropped during the accelerated UV light ageing, as well as after the thermo-oxidative treatment. On the other hand, ageing at 100% RH and at extreme alkaline/acidic environments did not cause a detectable change in the tyrosine amount [38].

Size exclusion chromatography (SEC)

SEC can be used to measure the molecular weight distribution of silk fibres. This can give an indication of the level of degradation of the material since the deterioration of silk leads to the breakage of the polymer chain. The breakage determines the formation of shorter polymers with a lower, and thus recognisable, molar mass. During the MODHT project, SEC analysis confirmed what was also observed with the other techniques: overall, the accelerated light ageing did not promote a degradation as extended as that of silk samples taken from historic hangings [20, 82]. Similar results were also obtained by Nilsson's research on historic silk [38, 39]. As underlined by Hallett and Howell in [82], SEC analysis can only be employed for monitoring chemical degradation in silk (as also reported by Thickett et al. [83]), not in wool. Indeed, the technique requires the samples to be dissolved and, while this can be accomplished by using a mild solvent with silk (thanks to the weak hydrogen structural bonds), in the case of wool a stronger solvent would be needed to break the stronger structural covalent links. This may cause the breakage of the polymer chain, and so compromise the outcomes of the analysis [82].

2.4 Conclusions: objectives and analytical approach of the current study

The literature review presented in Chapter 1 and Chapter 2 were helpful for defining which areas, within the study of historic tapestries, still need to be further investigated for ensuring a proper preservation of the textile artworks. Namely, the following broad research questions were identified as central and were selected for the project:

- 1) Which factors affect the structural stability of tapestries and how successfully can they be investigated by using analytical tools?
- 2) What are the mechanical degradation processes affecting tapestries while hung for their display?
- 3) How effectively can the structural stability of tapestries be improved using different display methods and conservation strategies?

More specifically, the current work aimed to fill the following knowledge gaps encountered in the literature review:

- 1) To what extent the level of chemical degradation occurring within fibres affect the physical properties of tapestries? Does the weave structure play a role? Can the relationship between chemical and physical properties be studied directly on fragments from actual historic hangings, following up the work started through the MODHT project? Can the analysis of warp threads, unexposed to light, provide new insights on the degradation processes?
- 2) In Southampton, 3D DIC was shown to be a suitable tool for tracking strain across relatively small areas, but can it be employed to monitor larger areas, and different kinds, of historic textiles? If so, what type of information should be expected, would it be actually possible to track “invisible” weaknesses? Which factors affect the accuracy of the analysis? Can DIC be used for evaluating conservation strategies?

- 3) Can sloping boards effectively prevent the elongation of tapestries? Which factors may contribute to the efficacy of the system? When considering conservation treatments, how the use support and stitching techniques may differently affect strain distribution in a textile object while hanging?

Through a review of past studies on the degradation of tapestries, Chapter 2 allowed to delineate the multi-analytical approach for answering the research questions. Based on the previous works, the experimental part of the thesis was designed as it follows:

- 1) For evaluating different factors affecting the structural stability of tapestries, mechanical and chemical testing was carried out on different historic tapestry fragments. For verifying the mechanical behaviour of specimens, uniaxial tensile testing was employed. In addition, samples were chemically characterised through ATR-FTIR and UHPLC-PDA. Namely, following the approach proposed during the MODHT project, ATR-FTIR was used for tracking chemical degradation in wool, while dye sources in the same historic threads were identified through UHPLC-PDA analysis. Wool samples were studied more in detail than silk ones, as tapestries, and in particular those investigated, are mainly made of wool. It should be highlighted that here ATR-FTIR was selected among a broader range of methods, as just discussed in Section 2.3. ATR-FTIR was chosen as it was demonstrated to be highly informative, well-established, straightforward (no need of pre-treatments), non-destructive, as well as the most accessible method, at least within the context of the current project. Although UHPLC-PDA analysis is ineffective in tracking markers of chemical degradation, it was included as it represents the most widespread technique for the characterisation of dyestuffs in textiles. Identifying dyes was defined as relevant since they may play a role in the degradation processes of fibres. The multi-analytical characterisation of samples from historic tapestries is described in Chapter 3.
- 2) For studying mechanical damage mechanisms occurring in tapestries while on display, DIC was used. The technique was further trialled, implementing the work started at the University of Southampton. Importantly, instead of employing 3D DIC, the 2D application of the

optical technique was tested, as it represents an easier and less expensive option, especially for *in situ* monitoring. The study on 2D DIC feasibility for tracking strain across textile objects is presented in Chapter 4.

- 3) When validating display and conservation approaches, these were tested first on (woollen) mock-ups, so to ensure reproducibility and to simplify the behaviour of historic hangings, which may differ from object to object. To speed up the propagation of mechanical damage, fixed-load experiments were carried out on the bespoke samples, while strain was tracked through DIC. In combination to the contactless technique, uniaxial tensile testing was used for further investigating the impact of stitching and support techniques. The experiments on the efficacy of sloping boards, an untraditional but increasingly popular display method, are discussed in Chapter 5. Among the current conservation approaches for improving structural stability in woven hangings, the most widespread in Europe, i.e. patch/full support and laid/brick couching, were evaluated as reported in Chapter 6.

References

1. Phipps, E., *Looking at textiles : a guide to technical terms*. 2011, Los Angeles, Calif.: J. Paul Getty Museum. vi, 94 p.
2. Rippon, J.A., *The Structure of Wool*, in *The Coloration of Wool and other Keratin Fibres*, D.M. Lewis and J.A. Rippon, Editors. 2013, John Wiley & Sons in association with the Society of Dyers and Colourists Bradford. p. 1-42.
3. Huson, M.G., *Properties of wool*, in *Handbook of properties of textile and technical fibres*, A.R. Bunsell, Editor. 2018, Elsevier Ltd. p. 59-103.
4. Swift, J.A. and J.R. Smith, *Microscopical investigations on the epicuticle of mammalian keratin fibres*. *Journal of Microscopy*, 2001. **204**(3): p. 203-211.
5. Negri, A.P., H.J. Cornell, and D.E. Rivett, *A Model for the Surface of Keratin Fibers*. *Textile Research Journal*, 1993. **63**(2): p. 109-115.
6. Leeder, J.D., D.G. Bishop, and L.N. Jones, *Internal Lipids of Wool Fibers*. *Textile Research Journal*, 1983. **53**(7): p. 402-407.
7. Bryson, W.G., et al., *The Cell Membrane Complex of Wool*. 1992, Wool Research Organisation of New Zealand.
8. Timár-Balázsy, A.g. and D. Eastop, *Chemical principles of textile conservation*. 1998, London: Routledge. 480 p.
9. Ballard, M.W., *How backings work: the effect of textile properties on appearance in Lining and backing: the support of paintings, paper and textiles. Papers delivered at the UKIC Conference, 7-8 November 1995*. 1995, United Kingdom Institute for Conservation of Historic and Artistic Works: London. p. 34-39.
10. Hearle, J.W.S., *A critical review of the structural mechanics of wool and hair fibres*. *International Journal of Biological Macromolecules*, 2000. **27**: p. 123-138.
11. Cook, J.G., *Handbook of textile fibres*. 5th ed. 2001, Cambridge: Woodhead Publishing Limited. 205 p.
12. Ballard, M.W., *Hanging Out Strength, Elongation and Relative Humidity: Some Physical Properties of Textile Fibers*, in *ICOM committee for conservation, 11th triennial meeting in Edinburgh, Scotland, 1996: Preprints*, J. Bridgland, Editor. 1996, James & James: London. p. 665-669.
13. Howell, D., *Some Mechanical Effects of Inappropriate Humidity on Textiles*, in *ICOM committee for conservation, 11th triennial meeting in Edinburgh, Scotland, 1996: Preprints*, J. Bridgland, Editor. 1996, James & James: London. p. 692-697.
14. May, E., et al., *Conservation science: heritage materials*. 2006, Cambridge: Royal Society of Chemistry.
15. Duffus, P., *Manufacture, analysis and conservation strategies for historic tapestries*, in *Faculty of Engineering and Physical Sciences*. 2013, University of Manchester.
16. Lewis, D.M., *Damage in wool dyeing*. *Review of Progress in Coloration and Related Topics*, 1989. **19**(1): p. 49-56.
17. Hacke, M., et al. *Investigation into the Nature and Degradation of Historical Wool Tapestries*. in *11th International Wool Textile Research Conference*. 2005. Leeds, UK.
18. Batcheller, J., et al., *Investigation into the nature of historical tapestries using time of flight secondary ion mass spectrometry (ToF-SIMS)*. *Applied Surface Science*, 2006. **252**(19): p. 7113-7116.

19. Smith, G.J., I.J. Miller, and V. Daniels, *Phototendering of wool sensitized by naturally occurring polyphenolic dyes*. Journal of Photochemistry and Photobiology A: Chemistry, 2005. **169**(2): p. 147-152.
20. Quye, A., et al., *'Wroughte in gold and silk' : preserving the art of historic tapestries*. 2009, Edinburgh: NMS Enterprises Limited-Publishing. viii, 134 p.
21. Hacke, A.M., *Investigation into the Nature and Ageing of Tapestry Materials*, in *Faculty of Engineering and Physical Sciences*. 2006, University of Manchester
22. Davidson, R.S., *The photodegradation of some naturally occurring polymers*. Journal of Photochemistry and Photobiology B, 1996. **33**: p. 3-25.
23. Smith, G.J., *New Trends in Photobiology (Invited Review): Photodegradation of keratin and other structural proteins*. Journal of Photochemistry and Photobiology B, 1995. **27**: p. 187-198.
24. Millington, K.R., *Photoyellowing of wool. Part 1: Factors affecting photoyellowing and experimental techniques*. Coloration Technology, 2006. **122**(4): p. 169-186.
25. Milligan, B., *The Degradation of Automotive Upholstery Fabrics by Light and Heat*. Review of Progress in Coloration and Related Topics, 1986. **16**(1): p. 1-7.
26. Feller, R.L., *Accelerated Aging: Photochemical and Thermal Aspects*. 1994, United States of America: The J. Paul Getty Trust.
27. Millington, K.R., *Photoyellowing of wool. Part 2: Photoyellowing mechanisms and methods of prevention*. Coloration Technology, 2006. **122**(6): p. 301-316.
28. Schäfer, K., D. Goddinger, and H. Höcker, *Photodegradation of tryptophan in wool*. Journal of the Society of Dyers and Colourists, 1997. **113**(12): p. 350-355.
29. Dyer, J.M., S.D. Bringans, and W.G. Bryson, *Characterisation of photo-oxidation products within photoyellowed wool proteins: tryptophan and tyrosine derived chromophores*. Photochemical & Photobiological Sciences, 2006. **5**(7): p. 698-706.
30. Murugesh Babu, K., *Silk: processing, properties and applications*. 2013, Cambridge: Woodhead Publishing in association with the Textile Institute. 264 p.
31. Hutton, E. and J. Gartside, *The Moisture Regain of Silk i. Adsorption and Desorption of Water by Silk at 25° C*. Journal of the Textile Institute Transactions, 1949. **40**(3): p. T161-T169.
32. Wiegerink, J.G., *The Moisture Relations of Textile Fibres at Elevated Temperatures*. Textile Research, 1940. **10**(9): p. 357-371.
33. Yazawa, K., et al., *Influence of Water Content on the B-Sheet Formation, Thermal Stability, Water Removal, and Mechanical Properties of Silk Materials*. Biomacromolecules, 2016. **17**(3): p. 1057-1066.
34. Luxford, N., *Silk durability and degradation*, in *Understanding and improving the durability of textiles*, P.A. Annis, Editor. 2012, Woodhead Publishing: Oxford; Philadelphia. p. 205-232.
35. Luxford, N., *Reducing the Risk of Open Display: Optimising the Preventive Conservation of Historic Silks*, in *Faculty Of Law, Arts & Social Sciences*. 2009, University of Southampton.
36. Luxford, N., D. Thickett, and P. Wyeth. *Applying preventive conservation recommendations for silk in historic houses*. in *Proceedings of the joint*

- interim conference. Multidisciplinary conservation: a holistic view for historic interiors*. 2010. Rome: ICOM-CC.
37. Nilsson, J., *Ageing and conservation of silk*. 2015, University of Gothenburg.
 38. Vilaplana, F., et al., *Analytical markers for silk degradation: comparing historic silk and silk artificially aged in different environments*. Analytical and Bioanalytical Chemistry, 2015. **407**: p. 1433-1449.
 39. Nilsson, J., et al., *The Validation of Artificial Ageing Methods for Silk Textiles Using Markers for Chemical and Physical Properties of Seventeenth-Century Silk*. Studies in Conservation, 2010. **55**(1): p. 55-65.
 40. Zhang, X., I. Vanden Berghe, and P. Wyeth, *Heat and moisture promoted deterioration of raw silk estimated by amino acid analysis*. Journal of Cultural Heritage, 2011. **12**(4): p. 408-411.
 41. Hacke, M., *Weighted silk: history, analysis and conservation* Studies in Conservation, 2008. **53**(sup2): p. 3-15.
 42. *Tapestry Conservation: Principles and Practice*. Butterworth-Heinemann series in conservation and museology, ed. F. Lennard and M. Hayward. 2006, Oxford: Butterworth-Heinemann. xxv, 247 p.
 43. Wilson, H., C. Carr, and M. Hacke, *Production and validation of model iron-tannate dyed textiles for use as historic textile substitutes in stabilisation treatment studies*. Chemistry Central Journal, 2012. **6**(1): p. 44.
 44. Miller, J.E.R., Barbara M., *Degradation in Weighted and Unweighted Historic Silks*. Journal of the American Institute for Conservation, 1989. **28**(2): p. 97-115.
 45. Appel, W.D. and D.A. Jessup, *Accelerated ageing test for weighted silk*. Journal of Research of the National Bureau of Standards, 1935. **15**: p. 601-608.
 46. Ballard, M.W., R.J. Koestler, and N. Indictor, *Weighted silks observed using energy dispersive X-ray spectrometry*. Scanning electron microscopy, 1986(II): p. p. 499-506.
 47. Odlyha, M., et al., *Thermal Analysis of Model and Historic Tapestries*. Journal of Thermal Analysis and Calorimetry, 2005. **82**: p. 627-646.
 48. Fuster López, L., et al., *Effects of mordants on the mechanical behaviour of dyed silk fabrics: preliminary tests on cochineal dyestuffs*. Arché, 2007. **2**: p. 115-120.
 49. Vanden Berghe, I. and J. Wouters, *Identification and condition evaluation of deteriorated protein fibres at the sub-microgram level by calibrated amino acid analysis*, in *Scientific Analysis of Ancient and Historic Textiles: Postprints*. 2005, Archetype Publications Ltd.: London. p. 151-158.
 50. Vanden Berghe, I., *Towards an early warning system for oxidative degradation of protein fibres in historical tapestries by means of calibrated amino acid analysis*. Journal of Archaeological Science, 2012. **39**(5): p. 1349-1359.
 51. Dulieu-Barton, J.M., et al., *Deformation and strain measurement techniques for the inspection of damage in works of art*. Reviews in Conservation 2005. **6**: p. 63-73.
 52. Dulieu-Barton, J.M., et al., *Assessing the feasibility of monitoring the condition of historic tapestries using engineering techniques*. Key Engineering Materials, 2007. **347**: p. 187-192.

53. Ye, C.C., et al., *Applications of polymer optical fibre grating sensors to condition monitoring of textiles*. Journal of Physics: Conference Series 2009. **178**: p. 012020.
54. Ye, C.C., et al., *Condition monitoring of textiles using optical techniques*. Key Engineering Materials, 2009. **413-414**: p. 447-454.
55. Khennouf, D., et al., *Assessing the Feasibility of Monitoring Strain in Historical Tapestries Using Digital Image Correlation*. Strain, 2010. **46**(1): p. 19-32.
56. Lennard, F. and J.M. Dulieu-Barton, *Quantifying and visualizing change: Strain monitoring of tapestries with digital image correlation*. Studies in Conservation, 2014. **59**(4): p. 241-255.
57. Khennouf, D., et al., *Application of digital image correlation to deformation measurement in textile*, in *Photomechanics 2008: International Conference on Full-Field Measurement Techniques and their Applications in Experimental Solid Mechanics*. 2008: Loughborough, UK.
58. Dulieu-Barton, J.M., et al. *Optical fibre sensors for monitoring damage in historic tapestries*. in *XIth International Congress on Experimental and Applied Mechanics*. 2008. Orlando, USA.
59. Lennard, F., et al., *Progress in strain monitoring of tapestries*, in *ICOM Committee for Conservation. Triennial meeting, 15th, New Delhi, India, 2008*, J. Bridgland, Editor. 2008, Allied Publishers Pvt. Ltd. p. 843-848.
60. Dulieu-Barton, J.M., et al. *Long term condition monitoring of tapestries using image correlation*. in *Society for Experimental Mechanics (SEM) Annual Conference*. 2010. Indianapolis, USA.
61. Lennard, F., et al., *Strain monitoring of tapestries: results of a three-year research project*, in *ICOM-CC 16th Triennial Conference, Lisbon, 2011: Preprints*, J. Bridgland, Editor. 2012, International Council of Museums: Paris. p. 1-8.
62. Williams, H.R., et al., *Application of digital image correlation to tapestry & textile condition assessment*, in *Proceedings of AIC Textile Specialty Group*. 2009. p. 156-170.
63. Bilson, T., D. Howell, and B. Cooke, *Mechanical Aspects of Lining 'Loose Hung' Textiles*, in *Fabric of an exhibition: an interdisciplinary approach. Preprints 1997*, Canadian Conservation Institute: Ottawa. p. 63-69.
64. Máximo Rocha, P., D. D'Ayala, and C. Vlachou-Mogire, *Methodology for tensile testing historic tapestries*. IOP Conference Series: Materials Science and Engineering, 2018. **364**: p. 012003.
65. Bratasz, L., et al., *Risk of Climate-Induced Damage in Historic Textiles*. Strain, 2015. **51**(1): p. 78-88.
66. Asai, K., et al., *Tapestry conservation traditions: an analysis of support techniques for large hanging textiles*, in *15th Triennial Conference New Delhi*. 2008: New Delhi. p. 967-975.
67. Hofenk de Graaff, J.H., F. Boersma, and W.G.T. Roelofs, *Tapestry Conservation (Part III Scientific Research 'Linen versus Cotton')*. 1998.
68. Catic, E.M., *A Research Project to Measure the Effectiveness of Stitching Methods when Stabilizing Weak Areas in Tapestries*. 2019, University of Glasgow.
69. Hofenk de Graaff, J.H., *Tapestry Conservation: Support Methods and Fabrics*. 1997.
70. Nilsson, J., et al., *Evaluation of stitched support methods for the remedial conservation of historic silk costumes*. e-conservation Journal, 2015(3).

71. Benson, S.J., F. Lennard, and M.J. Smith, *'Like-With-Like': A Comparison of Natural and Synthetic Stitching Threads used in Textile Conservation*, in *ICOM Committee for Conservation (ICOM-CC). Triennial meeting, 17th, Melbourne, Australia, 2014: Preprints*, J. Bridgland, Editor. 2014, The International Council of Museums: Paris.
72. Sutherland, H. and F. Lennard, *"Each to their own"? An investigation into the spacing of laid-thread couching as used in textile conservation*. Newsletter of the ICOM Committee for Conservation, Working Group of Textiles, 2017. 39.
73. Schön, M., *The Mechanical and Supporting effect of stitches in Textile Conservation*. 2017, Göteborgs Universitet.
74. Odlyha, M., C. Theodorakopoulos, and R. Campana, *Studies on woollen threads from historical tapestries*. Autex Research Journal, 2007. 7(1): p. 9-18.
75. Jones, D.C., C.M. Carr, and W.D. Cooke, *Investigating the Photo-Oxidation of Wool Using FT-Raman and FT-IR Spectroscopies*. Textile Research Journal, 1998. 68(10): p. 739-748.
76. Carr, C.M. and D.M. Lewis, *An FTIR spectroscopic study of the photodegradation and thermal degradation of wool*. Journal of the Society of Dyers and Colourists, 1993. 109(1): p. 21-24.
77. Kissi, N., et al., *Developing a non-invasive tool to assess the impact of oxidation on the structural integrity of historic wool in Tudor tapestries*. Heritage Science, 2017. 5(49).
78. Garside, P., S. Lahlil, and P. Wyeth, *Characterization of Historic Silk by Polarized Attenuated Total Reflectance Fourier Transform Infrared Spectroscopy for Informed Conservation*. Applied Spectroscopy, 2005. 59(10): p. 1242-1247.
79. Koperska, M.A., et al., *Degradation markers of fibroin in silk through infrared spectroscopy*. Polymer Degradation and Stability, 2014. 105: p. 185-196.
80. Koperska, M.A., T. Łojewski, and J. Łojewska, *Evaluating degradation of silk's fibroin by attenuated total reflectance infrared spectroscopy: Case study of ancient banners from Polish collections*. Spectrochimica Acta Part A: Molecular and Biomolecular Spectroscopy, 2015. 135: p. 576-582.
81. Badillo-Sanchez, D., et al., *Understanding the structural degradation of South American historical silk: A Focal Plane Array (FPA) FTIR and multivariate analysis*. Scientific reports, 2019. 9(1): p. 1-10.
82. Hallett, K. and D. Howell, *Size exclusion chromatography of silk: inferring the tensile strength and assessing the condition of historic tapestries*, in *ICOM Committee for Conservation. Triennial meeting, 14th, The Hague, Netherlands, 2005: Preprints*, I. Verger, Editor. 2005, James & James/Earthscan: London. p. 911-919.
83. Thickett, D., N. Luxford, and P. Lankester. *Environmental Management Challenges and Strategies in Historic Houses*. in *The artifact, its context and their narrative: multidisciplinary conservation in historic house museums* 2012. Los Angeles: ICOM-CC.

3 Characterisation of physical and chemical properties of historic tapestries

Chapter 3 aimed to define the physical and chemical properties of historic tapestries and to highlight factors that may affect them. To gather information on the mechanical behaviour, specimens taken from seven historic hangings were uniaxially tensile tested. In addition to the data gathered on Young's modulus and tensile strength, ATR-FTIR and UHPLC-PDA analysis were carried out on threads taken from the same historic samples. ATR-FTIR was used as a tool to define chemical deterioration of wool due to cystine oxidation, following the method applied to tapestries first proposed by Odlyha et al. [1]. On the other hand, UHPLC-PDA was employed to identify the natural dye sources within the woollen samples, to observe whether the dyeing process may have contributed to the degradation. This multi-analytical approach intended to follow up findings from the MODHT project [2], as discussed in Chapter 2. Importantly, the characterisation of tapestries reported in this chapter considered the influence of more variables than those evaluated in the past works from the MODHT project and others. For instance, the impact of structural differences in the weave structure on the mechanical response was also evaluated.

In addition to the specimens from actual tapestries, a wool rep fabric with similar weave structure was uniaxially tensile tested. Evaluating the physical properties of the newly woven fabric was needed as the textile was employed in the following chapters for assessing the efficacy of conservation and display methods.

While the choice of the techniques was justified in Section 2.4, the experimental design of Chapter 3 is described in Table 3.1.

Table 3.1 Experimental design of Chapter 3.

Hypothesis	Case studies	Techniques	Methodological limits
The weave structure affects the tensile properties of historic tapestries	37 samples (warp and weft direction) from 7 historic tapestries with different weave patterns	Uniaxial tensile testing	Due to the contained number of samples, the applicability of the outcomes can be limited; the small areas of fragments available determines a reduction in size and number of specimens tested (in comparison to what indicated by British Standard)
The newly hand-woven wool rep fabric has a mechanical behaviour similar to that of historic tapestries and, therefore, it can be employed as a representative material for testing conservation strategies	Samples from the wool rep fabric (5 per direction, weft and warp)	Uniaxial tensile testing	Besides the potential similar physical properties, the wool rep fabric will still show differences when compared to historic tapestries (e.g. lack of ageing and lower areal density)
The amount of CA can indicate the level of chemical degradation of wool threads from historic tapestries and it can help identifying factors responsible for such degradation	30 wool thread samples (warp and weft directions) from 7 historic tapestries	ATR-FTIR	Due to the contained number of samples, the applicability of the outcomes can be limited
The dye source affects the tensile properties of wool threads in historic tapestries	12 differently coloured wool thread samples (weft direction) from 7 historic tapestries.	UHPLC-PDA	Due to the contained number of samples, the applicability of the outcomes can be limited


3.1 Materials and methods

3.1.1 Historic tapestry fragments




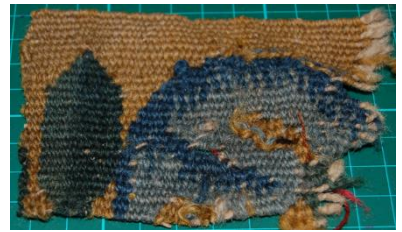


Samples from seven different tapestry fragments, belonging to the Karen Finch Reference Collection (study collection based at the CTCTAH, no information on provenance, date or history of the objects), were tested to define chemical and physical properties. The historic fragments are reported in Table 3.2, alongside some structural features, namely: thread count, fibre composition, thickness and areal density. At first, the fibre composition was assessed through a visual examination, also involving light microscopy, and then verified through ATR-FTIR analysis.

Depending on the type of analysis, the samples taken from the seven historic pieces were selected according to specific characteristics, such as colour (HPLC-PDA and ATR-FTIR analysis) and presence/absence of heterogeneities in the weave structure (tensile testing). This allowed the consideration of the influence of more variables in the properties of the specimens, expanding the research carried out within the context of the MODHT project and by other more recent studies (revised in Section 2.2 and 2.3). Important differences from the approach employed in the previous studies are: I) actual historic fragments were tensile tested, instead of bespoke mock-ups and artificially aged yarns/fibres [2, 3]; II) the impact of the meso-structural elements in the weave, e.g. thread count, were evaluated alongside the chemical features [2, 4-6].

Table 3.2. Historic tapestries tested.

Code	Thread count per 10 mm (warp x weft) ¹	Fibre materials (warp; weft)	Average thickness [mm]	Areal density [Kg/m ²]	Image
T1	7 x 18	Wool; wool, silk	0.99	0.73	

¹ A thread counter was used and the measurement was repeated in three different sites. The data from the inspection of three sites in each fragment were eventually averaged.

T2	7 x 32	Wool; wool, silk	1.16	0.81	
T3	4 x 14	Wool; wool	1.24	0.88	
T4	5 x 14	Wool; wool, silk	1.12	0.90	
T5	5 x 12	Wool; wool	1.12	0.58	
T6	7 x 26	Wool; wool, silk	1.21	0.77	
T7	7 x 20	Wool; wool, silk	1.14	0.80	

3.1.2 Newly woven wool rep fabric

In addition to samples cut from historic hangings, specimens from a hand-woven wool rep (or ribbed weave) fabric were uniaxially tensile tested. As described in

the following chapters, the fabric was later employed to create replicas for studying the efficacy of conservation and display approaches. The tensile tests presented here aimed to ensure a certain proximity in the mechanical response between the newly woven textile and tapestries.

The contemporary rep fabric was supplied by Context Weavers and it was selected as it is the most similar, and commercially available, textile to tapestries. It should be noted that requesting to produce a new tapestry fabric was not considered as a valuable option, as the process would have been too expensive and slow, and likely unable to create a textile with identical features to those from naturally aged tapestries. Important common features between the wool rep and historic hangings are the meso-structure, described as a plain-weave (depicted in Figure 3.1), and the use of wool as a constituent material. The wool rep has a thread count of 8 wefts X 23 warps per 10 mm, and an areal density of 0.41 kg/m². Besides the lower areal density, as illustrated in Figure 3.2, the newly woven wool rep differs from historic hangings as it is warp-faced instead of being weft-faced. This means that the contemporary material is made of tightly twisted warp threads and bulky weft yarns, whereas tapestry weave has opposite features, tightly twisted weft threads and bulky warp yarns.



Figure 3.1. Weave structure of the wool rep fabric (59x magnification).

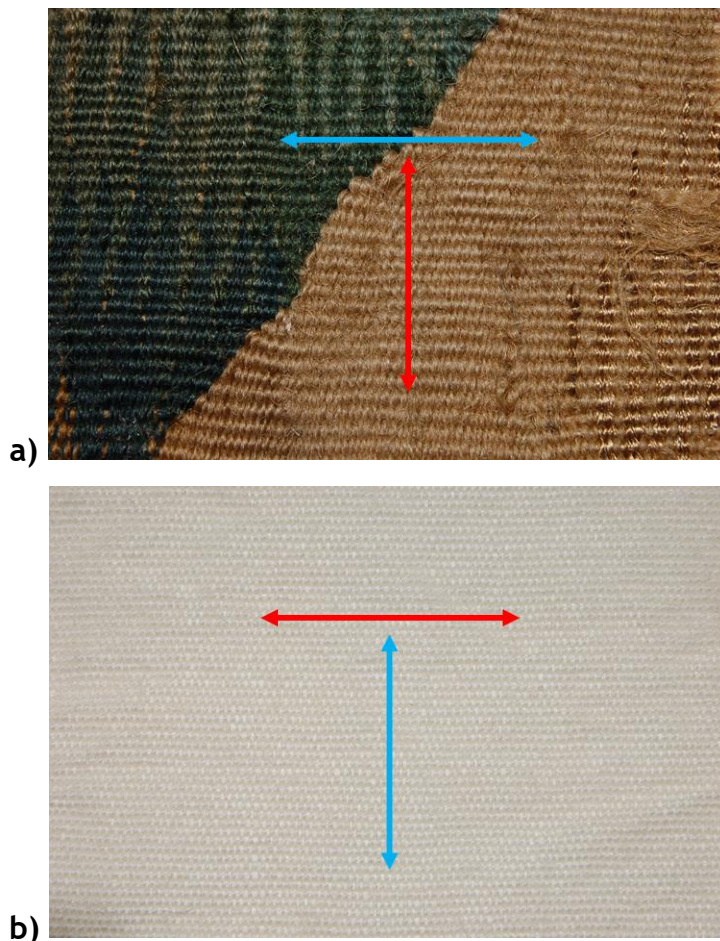


Figure 3.2. Detail of the weave structure of the historic tapestry fragment T6 (a) and the wool rep fabric (b). In both figures, the red arrows indicate weft direction, while the blue arrows warp direction. Historic tapestries are hung in the weft direction.

The use of the newly woven fabric for testing conservation and display methods ensured different advantages, including the possibility of applying a speckle pattern and assuring the repeatability of the experiments. As discussed in Chapter 4, applying a speckle pattern on the specimens was beneficial during the DIC processing stage.

Furthermore, the wool rep textile was selected in accordance with previous tests carried out by the research group at the University of Southampton. During the past project, a wool rep fabric was employed for tensile testing and preliminary DIC trials. The fabric used for this thesis is thought to be the same employed in Southampton, however, since no details on the supplier are reported in the past published works [7-10], this cannot be surely stated.

3.1.3 Uniaxial tensile testing

Uniaxial tensile testing was performed on historic tapestry samples using an Instron 5544 mechanical tester, according to the British standard [11]. The tester was attached to a hydraulic pump to ensure proper closure of the clamps and it was fitted with a 1kN loadcell. To avoid the slippage of the textile specimens, rubber coated jaw faces were employed. Testing was done in a controlled environment of $20.0 \pm 2^\circ \text{C}$ and $50.0 \pm 5\% \text{ RH}$, where all the samples were conditioned for at least 24 hours prior to the analysis. Tests were carried out at an extension rate of 10 mm/min. As previously indicated, the thickness of the specimens was measured with a digital micrometre (three measurements per sample).

In total, 37 samples were tested, as reported in Table 3.3. As illustrated in Table 3.3, the samples were from seven historic fragments (already described in Table 3.2) and they presented features, such as the weave pattern, that could impact the mechanical response. As mentioned in Section 3.1.1, studying the effects of structural features on the physical behaviour represents an important difference from previous studies. Indeed, in the case of the MODHT project, only the effects of dyeing processes and artificial ageing were evaluated on mock-ups [2]. Indeed, it should be underlined that few studies up to now have carried out tensile testing on actual tapestry fragments [4, 5, 12].

The uniaxial tensile properties of samples were verified in both the weft and warp direction and, from each fragment, at least two specimens per direction were investigated. The specimens were around 40 x 10 mm, thus five times smaller than standard recommendations (200 x 50 mm) [11]. Reducing dimensions and number of specimens was needed considering the limited size of the historic pieces. It should be underlined that the chosen samples were almost exclusively made of wool; a very limited amount of silk threads was present in a few of the pieces. This strategy allowed to direct the investigation towards the degradation of wool, so as to better link the results to those from the other analytical techniques. It is important to underlined that the tensile testing allowed to gather data expressed as load and extension. Since load and extension depend on the size of the specimen, they were converted into stress and strain, not affected by sizes and so more easily comparable. Stress was

calculated as load divided by cross-sectional area of the sample. Strain was measured as the ratio of deformed length to original length.

Table 3.3. Specimens from the historic fragments characterised through uniaxial tensile testing.

Tapestry Code	Direction	Sample Code	Weave pattern
T1	Warp	T1_Wa1	Homogeneous
		T1_Wa2	Homogeneous
		T1_Wa3	Heterogeneous, circular pattern
		T1_Wa4	Heterogeneous, circular pattern
	Weft	T1_We1	Homogeneous
		T1_We2	Homogeneous
		T1_We3	Heterogeneous, triangular pattern
		T1_We4	Heterogeneous, triangular pattern
T2	Warp	T2_Wa1	Heterogeneous, stripes in weft direction
		T2_Wa2	Heterogeneous, stripes in weft direction
	Weft	T2_We1	Heterogeneous, stripes in weft direction
		T2_We2	Homogeneous
		T2_We3	Heterogeneous, stripes in weft direction
		T2_We4	Heterogeneous, stripes in weft direction
T3	Warp	T3_Wa1	Heterogeneous, stripes in weft direction
		T3_Wa2	Heterogeneous, stripes in weft direction
		T3_Wa3	Heterogeneous, stripes in weft direction
	Weft	T3_We1	Homogeneous
		T3_We2	Homogeneous
T4	Warp	T4_Wa1	Homogeneous
		T4_Wa2	Homogeneous
	Weft	T4_We1	Homogeneous
		T4_We2	Homogeneous
		T4_We3	Homogeneous
		T4_We4	Homogeneous
T5	Warp	T5_Wa1	Homogeneous
		T5_Wa2	Homogeneous
	Weft	T5_We1	Homogeneous
		T5_We2	Heterogeneous, diagonal slit
T6	Warp	T6_Wa1	Homogeneous
		T6_Wa2	Heterogeneous, hatching weft direction
	Weft	T6_We1	Heterogeneous, hatching weft direction
		T6_We2	Heterogeneous, hatching weft direction
T7	Warp	T7_Wa1	Heterogeneous, stripes in weft direction
		T7_Wa2	Heterogeneous, stripes in weft direction
	Weft	T7_We1	Heterogeneous, diagonal slit
		T7_We2	Heterogeneous, diagonal slit

As mentioned in the previous paragraph, specimens from the wool rep fabric were also uniaxially tensile tested. The newly woven samples were characterised using the same equipment and conditions selected for the analysis of the historic fragments just described. Thanks to the larger availability of wool rep fabric, the measurements were repeated five times per direction (weft and warp), and using samples of the actual size indicated by the standard, 200 x 50 mm.

3.1.4 ATR-FTIR

Warp and weft samples, around 5 mm long, were collected from the tapestry fragments before the mechanical characterisation for enabling the analysis with ATR-FTIR. Samples and codes are reported in Table 3.4. It is important to underline that, differently from the MODHT project, warp samples were included in this study. After the non-destructive analysis, some of the coloured weft samples were further investigated using UHPLC-PDA, as also indicated in Table 3.4.

The analysis was carried out using a Perkin Elmer Spectrum One FTIR Spectrometer with a Universal Sampling Attenuated Total Reflectance accessory, a diamond/thallium bromoiodide (C/KRS-5) ATR crystal with a penetration depth of up to 2 μm , and Spectrum software version 5.0.1. The spectra were collected over the region of 4000-400 cm^{-1} , at a resolution of 4 cm^{-1} , and averaging 32 scans. The samples were held on the ATR using a clamping force of approximately 50 N. The spectra were analysed using Bio-Rad Laboratories KnowItAll® software, Windows version 10.0.15063. Each spectrum was viewed as absorbance mode. For each sample the analysis was repeated three times, and the resulting spectra were averaged using the software. The averaged spectra were baseline corrected and normalised at the peak high of Amide III at 1232 cm^{-1} and then processed to obtain the second derivate spectra. From the second derivate spectra, areas of peak at 1232 cm^{-1} and 1040 cm^{-1} were calculated. The spectral processing procedure just described was based on the method used in other works, also for studying tapestries [1, 6, 13].

Table 3.4. Samples from the historic fragments analysed through ATR-FTIR. As indicated, some of the samples were also analysed through UHPLC-PDA.

Tapestry code	Direction	Sample Code	Sample Colour	UHPLC-PDA
T1	Warp	T1_Wa	White, likely undyed	
	Weft	T1_We.DBrown	Dark brown	X
		T1_We.Yellow	Yellow	X
		T1_We.LBrown	Light brown	
		T1_We.Red	Red	
		T1_We.YellowS	Yellow	
		T1_WeWhiteS	White	
T2	Warp	T2_Wa	White, likely undyed	
	Weft	T2_We.DBrown	Dark brown	X
		T2_We.Red	Red	X
		T2_We.LBrown	Light brown	
		T2_We.Pink	Pink	
		T2_WeWhiteS	White	
T3	Warp	T3_Wa	White, likely undyed	
	Weft	T3_We.Brown	Brown	X
		T3_WeBlack	Black	X
T4	Warp	T4_Warp	White, likely undyed	
	Weft	T4_We.Beige	Beige	X
		T4_We.BeigeS	Beige	
T5	Warp	T5_Wa	White, likely undyed	
	Weft	T5_We.Beige	Beige	X
		T5_We.Blue	Blue	X
		T5_We.Green	Green	
T6	Warp	T6_Wa	White, likely undyed	
	Weft	T6_We.Beige	Beige	X
		T6_We.BeigeS	Beige	
T7	Warp	T7_Wa	White, likely undyed	
	Weft	T7_We.Purple	Purple	X
		T7_We.Beige	Beige	X
		T7_We.BeigeSM	Beige	

3.1.5 UHPLC-PDA

A Waters® ACQUITY UPLC H-Class system was employed for identifying marker compounds related to dye sources in historic samples (Table 3.4). The UHPLC equipment, belonging to the CTCTAH, was controlled by ACQUITY UPLC Console

and it included: a sample manager, a temperature-controlled column, a quaternary-solvent manager, a PDA detector. Through the auto-sampler system, for each analysis a fixed volume of 4 μl was taken from the extract and injected into a pre-column, eventually leading to the column. The pre-column, a C18 BEH shield Van Guard (5 mm \times 2.1 mm I.D., particle size 1.7 μm), aimed to avoid particulates contaminating the column, a shielded Waters C18 Ethylene Bridged Hybrid (BEH) (150 mm \times 2.1 mm I.D., particle size 1.7 μm).

The mobile phase eluents were: 10% methanol (v/v) in ultrapure water as solvent A; pure methanol as solvent B; 1% formic acid (v/v) in ultrapure water as solvent C. The following programme was used for the elution: 0-1.33 min 80% A, 10% B, 10% C; 1.33-2.33 min linear gradient to 74% A, 16% B, 10% C; 2.33-5.33 min linear gradient to 55% A, 35% B, 10% C; 5.33-9 min held at 55% A, 35% B, 10% C; 9-14 min linear gradient to 30% A, 60% B, 10% C; 14-25 min linear gradient to 5% A, 85% B, 10% C; 25-26 min linear gradient to 100% B; 26-30 min held at 100% B; 30-32 min linear gradient to 80% A, 10% B, 10% C; 32-40 min held at 80% A, 10% B, 10% C. During the 40-min elution gradient, the flow was set at 0.2 ml/min and the column temperature at 40 °C. The same gradient has been previously used at the CTCTAH for characterising dye sources in historic textiles [14, 15].

Data collection and examination were carried out through Empower 3 software system from Waters®. Spectral data were collected in the range 200 to 800 nm and with a resolution of 1.2 nm. At first, the data were processed at 254 nm, a useful wavelength to reveal the presence of dye-related compounds. Then, depending on the colour of sample/extract and/or possible dye sources, chromatograms were acquired at other wavelengths, to ensure that the characteristic markers were detected.

The marker compounds were identified thanks to specific UV-Vis absorbance spectra and retention time (RT). To allow a proper characterisation, spectra and RT of main components detected in the extracts were compared with those from reference materials (analysed in the same conditions), within UHPLC-PDA software libraries. These libraries have been enriched and employed during other projects at the CTCTAH [14-16].

3.1.5.1 Extraction method

The standard extraction method for historic textile samples developed and used at the CTCTAH [15, 17] was employed in the current work (samples are reported in Table 3.4). The method consists of the following steps. First, the sample (consisting of threads with maximum length of 5 mm) was treated with 50 μl of DMSO at 80 °C for 10 min. Then, the extract was transferred and stored into a new vial, while 75 μl of oxalic acid solution were added to the sample. The vial containing the sample was heated for 15 min at 80 °C; after, the new extract was evaporated to dryness using a Rotavapor (6-8 bar for around 30 min). At this point, the DMSO extract was placed back in the vial with the sample to reconstruct the dried residue. Using a micropipette, the combined extract was transferred on the tip of a filter placed on a syringe and eventually injected into a teardrop vial insert.

3.2 Results and discussion

3.2.1 Uniaxial tensile testing

3.2.1.1 Samples from historic tapestry fragments

Uniaxial tensile testing was carried out on the historic tapestry samples to determine the general mechanical behaviour and related properties, namely Young's modulus and tensile strength. Tensile testing tapestry fragments is often not possible, as it is difficult to find samples of a useful size to carry out valid destructive analysis. Because of this, only few studies in the past were able to test specimens from actual artworks [4, 5, 12]. In this research the advantage was to access the study reference collection at the CTCTAH, so as to enrich knowledge on the mechanical properties of historic hangings.

From a general perspective, the shape of the stress-strain curves of historic samples presented some common features, with some differences between warp and weft directions. The results gathered agreed with what was reported by previous studies on tapestries (historic and newly woven) [2-5, 18], and, more broadly, with the mechanical behaviour of wool illustrated in Chapter 2. Figure 3.3 depicts the typical shape of stress-strain curves obtained. Namely, in Figure 3.3 the graphs of samples T1_Wa1 (warp direction) and T1_We1 (weft direction)

are shown. Both samples were taken from the same historic piece, T1, they were made of wool and had a homogeneous weave pattern.

As illustrated in Figure 3.3, initially stress-strain curves presented a plateau, also indicated as a slack region [19]. The plateau was due to samples adjusting before actual tension took place and to the de-crimping of threads. This region was greater in tapestry samples tested in the weft direction, probably because weft threads were crimped during the weaving and they were tightly twisted. Once de-crimping ended, specimens showed an elastic behaviour. Generally speaking, in the elastic, or Hookean, region, stress and strain are directly proportional and reversible deformations occur. The slope of the linear regression calculated in the elastic region indicates the Young's modulus [4, 5]. Young's modulus relates to the stiffness of the material: the greater the slope, the greater the stiffness. Nevertheless, it is noted that the term *stiffness* differs from *stiffness modulus*. Indeed, the former property depends on the sizes of the tested specimen, while the latter (modulus) is unaffected by them [20].

As discussed later in detail, different factors could affect the modulus in the studied textiles. However, it can be stated that typically tapestry weft samples were more flexible than warp ones. After the elastic region, irreversible deformations started: from this moment on, specimens could no longer return to the original length. As described in Chapter 2, the so-called yield point indicated the end of the elastic behaviour and the beginning of the (mainly) inelastic one [21]. Eventually, stress began to decrease because of the progressive failure of threads. As also shown by Figure 3.3, the breaking point of each of the seven warp threads of sample T1_Wa1 (blue line) was evident: every drop in stress values corresponds to the failure of a thread.

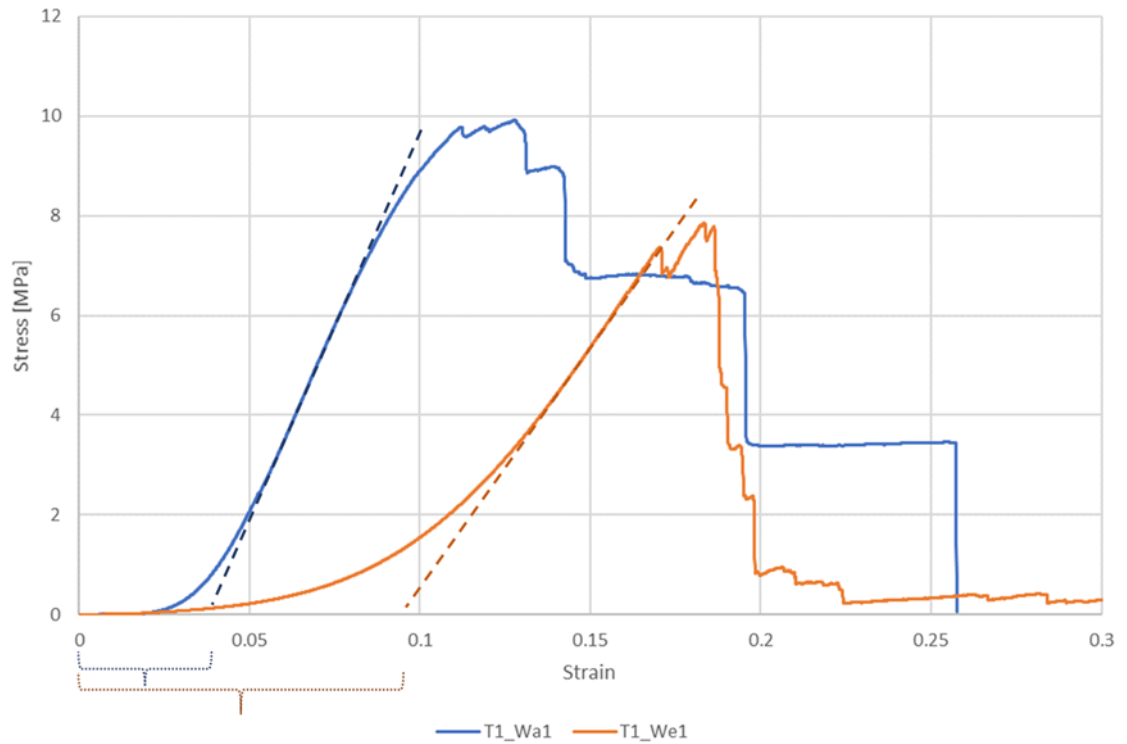


Figure 3.3. Stress-strain curves of sample T1_Wa1 (warp direction) and T1_We1 (weft direction). The dotted lines highlight the elastic region, while the brackets the de-crimping one.

Figure 3.4 depicts stress-strain curves of three samples, all tested in the weft direction, from various tapestries, T1, T2 and T6. The shape of these curves presented a characteristic post-yield region, where stress remained approximately constant and showed some recovery. This trend is not unexpected for wool, as this fibrous material usually retains a certain elasticity also after the yield point (Section 2.1.1.2) [21].

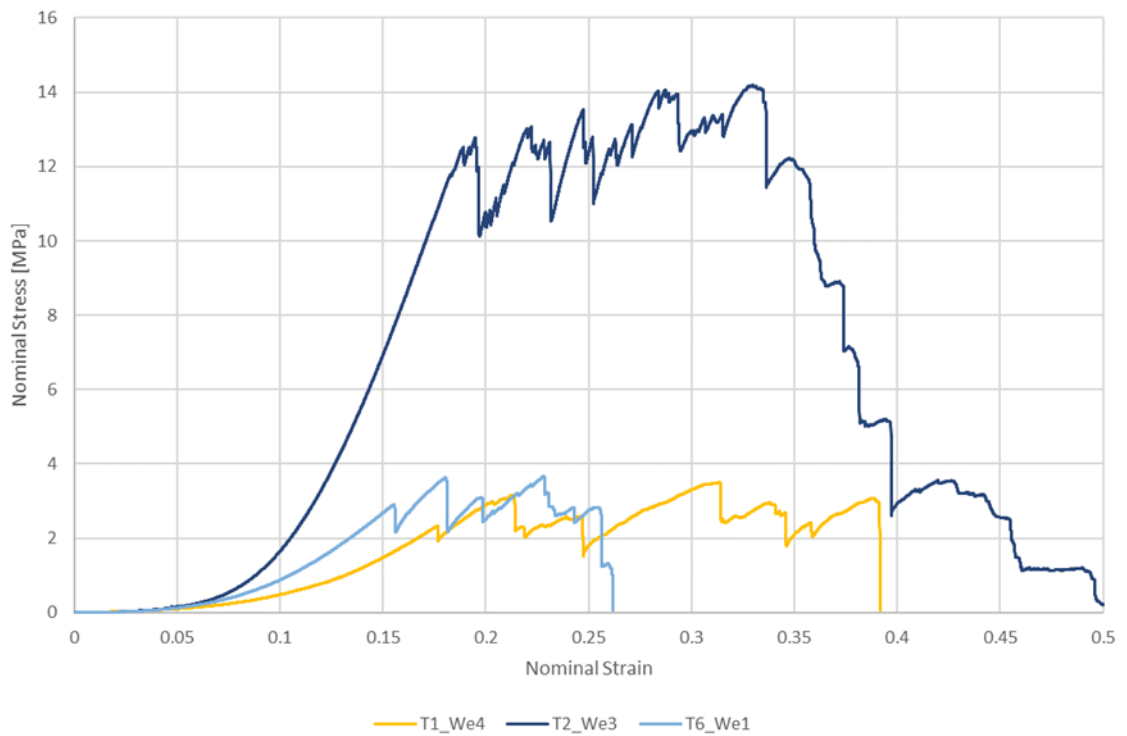


Figure 3.4. Stress-strain curves of sample T1_We4, T2_We3, T6_We1 (weft direction).

The data from the uniaxial tensile testing of historic samples are summarised in Table 3.5. In opposition to the similarities noted in the stress-strain curves, when looking at the detailed data on tensile properties, they demonstrated remarkable dissimilarities. Significant differences from sample to sample could be found in both the modulus and stress at failure, but also in nominal strain at the breaking point. These data prove how difficult it can be to define generic but representative features for this kind of artworks. This is an important caveat especially when such mechanical properties are needed to build an accurate model, as attempted by other studies [5].

From the data in Table 3.5, it can be observed that the least “stiff” and weakest tapestry was T5, since it showed the lowest Young’s modulus, as well as breaking stress in both warp and weft direction. In contrast, for the opposite reasons, sample T2 showed the greatest tensile strength. The extreme fineness of the weave of T2 (7 warp x 32 wefts per cm) may have been one of the factors that contributed to its relatively high strength, especially in comparison to tapestries with a significantly lower thread count, i.e. T5 (5 warps x 12 wefts per cm).

Table 3.5. Uniaxial tensile properties of the samples from historic tapestries.

Tapestry Code	Direction	Sample Code	Strain at the End of the Crimp	Young's Modulus [MPa]	Stress at Failure [MPa]	Strain at Failure
<i>T1</i>	Warp	T1_Wa1	0.04	145.83	9.92	0.11
		T1_Wa2	0.02	169.33	12.62	0.09
		T1_Wa3	0.05	104.39	8.50	0.11
		T1_Wa4	0.04	164.62	13.16	0.09
	Weft	T1_We1	0.10	93.47	7.85	0.17
		T1_We2	0.10	97.47	7.77	0.16
		T1_We3	0.12	40.71	5.53	0.25
		T1_We4	0.12	28.57	2.31	0.18
<i>T2</i>	Warp	T2_Wa1	0.02	246.03	20.12	0.09
		T2_Wa2	0.03	247.26	17.65	0.09
	Weft	T2_We1	0.09	121.13	13.03	0.20
		T2_We2	0.12	75.49	17.56	0.34
		T2_We3	0.09	139.85	12.50	0.19
		T2_We4	0.09	98.84	18.44	0.30
<i>T3</i>	Warp	T3_Wa1	0.04	78.00	3.84	0.06
		T3_Wa2	0.07	111.68	8.05	0.13
		T3_Wa3	0.04	101.72	3.71	0.07
	Weft	T3_We1	0.10	4.43	0.99	0.33
		T3_We2	0.18	6.65	0.62	0.18
<i>T4</i>	Warp	T4_Wa1	0.04	61.80	3.29	0.08
		T4_Wa2	0.04	67.05	3.03	0.07
	Weft	T4_We1	0.16	17.69	1.83	0.23
		T4_We2	0.12	5.08	0.53	0.19
		T4_We3	0.13	24.57	3.71	0.24
<i>T5</i>	Warp	T5_Wa1	0.04	28.90	1.22	0.12
		T5_Wa2	0.09	13.08	0.54	0.06
	Weft	T5_We1	0.09	4.55	0.45	0.16
		T5_We2	0.12	3.99	0.60	0.18
<i>T6</i>	Warp	T6_Wa1	0.03	56.62	2.49	0.08
		T6_Wa2	0.04	124.24	8.09	0.09
	Weft	T6_We1	0.10	38.14	2.89	0.15
		T6_We2	0.11	59.84	5.00	0.16
<i>T7</i>	Warp	T7_Wa1	0.06	124.78	6.76	0.10
		T7_Wa2	0.05	85.34	5.59	0.11
	Weft	T7_We1	0.08	75.91	6.51	0.15
		T7_We2	0.09	78.86	7.72	0.18

To better discuss the different mechanical properties, in Figure 3.5 are reported the Young's moduli of the seven samples tested in the warp direction, while in

Figure 3.6 are depicted the results from specimens tensioned in the weft direction. Whenever it was possible to characterise more than one specimen from the same tapestry fragment, in the same direction, and with similar structure (i.e. homogeneous/uniform or heterogeneous), the data were averaged. In such cases, the error bar was included in the graph to indicate the standard error (SE), that also accounts the variability in the number of tested specimens. When considering the warp direction, it is observed that the Young's moduli ranged from a maximum of 246.64 MPa (T2) to a minimum of 20.99 MPa (T5). On the other hand, Young's moduli of weft specimens varied from 119.94 MPa (T2) to 3.99 MPa (T5).

From the data gathered, it is not possible to assess the influence of the heterogeneity of the weave structure. Indeed, in the case of sample T1, uniform specimens showed a higher stiffness, while specimens with heterogeneities from sample T6 had greater moduli. On the other hand, as previously mentioned, it is observed that the density of the weave had an impact on flexibility: the higher the thread count, the higher the Young's modulus.

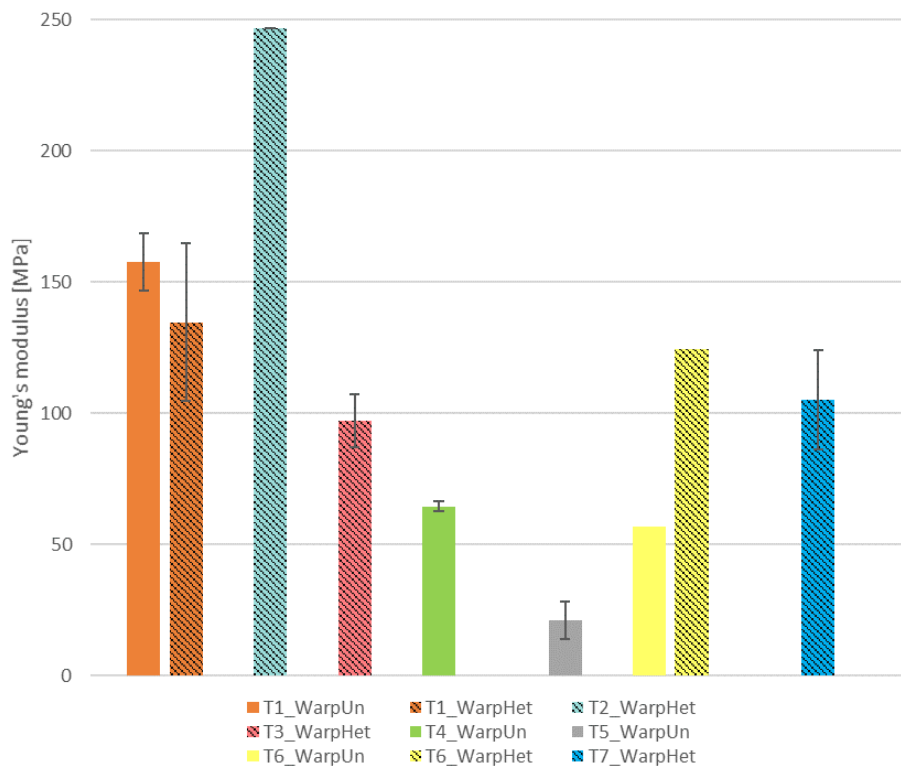


Figure 3.5. Young's moduli of specimens from historic tapestry fragments, tensioned in the warp direction. The bar indicates the SE, whenever it was possible to test more samples with uniform or heterogeneous weave structure.

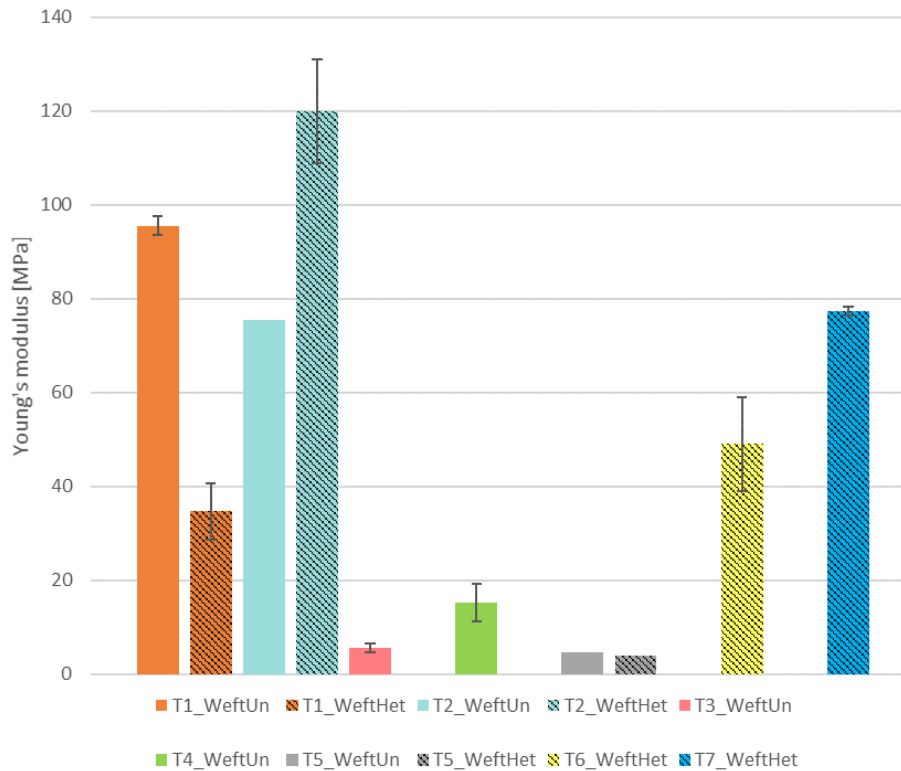


Figure 3.6. Young's moduli of specimens from historic tapestry fragments, tensioned in the weft direction. The bar indicates the SE, whenever it was possible to test more samples with uniform or heterogeneous weave structure.

Figure 3.7 and Figure 3.8 depict the breaking stress of the different samples tested in the warp and weft direction, respectively. In general, warp tapestry samples were shown to have higher tensile strength than weft ones, as also previously noted by Duffus [5]. This could be explained by the more direct exposure of weft threads than warp ones to environmental factors, that can be able to promote degradation processes affecting the mechanical behaviour. In particular, light can play an important role, as it can be responsible for photo-tendering process that may lead to a loss in strength [22], as discussed in Chapter 2, Section 2.1.1.3. The greater exposure of weft threads in comparison to warp ones is due to the tapestry weave structure, in which warp yarns are completely covered by the coloured wefts (Section 1.1.2). The detailed data indicate that in the case of warp direction, specimens failed from a maximum of 18.88 MPa (T2) to a minimum of 0.88 MPa (T5). In the case of weft direction, the data ranged from 17.56 MPa (T2) to 0.45 MPa (T5).

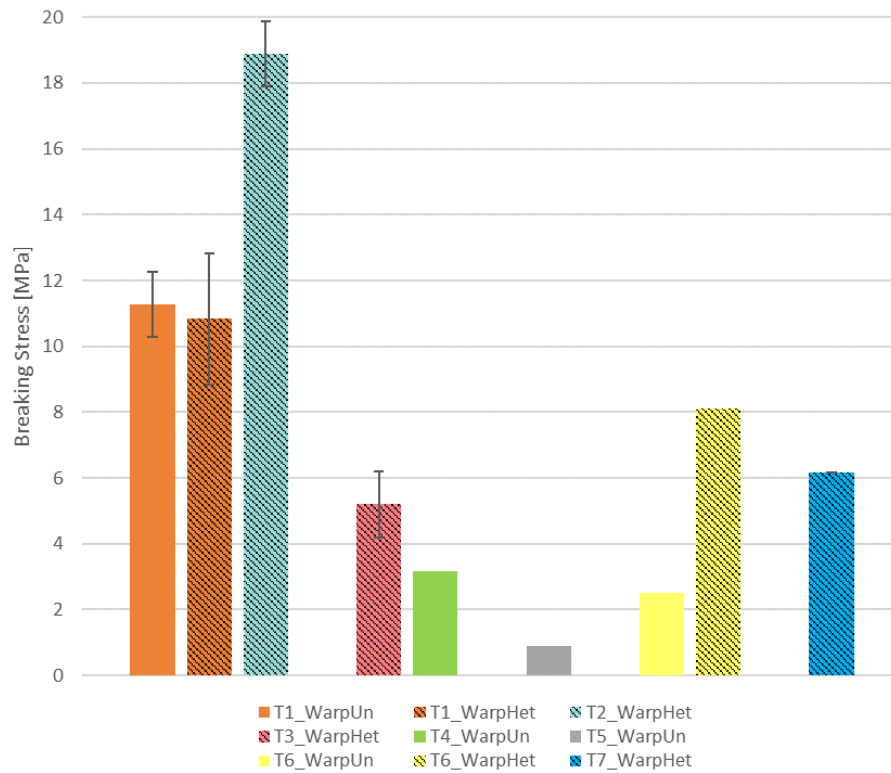


Figure 3.7. Breaking stress of specimens from historic tapestry fragments, tensioned in the warp direction. The bar indicates the SE, whenever it was possible to test more samples with uniform or heterogeneous weave structure.

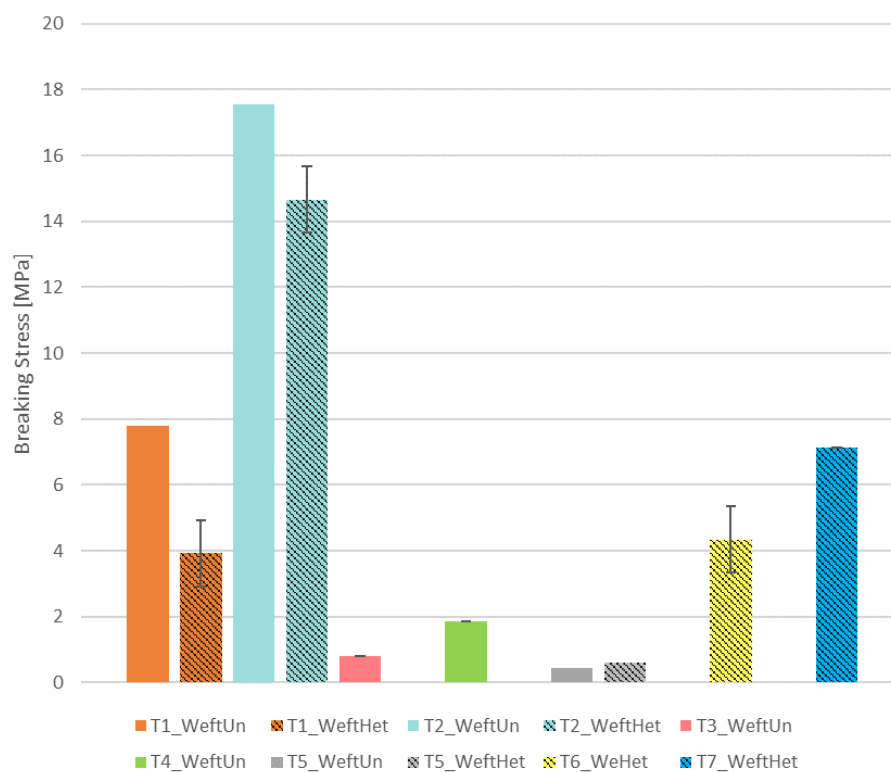


Figure 3.8. Breaking stress of specimens from historic tapestry fragments, tensioned in the weft direction. The bar indicates the SE, whenever it was possible to test more samples with uniform or heterogeneous weave structure.

It is interesting, though not surprising, to notice that in some cases the heterogeneities in the weave, especially those in the weft direction, determined the breaking point of specimens. This can be illustrated by Figure 3.9: during the uniaxial tensile test specimen T1_We3 failed in correspondence to the diagonal slit. Of course, the breaking mechanism greatly depended on the “geometry” of the pattern in the sample: if the change in colour was in the same direction of the tensioning, specimens would break uniformly. The variable influence of pattern justifies why, as reported in the data summarised by Table 3.5, not all samples with heterogeneities were weaker than ones with a homogeneous structure.

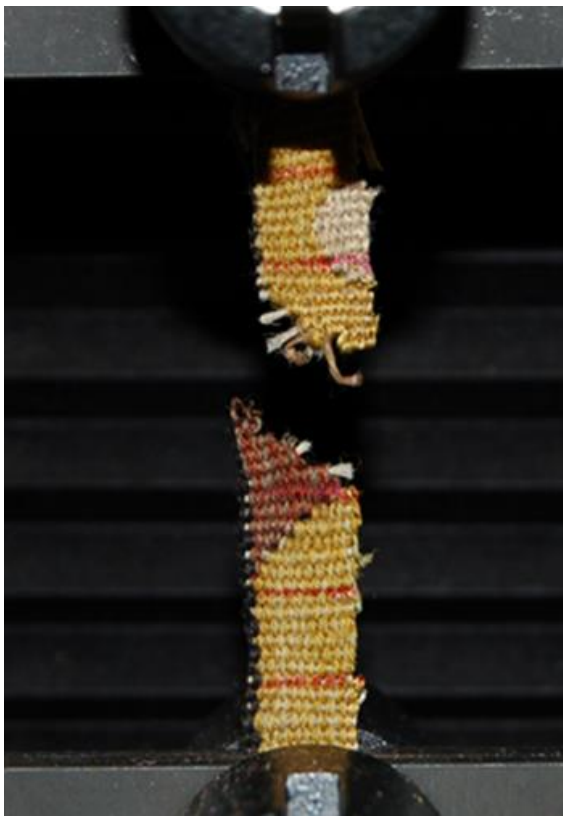


Figure 3.9. Sample T1_We3 at the end of the uniaxial tensile testing.

3.2.1.2 Newly woven wool rep fabric

As done for the specimens from actual tapestries, the wool rep fabric was uniaxially tensile tested. The characterisation aimed to assess the resemblance, in the mechanical behaviour, between historic hangings and the newly woven textile.

Figure 3.10 illustrates the typical stress-strain curve of the wool rep fabric in both warp and weft directions. The graphs indicate that the de-crimping region ended at greater strain in the warp direction, contrary to what was observed for the historic samples. Moreover, from the stress-strain curves, it is evident that the wool rep specimens tested in the weft direction had greater Young's moduli and were stronger than warp ones. These observations are confirmed by the data reported in Table 3.6. Indeed, from the data in the table, it is shown that weft samples had an average Young's modulus of 531 MPa, while warp ones had an average modulus of 98 MPa. When considering the stress at failure, specimens tested in the weft direction broke at around 23 MPa, while warp ones at around 10 MPa. All these observations seem to disagree with what was noted from the analysis of historic samples; nevertheless, it should be reminded that the new woollen fabric is warp-faced instead of weft-faced. Therefore, this clarifies why the physical features of warp yarns in the newly woven fabric resemble more those of historic weft threads. Besides these apparent discrepancies due to the different orientation of the weave, a certain similarity in the general mechanical behaviour can be stated from the shape of the stress-strain curves. For comparison, Figure 3.11 is shown.

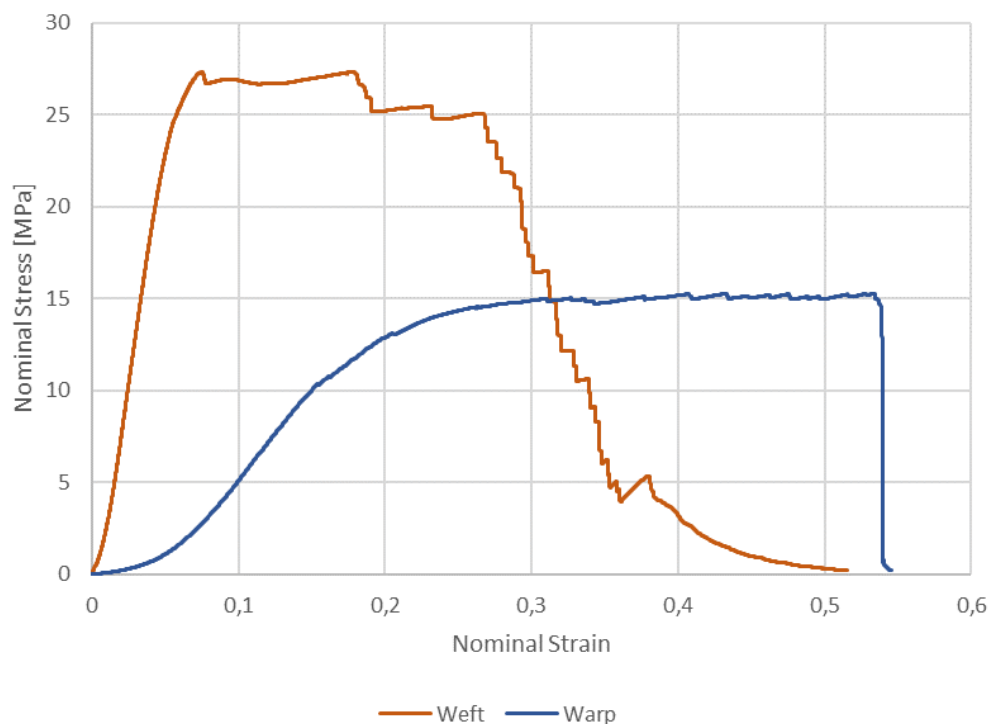


Figure 3.10. Stress-strain curves of samples of the warp-faced wool rep fabric in both weft (orange line) and warp direction (blue line).

Table 3.6. Uniaxial tensile properties of the wool rep fabric (average of five measurements per direction, the standard deviation, SD, is also indicated to show the variation of the data).

Direction	Strain at the End of the Crimp	Young's Modulus [MPa]	Stress at Failure [MPa]	Strain at Failure
Weft	0.02 ± 0.002	531 ± 32.326	23 ± 3.068	0.05 ± 0.007
Warp	0.08 ± 0.008	98 ± 5.816	10 ± 1.095	0.17 ± 0.016

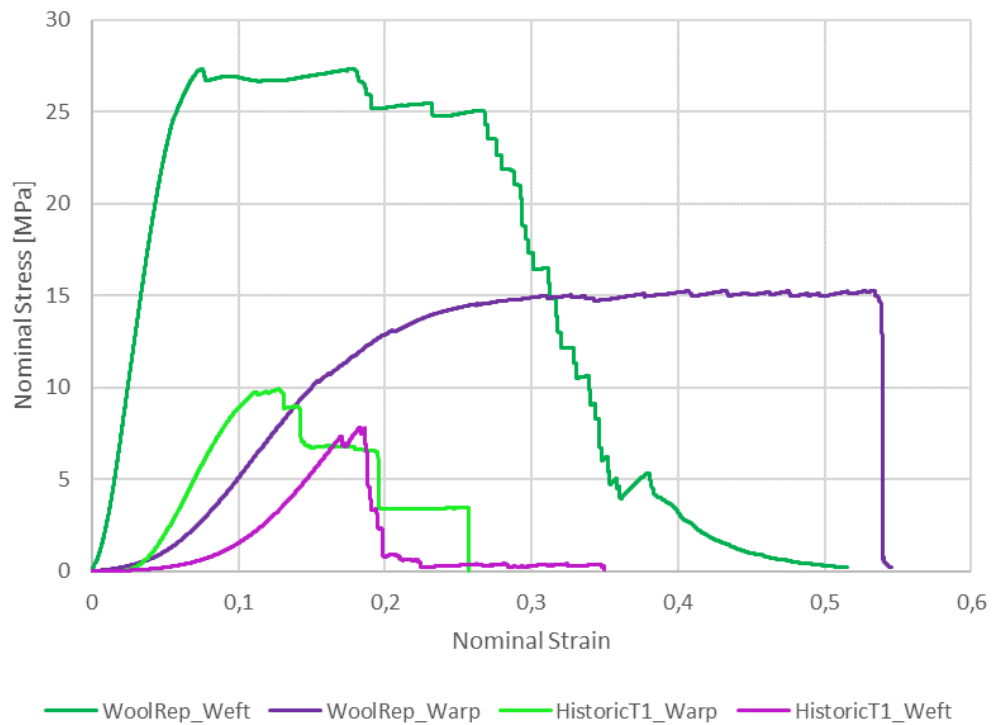


Figure 3.11. Stress-strain curves of samples from the warp-faced wool rep fabric and historic tapestry fragment T1.

When looking in more detail at the data (comparison between Table 3.5 and Table 3.6), the wool rep fabric demonstrated significantly higher moduli than the specimens from historic hangings, perhaps because of differences in the manufacturing process. Unsurprisingly, in general historic specimens were weaker than contemporary ones. However, this is not true in the case of T2, whose breaking stress values were close, or even higher, to those in Table 3.6. Again, the high thread count of T2, even greater than that of the wool rep fabric, may have determined its (relatively) remarkable strength.

3.2.2 ATR-FTIR

After the mechanical characterisation, samples collected from the historic tapestry fragments were analysed with ATR-FTIR.

In the first instance, the ATR-FTIR analysis clarified the fibre composition of the historic pieces under investigation, demonstrating that most of the samples were made of wool. Wool was identified because of the presence of some characteristic bands in the spectra. As an example, the spectrum of sample T1_We.Red is shown in Figure 3.12. Some of the peaks marked are distinctive of proteinaceous materials, namely: Amide I at 1635 cm^{-1} , due to C=O stretching; Amide II at 1514 cm^{-1} , linked to the combined vibrations of N-H and C-H [23, 24]; Amide III at 1232 cm^{-1} , caused by C-N stretching and N-H bending [1]. It should be noted that such peaks are at lower wavenumbers than those reported for wool when FTIR analysis is carried out in a transmission mode. This is due to shifts caused by the ATR approach [25]. Besides amide bands, wool samples presented representative peaks related to cystine and its degradation. This is discussed more in more detail later.

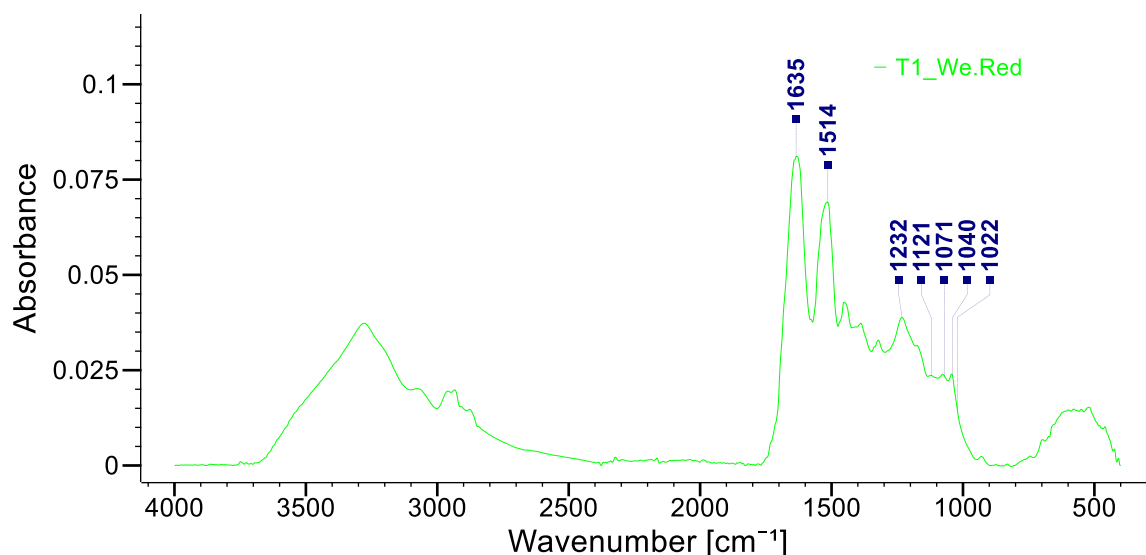


Figure 3.12. ATR-FTIR spectrum of sample T1_We.Red (average, baseline-corrected).

In addition to wool, in fewer cases silk was detected. Similarly to wool, some bands, in particular those at around 1620 cm^{-1} , 1510 cm^{-1} and 1230 cm^{-1} , can be ascribed to the presence of a proteinaceous material as linked to the vibration of aminoacidic groups. It is pointed out that, in comparison to wool, amide

bands in silk samples should be expected at slightly different wavenumbers; this is due to the influence of the characteristic structural protein conformation [26-28]. Other distinctive bands in the ATR-FTIR spectra of silk samples were at around: 1160 cm^{-1} (C-N stretching in tyrosine); 1000 and 970 cm^{-1} (skeletal stretching) [27, 29]. As an example, in Figure 3.13 the ATR-FTIR spectrum of T1_WeWhiteS is shown. Although different studies looked at methods for evaluating the level of degradation in silk through ATR-FTIR analysis (especially considering the band centred at 1700 cm^{-1} , linked to the vibration of C=O group) [26-30], this goes beyond the purposes of the current work and therefore is not further investigated.

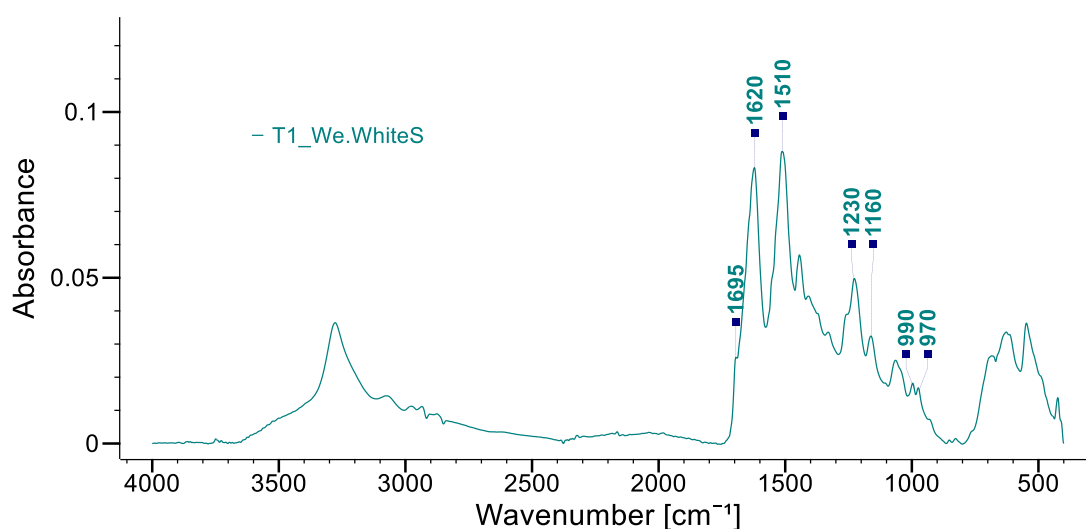


Figure 3.13. ATR-FTIR spectrum of sample T1_We.WhiteS (average, baseline-corrected).

When tracking chemical degradation of wool, although there may be some changes in the three amide bands, the most relevant variations occur between $1170\text{-}1000\text{ cm}^{-1}$ [1]. As first suggested by Odlyha et al. and mentioned in Section 2.3.1, by looking at key peaks in this region it is possible to compare the level of deterioration of different samples from historic tapestries [1]. The peaks of interest are related to cystine oxidation products, namely: cystine dioxide, $-\text{SO}_2\text{-S-}$, at 1121 cm^{-1} (CD); cystine monoxide, $-\text{SO-S-}$, at 1071 cm^{-1} (CM); cysteic acid, $-\text{SO}_3^-$, at 1040 cm^{-1} (CA); S-sulfonate/Bunte salt, $-\text{S-SO}_3^-$, at 1022 cm^{-1} (B-salt) [1, 6]. Results from the MODHT project revealed that, in historic samples, cystine is particularly converted into cysteic acid [1]. Because of this, the peak at 1040 cm^{-1} can be considered as the most informative for the purposes of the current work (the higher the CA amount, the greater the degradation). It is noted that,

besides the research carried out for the MODHT project, other studies have drawn similar conclusions, indicating the same peaks as the most useful to describe degradation of wool promoted by environmental factors such as light and temperature [13, 31, 32].

Results from the analysis of cystine degradation products are first discussed by considering woollen warp threads from the seven fragments. Since warp yarns in European tapestries were usually left undyed, focusing on the warp threads allows to first observe degradation paths of the fibrous material, without any interference of the colourants. Studying warp samples aimed to enrich the data gathered from the MODHT project, as only weft threads were investigated with the spectroscopic technique before. When looking at the spectra and signals between $1250\text{--}1000\text{ cm}^{-1}$, three groups can be distinguished. The first group, which includes sample T1_Wa and T2_Wa, is characterised by peaks related to CM and CA, and the lack of signal at 1022 cm^{-1} associated to B-salt. On the other hand, B-salt can be distinguished in sample T4_Wa, T6_Wa and T7_Wa, categorised within the second group. While, on the basis of absorbance values, specimens belonging to the so-called second group had a contained amount of CA, samples from the third group (T3_Wa and T5_Wa) presented an intense peak at 1040 cm^{-1} . Figure 3.14 illustrates the averaged spectra of sample T1_Wa, T5_Wa and T7_Wa to highlight the spectral differences of the three groups in the region of interest.

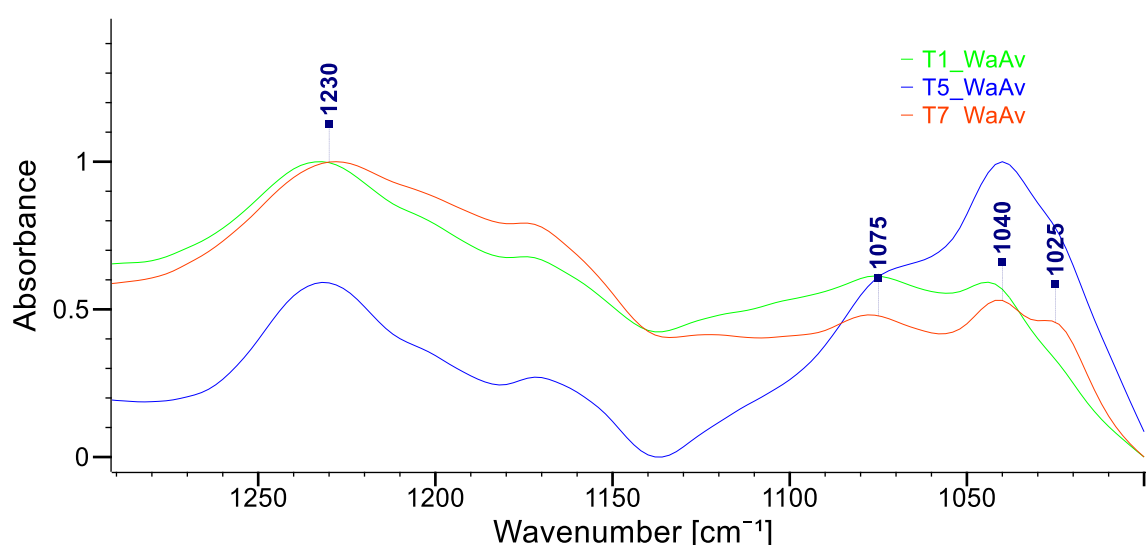


Figure 3.14. ATR-FTIR averaged spectra of wool warp samples from fragment T1, T5, and T7 (after baseline correction). Spectral differences in the intensity of peaks at around 1075 cm^{-1} (CM), 1040 cm^{-1} (CA), and 1022 cm^{-1} (B-salt) allow to differentiate three groups.

Interestingly, a similar (though not identical, as discussed later) subdivision into groups was made for the tapestry samples analysed by Odlyha et al. In the past study, this variation in the ratio of cystine degradation products was possibly justified by the exposure of artefacts at different ranges of wavelengths [1], following what was suggested in other studies [31, 33]. In addition to the wavelength, also the exposure time can be considered a determining factor, as reported by Carr and Lewis [13]. In their paper, ATR-FTIR spectra of wool specimens exposed to sunlight revealed that the B-salt peak increased only initially, while it dropped after 4 weeks. In opposition, the CA signal constantly grew during the 20-week experiment [13]. Importantly, it is remarked that such degradation processes were here observed on warp threads, not directly exposed to light. Because of this, it is thought that other environmental factors than light, e.g. temperature, RH and pollutants, contribute to the formation of oxidation products from cystine. The high impact of thermo-hygrometric conditions on the degradation of wool within historic hangings was previously observed by Duffus, who tracked the formation of radicals from cysteine through electron paramagnetic resonance (EPR) [5]. Importantly, Luxford et al. noted the formation of high humidity microclimates behind tapestries displayed in historic houses. The authors considered these microclimates possibly responsible for the great chemical deterioration of *silk* threads taken from the back of historic hangings and analysed during the MODHT project through ATR-FTIR [34]. Having found that also unexposed wool warp samples from tapestries may be significantly (chemically) degraded, this seems to confirm the observations from the past study: humidity may play a relevant role in determining the poor condition of tapestries.

Furthermore, in comparison to the classification by Odlyha et al., a main difference is noted. In the past work, specimens from the third group showed CA as the principal degradation product, however the corresponding signal at 1040 cm^{-1} was not as intense as in T3_Wa and T5_Wa. In some other cases, a particularly high sulphonate absorbance band was revealed by Odlyha et al., but this was attributed to the possible use of alum as mordant, normally $\text{KAl}(\text{SO}_4)_2 \cdot 12\text{H}_2\text{O}$. In the past paper, it is stated that the use of alum (possibly because of the SO_4^{2-} group, although this was not clearly stated) caused a band

between 1200 cm^{-1} and 980 cm^{-1} so intense as to obscure the CA peak, that therefore could not be quantified [1].

Considering the current work, since the warp threads are visibly undyed, the interference from alum seems unlikely. Nevertheless, to further study this aspect, reference samples from the MODHT project (stored at the CTCTAH) were analysed and compared with an undyed wool sample from the newly woven rep fabric. The two MODHT mock-ups had been dyed with logwood and mordanted with alum and an iron salt, also presenting the SO_4^{2-} group, Fe(II)SO_4 . The spectra from the analysis of the three samples are depicted in Figure 3.15. From Figure 3.15, the intensity and shape of peak at 1040 cm^{-1} of Ref_LogAl, mordanted with alum, was demonstrated to be similar to that of Ref_LogFe, mordanted with Fe(II)SO_4 . Undyed wool, as can be expected, did not present a pronounced peak around 1040 cm^{-1} . Combining the data, it can be said that the mordanting process might have contributed to the signal at 1040 cm^{-1} (slightly, and perhaps in combination to natural ageing). Nevertheless, the outcomes seem to disagree with what reported by Odlyha et al., since the sulphonate signal from alum proved not to be high enough to “obscure” the CA peak. Therefore, it can be concluded that the intense band in specimens belonging to the third group was not likely to be linked to the use of mordants.

Instead, it can be thought that other sources of sulphate (e.g. pollutants) may have played a role in determining strong signals at 1040 cm^{-1} . Namely, the exposure to environments rich in sulphur dioxide (SO_2) should be considered. Even if the concentration of SO_2 in the air has been constantly decreased since the 1980s, in the past this pollutant was highly present as largely released by fuels. This gaseous pollutant can lead to the formation of sulphate compounds possibly harmful for the cultural heritage, such as ammonium sulphate secondary aerosol ($(\text{NH}_4)_2\text{SO}_4$) [35], sulfuric acid (H_2SO_4), and gypsum ($\text{Ca}_2\text{SO}_4 \cdot 2\text{H}_2\text{O}$) when in presence of calcium carbonate [36]. Besides being formed through pollution, the latter soluble salt can be easily encountered historic buildings (e.g. in walls) and thus it should be included as a potential source of the sulphate signal in the investigated samples.

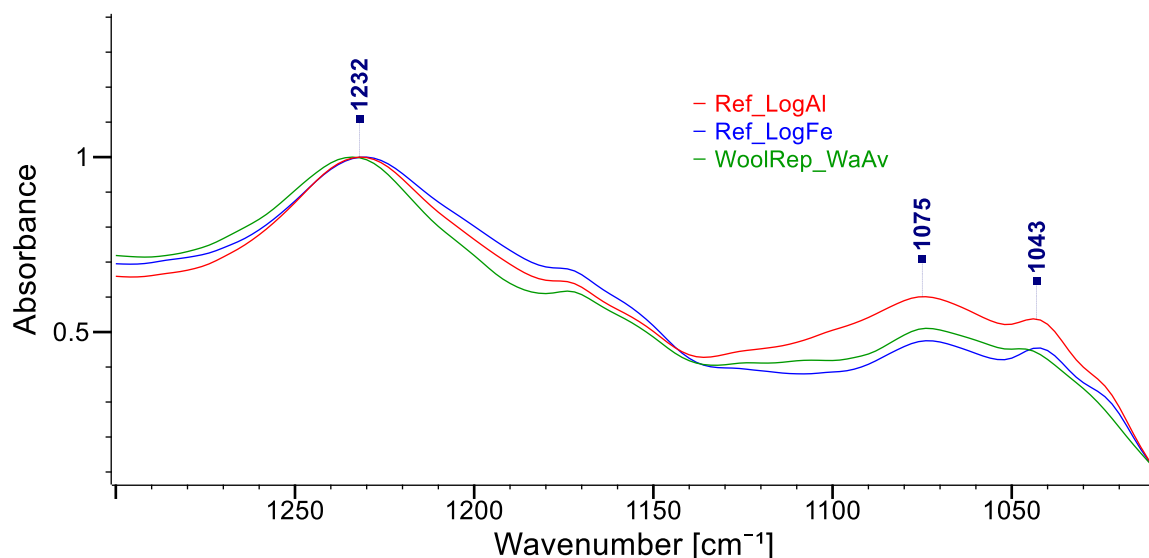


Figure 3.15. ATR-FTIR averaged spectra of wool reference samples prepared for the MODHT project and mordanted respectively with alum (Ref_LogAl) and iron salt (Re_LogFe). In addition, the spectrum of an undyed wool sample from the rep fabric is shown (green line).

When comparing the CA/Amide III peak ratio of the warp samples (second derivate spectra, as shown in Figure 3.16), some differences between fragments can be noted. As depicted in Figure 3.17, woollen warp from T5 appeared to be the most chemically degraded (highest CA signal), followed by T3; on the other hand, specimens from T7 present the lowest ratio, stating the most contained chemical deterioration due to the reaction from cystine to cysteic acid.

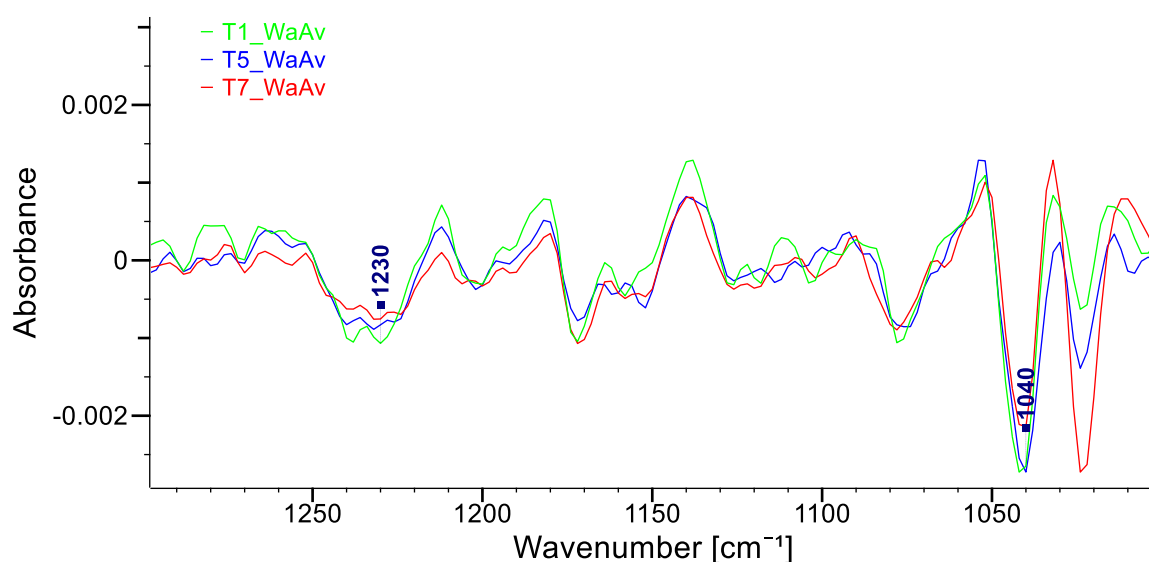


Figure 3.16. Second derivate ATR-FTIR spectra of warp samples from T1, T5, T7 (after average, baseline correction, normalisation, but no further processing/smoothing).

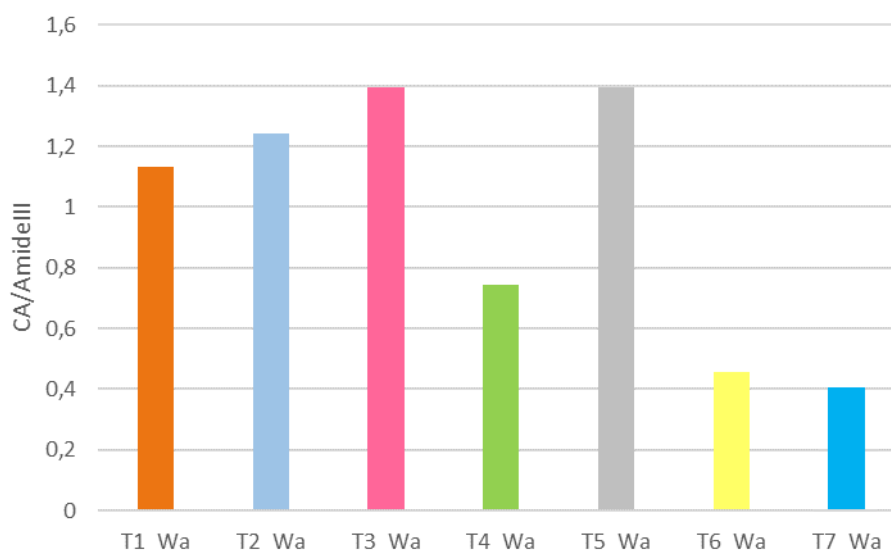


Figure 3.17. CA/AmideIII ratio from the analysis of the second derivate ATR-FTIR spectra of warp threads from historic samples.

As noted for warp samples, weft threads can also be grouped into the same three categories, indicated in Table 3.7. As an example, the spectra of weft samples from T1, T5, T4 are depicted in Figure 3.18. When looking at the data from the analysis of the second derivate spectra (Figure 3.19), some differences in the CA/AmideIII ratio can be noted from sample to sample. While the influence of the dyeing source is addressed later, in general it is highlighted that weft yarns from fragment T3 presented the most pronounced CA signal, and those from T7 the lowest.

The agreement between data from the analysis of warp and weft threads seems to suggest that the chemical degradation of wool partly depends on the dyeing conditions, and partly on the action of environmental parameters, and so on the ageing. Differences in the fibre treatment might justify variabilities in the CA/AmideIII ratio among samples from the same fragment. On the other hand, the ageing conditions, characteristic for each historic piece, may have determined the spectral similarities in threads collected from the same hanging.

Table 3.7. Classification of wool samples from the different tapestry fragments based on the intensity of peaks related to cystine oxidation products.

Group	Tapestry fragments	CD (1120 cm^{-1})	CM (1070 cm^{-1})	CA (1040 cm^{-1})	B-Salt (1022 cm^{-1})
I	T1, T2	X	X	X	
II	T4, T6, T7	X	X	X	X
III	T3, T5	X	X	X strong	X

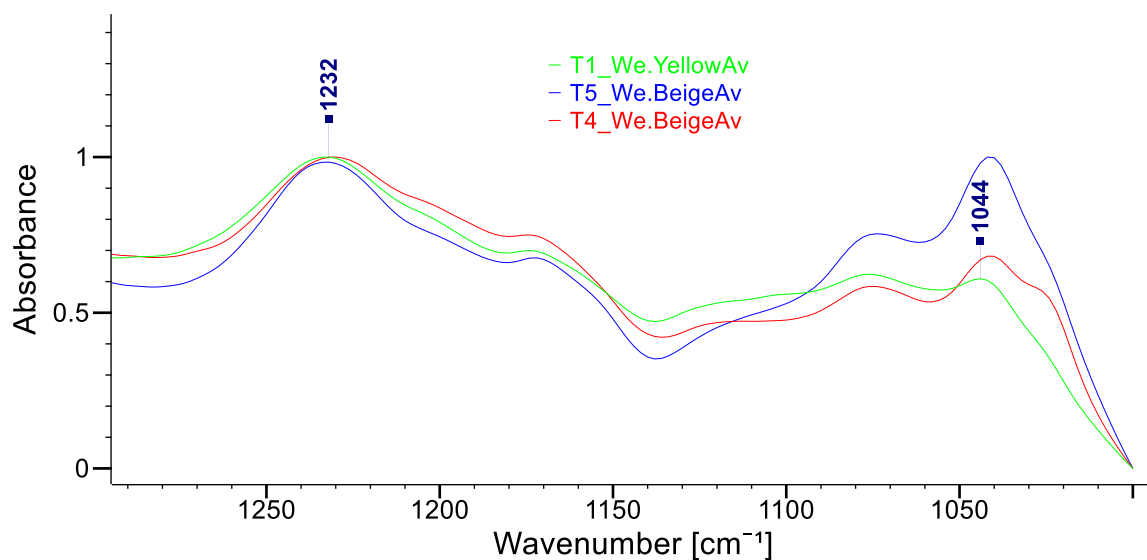


Figure 3.18. ATR-FTIR averaged spectra of wool weft samples from fragment T1, T5, and T4 (after baseline correction). All the specimens here presented were dyed with a luteolin-based source (Section 3.2.3).

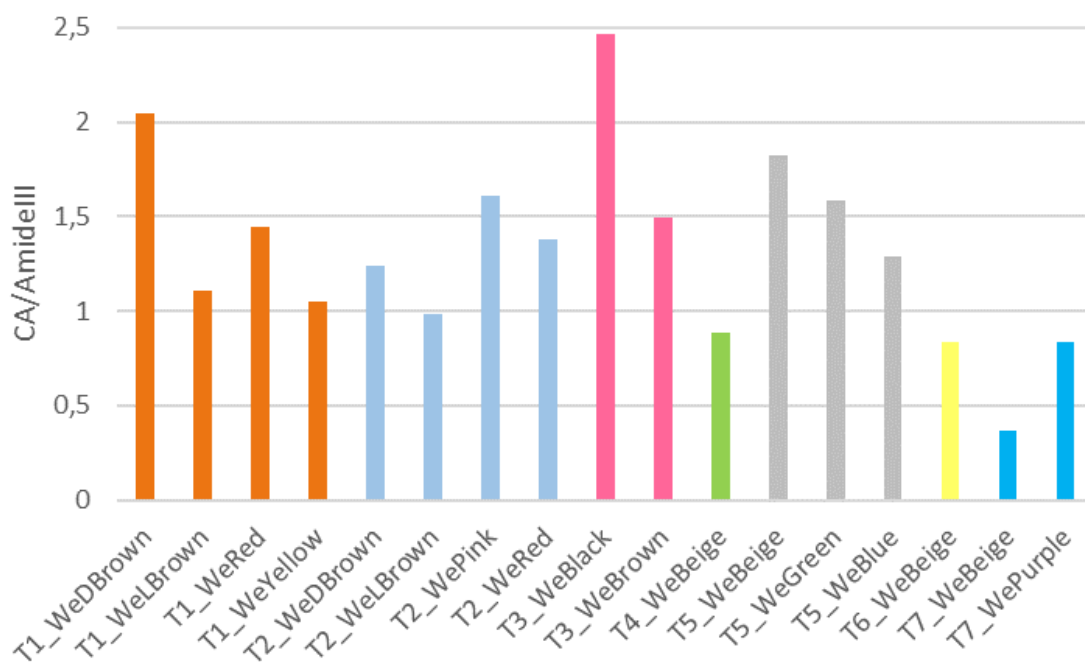


Figure 3.19. CA/AmideIII ratio from the analysis of the second derivate ATR-FTIR spectra of weft threads from historic samples.

When looking at the data in Figure 3.19, it is interesting to highlight that the tested samples show a CA level generally lower than that observed in the case of the weft threads collected from tapestries during the MODHT project. Namely, considering the results from the past study and reported in the published paper [1], the samples (all from tapestries of the Patrimonio National of Spain) showed, in most of the cases, a CA/AmideIII ratio between 2 and 3.5, with the exception of some extremely degraded wefts with a ratio above 4 [1]. All the wool threads with very high CA level were taken from the same tapestry, also demonstrating an intense oxidative degradation through the amino acid analysis [37]. During the MODHT project, differences in the chemical degradation of wool from the various case studies were justified by the variable conservation history and conditions experienced by each artwork [1, 37].

It should be pinpointed that some ATR-FTIR spectra showed peaks not related to wool. In the case of T3_We.Black and T3_We.Brown a signal at 1320 cm^{-1} was detected, as depicted in Figure 3.20. This peak can be attributed to the presence of calcium oxalate salts, such as weddellite ($\text{CaC}_2\text{O}_4 \cdot 2\text{H}_2\text{O}$) or whewellite ($\text{CaC}_2\text{O}_4 \cdot \text{H}_2\text{O}$). As reviewed by Rampazzi in 2019 [38], calcium oxalate salts have been found in various types of artworks, e.g. historic buildings [39], marble statues [40], paintings [41], barkcloth [42], cartoons (drawings) [43]. Nevertheless, prior to this study, its identification in woollen historical textiles is only seen in a few tapestry samples from the MODHT project [1]. When considering paintings or stone artefacts, it is still not clear whether the origin of calcium oxalate films is biological (from lichens and other microorganisms) or chemical (e.g. promoted by organic materials from past treatments or from the painting technique) [38, 44]. In the wool samples here studied, the origin of oxalate salts could be related to materials employed during the dyeing process, such as plants and/or urea [45].

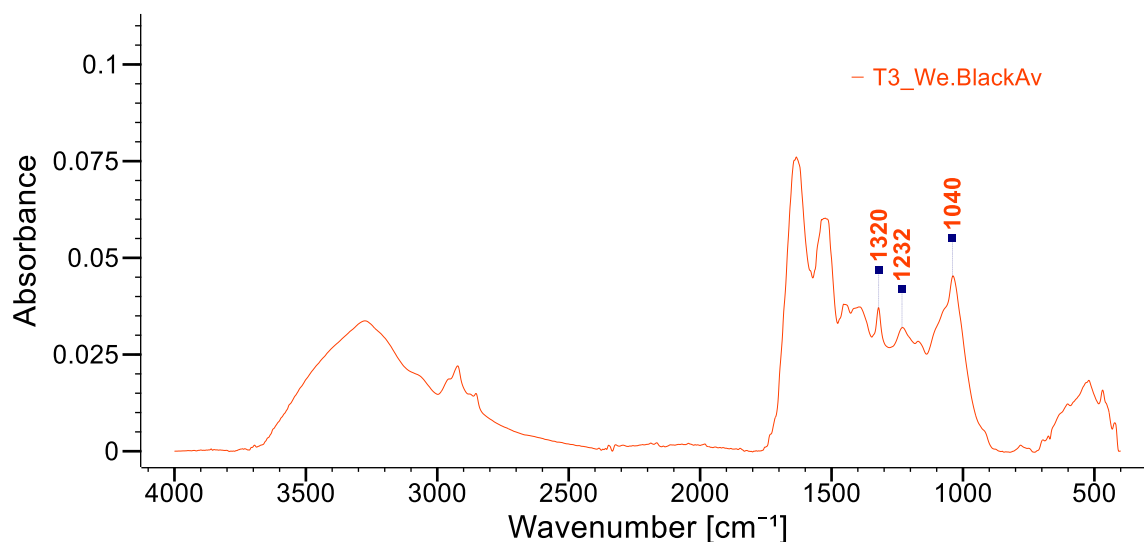


Figure 3.20. ATR-FTIR averaged spectrum of sample T3_We.Black: the peak at 1320 cm^{-1} can be linked to the presence of calcium oxalate salts.

3.2.3 UHPLC-PDA

In Table 3.8 are reported the main components, associated to dye sources, identified through UHPLC-PDA analysis of samples taken from the historic tapestries. When considering the analysed samples, it can be observed that the range of dyes used in the different hangings is quite limited. Namely, recurrent sources are: luteolin-containing plants (especially weld); indigo-type dye; soluble redwoods. Luteolin-based sources were employed to obtain yellow and beige hues, indigoid dyes for blue shades, while soluble redwoods for brownish ones. As discussed later, sometimes more colourants were identified within the same sample. Mixing different dyestuffs was traditionally done to obtain a wider range of shades.

In addition to three sources just mentioned, other dyestuffs were revealed, namely: madder, red scale insects, tannins, young fustic, and possibly logwood. The colourants identified within the fragments agree with those traditionally employed for European historic hangings, as confirmed by other studies (Section 1.1.3).

Table 3.8. Main compounds, and related dye sources, revealed in the wool samples from historic tapestry fragments.

Sample Code	Sample Colour	Compounds Identified	Dye Source
T1_We.DBrown	Dark brown	Ellagic acid, Gallic acid, Unkn. Shibayama	Tannins (+ logwood ?)
T1_We.Yellow	Yellow	Luteolin, Chrysoeriol, Apigenin, Sulfuretin,	Weld + young fustic
T2_We.DBrown	Dark brown	Alizarin, Purpurin, Xanthopurpurin	Madder-type dye
T2_We.Red	Red	Dcll, Carminic acid	Red scale insects (cochineal species)
T3_We.Brown	Brown	Type C	Soluble redwoods
T3_We.Black	Black	Ellagic acid	Tannins
T4_We.Beige	Beige	Luteolin, Chrysoeriol, Apigenin	Weld
T5_We.Beige	Beige	Luteolin, Apigenin (traces)	Luteolin-based source
T5_We.Blue	Blue	Isatin, Indigiton	Indigotin-based source
T6_We.Beige	Beige	Luteolin, Chrysoeriol, Apigenin	Weld
T7_We.Purple	Purple	Type C, Indigotin	Soluble redwoods + indigotin-based source
T7_We.Beige	Beige	Type C	Soluble redwoods

Below, the chemical compounds that allowed the characterisation, and the related dye sources, are described in detail.

Luteolin-based sources

Luteolin is a high lightfast flavonoid yellow component contained, together with related glycoside forms, in several plants [46]. Among the botanical sources containing luteolin, historically in Europe the most widespread for dyeing were: weld (*Reseda luteola* L.), sawwort (*Serratula tinctoria* L.), and dyer's broom (*Genista tinctoria* L.). Since luteolin (UV-Vis absorbance spectrum in Figure

3.22a) can be found in different plants, its identification alone does not allow to univocally distinguish the dyeing source. Therefore, in the past decade, studies were carried out to isolate other dyeing components to further discriminate luteolin-based plants [47-50].

In the case of dyer's broom, also called dyer's greenweed [46], genistein can be a helpful marker as it is not contained in either sawwort or weld [51, 52].

Genistein is an isoflavone whose UV-VIS absorbance spectrum presents two main peaks at 208 and 260 nm [52]. Since this compound does not greatly absorb in the yellow region (300-400 nm), it does not contribute to determining the final colour through the dyeing process [53]. In addition to genistein, Troalen et al. [48] reported that other compounds, indicated as Gt₁₋₄, and in particular Gt₃ (probably isopruneitin), can be useful to recognise the use of dyer's broom.

When genistein is not found through the chromatographic analysis, the presence of chrysoeriol may allow to differentiate between weld and sawwort. Indeed, this flavonoid component is present within weld, but it is absent in sawwort. Although chrysoeriol may be expected also in samples dyed with dyer's broom [54], when identified together with luteolin and in the absence of genistein, it likely refers to weld [52].

Due to the presence of both luteolin and chrysoeriol, and the lack of genistein, weld was identified in four samples taken from tapestries T1, T4 and T6. In Figure 3.21 the chromatogram from the analysis of sample T4_We.Beige is depicted as an example. From the chromatogram, it can be observed that the main markers for weld, luteolin and chrysoeriol, were eluted at 19.4 min and 20.9 min, respectively. The UV-Vis absorbance spectra of the three compounds are shown in Figure 3.22. It should be highlighted that often the analysis revealed the presence of other components, among which some may be associated to glycosides of the flavonoid compounds [55]. Besides, as indicated in Figure 3.21, apigenin was also found in samples dyed with weld. The yellow flavone apigenin is typical of several plants, though not exclusively luteolin-based ones [46] (e.g. safflower, *Carthamus tinctorius* L. [56]).

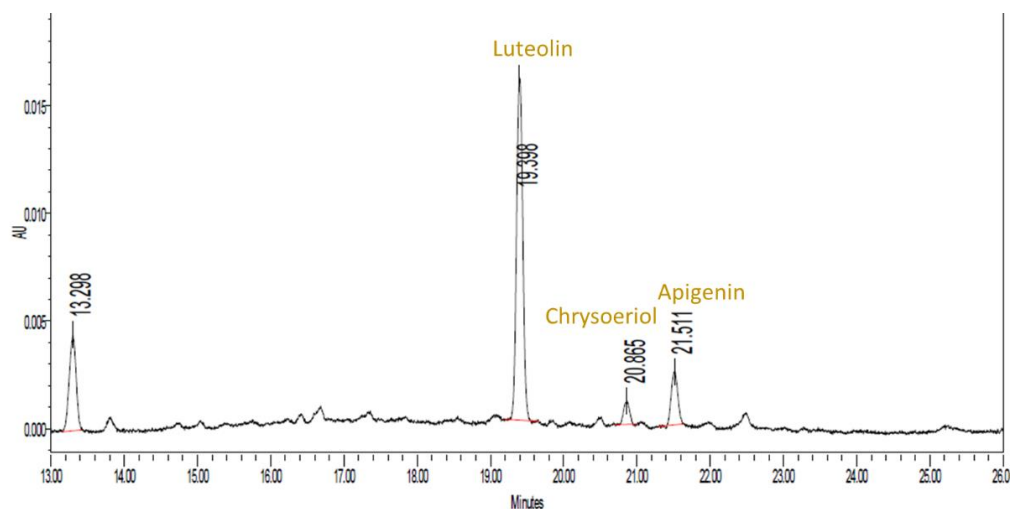


Figure 3.21. Chromatogram, acquired at 350 nm, from the analysis of sample T4_We.Beige.

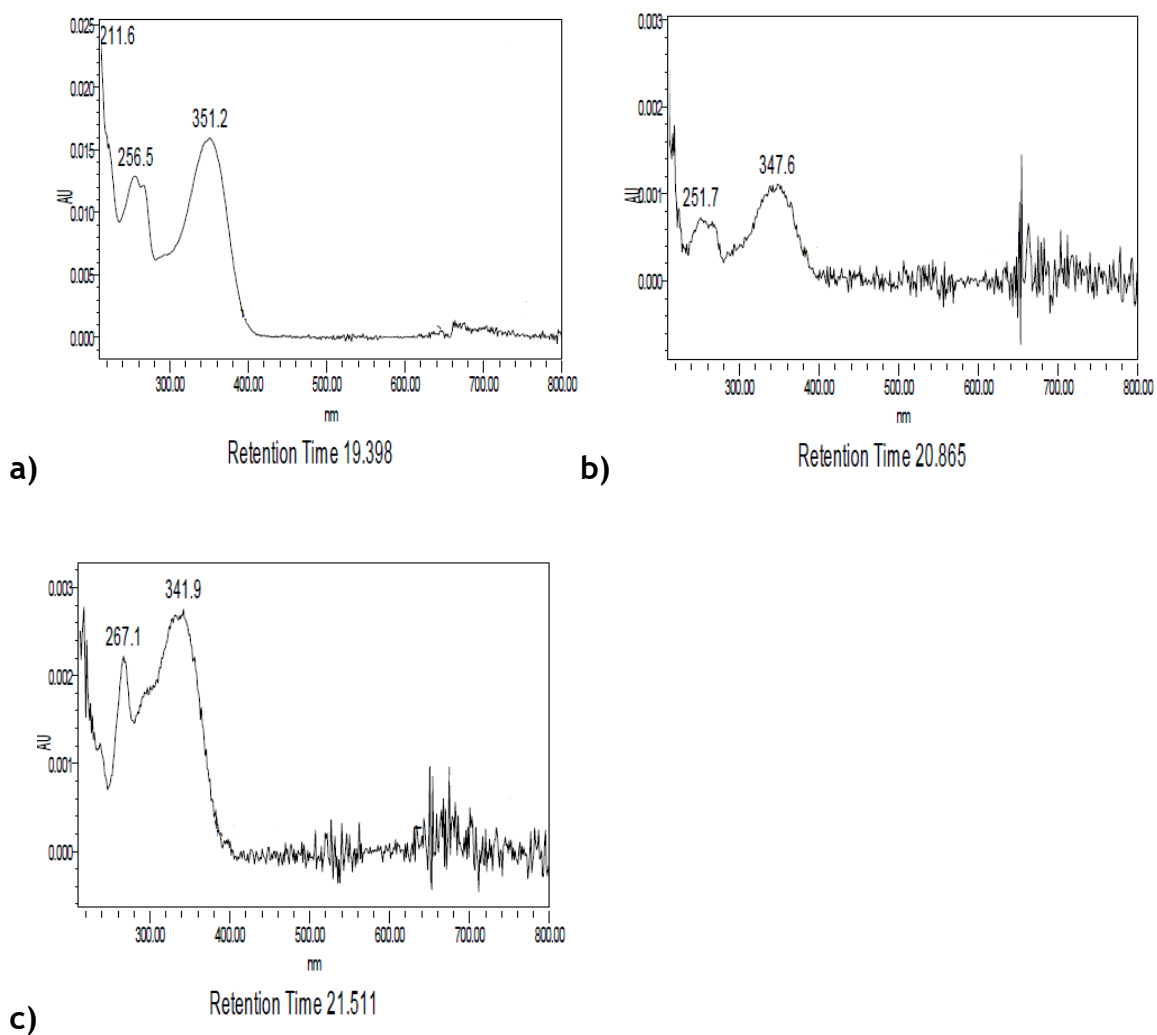


Figure 3.22. UV-Vis abs spectra of: a) luteolin; b) chrysoeriol; c) apigenin.

It is noted that, in the case of sample T5_We.Beige, only luteolin was revealed, impeding a precise characterisation of the dye source.

Interestingly, in sample T1_We.Yellow, together with weld, another botanical source giving yellow-orangish shades was identified, young fustic (*Cotinus coggygria* Scop.). Young fustic was revealed thanks to the presence of sulfuretin, an orange aurone (UV-Vis absorbance spectrum in Figure 3.23), usually found in combination with fisetin [52, 54, 57]. Young fustic was mainly employed between the Middle Ages and the 19th century in Mediterranean countries, particularly in Italy [46]. Since this dyestuff is fugitive, Troalen highlighted that the use of young fustic for dyeing historic tapestries should be considered a rarity [54].

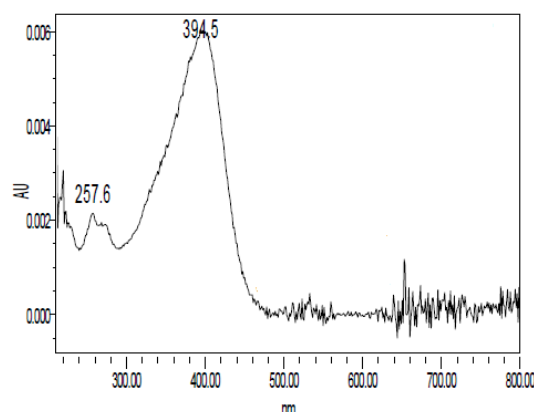


Figure 3.23. UV-Vis abs spectrum of sulfuretin.

Soluble redwoods

The term soluble redwoods refers to a group of trees of the *Caesalpinia* genus which includes Asian sappanwood (*Caesalpinia sappan* L.), and species native of South America, such as pernambuco wood (*Caesalpinia echinata* Lamarck) [46, 51]. The distinctive feature of soluble redwoods, also known as brazilwood, is the presence in the heartwood of brazilin. Brazilin is a colourless homoisoflavonoid compound that, through oxidation, leads to the production of the chromophore brazilein. Brazilein is the principal component responsible for the dyeing properties of redwoods; however, it is easily degraded due to its low photo-stability. Because of this, faded historic textiles only contain a low amount of brazilein, often too small to be detected. Since brazilein cannot be used as a marker, usually the identification of soluble redwoods is only possible thanks to a component indicated as (Novic) Type C compound, Orh or RW(2) [52, 57-60]. The chemical composition of the marker compound had been unknown

until 2018, when Peggie et al. reported that it corresponds to urolithin C [61]. Although in the paper it is underlined that further investigations are needed to properly understand how urolithin C is formed (presumably through ageing [62]), when detected, it can be unequivocally associated with the use of brazilwood [61].

The identification of Type C compound confirmed the use of brazilwood in tapestry fragments T3 and T7. In Figure 3.24, the chromatogram of T3_We.Brown is shown as an example: the marker compound Type C is eluted at 15.4 min. The characteristic UV-Vis absorbance spectrum of urolithin C is depicted in Figure 3.25.

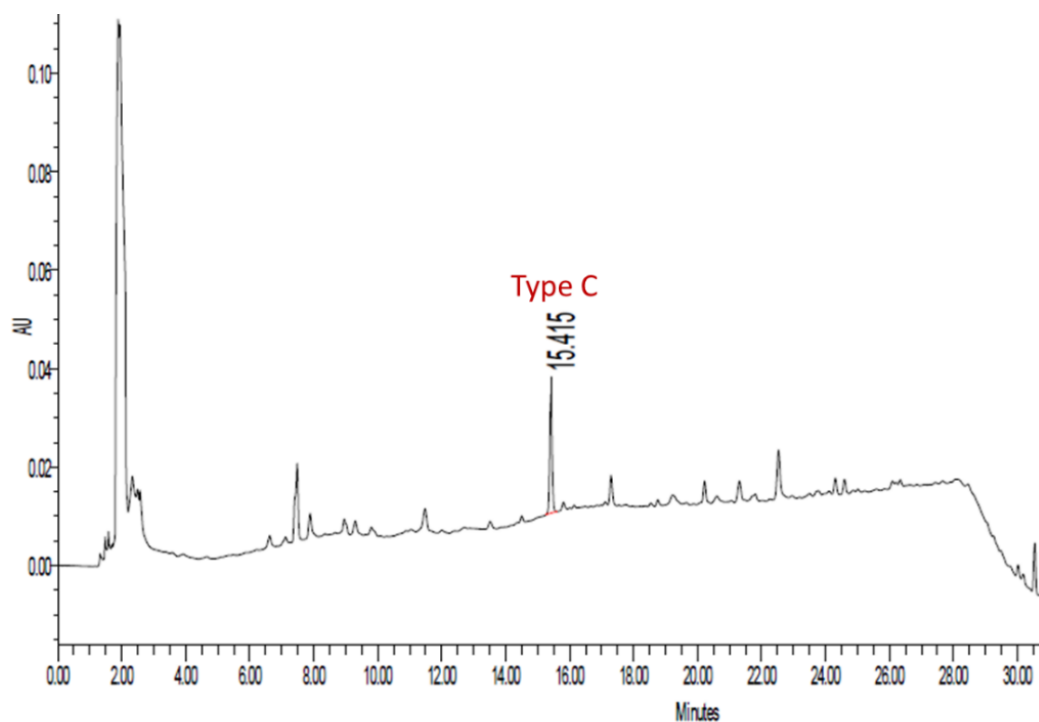


Figure 3.24. Chromatogram, acquired at 255 nm, from the analysis of sample T3_We.Brown.

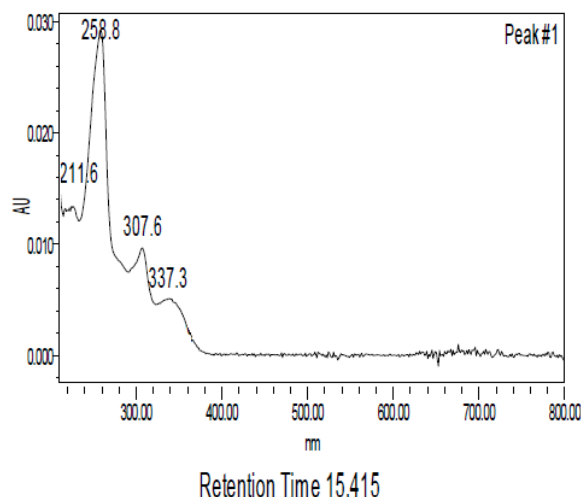


Figure 3.25. UV-Vis abs spectrum of urolithin C.

In the case of sample T7_We. Purple urolithin C was found in a mixture with an indigoid dye, as the combination of dye sources created a purplish hue on the textile.

Madder-type dye

Madder is a mordant dye obtained from the roots of a wide range of plants belonging to the *Rubiaceae* family. Depending on the geographical area, different plants have been used for dyeing. Among them, historically the most relevant one in Europe was *Rubia Tinctorium* L., usually referred to as dyer's madder or common madder [51, 63]. Madder plants contain several anthraquinones, some of them fundamental in determining the dyeing properties, like alizarin and purpurin [51, 64]. In general, for revealing the use of madder in historic textiles through HPLC-PDA, the main chromophores, i.e. alizarin and purpurin, should be detected [54, 65, 66]. Some studies have been carried out to differentiate the botanical sources on the basis of the ratio of the anthraquinones [67, 68]. Nevertheless, this can be challenging as the amount of the compounds may vary significantly depending on many different factors, such as the age of the plant [69].

A madder-type dye was detected in only one sample, T2_We.DBrown. As illustrated in Figure 3.26, within the sample both alizarin (RT 21.4 min) and purpurin (RT 25.3 min) were revealed; the UV-Vis abs spectra of the two markers are presented in Figure 3.27.

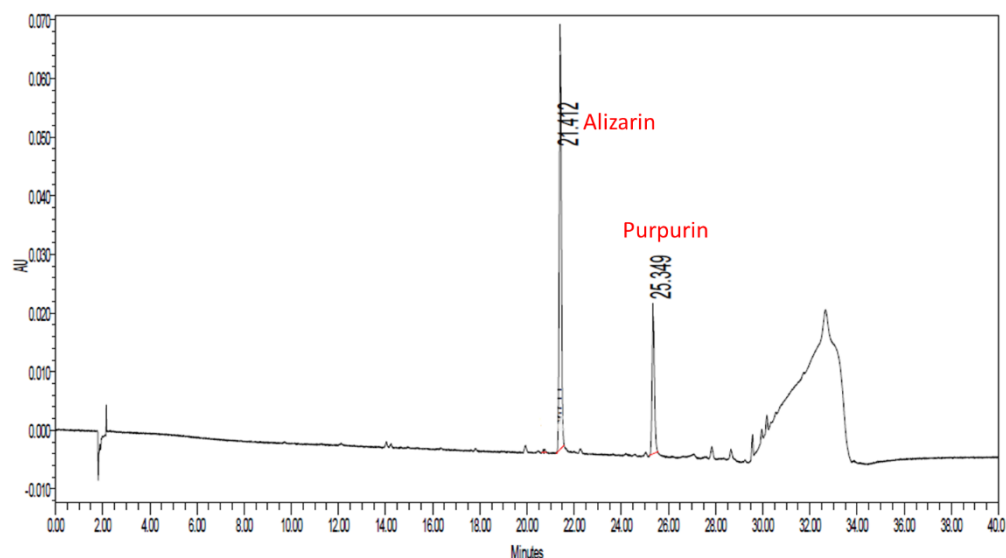


Figure 3.26. Chromatogram, acquired at 450 nm, from the analysis of sample T2_We.DBrown.

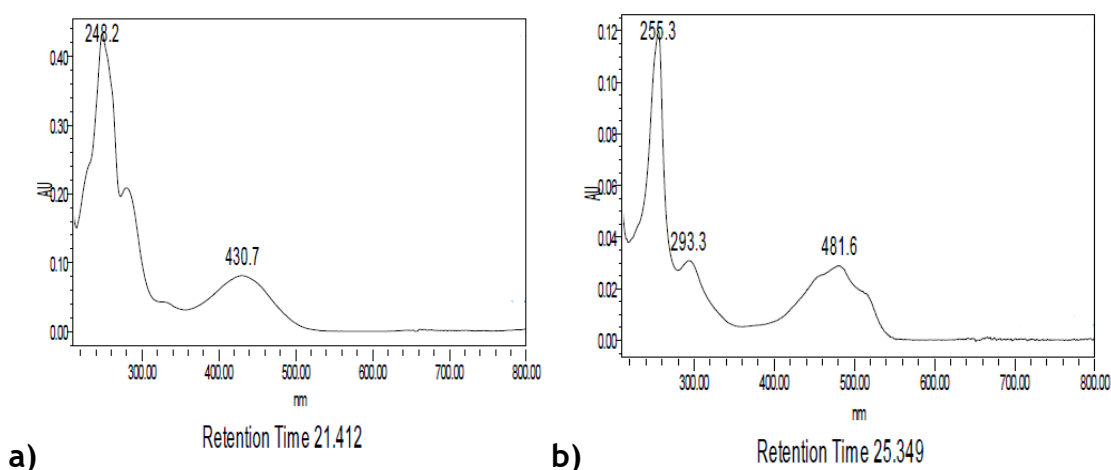


Figure 3.27. UV-Vis abs spectra of alizarin (a) and purpurin (b).

Red scale insects

Broadly speaking, red scale insects are plant parasites from the Coccidae superfamily; they all contain anthraquinones that define their ability to dye [46, 69]. Different species, originally from distinctive geographical areas, can be indicated as red dye insects, but the ones considered the most important in dyeing history are: American cochineal (*Dactylopius coccus* Costa); kermes (*Kermes vermilio* Planchon); Polish cochineal (*Porphyrophora polonica* L.); Armenian cochineal (*Porphyrophora hamelii* Brandt); lac (*Kerria lacca* Kerr).

HPLC-PDA analysis allows to easily distinguish lac from the other animal sources thanks to the univocal presence of laccaic acids as the main chromophores [57,

70]. On the other hand, the use of kermes can be successfully revealed when kermesic and flavokermesic acids are detected as principal compounds, since they are the predominant dyeing matters within this type of red scale insect [71-73].

When carminic acid is found to be the main component, this indicates the use of cochineal species. To further discriminate between *D. coccus*, *P. polonica*, and *P. hamelii*, Wouters and Verhecken suggested to evaluate the ratio of minor compounds, namely dcII (7-C-glucoside of flavokermesic acid [47]), flavokermesic and kermesic acid [74]. Nevertheless, it has been highlighted that this approach may be misleading as it does not consider changes in the ratios due to factors such as the extraction method, the dyeing conditions, the fibres, the larger number of cochineal species potentially available, the ageing [72]. For these reasons, when the historical contextualisation of the artworks does not allow to exclude some of the sources (e.g. [75]), studies can only generically report the use of a carminic acid containing insects [58, 71, 76]. Because of this, when a precise identification of the type of insects is needed, Serrano et al. advise to combine the qualitative and quantitative data from the chromatographic analysis with chemometric methods. This approach would enable to further discriminate species on the basis of statistical differences [72, 77, 78].

In the investigated fragments, carminic acid and dcII were only detected in sample T2_We.Red, as portrayed by the chromatogram and spectra in Figure 3.28 and Figure 3.29. Revealing the two markers in the red specimen from fragment T2, led to the identification of a red scale insect (cochineal species).

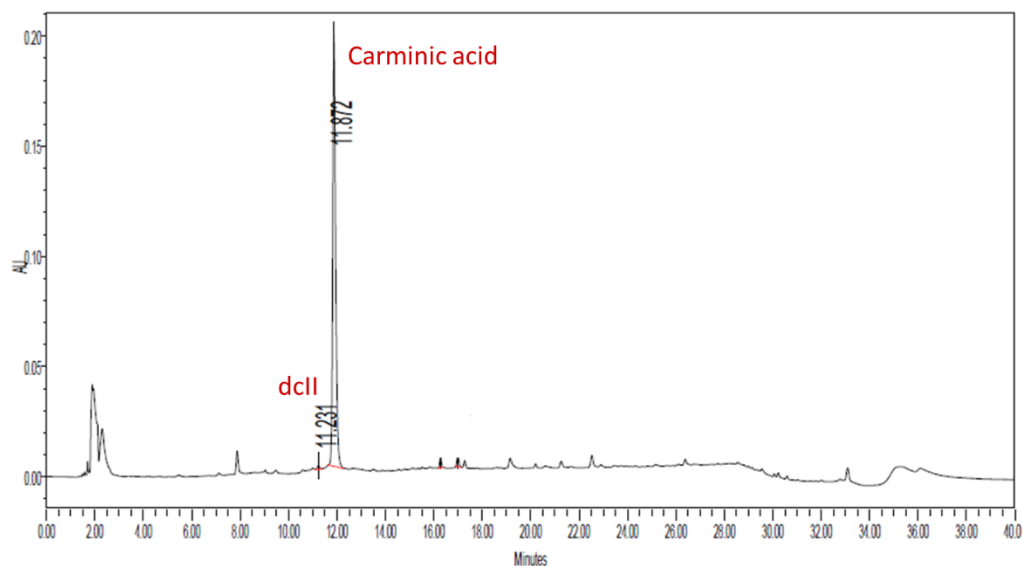


Figure 3.28. Chromatogram, acquired at 255 nm, from the analysis of sample T2_We.Red.

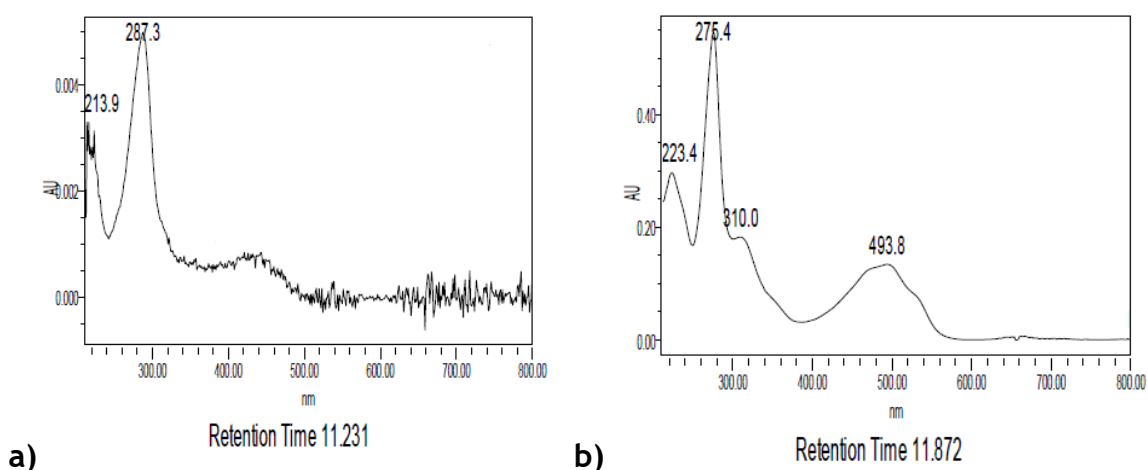


Figure 3.29. UV-Vis abs spectra of dcII (a) and carminic acid (b).

Tannins

Tannins, chemically described as polymeric polyphenols, have been widely used in the making of fine arts objects: from the preparation of leather [79], to the weighting of silk fibres [80] and the production of iron-galls inks [81]. Regarding the dyeing process, traditionally they were sometimes employed as assistants when combined with other colourants (like young fustic), with the purpose of enriching the intensity of the hue [51]. Alternatively, they were also used as colourants to produce grey, brown and black shades, when they were used together with metal salts for mordanting [51, 63, 69]. Tannins are contained within several plants, such as some from the *Fagaceae* family (oak galls) and

some *Alnus* species (alder bark) [46, 51]. Depending on the vegetal source, tannins are present in different parts of the plant and are formed through various processes. For instance, Aleppo galls are caused by wasps puncturing the buds of *Quercus infectoria* Oliv. for laying their eggs [51]. Based on the specific chemical structure, the number of vegetal tannins is vast; nevertheless, they are conventionally grouped into two main categories: hydrolysable tannins and condensed tannins. Hydrolysable tannins mainly contain gallic acid and ellagic acid; on the other hand, condensed tannins are made of flavonoids [79, 82].

When ellagic acid is detected through HPLC-PDA analysis within historic samples, this reveals the presence of hydrolysable tannins. Unfortunately, up to now, often the technique is unable to further discriminate the vegetal source [52, 54, 66, 83]. However, in the case of sources historically widespread in China, i.e. gallnut and acorn cup, Han et al. further characterised the related tannins (also by coupling the HPLC system with electrospray ionisation mass spectrometer as the detector), to enable a more precise identification [14, 84].

Based on the detection of ellagic acid, it can be stated that hydrolysable tannins were used for dyeing sample T1_We.DBrown and T3_We.Black. In addition to ellagic acid eluted at 14.6 min, gallic acid was revealed in T1_We.DBrown. The chromatogram showing the peaks related to the two markers is depicted in Figure 3.30, while the corresponding UV-Vis spectra are illustrated in Figure 3.31.

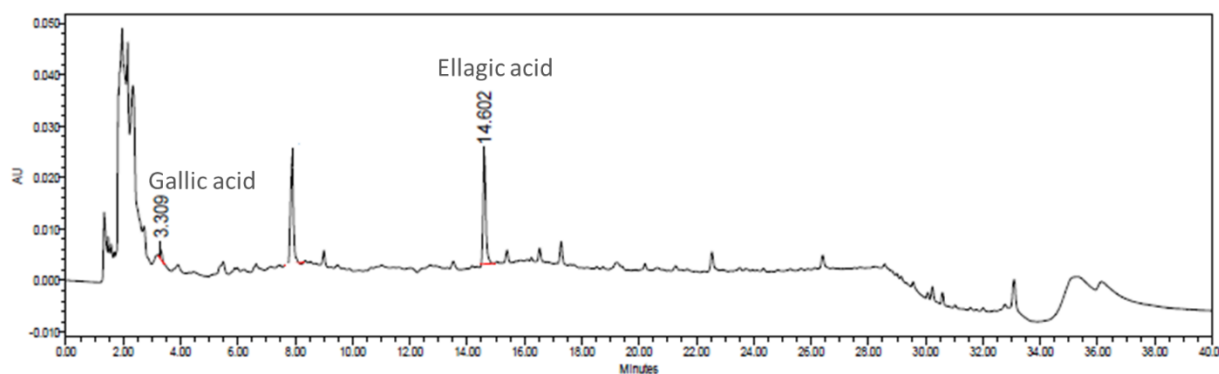


Figure 3.30. Chromatogram, acquired at 255 nm, from the analysis of sample T1_We.DBrown.

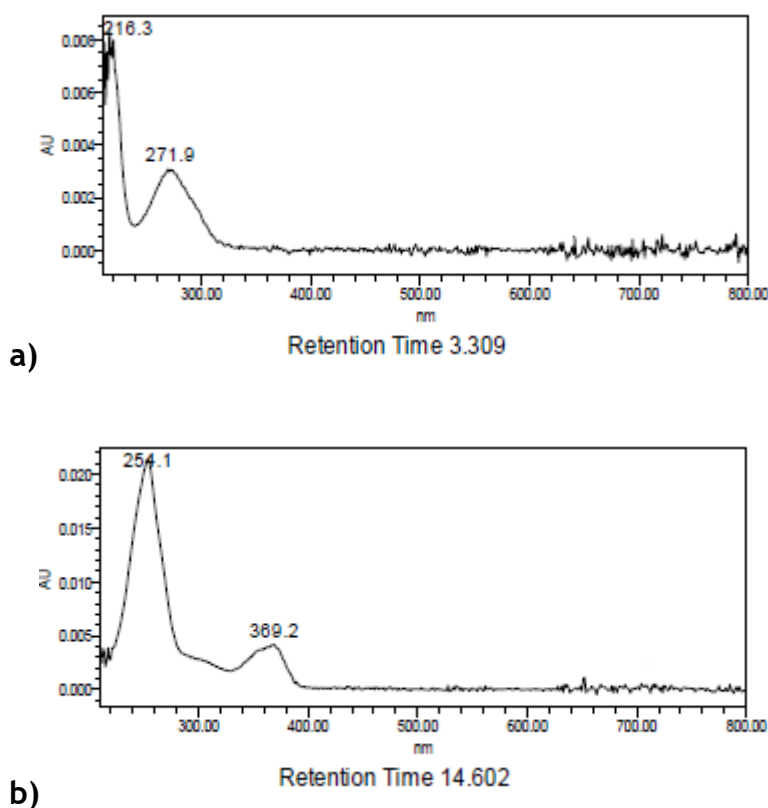


Figure 3.31. UV-Vis abs spectra of gallic acid (a) and ellagic acid (b).

Interestingly, besides ellagic and gallic acid, a coloured compound was revealed in specimen T1_We.DBrown. The component was eluted at 9 min and, as shown in Figure 3.32, its UV-Vis absorbance spectrum presented maximum wavelength at around 360, 290, and 250 nm. The marker is not reported among the references in the instrument libraries, nor in literature. Nevertheless, a small project, promoted by Dr Nobuko Shibayama and carried out at the Scientific Research Department of the Metropolitan Museum of Art in 2017, first attempted to associate the compound to logwood, *Haematoxylum campechianum* L. (native of the Yucatan peninsula) [85]. The dyeing properties of logwood, useful to obtain different colours like purple, blue and black, depend on the presence within the tree of homoisoflavanone haematoxylin. Although haematoxylin is colourless, it can be converted through oxidation by air into haematein, coloured but not lightfast [46]. Because of the low photo-stability of the principal dyeing component, the use of logwood in historical samples is usually based on the detection of a haematein derivate, first described by Hulme et al. in 2005 [86]. Since this marker is only solubilized when samples are treated with a HCl solution, if a mild extraction method is employed, as is usually now preferred, detecting logwood may be challenging [86]. Following the work

started by Shibayama, Wertz et al. possibly linked a compound found in Turkey red prints to logwood [87]. The component, with very similar RT and UV-Vis absorbance spectrum to the unknown compound here described, was revealed by Wertz et al. using the same equipment and methods as the current work. Further analysis involving mass spectrometry would be helpful in providing more precise information on the compound and its origin.

From an historical perspective, the combination of logwood and tannins as sources for the dark dyeing of sample T1_We.DBrown seems reasonable and in agreement with other research [46, 83]. However, logwood has been rarely detected in European tapestries [51]; this could be linked to: I) the difficulties of the HPLC-PDA analysis just discussed; II) the availability of the dyestuff. Indeed, although logwood has been imported into Europe from South America since the 16th century, laws and conflicts limited its trade. For instance, an English law issued in 1580 forbade the use of logwood as the colours obtained were too fugitive, and also to foster the trade of local woad [46].

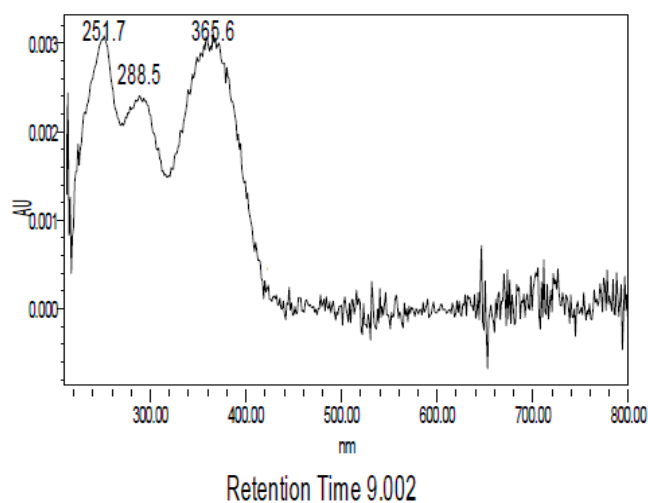


Figure 3.32. UV-Vis abs spectrum of unknown compound detected in T1_We.DBrown, possibly associated to logwood.

Indigotin-based sources

Indigotin represents the most widespread and historically relevant blue dyeing compound. This component, chemically classified as an indigoid chromophore, can be found in several plants from different botanical families diffused worldwide [46]. Among them, important ones are the European woad (*Isatis*

tinctoria L.) and the Asian indigo plant (*Indigofera tinctoria* L.). The dye, sometimes indicated with the generic term indigo, requires different steps for fixing into the fibres. Namely, the process includes a chemical reaction (reduction) to form a water-soluble compound from indigotin, that otherwise cannot be solubilised in water. Because of the type of dyeing method, indigo can be classified as vat colourant [46, 51]. In addition to indigotin, another coloured component within woad and indigo plants is indirubin. Although indigotin and indirubin are present in many botanical sources, they are formed from different chemical precursors, and via various processes [51, 88]. Regarding the use of HPLC-PDA analysis, in general the identification of indigotin states the use an indigo source, e.g. [42, 52, 54]. Due to the similar chemical composition and the many variables involved, recognising the exact dyeing plant employed is still difficult, as stated also by recent works [89].

Unsurprisingly, indigotin, UV-Vis absorbance spectrum in Figure 3.34, was detected in sample T5_We.Blue (chromatogram in Figure 3.33). While T5_We.Blue was likely only dyed with indigo, indigotin was found as minor compound in other weft threads of different colours (Table 3.8). As already mentioned, in such cases it is likely that indigo plants were employed together with other colourants and sources to obtain a wide range of shades.

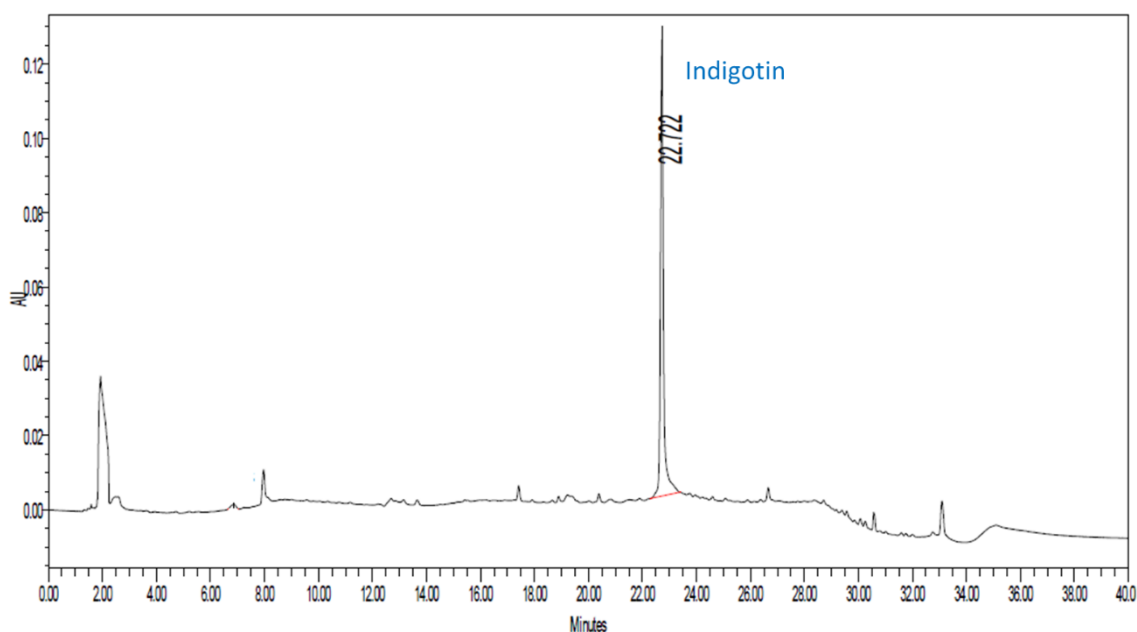


Figure 3.33. Chromatogram, acquired at 255 nm, from the analysis of sample T5_We.Blue.

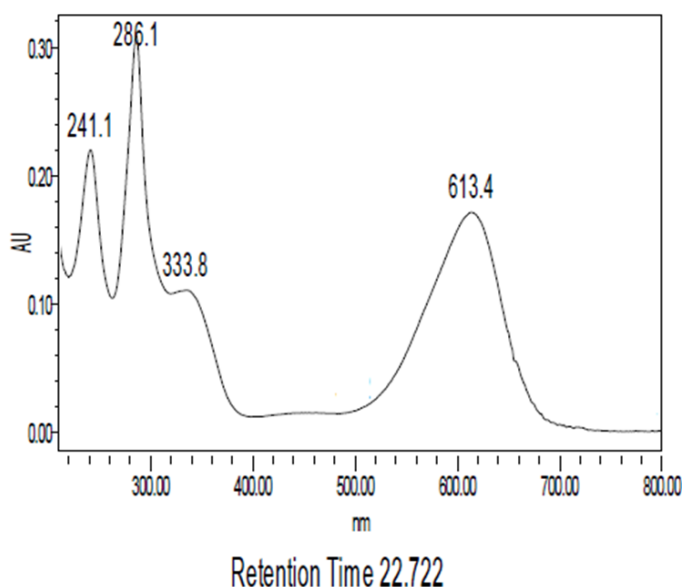


Figure 3.34. UV-Vis abs spectrum of indigotin.

3.2.4 Connecting the data from the multi-analytical investigation of historic samples

The results from both the tensile testing and the ATR-FTIR analysis were in agreement and proved the low strength and high chemical degradation of samples from fragments T3 and T5, in particular when considering the undyed warp threads. On the other hand, it is interesting to note that specimens from T2 showed the greatest breaking stress but, at the same time, a relatively high CA/Amide III ratio. These data seem to contradict themselves, but it could be hypothesised that the very dense weave structure of T2 largely impacted its tensile strength and so minimised effects linked to cystine conversion to CA.

In Figure 3.35 are depicted the combined data from the ATR-FTIR and UHPLC-PDA analyses. Looking at the graph, first it is pinpointed that, among samples from T1 and T3, threads dyed with tannins presented the greatest CA signal. Tannins are known to promote chemical degradation of wool, also linked to cystine oxidation, perhaps because of the combined use with the photosensitiser Fe^{3+} [2, 90]. This is usually acknowledged also by textile conservators, who are empirically aware of the high fragility of brownish/dark areas in tapestries [91]. Besides confirming the great weakness of wool dyed with tannins, it is noted that specimens with a luteolin-containing source showed a remarkable CA peak. In particular, this is true in comparison to samples dyed with indigo (T5).

Interestingly, these outcomes, although they are not relevant from a statistical perspective, agree with the findings from the MODHT project. During this past project, dyeing with weld was considered possibly detrimental due to the photo-tendering action of luteolin (thought this was not further linked to CA formation) [1]. On the other hand, the use of indigotin-based plants was thought not to impact wool degradation as the related dyeing conditions were usually not aggressive (i.e. high pH, low temperature) [2]. It is important to underline that further research, and a larger number of samples, are needed to define more precisely the chemical degradation processes promoted by the dyeing.

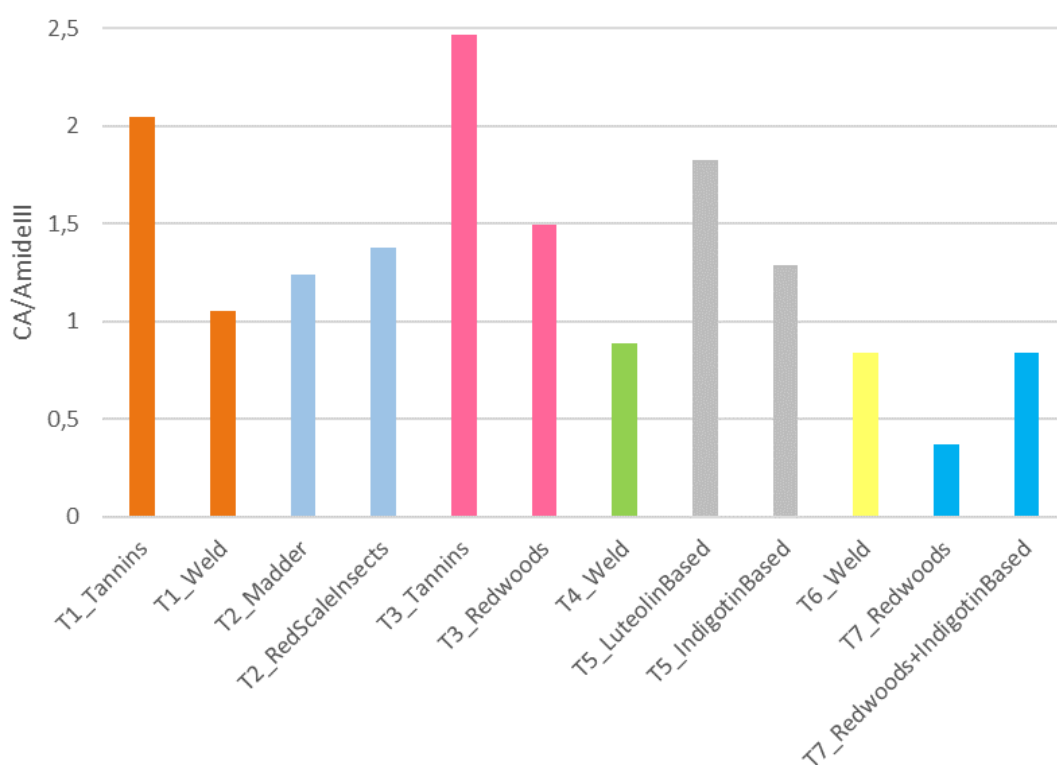


Figure 3.35. CA/AmideIII ratio and dye sources of weft threads from historic samples.

In conclusion, combining all the information from the three material analysis techniques again underpins that defining the state of degradation of tapestries is extremely complex. For the first time, the work reported here connected information on the chemical and physical properties of actual historic hangings, enriching the knowledge on the different factors behind structural damage. Importantly the results show that, even when the chemical degradation of wool (cystine oxidation) is found to be remarkable, the textile may still preserve a good tensile strength thanks to its characteristic weave and thread structure.

Similarly, the impact of the dyeing process, and so the treatment with aggressive conditions and/or materials, may affect the chemical degradation only partly. In addition, the (length of) exposure to different environmental factors should be considered a relevant caveat, though further research is needed to clarify which parameters are the most significant.

3.3 Conclusions

Chapter 3 aimed to investigate the tensile behaviour of tapestries and which factors may affect it. To do so, specimens from seven historic hangings, stored at the CTCTAH, were cut and uniaxially tensile tested. Furthermore, warp and weft threads were collected from the same samples and analysed through ATR-FTIR and UHPLC-PDA. While ATR-FTIR analysis was employed to help quantifying chemical degradation of wool due to cystine oxidation, UHPLC-PDA was used to identify dyeing sources. The multi-analytical strategy is built on previous studies on tapestries, nevertheless, it differs from them, as they examined chemical and physical variables separately and/or not on fragments from historic artworks. In addition to historic samples, uniaxial tensile testing was carried out on the wool rep fabric to be employed in the following chapters for studying the efficacy of conservation strategies. This allowed an assessment of the similarity between the newly woven textile and actual tapestries.

The results from the mechanical characterisation of tapestry fragments highlighted that, although all stress-strain curves presented similar features, properties like stress at failure and Young's modulus varied significantly. Besides variabilities linked to the chemical degradation of fibrous materials, the density of the weave seems to be a determining factor for understanding the tensile strength of the historic hangings. This is an important contribution to the findings from the MODHT project, as the previous study did not take into account the impact of differences in the weave on the structural stability.

The uniaxial tensile testing carried out on the wool rep fabric confirmed a certain similarity with the mechanical behaviour of historic hangings, especially when looking at the stress-strain curves. It is remarked that, since the newly woven wool fabric is warp-faced, and not weft-faced as are actual tapestries, warp threads have features like historic weft yarns, and vice versa. Therefore,

from this moment on, to avoid confusion the weft direction of the wool rep fabric is referred to as warp, and warp as weft.

The chemical characterisation of the historic woollen samples through ATR-FTIR and UHPLC-PDA analysis led to some similar observations to those from the MODHT project (e.g. the negative impact of tannins, spectral differences possibly due to the variable exposure to environmental factors). In general, the good agreement between the data here collected and those from the previous project confirmed the validity of the non-destructive approach (ATR-FTIR) for assessing the level of chemical degradation in wool. Nevertheless, the current study provided new insights on the interpretation of some spectral differences in naturally aged samples. Although it can be concluded that there are several parameters that may compete, including the dyeing process, tracking the amount of CA can be a helpful tool to gain a first estimation of the level of wool deterioration. A relevant observation drawn from the ATR-FTIR analysis is that humidity may greatly determine chemical deterioration of tapestry fibre materials, also in comparison to light. Importantly, this was observed through the investigation of warp threads (not studied before), unexposed to light.

References

1. Odlyha, M., C. Theodorakopoulos, and R. Campana, *Studies on woollen threads from historical tapestries*. Autex Research Journal, 2007. 7(1): p. 9-18.
2. Quye, A., et al., *'Wroughte in gold and silk' : preserving the art of historic tapestries*. 2009, Edinburgh: NMS Enterprises Limited-Publishing. viii, 134 p.
3. Hacke, A.M., *Investigation into the Nature and Ageing of Tapestry Materials*, in *Faculty of Engineering and Physical Sciences*. 2006, University of Manchester
4. Máximo Rocha, P., D. D'Ayala, and C. Vlachou-Mogire, *Methodology for tensile testing historic tapestries*. IOP Conference Series: Materials Science and Engineering, 2018. 364: p. 012003.
5. Duffus, P., *Manufacture, analysis and conservation strategies for historic tapestries*, in *Faculty of Engineering and Physical Sciences*. 2013, University of Manchester.
6. Kissi, N., et al., *Developing a non-invasive tool to assess the impact of oxidation on the structural integrity of historic wool in Tudor tapestries*. Heritage Science, 2017. 5(49).
7. Dulieu-Barton, J.M., et al., *Assessing the feasibility of monitoring the condition of historic tapestries using engineering techniques*. Key Engineering Materials, 2007. 347: p. 187-192.
8. Ye, C.C., et al., *Applications of polymer optical fibre grating sensors to condition monitoring of textiles*. Journal of Physics: Conference Series 2009. 178: p. 012020.
9. Khennouf, D., et al., *Assessing the Feasibility of Monitoring Strain in Historical Tapestries Using Digital Image Correlation*. Strain, 2010. 46(1): p. 19-32.
10. Lennard, F. and J.M. Dulieu-Barton, *Quantifying and visualizing change: Strain monitoring of tapestries with digital image correlation*. Studies in Conservation, 2014. 59(4): p. 241-255.
11. Standard, B., *BS EN ISO 13934-1:2013*. 2013.
12. Bilson, T., D. Howell, and B. Cooke, *Mechanical Aspects of Lining 'Loose Hung' Textiles*, in *Fabric of an exhibition: an interdisciplinary approach. Preprints 1997*, Canadian Conservation Institute: Ottawa. p. 63-69.
13. Carr, C.M. and D.M. Lewis, *An FTIR spectroscopic study of the photodegradation and thermal degradation of wool*. Journal of the Society of Dyers and Colourists, 1993. 109(1): p. 21-24.
14. Han, J., *The historical and chemical investigation of dyes in high status Chinese costume and textiles of the Ming and Qing dynasties (1368-1911)*, in *School of Cultural and Creative Arts College Of Arts*. 2016, University of Glasgow.
15. Wertz, J., *Turkey red dyeing in late-19th century Glasgow: Interpreting the historical process through re-creation and chemical analysis for heritage research and conservation*, in *School of Culture and Creative Arts College of Arts*. 2017, University of Glasgow.
16. Quye, A., D. Cardon, and J.B. Paul, *The Crutchley Archive: Red Colours on Wool Fabrics from Master Dyers, London 1716-1744*. Textile History, 2020: p. 1-48.

17. De Luca, E., et al., *Multi-technique investigation of historical Chinese dyestuffs used in Ningxia carpets*. Archaeological and Anthropological Sciences, 2016. **9**(8): p. 1789-1798.
18. Hacke, M., et al. *Investigation into the Nature and Degradation of Historical Wool Tapestries*. in *11th International Wool Textile Research Conference*. 2005. Leeds, UK.
19. Bratasz, L., et al., *Risk of Climate-Induced Damage in Historic Textiles*. Strain, 2015. **51**(1): p. 78-88.
20. Young, C.R.T., *Measurement of the Biaxial Tensile Properties of Paintings on Canvas*, in *Department of Mechanical Engineering*. 1996, Imperial College, University of London.
21. Smith, M.J., T.H. Flowers, and F.J. Lennard, *Mechanical properties of wool and cotton yarns used in twenty-first century tapestry: Preparing for the future by understanding the present*. Studies in Conservation, 2015. **60**(6): p. 375-383.
22. Millington, K.R., *Photoyellowing of wool. Part 1: Factors affecting photoyellowing and experimental techniques*. Coloration Technology, 2006. **122**(4): p. 169-186.
23. Derrick, M., D. Stulik, and J.M. Landry, *Infrared Spectroscopy in Conservation Science*. Scientific Tools for Conservation. 1999, Los Angeles: Getty Conservation Institute. x, 235 p.
24. Gilbert, A.S., *IR Spectral Group Frequencies of Organic Compounds*, in *Encyclopedia of Spectroscopy and Spectrometry*, J.C. Lindon, Editor. 2000, Academic Press. p. 1035-1047.
25. Bruni, S., et al., *Identification of Natural Dyes on Laboratory-Dyed Wool and Ancient Wool, Silk, and Cotton Fibers Using Attenuated Total Reflection (ATR) Fourier Transform Infrared (FT-IR) Spectroscopy and Fourier Transform Raman Spectroscopy*. Applied Spectroscopy, 2011. **65**(9): p. 1017-1023.
26. Garside, P., S. Lahlil, and P. Wyeth, *Characterization of Historic Silk by Polarized Attenuated Total Reflectance Fourier Transform Infrared Spectroscopy for Informed Conservation*. Applied Spectroscopy, 2005. **59**(10): p. 1242-1247.
27. Koperska, M.A., et al., *Degradation markers of fibroin in silk through infrared spectroscopy*. Polymer Degradation and Stability, 2014. **105**: p. 185-196.
28. Badillo-Sanchez, D., et al., *Understanding the structural degradation of South American historical silk: A Focal Plane Array (FPA) FTIR and multivariate analysis*. Scientific reports, 2019. **9**(1): p. 1-10.
29. Vilaplana, F., et al., *Analytical markers for silk degradation: comparing historic silk and silk artificially aged in different environments*. Analytical and Bioanalytical Chemistry, 2015. **407**: p. 1433-1449.
30. Koperska, M.A., T. Łojewski, and J. Łojewska, *Evaluating degradation of silk's fibroin by attenuated total reflectance infrared spectroscopy: Case study of ancient banners from Polish collections*. Spectrochimica Acta Part A: Molecular and Biomolecular Spectroscopy, 2015. **135**: p. 576-582.
31. Church, J.S. and K.R. Millington, *Photodegradation of wool keratin: Part I. Vibrational spectroscopic studies*. Biospectroscopy, 1996. **2**(4): p. 249-258.
32. Zeng, Y., et al., *Application of electron paramagnetic resonance spectroscopy, Fourier transform infrared spectroscopy-attenuated total*

- reflectance and scanning electron microscopy to the study of the photo-oxidation of wool fiber*. Analytical Methods, 2015. 7(24): p. 10403-10408.
33. Millington, K.R. and J.S. Church, *The photodegradation of wool keratin II. Proposed mechanisms involving cystine*. Journal of Photochemistry and Photobiology B: Biology, 1997. 39(3): p. 204-212.
 34. Luxford, N., D. Thickett, and P. Wyeth. *Applying preventive conservation recommendations for silk in historic houses*. in *Proceedings of the joint interim conference. Multidisciplinary conservation: a holistic view for historic interiors*. 2010. Rome: ICOM-CC.
 35. Grau-Bové, J. and M. Strlič, *Fine particulate matter in indoor cultural heritage: a literature review*. Heritage Science, 2013. 1(1): p. 8.
 36. Comite, V. and P. Fermo, *The effects of air pollution on cultural heritage: The case study of Santa Maria delle Grazie al Naviglio Grande (Milan)**. The European Physical Journal Plus, 2018. 133(12): p. 556.
 37. Vanden Berghe, I., *Towards an early warning system for oxidative degradation of protein fibres in historical tapestries by means of calibrated amino acid analysis*. Journal of Archaeological Science, 2012. 39(5): p. 1349-1359.
 38. Rampazzi, L., *Calcium oxalate films on works of art: A review*. Journal of Cultural Heritage, 2019. 40: p. 195-214.
 39. Calia, A., M. Lettieri, and G. Quarta, *Cultural heritage study: Microdestructive techniques for detection of clay minerals on the surface of historic buildings*. Applied Clay Science, 2011. 53(3): p. 525-531.
 40. Pinna, D., M. Galeotti, and A. Rizzo, *Brownish alterations on the marble statues in the church of Orsanmichele in Florence: what is their origin?* Heritage Science, 2015. 3(7).
 41. van Loon, A., et al., *Out of the blue: Vermeer's use of ultramarine in Girl with a Pearl Earring*. Heritage Science, 2020. 8(25).
 42. Tamburini, D., et al., *Scientific characterisation of the dyes, pigments, fibres and wood used in the production of barkcloth from Pacific islands*. Archaeological and Anthropological Sciences, 2019. 11(7): p. 3121-3141.
 43. Ioele, M., et al., *Chemical and spectroscopic investigation of the Raphael's cartoon of the School of Athens from the Pinacoteca Ambrosiana*. Applied Physics A, 2016. 122(12): p. 1045.
 44. Cariati, F., et al., *Calcium Oxalate Films on Stone Surfaces: Experimental Assessment of the Chemical Formation*. Studies in Conservation, 2000. 45: p. 180-188.
 45. Franceschi, V.R. and P.A. Nakata, *Calcium Oxalate in Plants: Formation and Function*. Annual review of plant biology, 2005. 56(1): p. 41-71.
 46. Cardon, D., *Le monde des teintures naturelles*. 2003, Paris: Belin. 783 p.
 47. Peggie, D.A., et al., *Towards the identification of characteristic minor components from textiles dyed with weld (Reseda luteola L.) and those dyed with Mexican cochineal (Dactylopius coccus Costa)*. Microchimica Acta, 2008. 162(3): p. 371-380.
 48. Troalen, L.G., et al., *Historical textile dyeing with Genista tinctoria L.: a comprehensive study by UPLC-MS/MS analysis*. Analytical Methods, 2014. 6(22): p. 8915-8923.
 49. Hulme, A.N., et al., *The chemical characterisation by HPLC-PDA and HPLC-ESI-MS of unaged and aged fibre samples dyed with sawwort (Serratula tinctoria L.)*. Dyes in History and Archaeology, 2017: p. 374-382.

50. Petroviciu, I., et al., *Flavonoid dyes detected in historical textiles from Romanian collections*. e-Preservation Science, 2014. 11: p. 84-90.
51. Kirby, J., et al., *Natural colorants for dyeing and lake pigments: practical recipes and their historical sources*. 2014, London: Archetype Publications Ltd in association with CHARISMA. 114 p.
52. Petroviciu, I., et al., *Dyes and biological sources in nineteenth to twentieth century ethnographic textiles from Transylvania, Romania*. Heritage Science, 2019. 7.
53. Paggie, D.A., *The development and application of analytical methods for the identification of dyes on historical textiles*, in *School of Chemistry*. 2006, University of Edinburgh.
54. Troalen, L.G., *Historic Dye Analysis: Method Development And New Applications In Cultural Heritage*, in *School Of Chemistry*. 2013, University Of Edinburgh.
55. Otłowska, O., et al., *Chromatographic and Spectroscopic Identification and Recognition of Natural Dyes, Uncommon Dyestuff Components, and Mordants: Case Study of a 16th Century Carpet with Chintamani Motifs*. Molecules 2018. 23(2): p. 339.
56. Wouters, J., C.M. Grzywacz, and A. Claro, *Markers for Identification of Faded Safflower (Carthamus tinctorius L.) Colorants by HPLC-PDA-MS - Ancient Fibres, Pigments, Paints and Cosmetics Derived from Antique Recipes*. Studies in Conservation, 2010. 55(3): p. 186-203.
57. Karapanagiotis, I., et al., *High-performance liquid chromatographic determination of colouring matters in historical garments from the Holy Mountain of Athos*. Microchimica Acta, 2007. 160(4): p. 477-483.
58. Karapanagiotis, I., et al., *Identification of materials in post-Byzantine textiles from Mount Athos*. Journal of Archaeological Science, 2011. 38(12): p. 3217-3223.
59. Karapanagiotis, I., et al., *Investigation of the colourants used in icons of the Cretan School of iconography*. Analytica Chimica Acta, 2009. 647(2): p. 231-42.
60. Manhita, A., et al., *Unveiling the colour palette of Arraiolos carpets: Material study of carpets from the 17th to 19th century period by HPLC-DAD-MS and ICP-MS*. Journal of Cultural Heritage, 2014. 15(3): p. 292-299.
61. Peggie, D.A., et al., *Historical mystery solved: a multi-analytical approach to the identification of a key marker for the historical use of brazilwood (Caesalpinia spp.) in paintings and textiles*. Analytical Methods, 2018. 10(6): p. 617-623.
62. Manhita, A., et al., *Ageing of brazilwood dye in wool - a chromatographic and spectrometric study*. Journal of Cultural Heritage, 2013. 14(6): p. 471-479.
63. Phipps, E., *Looking at textiles: a guide to technical terms*. 2011, Los Angeles: J. Paul Getty Museum. 94 p.
64. Shahid, M., et al., *Analytical methods for determination of anthraquinone dyes in historical textiles: A review*. Analytica Chimica Acta, 2019. 1083: p. 58-87.
65. Chahardoli, Z., I. Vanden Berghe, and M. Rocco, *Twentieth century Iranian carpets: investigation of red dye molecules and study of traditional madder dyeing techniques*. Heritage Science, 2019. 7.
66. Flowers, T.H., M.J. Smith, and J. Brunton, *Colouring of Pacific barkcloths: identification of the brown, red and yellow colourants used in*

- the decoration of historic Pacific barkcloths*. Heritage Science, 2019. 7(2): p. 1-15.
67. Mouri, C. and R. Laursen, *Identification of anthraquinone markers for distinguishing Rubia species in madder-dyed textiles by HPLC*. Microchimica Acta, 2012. 179(1): p. 105-113.
 68. Cuoco, G., et al., *Characterization of madder and garancine in historic French red materials by liquid chromatography-photodiode array detection*. Journal of Cultural Heritage 2011. 12: p. 98-104.
 69. Ferreira, E.S., et al., *The natural constituents of historical textile dyes*. Chemical Society Reviews, 2004. 33(6): p. 329-36.
 70. Szostek, B., et al., *Investigation of natural dyes occurring in historical Coptic textiles by high-performance liquid chromatography with UV-Vis and mass spectrometric detection*. Journal of Chromatography A, 2003. 1012(2): p. 179-192.
 71. Petroviciu, I., et al., *A discussion on the red anthraquinone dyes detected in historic textiles from Romanian collections*. e-Preservation Science, 2012. 9: p. 90-96.
 72. Serrano, A., et al., *Investigation of crimson-dyed fibres for a new approach on the characterization of cochineal and kermes dyes in historical textiles*. Analytica Chimica Acta, 2015. 897: p. 116-127.
 73. Zaffino, C., et al., *Online coupling of high-performance liquid chromatography with surface-enhanced Raman spectroscopy for the identification of historical dyes*. Journal of Raman Spectroscopy, 2016. 47(5): p. 607-615.
 74. Wouters, J. and A. Verhecken, *The scale insect dyes (Homoptera: Coccoidea). Species recognition by HPLC and diode-array analysis of the dyestuffs*. Annales de la Société entomologique de France (N.S.), 1989. 25: p. 393-410.
 75. Carò, F., et al., *Redeeming Pieter Coecke van Aelst's Gluttony Tapestry: Learning from Scientific Analysis*. Metropolitan Museum Journal, 2014. 49: p. 151-164.
 76. Surowiec, I., A. Quye, and M. Trojanowicz, *Liquid chromatography determination of natural dyes in extracts from historical Scottish textiles excavated from peat bogs*. Journal of Chromatography A, 2006. 1112(1): p. 209-217.
 77. Serrano, A., et al., *Analysis of natural red dyes (cochineal) in textiles of historical importance using HPLC and multivariate data analysis*. Analytical and Bioanalytical Chemistry, 2011. 401(2): p. 735-743.
 78. Serrano, A., et al., *Identification of Dactylopius cochineal species with high-performance liquid chromatography and multivariate data analysis*. Analyst, 2013. 138(20): p. 6081-6090.
 79. Falcão, L. and M.E. Araújo, *Tannins characterization in historic leathers by complementary analytical techniques ATR-FTIR, UV-Vis and chemical tests*. Journal of Cultural Heritage, 2013. 14: p. 499-508.
 80. Hacke, M., *Weighted silk: history, analysis and conservation* Studies in Conservation, 2008. 53(sup2): p. 3-15.
 81. da Costa, A.C., et al., *Scanning Electron Microscopic Characterization of Iron-Gall Inks from Different Tannin Sources - Applications for Cultural Heritage*. Chemistry and Chemical Technology, 2014. 8: p. 423-430.
 82. Degano, I., et al., *A Mass Spectrometric Study on Tannin Degradation within Dyed Woolen Yarns*. Molecules, 2019. 24(12): p. 2318.

83. Ortega Saez, N., et al., *Material analysis versus historical dye recipes: ingredients found in black dyed wool from five Belgian archives (1650-1850)*. *Conservar Património*, 2019. **31**: p. 116-132.
84. Han, J., et al., *Characterisation of chemical components for identifying historical Chinese textile dyes by ultra high performance liquid chromatography - photodiode array - electrospray ionisation mass spectrometer*. *Journal of Chromatography A*, 2017. **1479**: p. 87-96.
85. Costantini, R., N. Shibayama, and F. Carò. *Logwood blue: dyeing, fading and the possible marker compound for the HPLC-PDA identification by a mild extraction*. in *Dye in History and Archaeology 37*. 2018. Lisbon.
86. N. Hulme, A., et al., *Analytical characterisation of the main component found in logwood dyed textile samples after extraction with hydrochloric acid*, in *ICOM 14th Triennial Meeting. Preprints*. 2005. p. 783-788.
87. Wertz, J.H., A. Quye, and D. France, *Turkey red prints: identification of lead chromate, Prussian blue and logwood on Turkey red calico*. *Conservar Património: Studies in Historical Textiles*, 2019. **31**: p. 31-39.
88. Degani, L., C. Riedo, and O. Chiantore, *Identification of natural indigo in historical textiles by GC-MS*. *Analytical and Bioanalytical Chemistry*, 2015. **407**(6): p. 1695-1704.
89. Lech, K. and E. Fornal, *A Mass Spectrometry-Based Approach for Characterization of Red, Blue, and Purple Natural Dyes*. *Molecules*, 2020. **25**(14): p. 3223.
90. Sabatini, F., et al., *Investigating the composition and degradation of wool through EGA/MS and Py-GC/MS*. *Journal of Analytical and Applied Pyrolysis*, 2018. **135**: p. 111-121.
91. *Tapestry Conservation: Principles and Practice*. Butterworth-Heinemann series in conservation and museology, ed. F. Lennard and M. Hayward. 2006, Oxford: Butterworth-Heinemann. xxv, 247 p.

4 2D DIC for investigating mechanical damage mechanisms in tapestries

Chapter 4 discusses the usefulness of 2D Digital Image Correlation (DIC) for monitoring strain across historic hangings and tapestry-like materials when on display. The first section of the chapter presents a literature review on DIC, focusing on the related sources of errors. It is important to pinpoint, before the actual tests, which factors to look at to ensure the accuracy of measurements. This is particularly true when considering tapestries as case studies, since DIC needs to rely on a woven figurative design rather than an applied speckle pattern, usually employed as a correlation device. Besides the pattern, the impact of other factors is discussed in the first part of the chapter, by looking at past studies.

The following experimental part reports 2D DIC monitoring tests on different case studies, involving actual historic hangings and a wool rep fabric with tapestry-like weave structure. The experiments aimed to verify the feasibility of the optical technique for tracking displacements in larger areas of historic hangings than those previously researched ($\approx 10 \text{ cm}^2$) [1, 2]. Through the diversity of the textile objects monitored and the set-ups, different variables affecting the measurements were identified. Importantly, the 2D DIC monitoring tests also intended to investigate the potential mechanical damage mechanisms in woven hangings. Differently from the research presented in Chapter 3, here the structural stability of tapestries is studied from a macroscopic perspective and it focuses on the mechanical mechanisms occurring while the artwork is hanging.

4.1 Introduction

4.1.1 2D DIC: basic principles of the technique and common sources of errors

As briefly mentioned in Chapter 2, DIC can be defined as a contactless optical technique able to measure displacement and deformation occurring in an object subject to different loadings. Before and during the loading, images of the object are acquired, so to record the deformation. Once all the needed images

are taken, the post-processing phase begins: thanks to specific correlation algorithms, the deformation is eventually translated into displacement and strain.

DIC can be used for both 2D measurements as well as 3D ones. As suggested by the name, the 2D method can only track in-plane displacements, while 3D DIC, also called stereo-DIC, enables the measurement of out-of-plane displacements. The monitoring equipment varies depending on whether 2D or 3D DIC is used: only one camera is required for tracking 2D movements, while for 3D DIC two synchronised cameras are usually needed [3, 4].

DIC has been widely used and applied on a broad range of case studies and objectives, from defining deformations in nano/micro-scale specimens (e.g. [5, 6]) to large-scale structures such as walls (e.g. [7, 8]). In the cultural heritage sector, the use of DIC can be particularly appealing: the technique is contactless, the set-up is simple, and it allows *in situ* analysis. Compared to other state-of-the-art methods, the equipment needed is more affordable. Indeed, the technique only requires: one/two camera(s); a tripod; a DIC software. The latter can be the most expensive part of the set-up, although some open source software exists, such as Ncorr [9]. A limitation to the use of DIC is that no artificial speckle pattern, usually employed as a correlation device, can be applied on historic objects. This means that, differently from the common usage of DIC, when artworks are monitored the technique needs to rely on the intrinsic figurative pattern to track deformation.

Besides the work done on tapestries by the research group at the University of Southampton [1, 2], DIC has been employed to study deformations occurring in artworks such as: textile objects [10]; panel paintings [11-13]; canvas paintings [14-18]; wall leather decorations [19]; wood shipwrecks [20, 21].

4.1.1.1 Theoretical foundation and sources of error related to the correlation algorithm

Fundamentally, DIC works by defining how much a specific point of interest (P) has moved during a time-lapse, while capturing the movement through an image acquisition system. The point of interest is part of a square subset, which is

found within a region of interest (ROI). The region of interest is established at the beginning of the analysis, from the reference image. The reference image describes the point of interest before the occurrence of any deformation, at t_0 [22, 23]. An example of point of interest, subset, and ROI is provided in Figure 4.1.



Figure 4.1. Example of defining features in the DIC analysis: the ROI is the area indicated in red, the subset is marked by the blue line, and the point of interest corresponds to the green dot.

It should be noted that the shape and size of the subset are important variables that need to be properly selected, as they may impact the analysis accuracy. Indeed, the subset defines the amount of information available for correlation, therefore, the smaller the subset the lower the amount of information, and so the more difficult it could be to track the deformation. On the other hand, if the

subset is too big, relevant pieces of information may be overseen through averaging and not considered, leading to a miscalculation of the displacement [22-24]. This can be an issue especially when heterogeneous deformations occur [25]. Of course, the appropriate subset size (measured in pixels) would greatly depend on the speckle pattern and should be defined together with other parameters of the algorithm, such as the shape function (see below) [26]. At the beginning of the analysis, alongside the subset size, step size is chosen. The step size, defined in pixels, indicates the distance between subset centres, in both horizontal and vertical directions. The step size may vary from 1 pixel to half of the subset size and it defines the spatial resolution of data: the bigger the step size, the less the displacement measurements. Since selecting a small step size means more data to calculate, this affects the time for the analysis [25].

The deformation process tracked by DIC is schematically illustrated in Figure 4.2. From Figure 4.2, it can be seen that at t_1 , where $t_1 = t_0 + \Delta t$, P is no longer in the initial position. Therefore, the reference image at t_0 is compared to the deformed one, taken at t_1 . From the comparison of the two images, and in particular of the subset of interest at different times, the displacement of P can be calculated.

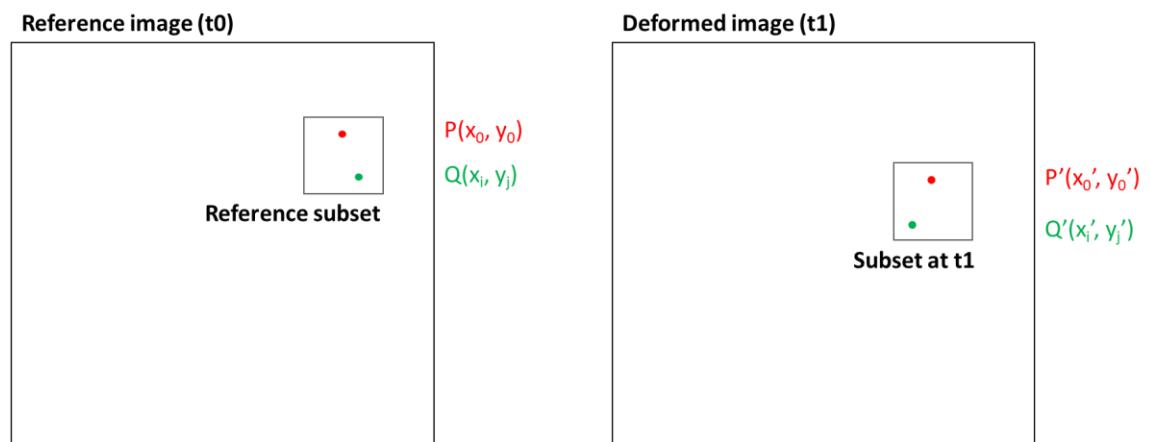


Figure 4.2. Scheme of a subset before and after deformation.

Specific algorithms enable the matching of the subset before and after deformation and so the tracking of the point of interest. These algorithms must include a proper correlation criterion, able to recognise and measure changes that have occurred in the subset over time by highlighting differences and

similarities [3]. Pan et al. in [27] classified the criteria used for DIC into four main categories: I) cross-correlation (CC); II) sum-squared difference (SSD); III) sum of absolute difference (SAD); IV) parametric sum of squared difference (PSSD). Tables summarising the most commonly used correlation-criteria for DIC can be found in review papers, e.g. [22]. In general, a good correlation criterion should not be affected by variables linked to the set-up, like uneven lightning, brightness, or contrast. Therefore, the choice of the correlation criterion is particularly important when the resolution of the images is not expected to be very high because of the experimental conditions [28].

Besides the correlation criterion, another important detail of DIC algorithm is the shape function. The shape, or displacement mapping, function describes the deformations that have occurred across the entire subset, therefore affecting all its different nodal points. When selecting the shape function, it is important to consider that different points in the same subset may move in various directions. This means that the displacement could not be accurately defined by a zero-order shape function, so a high order one should be preferred as it would better fit a broader range of deformations [26, 29].

Furthermore, different studies focused on the systematic errors caused by the fact that the coordinates of the point of interest in the deformed image may be between pixels, but the displacement is calculated considering the pixel as the minimum unit. To avoid this, algorithms able to register information at a sub-pixel level can be used [22, 30].

4.1.1.2 Experimental sources of errors

Speckle pattern

Speckle patterns, more precisely random intensity distributions, are fundamental in DIC analysis. Indeed, the speckle pattern carries the information on the deformation experienced by the specimen, allowing the algorithm to operate the correlation [31]. This correlation device can be artificially applied on the surface of the sample or sometimes it can consist of the natural intrinsic texture of the material, as later discussed. In any case, speckle patterns need to fulfil specific requirements since the quality greatly affects the accuracy and

precision of the measurements. As summarised by Dong and Pan in [31], a high quality speckle pattern requires: high contrast in the greyscale levels; non-periodic features; anisotropy (lack of orientation); stable and strong adherence to the sample surface.

When an artificial speckle is applied, some practical precautions should be taken into consideration to obtain and verify its good quality [32-36]. For instance, each subset should contain 2-3 speckles, so their size needs to conform to this [32], while avoiding any aliasing due to too small speckles (< 3 pixels) [33]. At the same time, ideally there should be 50-50% coverage of black and white [34], and speckle edges should be “soft” (with a transitional grey area) [36]. These features need to be adapted depending on the subset size, since larger subsets can allow bigger speckles [37] and/or lower density [34]. As also revised in [31], besides general qualitative indications, different theoretical assessments have been proposed to verify the quality of speckle patterns.

As mentioned above, in the current study, the application of an artificial speckle pattern can only be taken into consideration for bespoke mock-ups used as models, since no alteration can be done on actual historic objects.

Image quality: camera system and illumination

The image acquisition system, which can be a camera, but also a microscope, and the related settings greatly contribute to defining the resulting image quality and so the accuracy of DIC data. When a camera is used, the type of lens and sensor, its main components, may separately affect image quality [38]. Lenses and sensors are fundamental elements in a camera as the first enables to collect the light, while the latter permits the image to be formed and registered thanks to its sensitivity to the electromagnetic radiation [39].

For 2D DIC, Pan in 2009 recommended to use CCD (charge-coupled device) sensors [22], however later works found out that also state-of-the-art CMOS (complementary metal oxide semiconductor) sensors can lead to high quality images, feasible for DIC analysis [40]. In 2017, Hijazi and Kähler experimentally assessed the different and separate contribution of lenses and sensors on 2D DIC errors [38]. It was shown that the imaging sensor and type of camera scarcely

influence the accuracy of the data, while they may be more affected by the quality of the lenses [38]. Nevertheless, low cost devices like camera phones have also been employed for DIC measurements [41, 42]; in this case, the accuracy of the data was shown to be improved when applying appropriate error correction approaches [42].

An even illumination is needed to ensure a stable contrast over the specimen surface (and speckle pattern) during the monitoring, to enable proper correlation. Indeed, fluctuations in the light source may lead to drastic drops/growths in the greyscale level, eventually resulting in errors [24]. Because of that, for 2D DIC, adjusting the exposure time of the camera is important. When no displacement is expected to occur during the capture (slow deformations), a high exposure time can be set to avoid errors from an uneven illumination [4]. In particular, an adequate adjustment of the exposure time may play an important role in the accuracy of data from *in situ* experiments, when the environmental illumination is irregular and/or too low. As assessed by Wang et al., this can play an important role for cultural heritage applications, such as long-term monitoring in museums, since only low and uneven lighting is available [21].

Another variable to consider is the type of light source. A constant white light source is usually employed for tests in laboratory environments [43]. To allow an efficient *in situ* monitoring, Pan et al. presented a monochromatic light illuminated active imaging DIC method. The monitoring kit, besides a CMOS camera, included two monochromatic light sources and an optical bandpass filter, able to avoid the interference of unstable ambient light [43].

Furthermore, it is noted that lenses and sensors can temporarily deform because of the temperature increase (up to 10 °C) that occurs when the cameras are switched on. The phenomenon can last one or two hours and its intensity may depend on the type of lens [44] (telecentric lenses appeared to be scarcely affected by self-heating effect [45]).

Out-of-plane displacement

Three fundamental and basic requirements to ensure 2D DIC operates properly are: I) specimens have a planar surface; II) mainly in-plane deformations occur; III) the sensor plane of the camera is parallel to the specimen surface [4, 46]. These three factors are all linked to the inability of the 2D application of DIC to measure out-of-plane displacements.

Figure 4.3 depicts how out-of-plane motions of the specimen can lead to errors in the DIC analysis when using a standard lens [45, 46]. Z represents the distance between the object and the camera, while L the image distance. When the object moves of a distance ΔZ towards the lens, the out-of-plane displacement would affect the image dimensions (X , Y) and so the strain calculated by the DIC software.

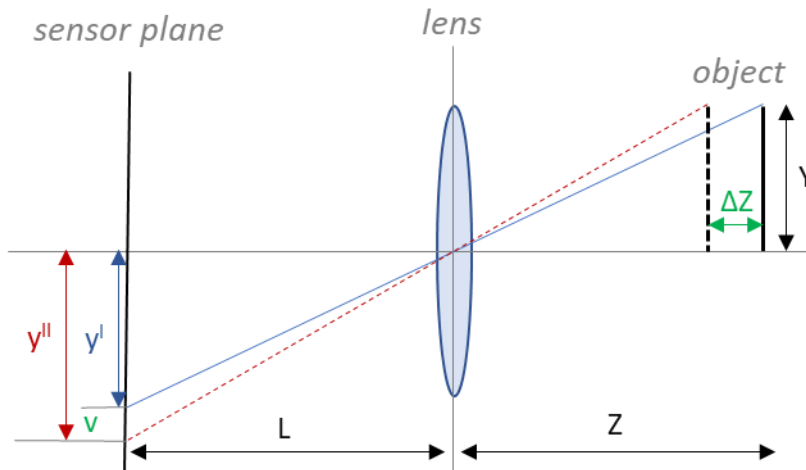


Figure 4.3. Effect of out-of-plane movement of the specimen (translation towards the lens) on the in-plane displacements calculated by DIC.

As defined by Sutton et al. [46], the resulting displacement (u horizontal, v vertical) and error strain can be measured as:

$$u(\Delta Z) \approx -L/(Z) X \cdot \Delta Z/Z \quad \text{Eq (1)}$$

$$v(\Delta Z) \approx -L/(Z) Y \cdot \Delta Z/Z \quad \text{Eq (2)}$$

$$\epsilon \approx -\Delta Z/Z \quad \text{Eq (3)}$$

When ΔZ is negative, meaning when the object is moved towards the camera, the error strain is positive, i.e. a higher extension (y direction). On the other hand, when a translation away from the lens occurs (positive ΔZ), the strain error is negative. By increasing the distance between lens and specimen (Z) the influence of some unavoidable out-of-plane displacements can be contained [46]. Besides, the use of telecentric lenses instead of standard ones can also help to increase the accuracy of the measurement [46].

4.1.2 Evaluating the usefulness of DIC as a tool to measure strain across historic hangings through synthetic deformation fields

Before employing 2D DIC for monitoring strain across large areas of historic hangings, the feasibility of the technique was first evaluated using a theoretical approach involving finite element analysis (FEA). This was done by Dr Alsayednoor, post-doctoral researcher working on the project and the main outcomes were presented in an article published in 2019 [47]. The method used by Dr Alsayednoor is based on the comparison of the 2D DIC outcomes from the analysis of the synthetic deformation of two images: I) a standard speckle pattern; II) the *Florence* tapestry from the Burrell Collection, Glasgow Museums (Figure 4.13). It is noted that a similar approach for validating DIC set-ups, by using FEA, can also be found in other studies [48, 49].

The comparison aimed to highlight whether the image of the tapestry was able to give results as accurate as those from the analysis of the speckled figure. Both starting images were deformed by applying displacement fields as indicated by the simulation; then the two sets of images were processed through DIC, to eventually compare the resulting strain data (calculated through VIC by Correlated Solutions). FEA was therefore used as a tool for predicting how a tapestry-like material would deform under the effects of self-weight loading, as the image was modified through the interpolation with the nodes of the FEA model. To make the prediction reasonably close to actual cases, the model (made through Abaqus) was fitted with parameters obtained from the mechanical characterisation of tapestry samples (the tests are presented in Section 3.2.1.1). Different scenarios were considered and modelled, adding

heterogeneities such as the presence of: I) stitched slits; II) open slits; III) local support patches.

In general, the work was able to assess that probably DIC analysis would be successful, in the case of the tapestry under investigation and when such (relevant) deformations occur. It was stressed that the technique may still lead to inaccurate strain data, especially in case of different/less busy figurative designs. In addition, actual measurements may be influenced by the out-of-plane movements of the textile object. The approach followed in the paper was indicated as a helpful pre-experimental strategy able to verify the suitability of a specific tapestry for DIC analysis, before conducting any monitoring.

Despite some advantages, it should be pinpointed that the proposed pre-testing analysis presents a relevant limit, as it does not take into consideration experimental variables that may affect image quality. Indeed, the quality of the pattern and its suitability as correlation device depends on factors such as resolution and brightness. So, in general, to assess *a priori* whether a set of images of a specific tapestry could lead to accurate DIC data, a picture of the object in the same experimental conditions should be processed through the suggested pre-testing tool. However, this can be counterproductive, as it will lengthen the testing time.

4.2 Materials and methods

In this chapter, 2D DIC was employed to monitor strain across different textile objects. The tests aimed: I) to verify the feasibility of the optical technique in measuring displacements across case studies with different features; II) to investigate which parameters may affect the accuracy of the data; III) to study the mechanical damage mechanisms occurring in historic hangings once hung for their display. The studied textiles included one newly woven wool rep fabric with two speckle patterns applied, and five historic hangings. In the following paragraphs the case studies are described in detail, together with the monitoring set-up and data processing.

It should be noted that the 2D DIC approach was preferred for the project due to limitations that 3D system may cause when setting the monitoring *in situ*. In

particular, this was first noted when preparing the monitoring of the contemporary tapestry in Stirling Castle, for which a camera was placed on the opposite wall of the hanging. Having a second camera for the 3D monitoring would have been problematic since the two needed to be synchronised and so at a fixed position, but the periodic need of changing the battery and memory card would have prevented that. Nevertheless, as just discussed in Section 4.1.1.2, it is important to underline that out-of-plane movements can lead to errors, so the 2D approach could be non-ideal for tapestries. As later discussed, the occurrence of 3D movements was tentatively prevented through monitoring most of the case studies against a board/wall that limited air circulation.

4.2.1 Case studies

4.2.1.1 Wool rep sample

Strain across a wool rep sample (37 x 37.5 cm) was monitored for 48 hours using 2D DIC (specifications and mechanical behaviour of the fabric are described in Chapter 3). Two speckle patterns were applied to the sample, as shown in Figure 4.4: I) a pattern with random dots of around 1 mm in diameter, obtained by using both a Stabilo OHPen Universal Marker™ (Fine, black) and a Sharpie Permanent Marker™ (fine, black); II) a spray pattern obtained by using a Montana Gold NC-Acrylic™ professional black spray paint.

The test aimed to evaluate whether the two patterns can be used successfully as devices for DIC correlation. This would be helpful in defining the experimental conditions for the tests reported in the following chapters.

Figure 4.4 represents the monitoring set-up. The sample was pinned from the top edge to a vertical board and the camera was placed parallel to the object, taking one picture per hour. A data logger was put close to the board, so as to monitor the environmental conditions.



Figure 4.4. Monitoring set-up of the wool rep sample with two speckle patterns applied: spray (left side), and dots (right side).

4.2.1.2 Tapestries

Five different tapestries were selected for testing the feasibility of 2D DIC in measuring strain across historic textile objects. Using various artworks with distinctive features (e.g. size, areal density, thread count, fibrous materials, figurative design) aimed to discriminate the impact of such variables in the analysis. Furthermore, factors affecting the image quality were also indirectly researched. Indeed, the monitoring set-up differed from case study to case study depending on the object and/or location specifications, e.g. different size of the artwork and/or the available lighting. The impact of these factors on the resulting image quality was also considered.

In addition to the evaluation of the usefulness of the contactless technique, monitoring five tapestries enabled to study mechanical damage mechanisms affecting historic hangings while on display. A relevant aspect to consider through the investigation of historic case studies is whether the DIC approach could help locate defects before these become visible. Indeed, as discussed in Chapter 2, during the project in Southampton the optical method was proposed

as a possible preventive tool for anticipating damage and thus for indicating areas at risk and in need of conservation.

TapestryFragment_1

TapestryFragment_1, illustrated in Figure 4.5, belongs to the Karen Finch Reference Collection, based at the CTCTAH. The textile object, 160 cm high x 40 cm width, has an areal density of 1.14 kgm^{-2} and it is made of wool (information confirmed by FTIR-ATR analysis of samples from weft and warp yarns). As Figure 4.5 shows, at the time of the test, the fragment was structurally weak: it presented several open slits (highlighted by the red line in the picture) and some detached parts.



Figure 4.5. TapestryFragment_1, Karen Finch Reference Collection, CTCTAH. Two open slits are highlighted in red.

Also when looking at the back of the tapestry it can be deduced that the fragment had a complex conservation history: some patches, made of pieces of hangings, were stitched on the back (Figure 4.6).



Figure 4.6. Detail of the back of TapestryFragment_1.

TapestryFragment_1 was selected for monitoring strain through 2D DIC (200-hour test) partly because of its weak condition, as it was thought that the effects of mechanical damage mechanisms would be more evident in such a poorly conserved piece.

TapestryFragment_1 has a relatively low thread count, namely 4 warps x 14 wefts per 10 mm. A magnified picture of the coarse weave structure of the historic hanging is provided in Figure 4.7.



Figure 4.7. Weave structure of TapestryFragment_1 showing horizontal warps and vertical wefts, as it would hang (55x magnification).

TapestryFragment_2

A second tapestry fragment belonging to the Karen Finch Reference Collection was monitored using 2D DIC for 168 hours. TapestryFragment_2 is depicted in Figure 4.8. Like TapestryFragment_1, it is characterised by different damaged areas. Namely, on the left part, extensive areas of bare warps are shown, while on the right, a large open slit is present, as better portrayed in Figure 4.9. The fragment has an irregular shape: it is 16.5 cm high on the right side and 61.5 cm on the left side. The top has a maximum width of 141.5 cm.



Figure 4.8. TapestryFragment_2, Karen Finch Reference Collection, CTCTAH.



Figure 4.9. Detail of the front of TapestryFragment_2 showing an open slit.

Differently from the first fragment, in this case it can be noted that the figurative design is less busy, especially on the left-side area and bottom right-side part, where a homogeneous brownish pattern is present. This could mean

that the response of the correlation algorithm in tracking strain may be different as the level of contrast here is less marked.

Preliminary FTIR-ATR analysis assessed that TapestryFragment_2 is made of wool (warp and weft) and silk (weft). Unlike TapestryFragment_1, this historic textile has a relatively fine weave, as shown in Figure 4.10 (9 warps x 25 wefts per 10 mm).



Figure 4.10. Weave structure of TapestryFragment_2 showing horizontal warps and vertical wefts, as it would hang (57x magnification).

Kesi

In addition to historic tapestries from the European tradition, strain across a *kesi*, also belonging to the Karen Finch Reference Collection, was monitored. The circular shaped textile object, with a diameter of 80 cm, is shown in Figure 4.11. It is important to note that the *kesi* is extremely light-weight, 11.40 g, especially when compared to the other tapestries studied.



Figure 4.11. *Kesi*, Karen Finch Reference Collection, CTCTAH.

As mentioned in Chapter 1, *kesi* have the typical tapestry weave structure but they are mainly made of silk, instead of wool. Moreover the weave of *kesi* is very fine (i.e. 22 warps x 15 wefts per 10 mm, in this case study) and may present painted areas and metal threads, as shown in the magnified pictures of Figure 4.12. Through Figure 4.12, the complexity of the weave of *kesi* can be observed, also noting how the geometry of weft yarns is not as regular as in the case of European tapestries. Indeed, it includes a round-shaped pattern, usually termed eccentric weaving. Another detail to highlight is that, when the studied *kesi* is displayed, coloured weft yarns run horizontally, and not vertically like in European traditional tapestries. As depicted in Figure 4.11, during the monitoring the *kesi* was displayed hanging vertically against a magnetic board. The Chinese artwork was suspended from the board using some small magnets placed on the top border.

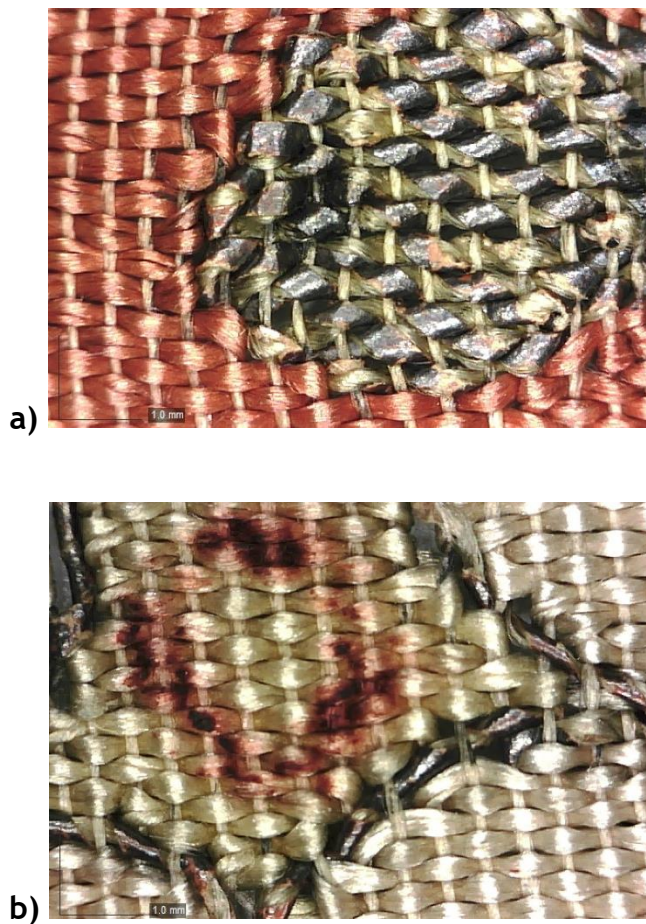


Figure 4.12. Details of weave structure of *kesi* (58x magnification): a) area with metal threads; b) painted decoration and metal threads.

Historic tapestry conserved with full support

A historic tapestry from the Burrell Collection belonging to Glasgow Museums was monitored for 100 hours after being conserved with a full support treatment. The tapestry is called *Two Episodes from a Chivalric Romance, perhaps the tale of Florence of Rome*, abbreviated from this moment on to *Florence*. This test represents the first attempt of monitoring a historic hanging in its entirety, but also a first investigation through DIC on the mechanical behaviour of a tapestry after conservation.

Table 4.1 gathers historical and manufacturing details of the studied tapestry, while Figure 4.13 depicts the historic hanging. From Figure 4.13b, taken in transmitted light, the poor mechanical condition of the tapestry before conservation is evident: there were many (failed) slits and areas of loss across the entire surface.



a)



b)

Figure 4.13. Florence tapestry: a) direct light; b) transmitted light. Registration number: 46.93. © CSG CIC Glasgow Museums Collection.

Table 4.1. Details of *Florence* tapestry.²

Title	Two Episodes from a Chivalric Romance, perhaps the tale of Florence of Rome
Date of manufacture	Late 15 th century
Provenance	Burgundy
Size, height [cm]	207 (left) x 210 (right)
Size, width [cm]	298 (top) x 301 (bottom)
Weight [kg]	4.9 (before wet cleaning, although no extensive loss of original material was noticed after the treatment)
Fibre, warp	Wool (Z twist 3 x 5 plied)
Fibre, weft	Wool (Z twist 2 x 5 plied); Silk (Z twist 2 x 5 plied)
Thread count	7 warps x 11 wefts per 10 mm

The tapestry underwent two main phases of the conservation process: while the first consisted of the application of a linen full support stitched through a grid lined system (42.5 mm distance between grid lines, leaving 10 mm excess of fabric), the second concerned local treatments, like slits re-stitching. The local treatments were carried out through the support fabric. The strain monitoring, whose results are presented in this chapter, was carried out right after the first phase of conservation, i.e. the application of the linen full support.

Contemporary tapestry at Stirling Castle

Besides the historic hangings described in the previous paragraphs, a contemporary tapestry was monitored using 2D DIC. The tapestry, originally called *The Mystic Hunt of the Unicorn* but here referred with the name *Unicorn tapestry* for simplicity (details in Figure 4.14), was woven by the West Dean Tapestry Studio. This was done as part of a project that involved the Studio between 2001 and 2013, aiming to reinterpret the series of the *Hunt of the Unicorn*, originally made in the Netherlands between the late XV-early XVI century. The historic set of tapestries now belongs to the Metropolitan Museum of Art and it is on display at the Cloisters Museum [50, 51]. The weaving of the new series was commissioned by Historic Scotland and it is part of a big

² Data taken from the condition report by Meggie Dobbie (Glasgow Museums), 2011.

renovation project by the organisation, aiming to reproduce the original appearance of the XVI century Scottish castle [51].



Figure 4.14. Details of *Unicorn tapestry*. The figurative design of the contemporary piece was greatly inspired by that of *The Unicorn Surrenders to a Maiden* belonging to the Metropolitan Museum of Art (accession number: 38.51.2).

Also for ethical reasons, the new *Hunt of the Unicorn* set was woven introducing some significant differences from the original pieces. For instance, the new weave structure is less fine (4 warps, instead of 8, per 10 mm) and the metal threads are wrapped in gold instead of silver leaf [51]. In addition, the warp threads are made of cotton, not wool, and the woollen weft yarns are dyed with synthetic colourants instead of natural ones. In 2015, Smith et al. published a study on the mechanical properties of the fibrous materials employed in the contemporary hangings, with the aim of providing information on the conditions of wool and cotton yarns at t_0 , before the occurrence of any degradation process [50].

Regarding the size, it is reported that the contemporary tapestries are around 10% smaller than the original ones [51], meaning that the case study has a total length of around 180 cm.

Once completed, the contemporary tapestries were hung on the wall of Stirling Castle (Queen's Inner Hall), where the artwork has been monitored since first hung (June 2015) until August 2020.

4.2.2 Monitoring set-up and strain calculation

The strain monitoring of both wool rep sample and actual tapestries was carried out by taking one picture per hour, although the duration of the test varied from case study to case study (Table 4.2). This was done automatically, using an auto shutter connected to the camera, alongside a charger kit that prevented the use of batteries. At all times, the camera was fitted on a tripod (in the case of the monitoring at Stirling, fixed on the wall). All these precautions were needed to maintain a constant distance between lens and specimen and to prevent any movement of the camera.

The first picture was taken within around the first 10 seconds of the textile object being hung (to track displacement post self-weight loading) but after two hours of the camera being turned on, to avoid lenses distortion. A Canon EOS 1000D™ (manual mode, no flash, 100 ISO, f/8 aperture, exposure time 1/4 s)³ was employed for all the tests, except for the monitoring of the tapestry at Stirling, where a Nikon D7000 was employed. Both cameras have a CMOS sensor.

2D DIC analysis was performed on the acquired images using Vic-2D 2009 by Correlated Solutions. The following parameters were employed: optimised 8-tap interpolation shape function, normalised squared differences and Gaussian weights, exhaustive search, low-pass filter, and incremental correlation. These parameters were chosen following recommendations from Dr Alsayednoor, who found them to be the most suitable for accurate results in similar conditions [47]. Since such details of the correlation algorithm were evaluated by the post-

³ The camera set-up was selected following recommendations from Iona Shepherd (Glasgow Life), Santiago Arribas Peña (photographer with Historic Scotland), Stephen McCann and Sam Dyer (University of Glasgow Photo Unit). The recommendations took into consideration the different lighting conditions and the need to avoid image noise.

doctoral researcher working on the project, they were not further considered in this thesis. A subset size of 61 and a step size of 5 were selected for all case studies. In certain cases, the analysis was repeated by processing the set of images with a lower subset size (31) or step size (3), so as to assess the impact of such parameters in the measurement of displacement. The Hencky strain was calculated using the DIC software and the data were then transferred to MATLAB to allow further analysis. In particular, through MATLAB, strain data across specific areas of the investigated objects were averaged, following the method first proposed by the research group in Southampton [1]. Namely, once the data were transferred in MATLAB, a strain map of the object at the end of the test was opened and, from that, the area of interest was selected. MATLAB mean function was then used for averaging the data so as to obtain one strain value representing the deformation of the area during each moment of the monitoring. This allowed the definition of deformations affecting the overall surface of the studied textiles, even when local strain data were expected to be unreliable from what indicated by the sigma maps. Furthermore, the method was useful to study how different regions of the object moved, in particular to distinguish the behaviour across open slits from that across the rest the artwork.

Table 4.2 provides details of the monitoring tests and details of the experimental design, highlighting the justifications that led to the choice of the case studies. It is added that artificial lighting was used during all the experiments (except for *Unicorn tapestry*, illuminated by natural light) and that all the textile objects were displayed against a vertical surface, i.e. a board or the wall (not covered to prevent friction), to avoid out-of-plane movements (except for *Florence*, which was free-hanging).

A data logger (Hanwell Pro ML4000) was placed close to all case studies to record the environmental conditions (RH and temperature) every 15 minutes. This was needed as the environmental parameters were unstable in all the monitoring locations. Temperature data are not discussed in the following paragraphs as they were found to be usually more stable than RH and always unrelated to strain measurements.

Table 4.2. Details of monitoring tests and of the experimental design.

Object code	Hypothesis	Monitoring Location	Test duration	Limitations of DIC analysis
Wool rep	The wool rep fabric, with a proper speckle pattern applied, can be used as a representative material for evaluating the efficacy of conservation strategies through DIC	Photo Studio Robertson Building	48 hours	Possible out-of-plane movements, contained by the presence of a board behind the object
TapestryFragment_1	DIC can be used to track strain across areas of tapestries larger than 10 cm ² and it allows to gather data on the mechanical behaviour, especially in the case of highly damaged artefacts	Photo Studio Robertson Building	200 hours	Possible out-of-plane movements, contained by the presence of a board behind the object
TapestryFragment_2	DIC can be used to track strain across areas of tapestries larger than 10 cm ² and it allows to gather data on the mechanical behaviour, even when the pictorial motif is homogeneous	Project Room Robertson Building	168 hours	Possible out-of-plane movements, contained by the presence of a board behind the object
<i>Kesi</i>	Silk artefacts, besides wool hangings, can be successfully monitored through DIC	Project Room Robertson Building	68 hours	Possible out-of-plane movements, contained by the presence of a board behind the object
<i>Florence</i>	Information on the mechanical behaviour of tapestries, especially recently conserved ones, can be gathered from their full-field monitoring	Textile Conservation Studio Glasgow Life	100 hours	Air circulation promoted by conservators working below the tapestry (suspended from a batten) possibly leading to out-of-plane movements
<i>Unicorn tapestry</i>	Information on the mechanical behaviour of tapestries, especially contemporary ones exposed to wide RH levels, can be gathered	Queen's Inner Hall Stirling Castle	5 years ⁴	Uneven lighting; movement of the camera when changing battery/memory card; possible

⁴ It is noted that data were not reliably gathered for all the 5-year period, as discussed in Section 4.3.2.5.

	from their full-field monitoring			out-of-plane movements, contained by the presence of the wall behind the object
--	----------------------------------	--	--	---

4.3 Results and discussion

4.3.1 Wool rep sample

Strain across a wool rep fabric sample with two different speckle patterns applied (dots and spray) was monitored through 2D DIC for 48 hours. This test aimed to evaluate the suitability of two patterns as means for correlation. The results were useful to define the experimental conditions for the following chapters, as wool rep specimens were employed to compare treatments and display methods for tapestries.

4.3.1.1 Causes of strain

The average strain (longitudinal and horizontal) calculated across the entire surface of the wool rep fabric is plotted in Figure 4.15. Together with the strain, humidity fluctuations are reported in the same graph. From Figure 4.15, it is clear that there is no direct proportionality between time and strain, since there was not a constant increase in either ϵ_{xx} or ϵ_{yy} during the 48 hours of monitoring. However, strain in both directions was demonstrated to change according to variations in humidity, that fluctuated between a maximum of 53.4% and a minimum of 45.3%.

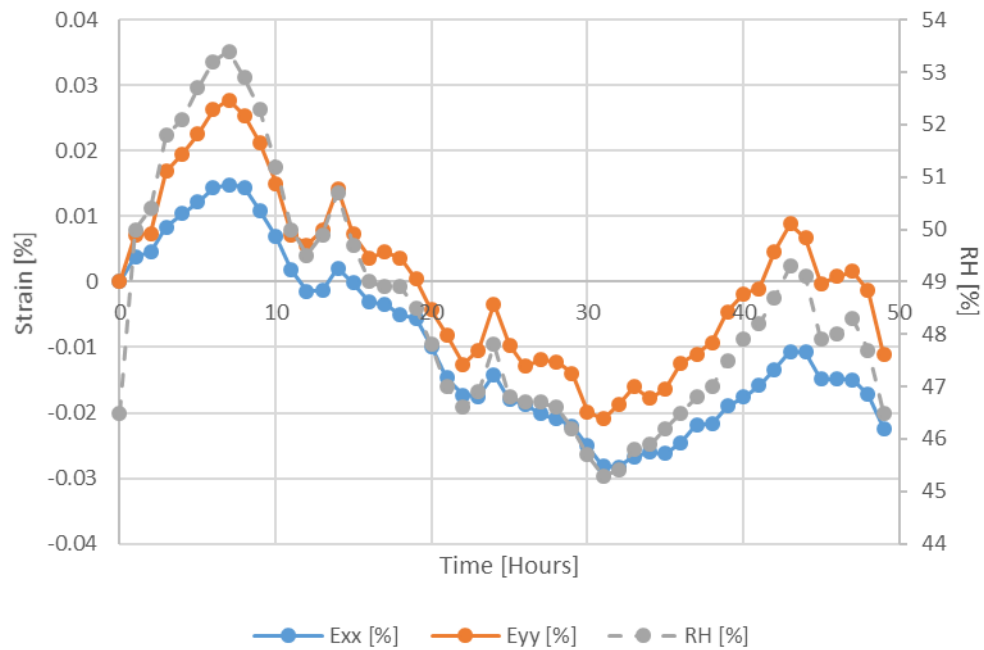
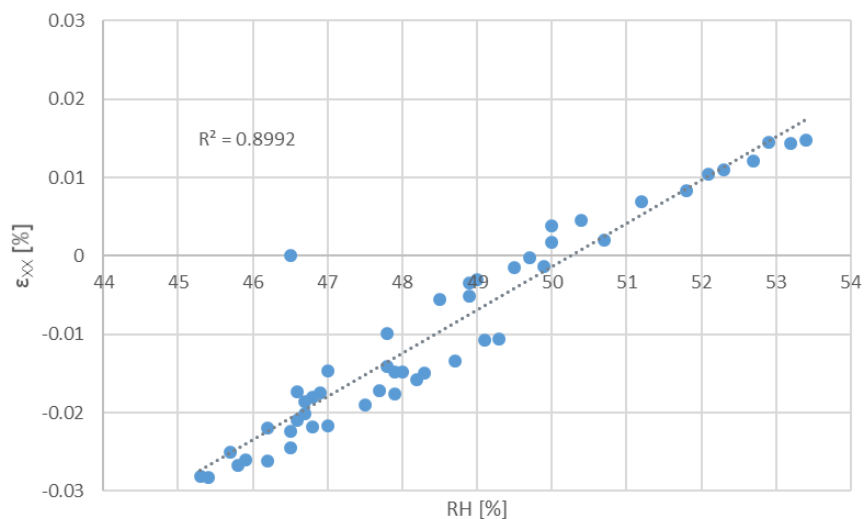
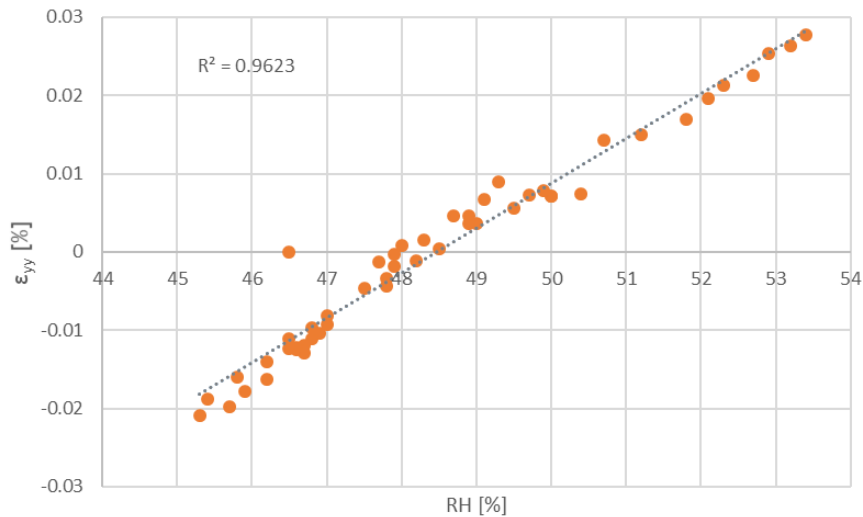


Figure 4.15. Mean ϵ_{xx} and ϵ_{yy} [%] of the wool rep sample with two speckle patterns during the 48-hour monitoring. RH [%] is indicated by the dotted line.

In Figure 4.16 the good linear relationship between strain, both ϵ_{yy} and ϵ_{xx} , and RH is stated, as the coefficients of determination, R^2 (a statistical measure to define the linearity between two variables), are close to 1. Longitudinal strain data gave a better fit (R^2 0.96) than ϵ_{xx} (R^2 0.90).



a)



b)

Figure 4.16. Mean strain [%], longitudinal (a) and horizontal (b), during the 48-hour monitoring of the wool rep sample plotted against RH [%].

The registered extensions/contractions, especially those in the vertical direction, were probably due to variations in weight of the woollen sample because of absorption/desorption of water from the environment. This indicates the occurrence of fatigue mechanisms. However, since changes occurred also in the horizontal direction, this reveals that humidity variations were also responsible for the swelling of the fibrous material.

As mentioned in Chapter 2, when considering the effects of fatigue, it is important to underline that the linear relationship between strain, due to changes in weight, and RH can only be observed within specific intervals, such as the one experienced during the monitoring (45-53% RH). Indeed, the response of moisture content within natural fibres, thus including wool, from 0 to 100% RH, is sigmoidal and not linear. In addition, the complex relationship between moisture uptake and humidity conditions is also linked to: I) the difference in rate between absorption and desorption; II) the hysteresis phenomenon; III) the prolonged time needed for the water content to reach the equilibrium [10, 52]. As mentioned in Section 2.2.1.2, this means that data gathered on the strain response of the case studies here investigated to RH fluctuations would be unable to build an accurate mathematical model for predicting the mechanical behaviour of tapestries. In general, the damage function would not be linear, and additionally it would need to consider several parameters characteristic of each artwork, as also proved by the tests in Chapter 3. Although *modelling* the

behaviour of historic hangings goes beyond the objectives of the current study, gathering more data though the *monitoring* represents a crucial step [53].

In Figure 4.17 the strain maps of the sample are shown. It is interesting to note that the ϵ_{yy} map reveals alternating areas of high and low strain on the side with the spray pattern applied (left side of the sample, indicated by the dotted red line). On the other hand, ϵ_{yy} across the right-side area with dots is more homogeneous.

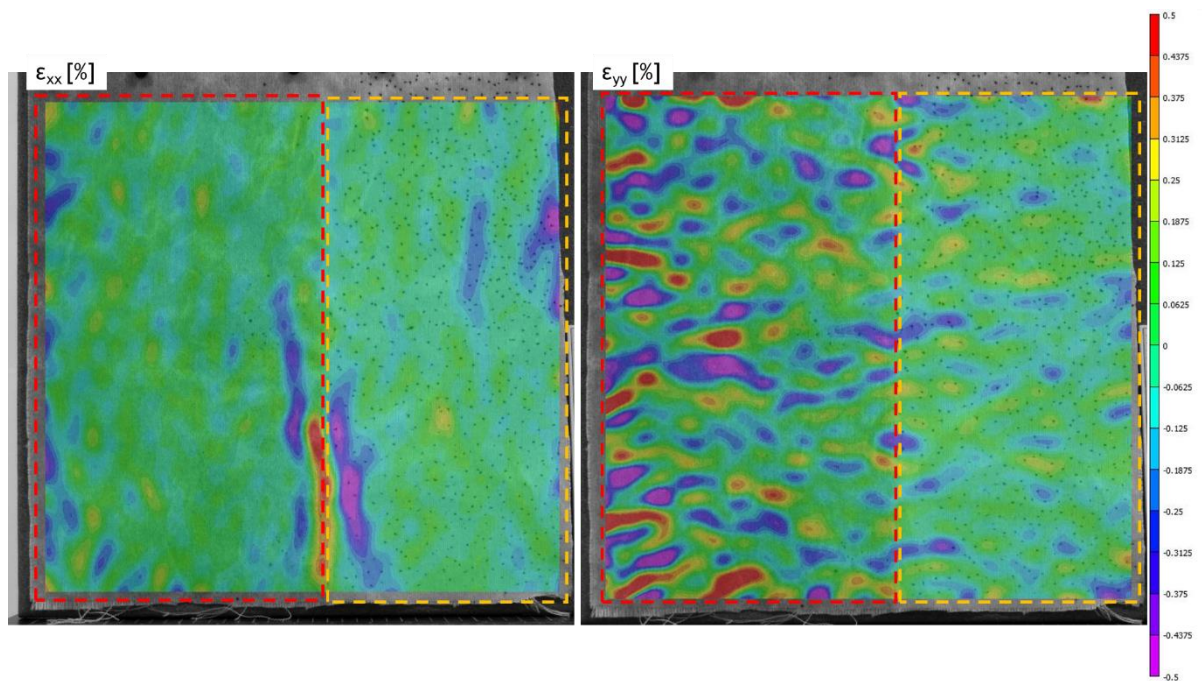


Figure 4.17. Strain maps, ϵ_{xx} and ϵ_{yy} [%], of the wool rep sample with two speckle patterns (spray pattern on the left side, dotted pattern on the right side) at the end of the 48-hour monitoring.

4.3.1.2 Evaluation of artificial speckle patterns as correlation devices

Some first observations on the accuracy of the two patterns can be drawn from the error map in Figure 4.18. Figure 4.18 illustrates the errors in the investigated area expressed in sigma, where sigma represents the confidence interval for the match at that point in pixels. In Vic-2D software, high sigma indicates low confidence, while the closer sigma is to 0, the more (statistically) likely the values are to be correct [54]. It is highlighted that no further explanation is given by Correlated Solutions on how the data are generated in Vic-2D [54].

From Figure 4.18, it can be stated that the spray pattern gave less accurate results compared to the dotted one. It seems likely that this contained efficiency mainly affects the accuracy of strain data on a small-scale level; this would justify the alternating (small) areas of high and low strain observed in the strain map of Figure 4.17. The lower accuracy of the spray pattern may be due to the textile features: the wool fabric presents a hairy surface that prevented the paint from properly depositing, hence the paint only stained the hairs. This eventually resulted in a relatively homogeneous black pattern, not properly adhered to the moving surface.

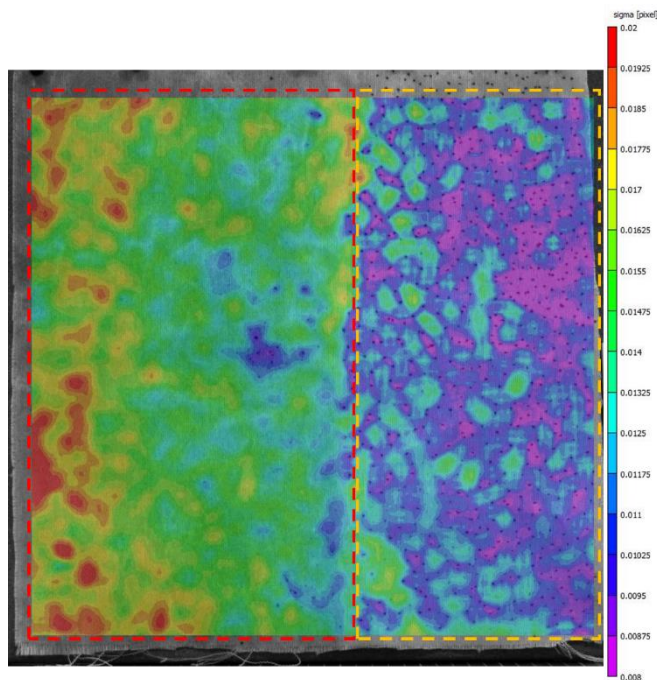


Figure 4.18. Error map expressed in sigma [pixel] of the wool rep sample with two speckle patterns (spray pattern on the left side, dotted pattern on the right side) at the end of the 48-hour monitoring.

The average longitudinal strain data across the two areas with sprayed and dotted patterns were then calculated, separately to allow their comparison. From the observations drawn in the previous paragraph, it is expected that the strain data from the analysis of the dotted pattern would better fit the RH values. This is confirmed when looking at graphs in Figure 4.19, depicting the linear fitting of strain against humidity. Since the coefficient of determination R^2 is very close to 1, ≈ 0.97 , this proves the good fitting of the data from the pattern with dots. It should be underlined that the average strain from the sprayed area was also shown to be directly proportional to RH, however with a

worse fitting ($R^2 \approx 0.94$) perhaps indicating lower accuracy and higher errors. It is important to note that two groups of ϵ_{yy} data in Figure 4.19 are clearly represented by different equations, with different slope as well as x axis crossing. This likely reflects divergency in the accuracy.

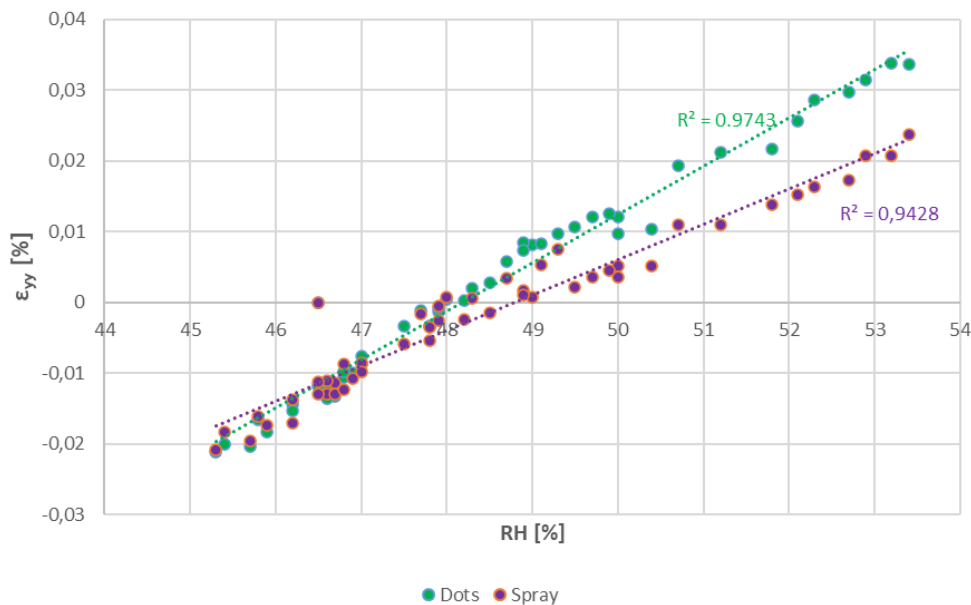


Figure 4.19. Mean longitudinal strain calculated across the area with dotted pattern (green) and sprayed pattern (purple) against RH [%].

From a quantitative point of view, the maximum longitudinal strain reached was around 0.03%, that, considering a total length of 37 cm, corresponds to an extension of around 0.01 cm. On the other hand, the minimum strain was -0.02% and it can be translated as a compression of around 0.007 cm. Therefore, the DIC outcomes demonstrated that only minimal and reversible variations occurred. Nevertheless, the technique proved to be sensitive enough to properly detect such displacements, more accurately when the dotted pattern was used.

Both the very good linearity between strain and RH, as well as the reasonable quantitative strain data, established the viability of 2D DIC as a monitoring tool in similar experimental conditions. Although the past research in Southampton already looked at the influence of dotted patterns applied on a similar wool rep fabric (see review in Section 2.2.1) [1, 55], the outcomes could not be directly related to the current study. Therefore, the tests presented in this section were needed to better adapt to the aims and methodology of the research in this

thesis. As a main difference, here 2D DIC was selected, while 3D DIC was preferred by the previous research group. In addition, the sizes of woollen mock-ups for testing conservation approaches (Chapter 5 and 6) would need to be bigger than those considered in the experiments from 2010 (15 x 5 cm [1]). Because of this, a larger wool rep sample was here tested.

4.3.1.3 Evaluation of DIC parameters: subset size, step size

The 2D DIC analysis of the wool rep fabric was repeated using different parameters than those employed for the strain measurements presented in sections 4.3.1.1 and 4.3.1.2. In the previous paragraphs the set of images was processed using a subset size of 61 and a step size of 5, while in this paragraph lower subset and step sizes were selected to analyse the same set of images. The aim of this series of tests was to understand whether these DIC parameters may have an impact on the data.

Figure 4.20 presents the strain data calculated across the dotted area of the wool rep sample, when using the different parameters. Similarly, Figure 4.21 shows the trend of the strain data measured, with the various subset and step sizes, across the area with the sprayed pattern. Already from these graphs, it can be noted that the strain calculation seems to be scarcely affected by decreasing the step size from 5 to 3, or the subset size from 61 to 31. Indeed, a more significant difference was underlined between the measurements on the two areas with different patterns (Section 4.3.1.2).

It should be underlined that, since the real value of strain and displacement is not known, it is not possible to properly define accuracy. Therefore, in this case the deviance from the 61_5 data is considered. In general, such parameters are proposed as the most convenient in comparison to the others. Indeed, a step size of 5 would shorten the correlation calculation time, while a subset size of 61 can be considered more appropriate to the type of homogeneous deformation studied [47].

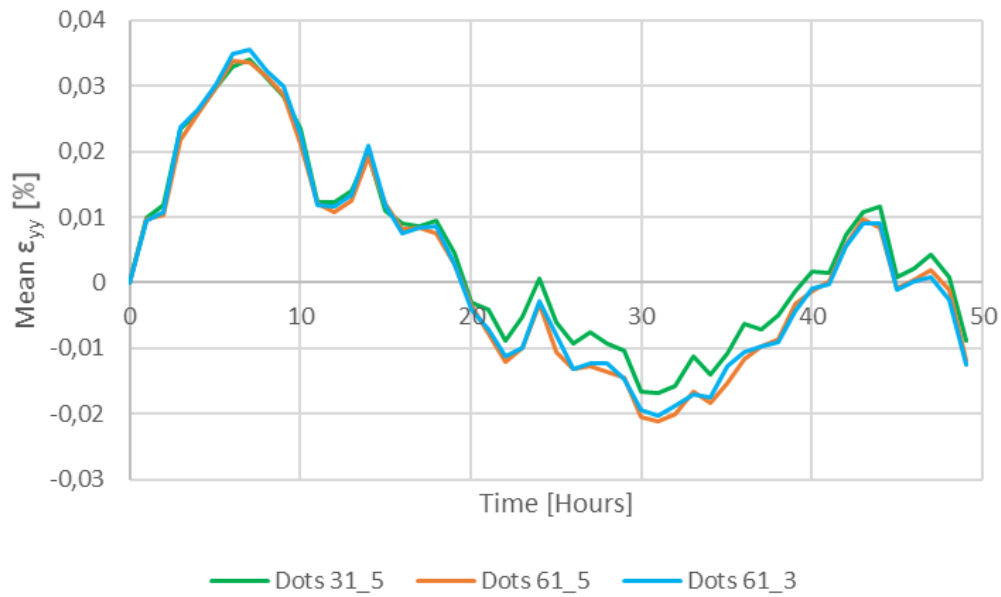


Figure 4.20. Mean ε_{yy} [%] calculated across the area with dotted pattern using different DIC parameters: 31 as subset size, 5 as step size (green line); 61 as subset size, 5 as step size (orange line); 61 as subset size, 3 as step size (blue line).

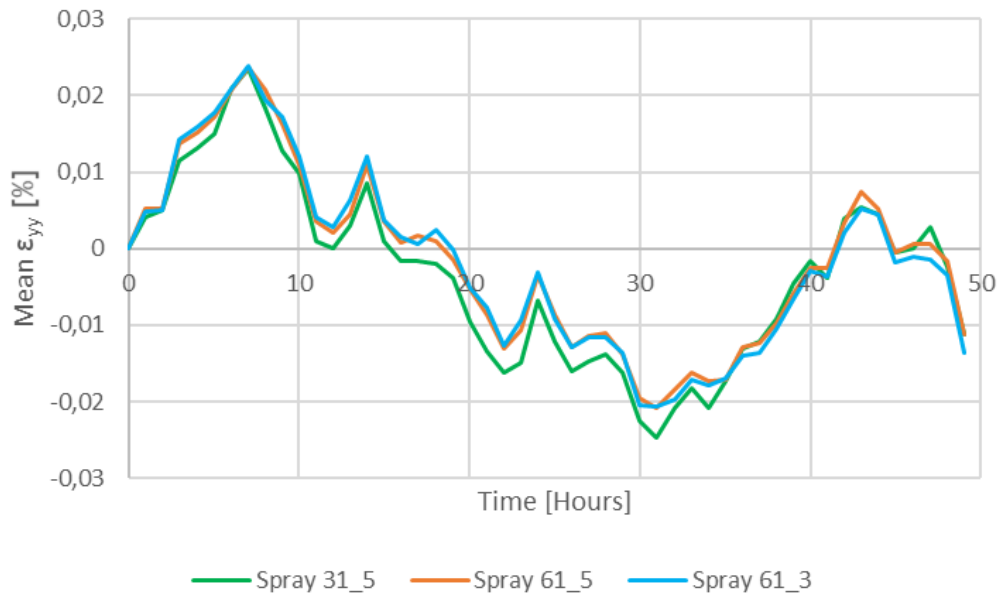


Figure 4.21. Mean ε_{yy} [%] calculated across the area with sprayed pattern using different DIC parameters: 31 as subset size, 5 as step size (green line); 61 as subset size, 5 as step size (orange line); 61 as subset size, 3 as step size (blue line).

The good agreement of the data obtained from processing the images with the different sets of parameters is also stated from the linear fitting, as shown in Figure 4.22. The R^2 values from the fitting of the three different sets of data are reported in Table 4.3: in all three cases, R^2 is between 0.97-0.98. Importantly, slope and x axis crossing of the three plots are alike. This differs from what observed from the comparison of the two patterns (Figure 4.19). Because of this,

it can be suggested that subset and step sizes had less an impact on the accuracy of data than the type of pattern applied.

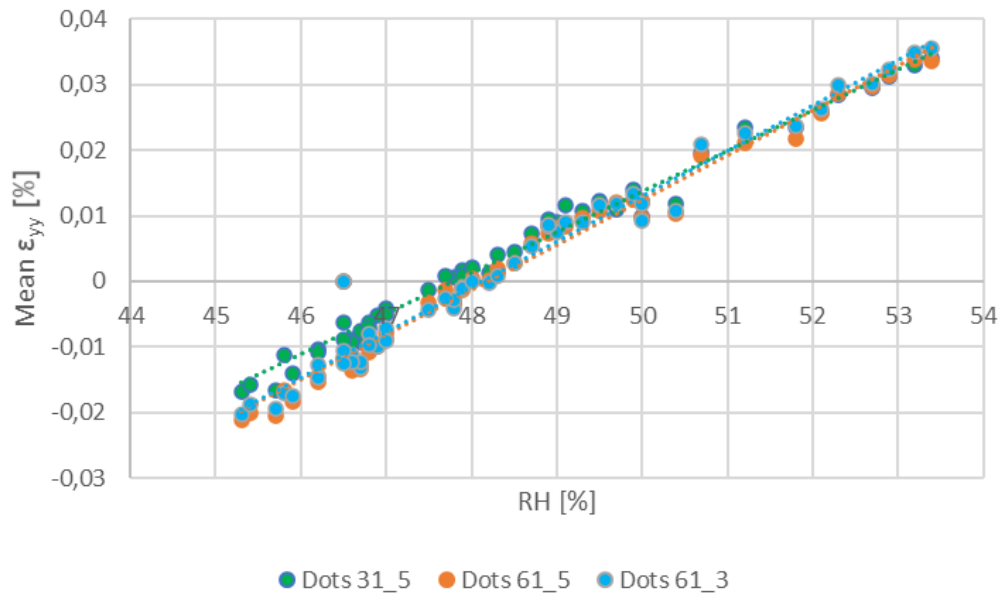


Figure 4.22. Mean ϵ_{yy} [%] calculated across the area with dotted pattern using different DIC parameters.

Table 4.3. R^2 from the linear fitting of ϵ_{yy} [%] calculated from the DIC analysis of the wool rep sample (dotted pattern) with different parameters.

Subset Size - Step Size	R^2
31 - 5	0.9786
61 - 5	0.9743
61 - 3	0.9770

4.3.2 Tapestries

As done for the wool rep sample, 2D DIC was used to monitor strain across five different tapestries. The test aimed to define the usefulness of DIC when considering actual historic textile objects as case studies. Moreover, the experiments pointed to the identification of mechanical damage mechanisms affecting tapestries when on display.

4.3.2.1 TapestryFragment_1

Strain across TapestryFragment_1 was monitored for 200 hours using 2D DIC. At the time of the experiment, the historic hanging was evidently in weak condition.

Figure 4.23 and Figure 4.24 report globally averaged ϵ_{xx} and ϵ_{yy} data obtained from the monitoring of TapestryFragment_1, respectively. In the two figures RH fluctuations are also indicated. It is clear that the overall strain across the entire surface of the fragment, in both the horizontal and longitudinal direction, is strongly linked to the variations in humidity. This shows the occurrence of fatigue and swelling, as observed for the wool rep fabric (Paragraph 4.3.1.1). It is highlighted that mean ϵ_{yy} was greater than ϵ_{xx} . This can be expected, as self-weight loading would contribute to the longitudinal extension of the fragment, and more greatly in this case study since the fragment has a longitudinal shape and so its weight is mainly distributed in the vertical direction. On the other hand, loading is not expected to impact strain variations in the horizontal direction, therefore swelling can be considered responsible for ϵ_{xx} variations.

It is noted that, although changes in lengths promoted by RH variations are expected to be reversible and discrete, these can be detrimental on a long term due to their cycling nature, possibly determining failure. Indeed, strain cycling may lead to fretting process, as neighbouring threads move against each other with friction. Therefore, when historic hangings are exposed to uncontrolled environments, the constant friction can cause the rupture of wool, already strained by the self-weight loading. As mentioned in Chapter 2, the actual damage caused by fretting fatigue in tapestries is still debated [10].

Nevertheless, according to the study conducted in 2015 by Bratasz et al., no remarkable damage should occur over a 274-year period in tapestries that experience strain (up to 1%) due to RH fluctuations [10].

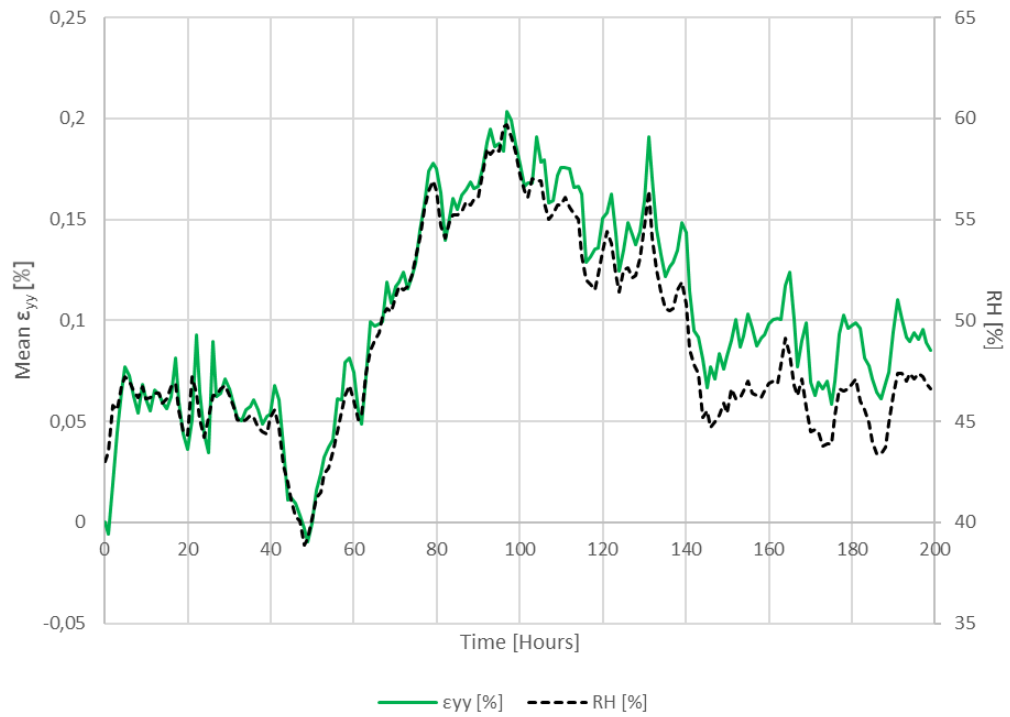


Figure 4.23. Mean ε_{yy} [%] calculated across the entire surface of TapestryFragment_1 against time. RH [%] fluctuations are indicated by the dotted line.

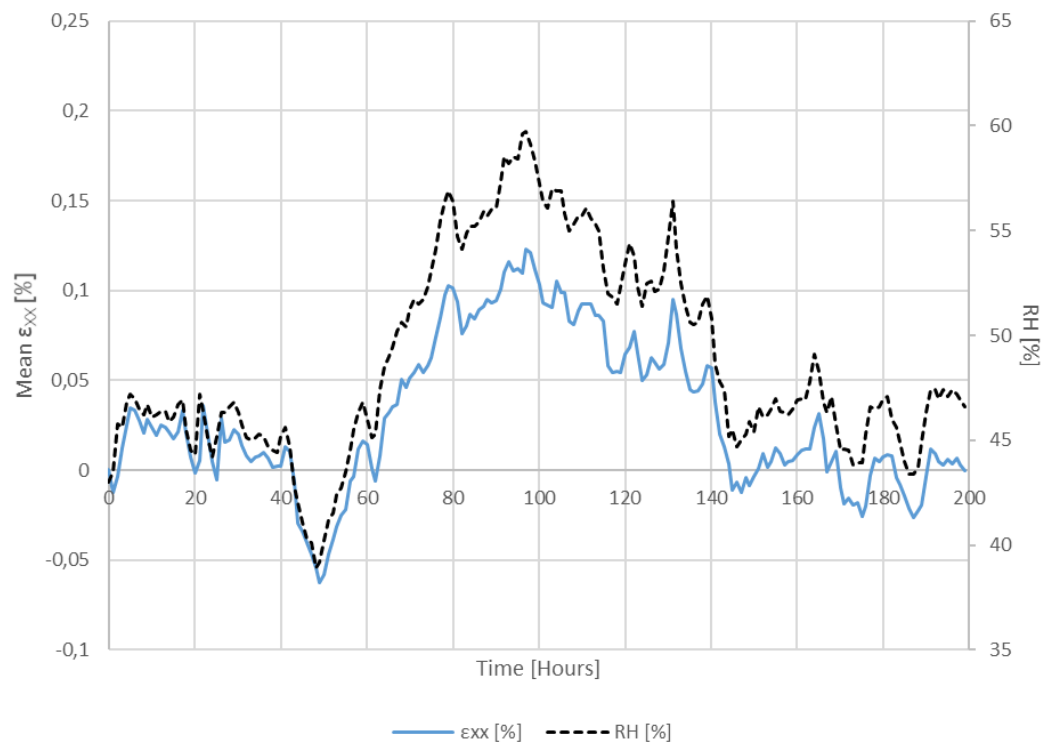


Figure 4.24. Mean ε_{xx} [%] calculated across the entire surface of TapestryFragment_1 against time. RH [%] fluctuations are indicated by the dotted line.

The good linear fitting of the strain data against the RH values, indicated by Figure 4.25 and Figure 4.26, confirms the accuracy of the outcomes from the DIC

analysis. In this case, this is particularly important as it proves the feasibility of 2D DIC for monitoring larger areas of historic textiles than those previously researched [2].

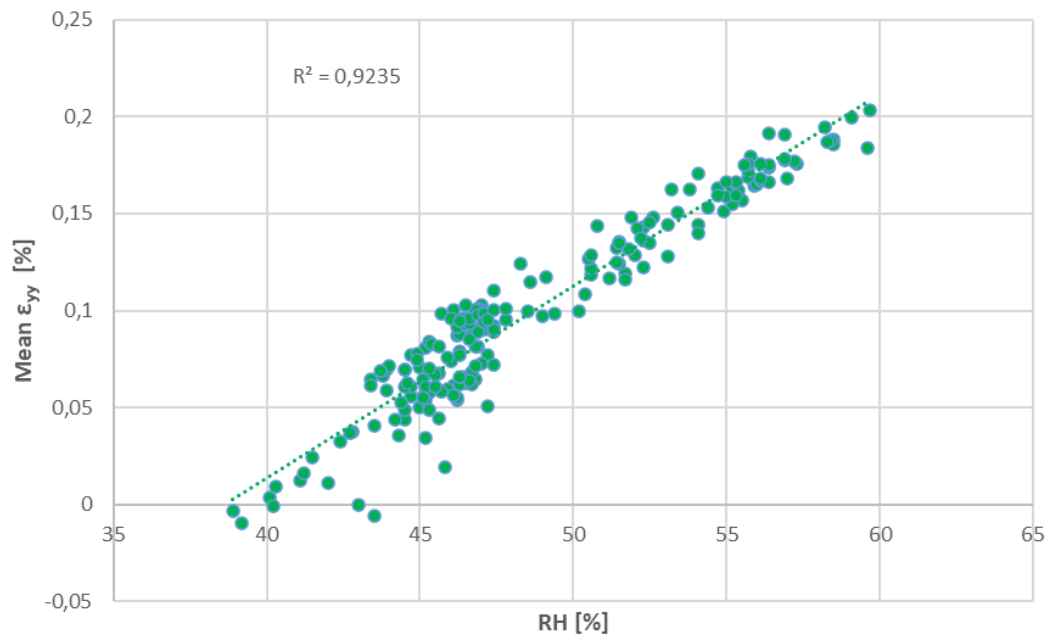


Figure 4.25. Mean ϵ_{yy} [%] across TapestryFragment_1 plotted against the changes in RH [%].

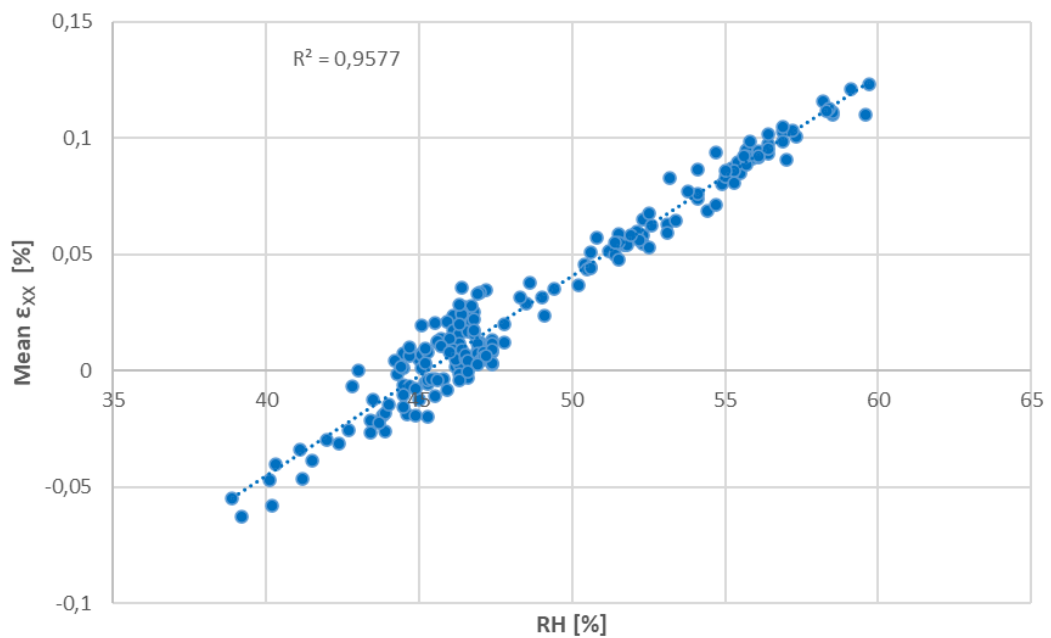


Figure 4.26. Mean ϵ_{xx} [%] across TapestryFragment_1 plotted against the changes in RH [%].

Figure 4.27 shows the error map of TapestryFragment_1. Since the sigma values across the entire surface are largely comparable, this can indicate that, in general, the figurative pattern was successful as the correlation device.

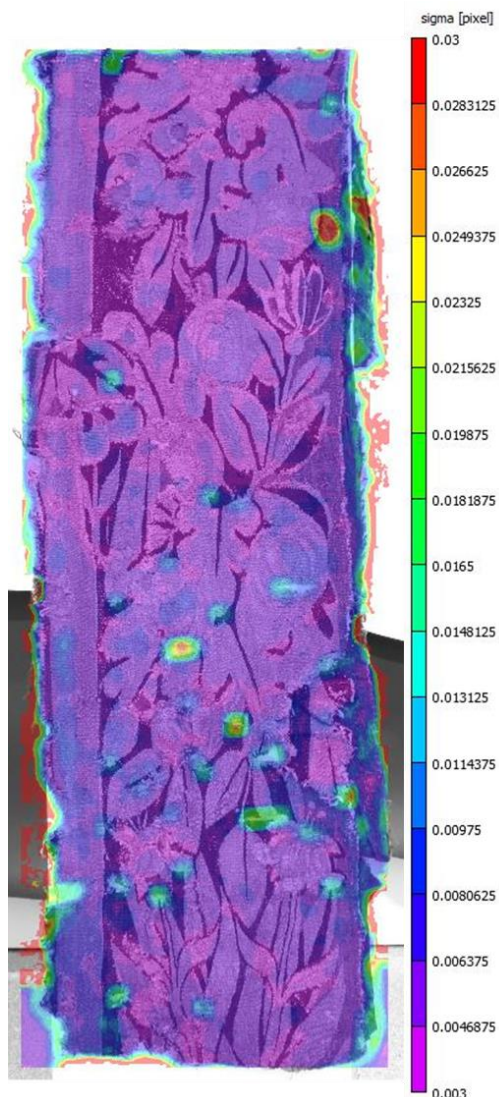


Figure 4.27. Error map expressed in sigma [pixel] of TapestryFragment_1 at the end of the 200-hour monitoring.

Figure 4.28 depicts the longitudinal strain map of the historic hanging at the end of the experiment. Overall, the fragment appeared to be largely affected by a longitudinal strain below 0.15%, as also indicated by the data plotted in Figure 4.23. From the map, some weak and damaged areas can be easily located, as they correlate to regions of high local strain, pinpointed in red. These locations of high strain mainly correspond to pre-existing open slits, such as those within the dotted squares in Figure 4.28. When observing the strain maps at different moments, it could be noted that the high strain across the slits progressively

augmented, while the overall strain changed unevenly with time as it followed the unstable humidity.

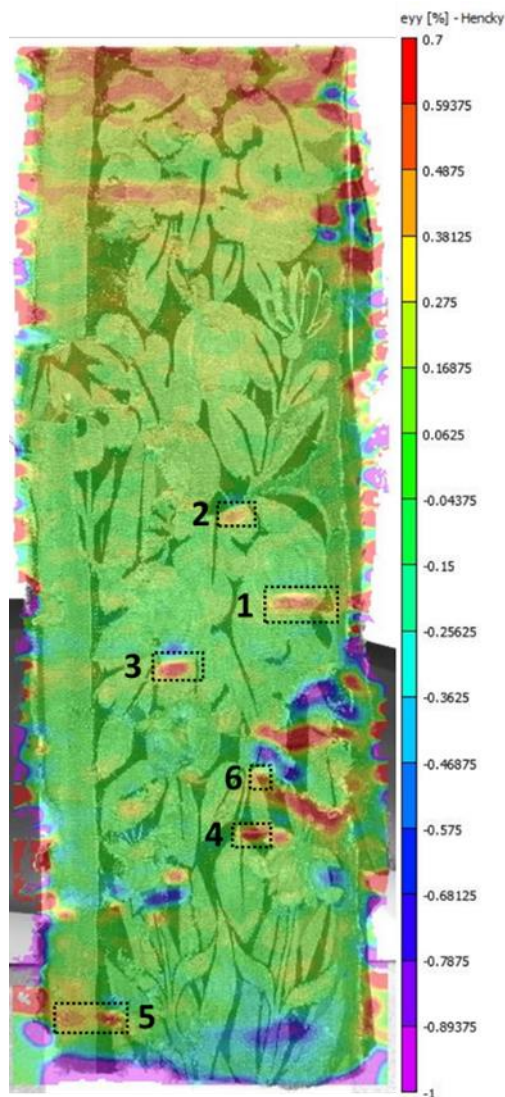


Figure 4.28. Longitudinal strain map of TapestryFragment_1 at the end of the 200-hour monitoring.

This observation was validated thanks to strain data registered across the six open slits. In these damaged areas, ϵ_{yy} augmented with time, as shown by the graphs in Figure 4.29. It is important to underline that the data describing the deformation affecting the slits cannot be defined as actual strain. Indeed, the slits progressively enlarged during the experiment, so the data portray the interpolated displacement, rather than the strain. Therefore, from this moment on, the outcomes averaged from the slits/damaged areas are referred to as *pseudo strain*.



Figure 4.29. Pseudo ϵ_{yy} [%] acting across the slits versus time. RH [%] fluctuations are indicated by the dotted line.

As just said, pseudo strain was largely influenced by time. However, the environmental conditions may have had some (limited) effects on it. For instance, it is clear that the steep rise in humidity registered between the 60th and the 80th hours promoted a more drastic increase in the local pseudo ϵ_{yy} . Since pseudo strain was shown to mainly depend on time, it can be suggested that the mechanical damage mechanism occurring in the weak areas can be defined as creep. Such time-dependent mechanism is expected to be, at least partly, irreversible, causing much faster and more evident damage processes than those due to fatigue.

Besides the high strain in correspondence to the damaged areas, also the top border seemed to extend more than the rest of the fragment. However, it is thought that the high ϵ_{yy} data are unrelated to creep-like mechanisms, or to the self-weight loading expected when going from the unloaded horizontal position to the vertical one, as modelled by Duffus [56] and in Section 5.1.4. Instead, it is hypothesized that the high strain could be due to: I) errors caused by out-of-plane movements; II) the un-crimping of weft yarns. The first option seems more likely, as the outcomes from other tests carried out on the same tapestry fragment, and presented in the following chapters, do not show the same strain at the top border.

It is important to underline that, besides the open slits just described, no other defects could be tracked through the strain maps. This indicates that the technique was not able to detect other non-visible weak areas that may have been present in the artefact. Therefore, under the same experimental conditions, DIC seems unfeasible as a preventive tool for anticipating locations prone to creep. Nevertheless, it should be noted that the test only lasted 200 hours, so possibly the time span was too short for allowing minimal (and still invisible) defects to form and be tracked.

4.3.2.2 TapestryFragment_2

As done for TapestryFragment_1, strain across another piece of historic hanging was monitored through 2D DIC, in this case for 168 hours. TapestryFragment_2 was also in evident weak condition and it presented extensive areas of loss. The experiment further trialled DIC feasibility for monitoring strain across actual textile objects, and, in particular, the sensitivity of the optical technique to a different figurative pattern.

In Figure 4.30 the sigma values across the entire surface of TapestryFragment_2 are mapped, giving a first indication of error distribution. It is shown that the areas with the less busy figurative pattern, namely the brownish/reddish part at the bottom right corner, were probably going to provide less accurate data (high sigma, low confidence) than those from the top right-side area (low sigma, high confidence), e.g. in correspondence to the detailed oval motif, already depicted in Figure 4.9. As first discussed in Section 4.3.1.2, the sigma map provides an indication of the accuracy of strain data, highlighting the ability of the pattern of ensuring proper correlation.

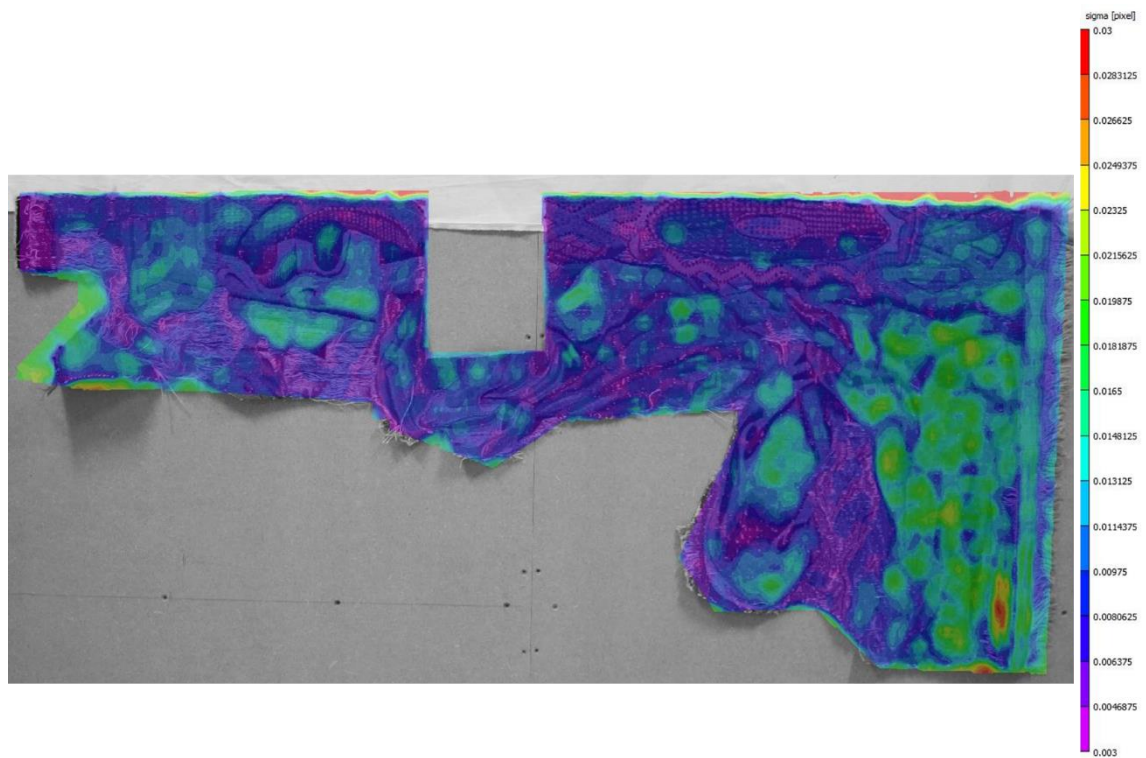


Figure 4.30. Error map expressed in sigma [pixel] of TapestryFragment_2 at the end of the 168-hour monitoring.

Figure 4.31 presents the strain map at the end of the 168-hour monitoring of TapestryFragment_2. Figure 4.31 illustrates the difficulty of the optical technique in properly tracking strain in certain areas, as predicted from the sigma mapping. As previously observed, wherever there were some issues with the measurements (i.e. areas of high sigma values, low level of confidence), in the strain map there are alternating small areas of relatively high and low strain. Namely, this can be observed in the region at the bottom right corner. Again, this likely indicates that the homogeneous pattern in this area did not allow proper correlation and led to errors. An area of high strain is shown at the bottom of the oval design. This area corresponds to a long open slit (detail in Figure 4.9), that presumably widened up during the test. It is underlined that no other defects or weak areas were clearly noted.

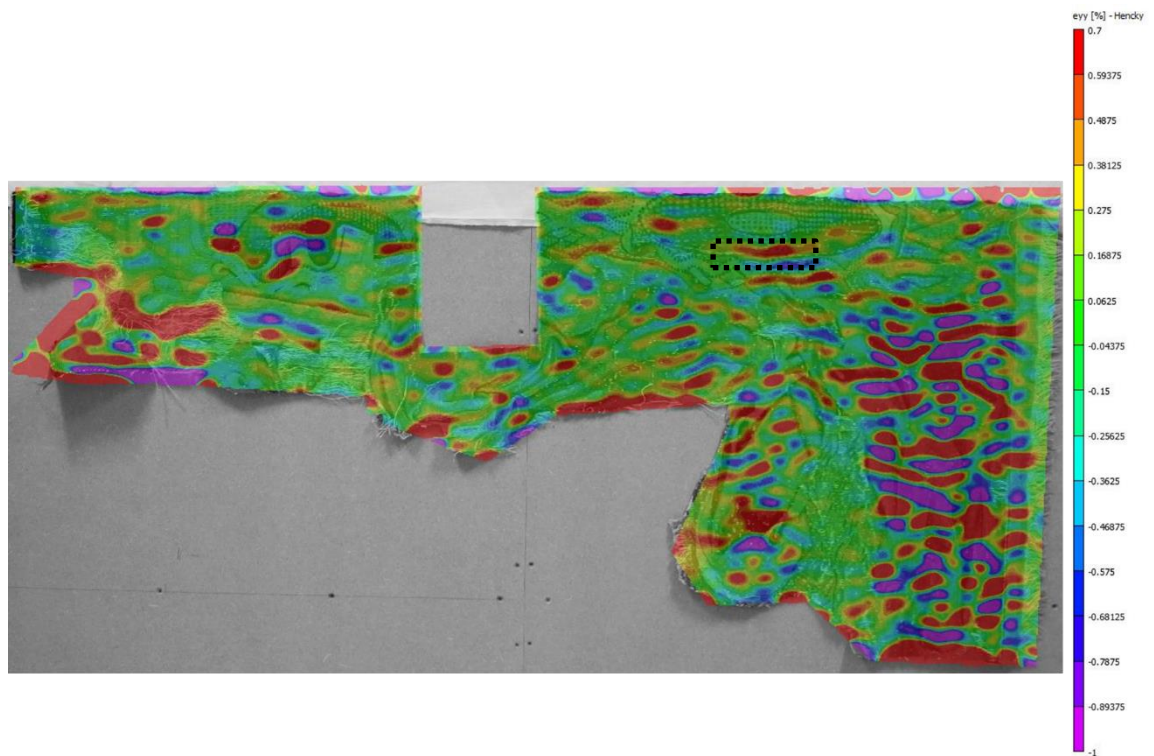


Figure 4.31. Longitudinal strain map of TapestryFragment_2 at the end of the 168-hour monitoring. The area delineated by the dotted line refers to an open slit.

The trend of the average longitudinal strain is illustrated in Figure 4.32, together with humidity variations. It is noted that strain data from areas with unsuitable pattern for correlation were excluded from the calculation of the average ϵ_{yy} . By looking at the graph in Figure 4.32, the influence of RH on the overall strain is clear. It should be pinpointed that humidity rose less remarkably than during the monitoring of TapestryFragment_1. In this case, the main increase in RH, from around 34% to around 43%, occurred during a time-lapse of 50 hours (60th-110th hour). Because of this, also the overall increase in length of the fragment linked to fatigue was more contained (maximum overall ϵ_{yy} 0.13%) than that registered in the previous test. Another factor that may have contributed to the less extensive longitudinal strain on TapestryFragment_2 can be linked to its horizontal, rather than vertical, shape. The very good linearity between strain and humidity was observed also for overall ϵ_{xx} , confirming the occurrence of fatigue and swelling in both longitudinal and horizontal direction.

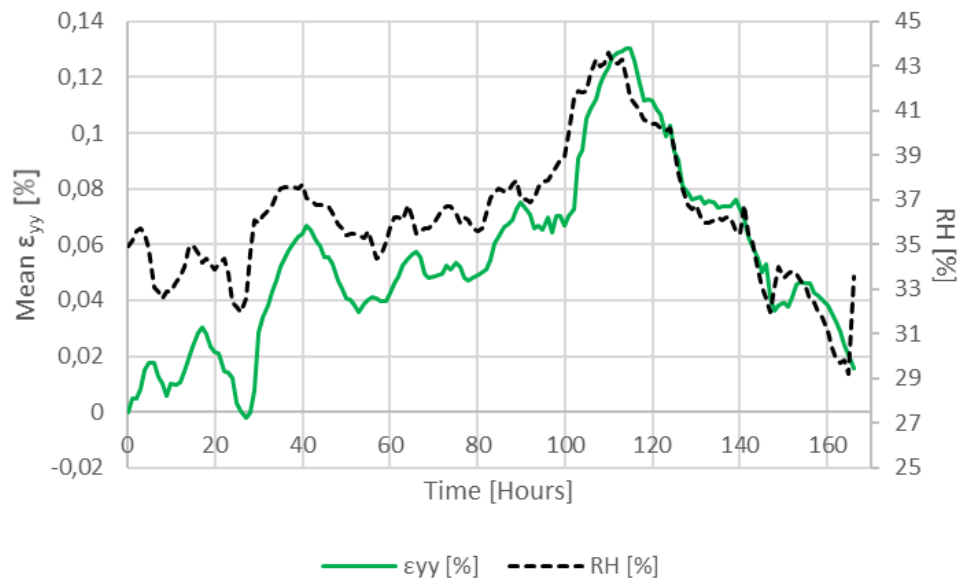


Figure 4.32. Mean ε_{yy} [%] calculated across TapestryFragment_2 against time. RH [%] fluctuations are indicated by the dotted line.

Figure 4.33 depicts the longitudinal pseudo strain registered across the long open slit below the oval motif. As noted for the slits in TapestryFragment_1, also in this case the data demonstrate that the damaged area enlarged progressively with time, possibly indicating the occurrence of a creep-like mechanism. Again, humidity appears to impact, up to a certain level, pseudo ε_{yy} .

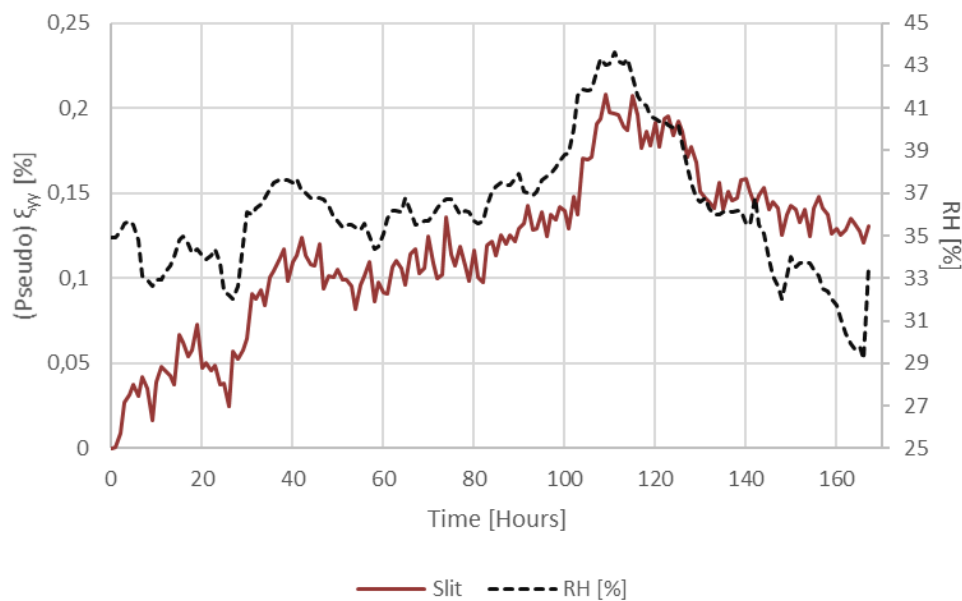


Figure 4.33. Pseudo ε_{yy} [%] calculated across the slit in TapestryFragment_2 against time. RH [%] fluctuations are indicated by the dotted line.

4.3.2.3 *Kesi*

In addition to European woollen tapestries, 2D DIC was employed to monitor strain across a light-weight Chinese silk *kesi* for 68 hours. This experiment aimed to further assess the feasibility of the optical method for studying mechanical deformations in textile objects, also when they include different manufacturing features than traditional European tapestries.

The error map and the strain map at the end of the monitoring are shown in Figure 4.34 and Figure 4.35, respectively. Both maps state that the pattern of the border of the textile object is probably unsuitable as the correlation device, since it shows relatively high sigma and it provides inaccurate strain data on a local level (alternated areas of high and low strain).

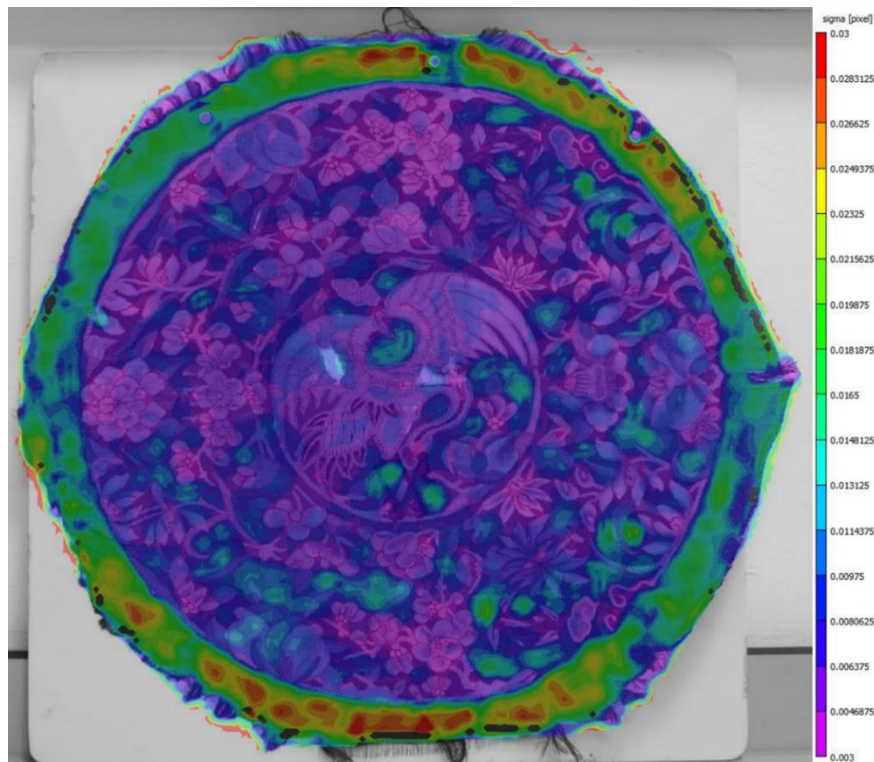


Figure 4.34. Error map expressed in sigma [pixel] of the *kesi* at the end of the 68-hour monitoring (61 subset size, 5 step size).

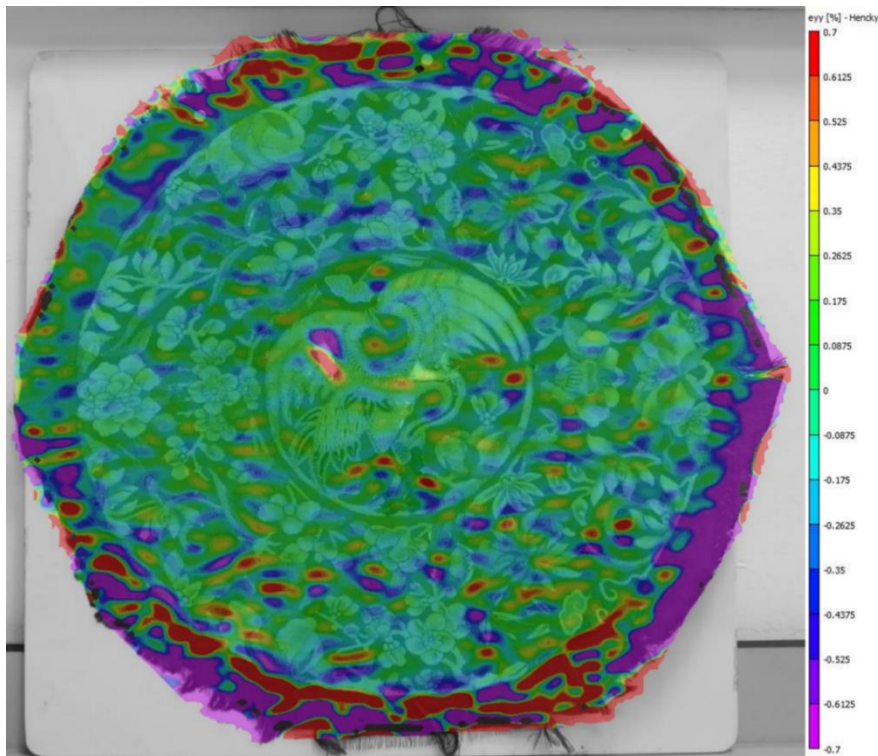


Figure 4.35. Longitudinal strain map of the *kesi* at the end of the 68-hour monitoring (61 subset size, 5 step size).

Figure 4.36 portrays the fluctuations in the ϵ_{yy} , averaged from the overall central area of the *kesi* (borders excluded), while Figure 4.37 shows length variations in the horizontal directions. As observed for the other case studies made of wool, the Chinese silk tapestry also extended and contracted following RH trends. Although tracking such changes is relevant as this demonstrates the validity of the monitoring technique also in this case study, these dimensional variations should be expected to happen since silk, like wool, is a hygroscopic material [57]. As discussed in more detail in Chapter 2, silk shows a more contained moisture regain than wool. This could partly explain the relatively low extension of the object during the RH increases, namely the one registered between 15-25 hours from 44% to 55% (maximum overall ϵ_{yy} 0.005%). Moreover, the low areal density of the *kesi*, in opposition to that of European tapestries, may have limited the effects linked to the self-weight loading. In general, the humidity decreased during the experiment, causing the object to contract rather than extend.

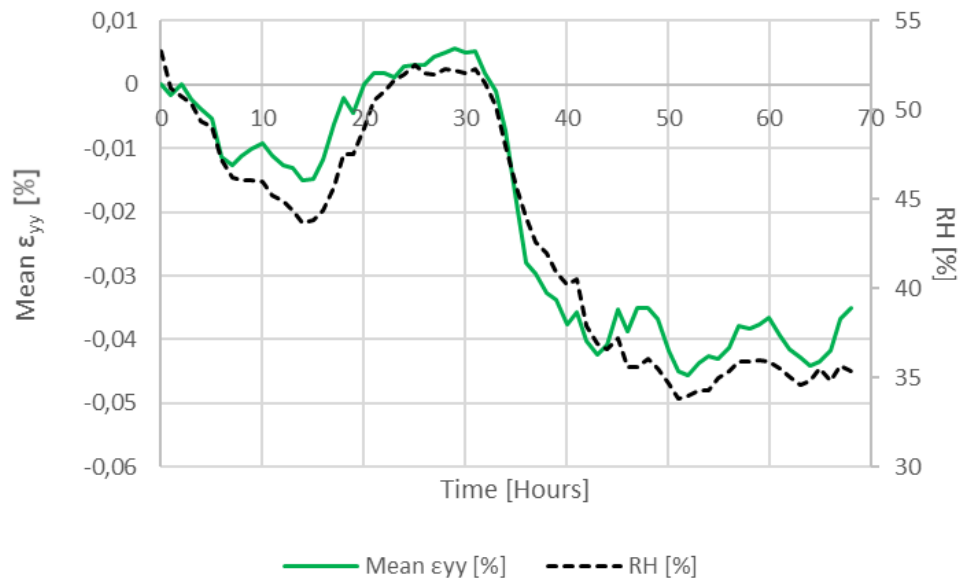


Figure 4.36. Mean ϵ_{yy} [%] calculated across the *kesi* against time. RH [%] fluctuations are indicated by the dotted line.

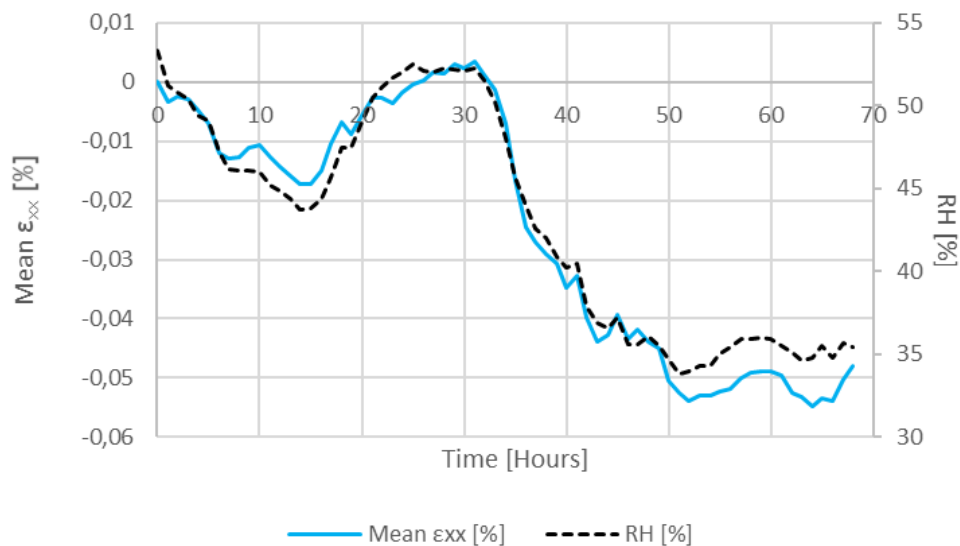


Figure 4.37. Mean ϵ_{xx} [%] calculated across the *kesi* against time. RH [%] fluctuations are indicated by the dotted line.

4.3.2.4 Historic tapestry conserved with full support

A historic tapestry from the Burrell Collection was monitored for 100 hours. Unlike the experiments presented in the previous sections that only dealt with relatively small historic hangings (though larger than those tested in Southampton [2]), in this case a 2x3 m tapestry was considered. Inevitably, capturing the entire surface of *Florence* causes a certain loss of detail (lower resolution), so this test was important to assess whether the full-field

application of DIC can be useful for textile objects of such sizes. Another objective was to define the mechanical damage mechanisms occurring across a historic hanging while on display right after being conserved with a linen full support.

Before starting the analysis, by looking at the pictures taken, it was clear that the lower part of the tapestry moved. These out-of-plane displacements were caused by the (contained) air circulation within the workshop, while the object was hanging freely from a batten. Since 3D movement affects the accuracy of 2D DIC analysis, only the top half of the hanging was considered as ROI.

Sigma values across the analysed area are plotted in Figure 4.38, while the related ϵ_{yy} map is shown in Figure 4.39. Figure 4.38 outlines as areas of higher sigma (lower accuracy) regions with homogeneous figurative patterns, such as the tower in the centre, or the architecture around the borders.

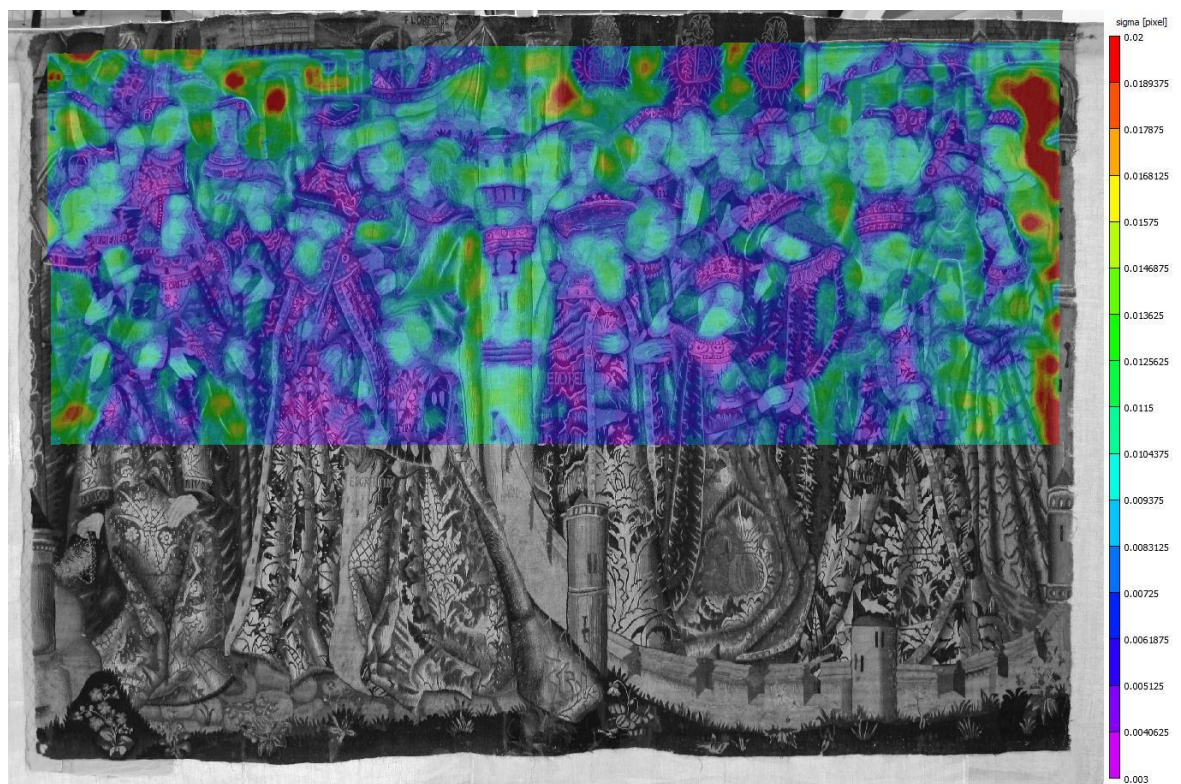


Figure 4.38. Error map expressed in sigma [pixel] of *Florence* at the end of the 100-hour monitoring (61 subset size, 5 step size).

By looking at the strain map of Figure 4.39, the same locations of high sigma correspond to areas of relatively high and low strain. Again, this can be linked to

DIC miscalculating local strain. As discussed later, the miscalculation can be due to the lack of contrast in the image, negatively affected by the low resolution on a small-scale level.

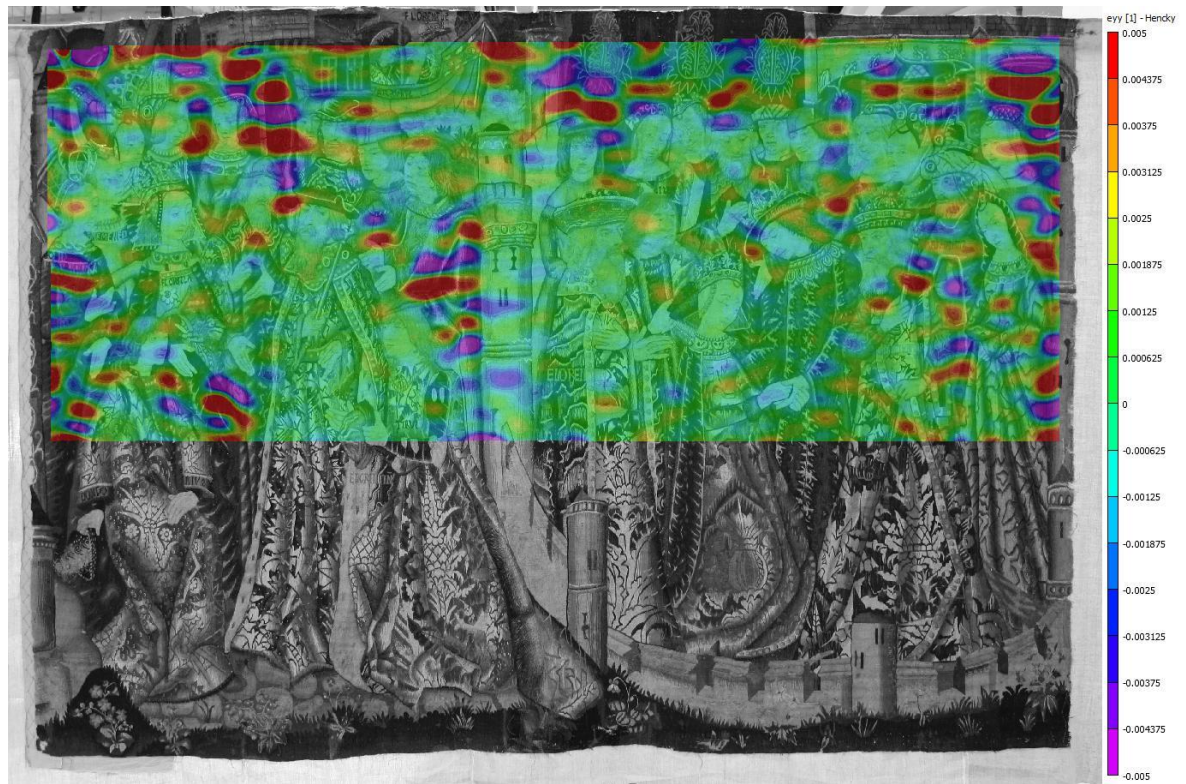


Figure 4.39. Longitudinal strain map of *Florence* at the end of the 100-hour monitoring (61 subset size, 5 step size).

Overall longitudinal strain across the upper half of the tapestry is shown in Figure 4.40. By looking at the graph, mean ϵ_{yy} was demonstrated to follow two different trends: one defining the behaviour during around the first 24 hours of monitoring, the other describing a different mechanical mechanism between the 25th and the 100th hours. Right after being hung, as well as during the entire first day of display, the tapestry was shown to elongate constantly with time. Importantly, this occurred regardless of a drastic drop in RH (from 44% to 35%) registered in the same time-lapse. After around the first 24 hours of display, the trend changed and strain across the historic hanging was found to depend more greatly on humidity.

From these observations, it can be suggested that at the beginning of the test a time-dependent deformation occurred, determining an overall elongation of the

textile object in the weft direction. The initial time-dependent mechanism can be justified by the uncrimping of the fibres and the re-adjusting of the weave structure subjected to the self-weight loading after a long period of storage. From the second day of display onwards, fatigue was the dominating mechanical damage mechanism.

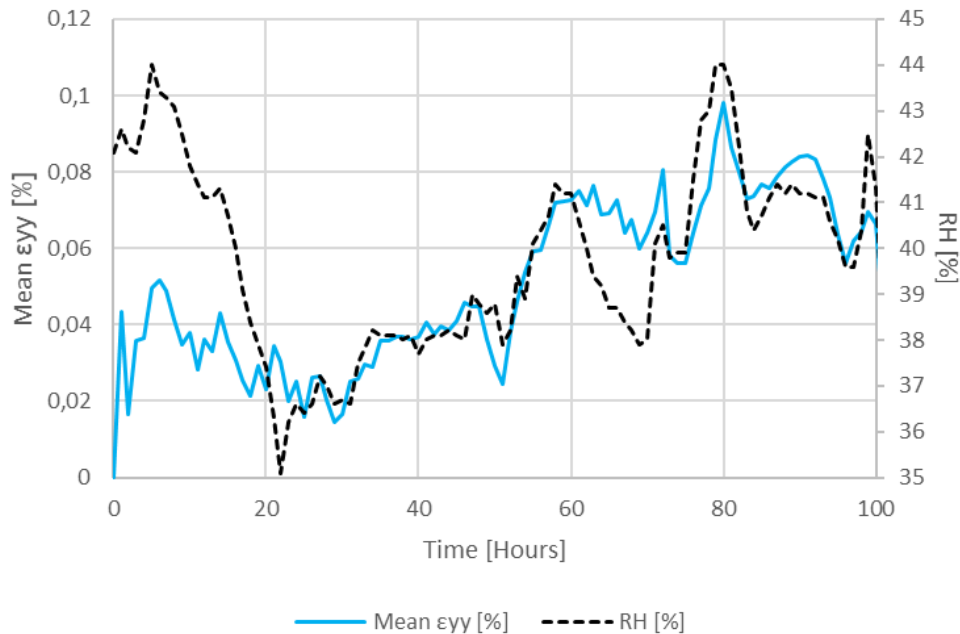


Figure 4.40. Mean ϵ_{yy} [%] during the 100-hour monitoring of *Florence* tapestry. RH [%] fluctuations are indicated by the dotted line.

The maximum overall strain registered was $\approx 0.1\%$, in correspondence to the maximum RH reached, 44%; this would indicate an extension of 0.06 cm (initial length analysed of ≈ 60 cm). Although the order of magnitude of strain data is comparable to that of other studies on fully conserved tapestries (considering a longer monitoring period, i.e. 25 days) [58], it is not possible from this test alone to define the (potential) supporting effects of the linen on the back: monitoring the tapestry before the conservation treatment would have enabled a better evaluation of the treatment.

The ability of DIC in demonstrating the occurrence of fatigue from the second day on gives a certain confidence to the overall strain data gathered, since it agrees with what was reported in the previous sections. However, it is noted that the linearity between strain and RH is not as good as that from other tests.

Indeed, as indicated by Figure 4.41, the R^2 is only 0.75. This poorer linearity could be linked to hysteresis effects, but it may also indicate a lower accuracy in the measurements. This could be due to different factors, namely: the insufficient greyscale contrast affecting the image processing algorithm; the appearance of out-of-plane displacements. Besides the figurative design, it is thought that the size of the monitored object prevented the acquisition of images with a high resolution on a small-scale level. This could have negatively affected (local) greyscale contrast and so strain calculation. For the same reason, such full-scale monitoring is probably unable to detect weak areas like slits, even when visible.

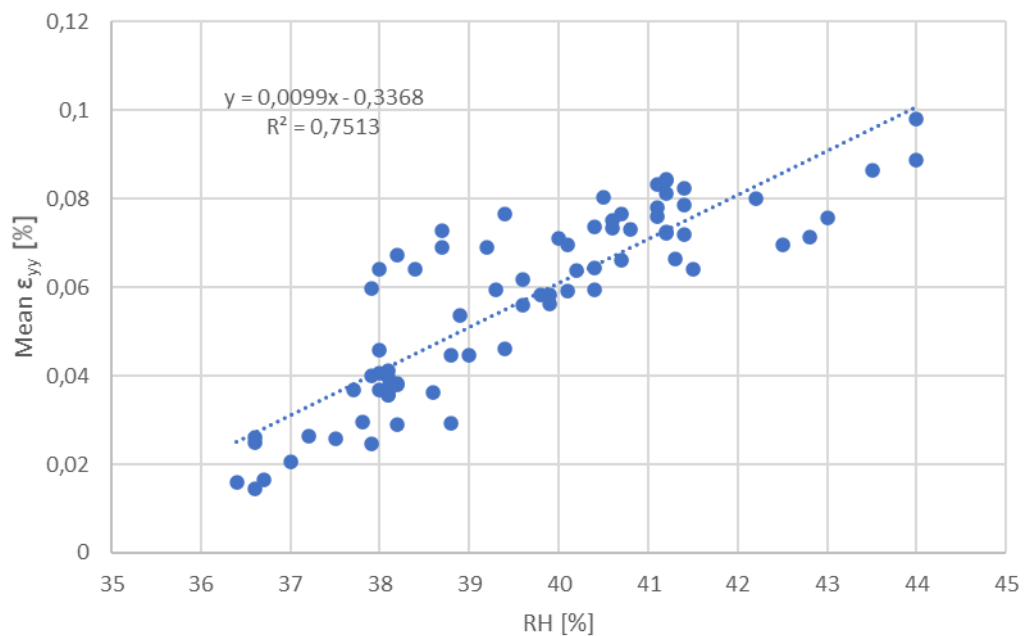


Figure 4.41. Mean ϵ_{yy} [%] across *Florence* tapestry against RH [%] (25-100 hours).

4.3.2.5 Contemporary tapestry at Stirling Castle

In addition to historic tapestries, a contemporary hanging, *Unicorn tapestry*, made of wool (weft) and cotton (warp) was monitored. As done for *Florence*, also in this case the full-field application of 2D DIC was tested. However, the monitoring lasted longer than in the previous cases, as it started in 2015, when the tapestry was first hung in the Castle, until August 2020. This was possible thanks to a camera placed on the opposite wall of the room, taking one picture per hour. The memory card was changed when full, i.e. around once a month. However, it was later found that whenever this was done, the device was

slightly moved, preventing the correlation of the sets of images acquired at different moments.

When observing the pictures taken during the long-term monitoring, a first potential issue for the DIC analysis was shown to be the uneven lighting. Indeed, no artificial lighting was used in the room, so the quality of pictures greatly depended on the natural light coming from the two windows at the sides of the tapestry. Because of this, most of the photos taken were very dark, and thus not suitable for correlation, as in the example in Figure 4.42. Whenever the image quality was too low, the VIC-2D software excluded the pictures from the analysis.



Figure 4.42. Picture from the monitoring of the *Unicorn tapestry*. The photo, taken at 10:30 pm on the 23/07/2015, was not suitable for 2D DIC analysis.

It was noted that, in the current position, the tapestry has the best light exposure at around 10:30 am. Therefore, it was possible to process through the software some of the photos taken at this time. In particular, all the images from the first month of monitoring, when the tapestry was first hung on the wall of the Queen's Inner Hall, were suitable for correlation. The first image of the monitoring, employed for the successful DIC analysis, is depicted in Figure 4.43.



Figure 4.43. Picture from the monitoring of the *Unicorn tapestry*. The photo, taken at 10:30 am on the 23/07/2015, was used for 2D DIC analysis.

Figure 4.44 illustrates error distribution from the analysis of pictures from the first month of monitoring. It is shown that the central area corresponding to the body of the unicorn did not allow any correlation. This was due to the strong lack of greyscale contrast, that prevented the calculation of strain across this area, as shown by the strain map in Figure 4.45. Because of that, the overall strain data from this first month of monitoring only considered the top half of the hanging, i.e. the area within the dotted line in Figure 4.45.

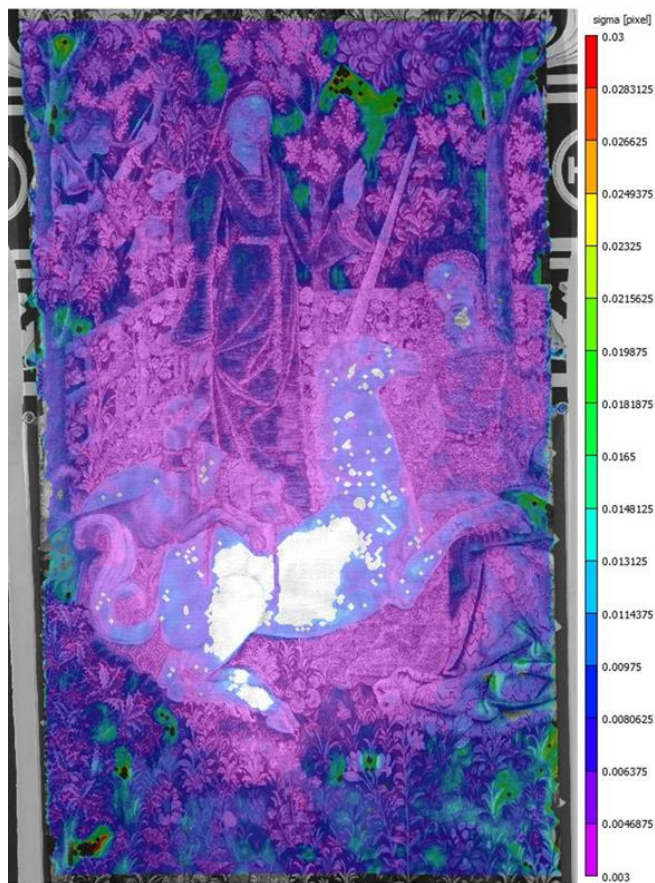


Figure 4.44. Error map expressed in sigma [pixel] of *Unicorn tapestry* at the end of the 30-day monitoring when first hung (23/07/2015).

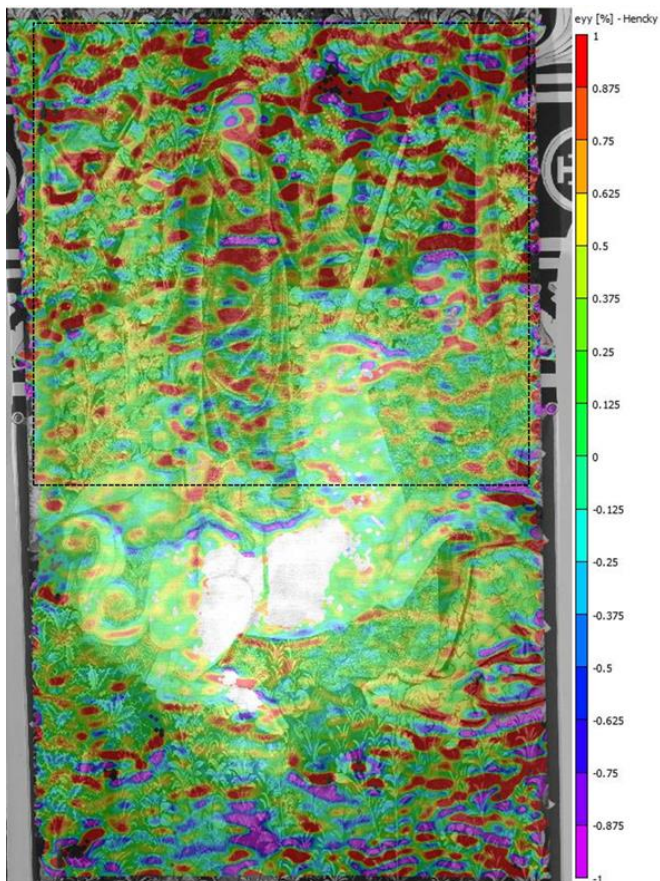


Figure 4.45. Longitudinal strain map of *Unicorn tapestry* at the end of the 30-day monitoring when first hung (23/07/2015).

The average longitudinal strain data calculated across the top half of the tapestry during the 30 days of monitoring are plotted in Figure 4.46, together with humidity fluctuations. It is interesting to note that, overall, the newly woven tapestry extended constantly in the weft direction within the first month. In particular, it is observed that mean ϵ_{yy} drastically increased during the first week. This occurred regardless of the uneven RH, indicating how time-dependent mechanisms like creep and uncrimping overcame the influence of fatigue. This was similar to what was observed in the first 24 hours of monitoring of *Florence* tapestry (Section 4.3.2.4). In this case uncrimping seems a reasonable factor as, straight after being woven, weft threads in a hanging are more tightly twisted from the manufacturing process, than after being displayed. It should be underlined that, after the first 30 days of hanging, the maximum overall ϵ_{yy} registered was 0.4%. Considering a total length of 90 cm of the analysed area, such strain would correspond to an extension of ≈ 0.36 cm.

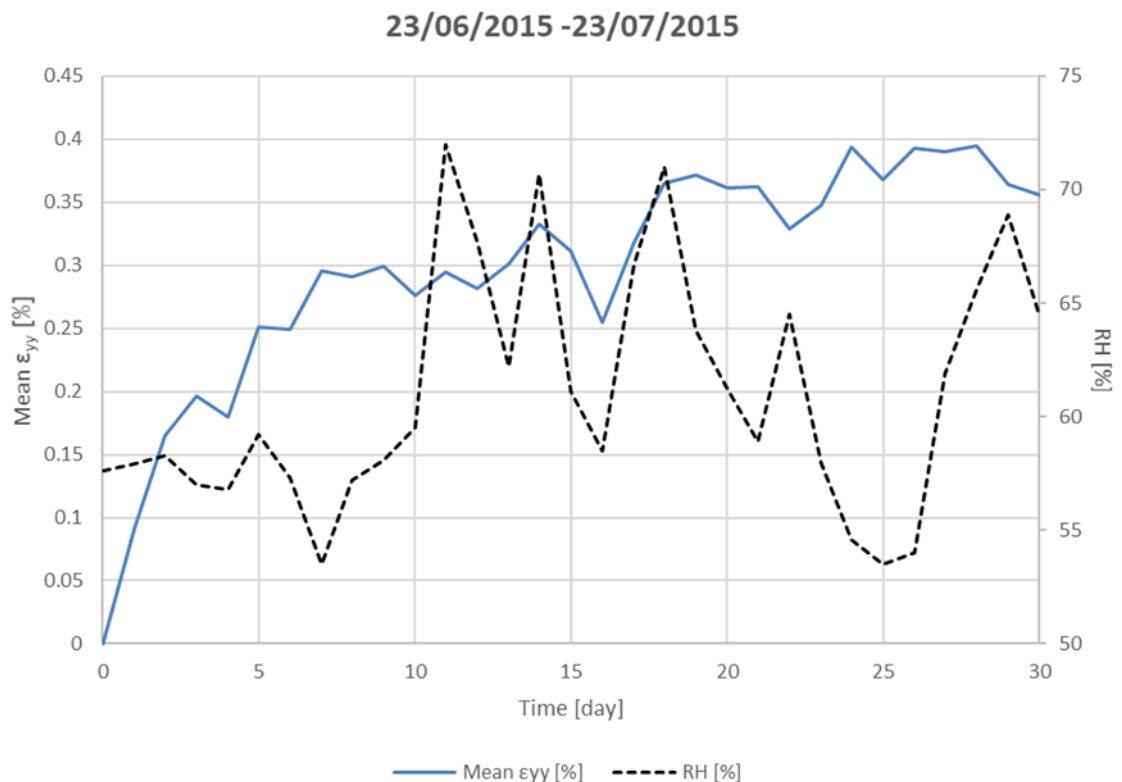


Figure 4.46. Mean ϵ_{yy} [%] during the first month of monitoring of *Unicorn tapestry*. RH [%] fluctuations are indicated by the dotted line (23/06/2015 – 23/07/2015).

The observations drawn in the previous paragraph on the greater influence of creep/uncrimping over fatigue occurring at the beginning of the display were confirmed by looking at the strain data calculated in June 2016, a year later. In Figure 4.47 are shown the trends of mean ϵ_{yy} , calculated across the top half of the tapestry, and RH. Although in this case it was possible to run the analysis only on ten pictures, covering a period of ten days (one picture a day, at 10:30 am), it is clear that fatigue dominated creep/uncrimping. This shows how, after the initial phase, the textile object adjusted to a certain length. Although this length may vary afterwards, elongations would be less remarkable and would alternate with contractions, all depending on humidity.

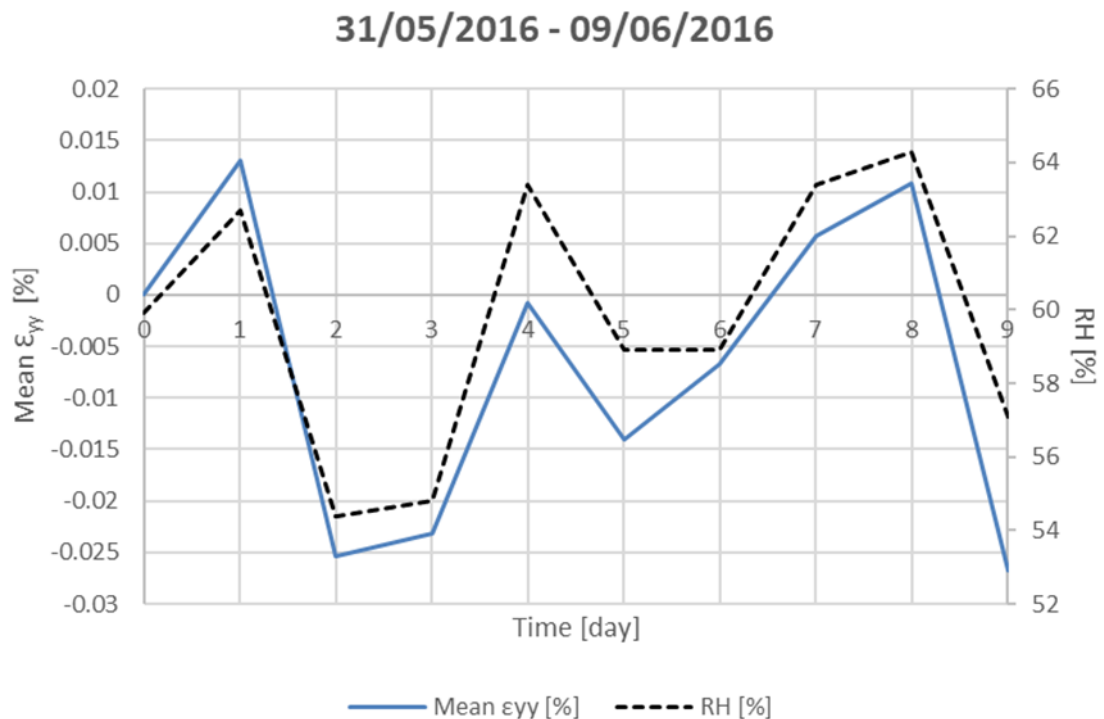


Figure 4.47. Mean ϵ_{yy} [%] during the ten days of monitoring of *Unicorn tapestry*, after around a year of it being on display (31/05/2016 – 09/06/2016). RH [%] fluctuations are indicated by the dotted line.

It is noted that the second set of images (taken in 2016) allowed a proper correlation of the entire surface of the tapestry. This includes the central area corresponding to the white body of the unicorn, as shown in the strain map of Figure 4.48. This was not possible when monitoring the same tapestry during the first month of display (Figure 4.45), demonstrating how the pattern alone does

not guarantee a successful analysis. In this case, probably the different light exposure of the textile object, due to a slight change in the position of the camera, allowed an increase in the greyscale contrast in the problematic area. The new camera position permitted a full-field strain calculation, but it did not ensure a constant (in time) light exposure of the tapestry, preventing the analysis of most of the images. All these observations indicate the need to properly evaluate such variables impacting image quality before starting *in situ* long-term tests.

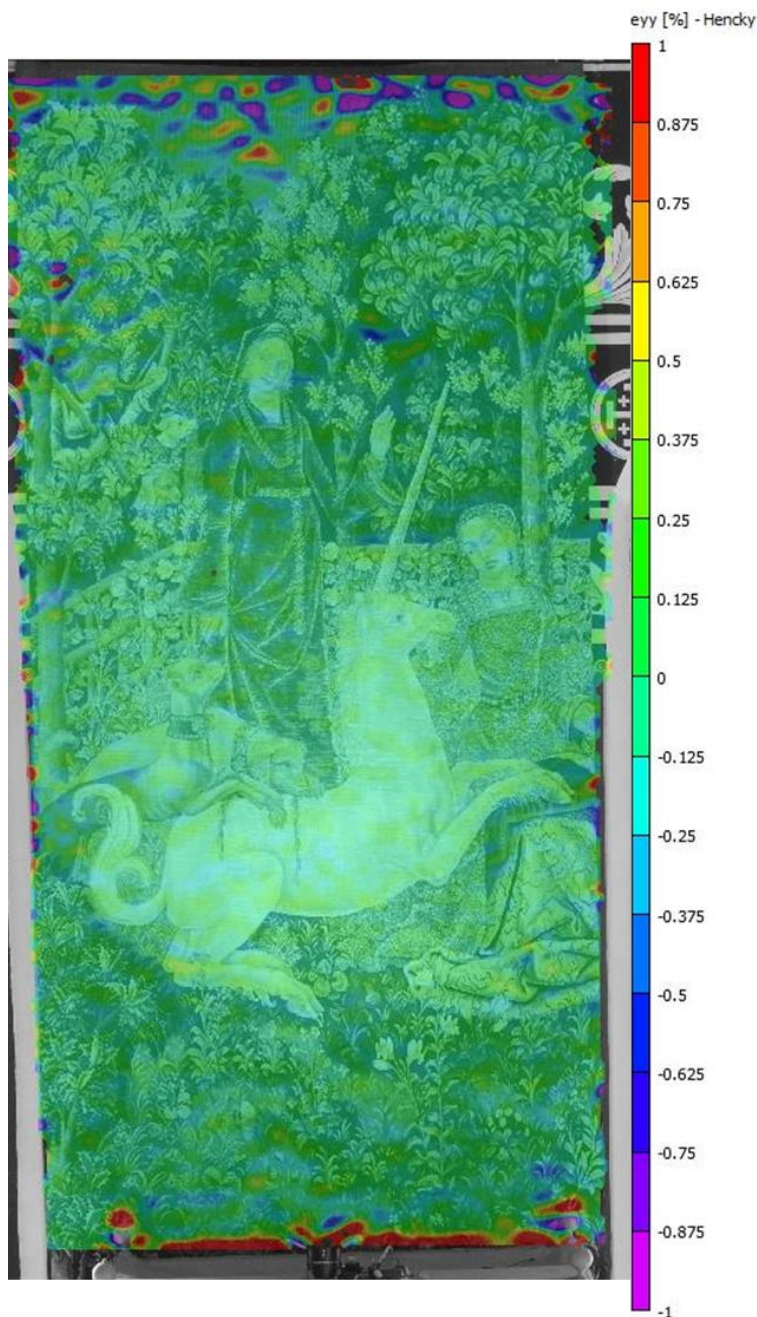


Figure 4.48. Longitudinal strain map of *Unicorn tapestry* at the end of 10-day monitoring after a year since first hung (09/06/2016).

Importantly, it should be noted that the contemporary tapestry in Stirling Castle was the only case study exposed to high ranges of RH. Indeed, while RH did not exceed 60% in all in the experiments described in in Sections 4.3.2.1 - 4.3.2.4 (taking place in mitigated environments, i.e. research laboratories and a conservation studio), the historic castle was shown to be more humid, reaching peaks up to 73% of RH. This observation is significant when defining the applicability of the outcomes: since a large number of tapestries are displayed in historic houses, they are probably exposed to high levels of RH [59, 60]. Therefore, a more extended investigation of the mechanical behaviour of woven hangings subject to wider RH ranges, including levels above 60%, would be beneficial for ensuring a proper understanding of the risk caused by humidity. Defining the mechanical response of the artworks at high RH is particularly crucial since, at high RH, the linear relationship between strain and moisture content in wool stops and the fibrous material undergoes shrinkage [10].

4.3.2.6 Evaluation of DIC parameters when monitoring historic tapestries: step size, subset size

As done for the wool rep sample (Section 4.3.1.3), images from the monitoring of the *kesi* and *Florence* tapestries were processed through VIC-2D with different subset (31 and 61) and step (3 and 5) size. Varying step and subset size aimed to highlight the impact of such parameters in strain calculation.

By comparing the error maps presented in the previous sections, i.e. Figure 4.34 and Figure 4.38, with those obtained using different parameters, Figure 4.49 (*kesi*) and Figure 4.50 (*Florence*), it is observed that lowering the subset size from 61 to 31 increased the overall sigma. On the other hand, the same maps do not highlight any significant difference in sigma values when using different step size, namely 3 and 5. From these observations, a certain impact of the subset size was expected to be found in the sets of strain data. In particular, it could be hypothesised that strain measurements obtained with a subset size of 31, instead of 61, would be less accurate.

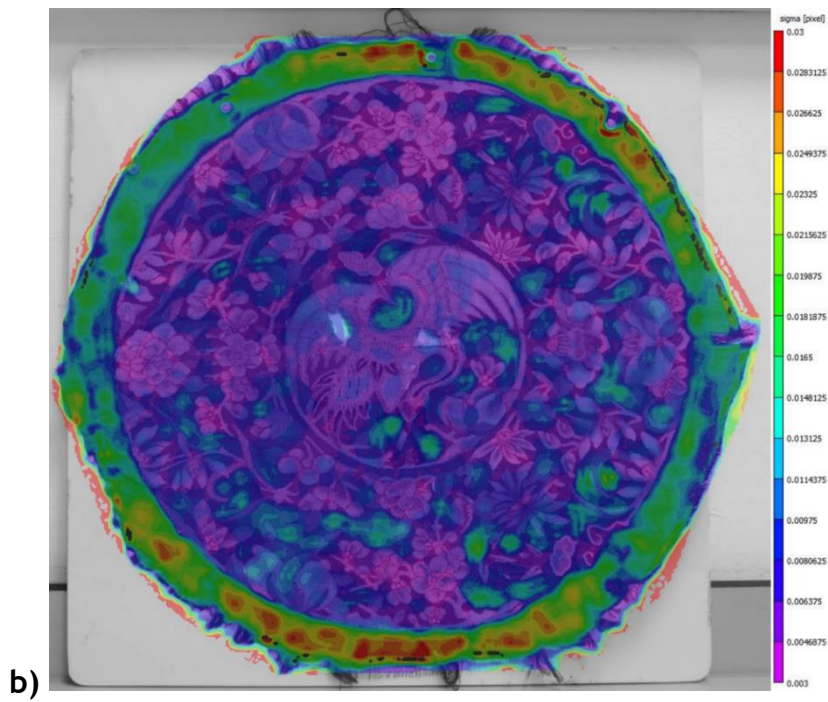
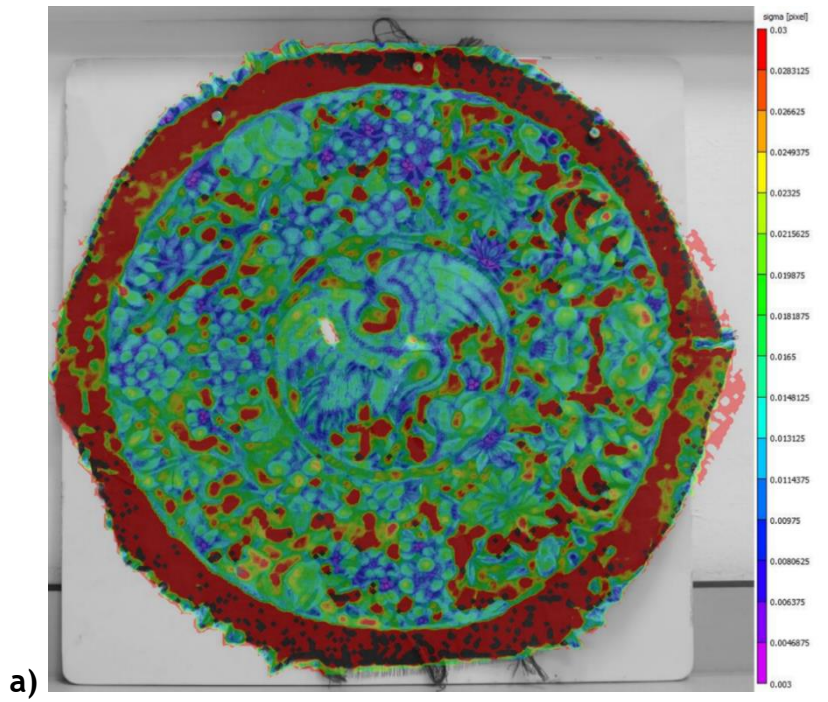


Figure 4.49. Error maps expressed in sigma [pixel] of the *kesi* at the end of the 68-hour monitoring: a) 31 subset size, 5 step size; b) 61 subset size, 3 step size.

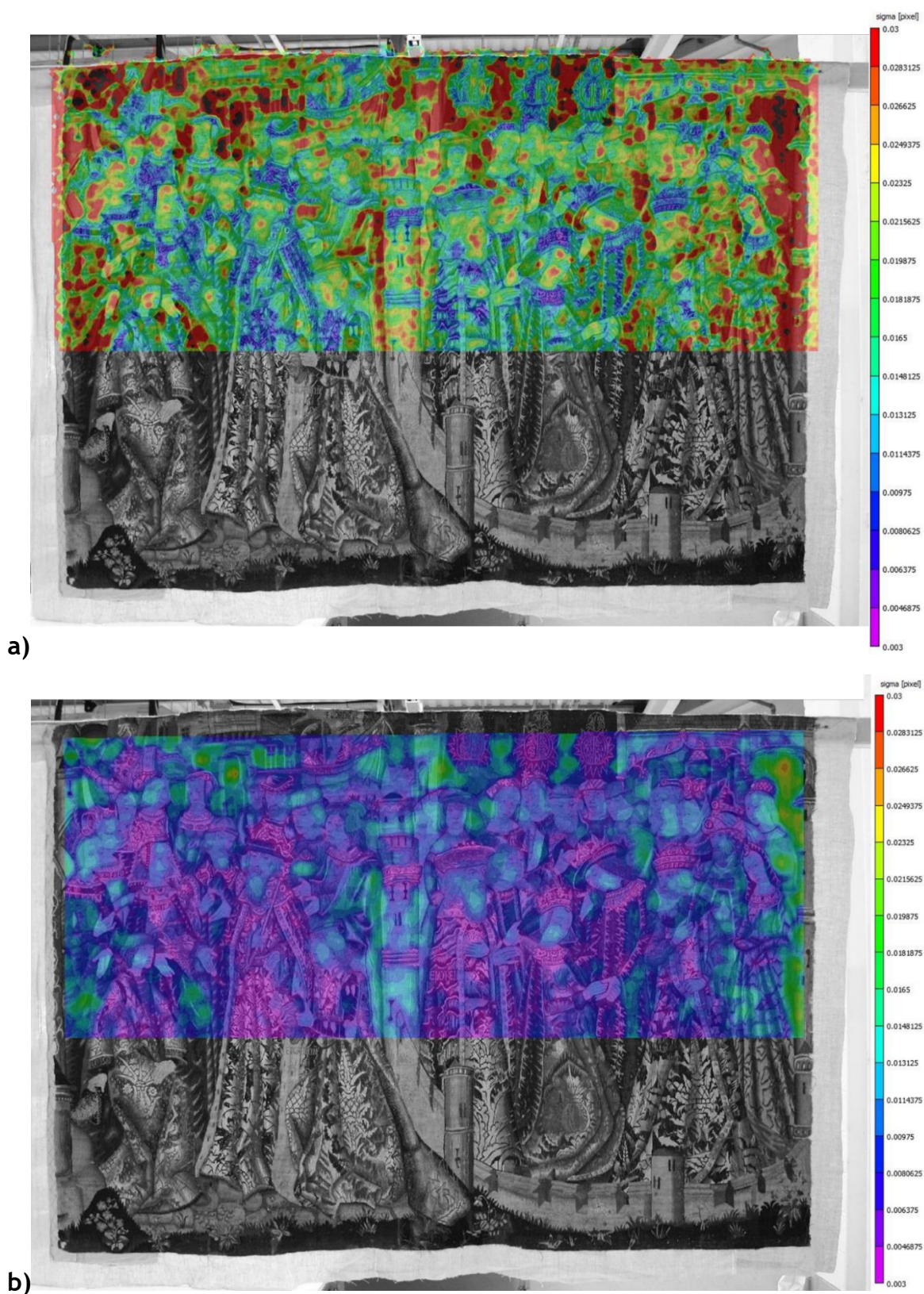


Figure 4.50. Error maps expressed in sigma [pixel] of the *Florence* tapestry at the end of the 100-hour monitoring: a) 31 subset size, 5 step size; b) 61 subset size, 3 step size.

The longitudinal strain maps of the silk and wool tapestries, with different subset and step sizes, are shown in Figure 4.51 and Figure 4.52, respectively. As noted in the previous paragraphs, the higher the sigma in a specific area, the lower seem to be the accuracy of strain measurements on a small scale. Indeed, Figure 4.51a and Figure 4.52a presented more alternating areas of high and low strain than Figure 4.51b and Figure 4.52b.

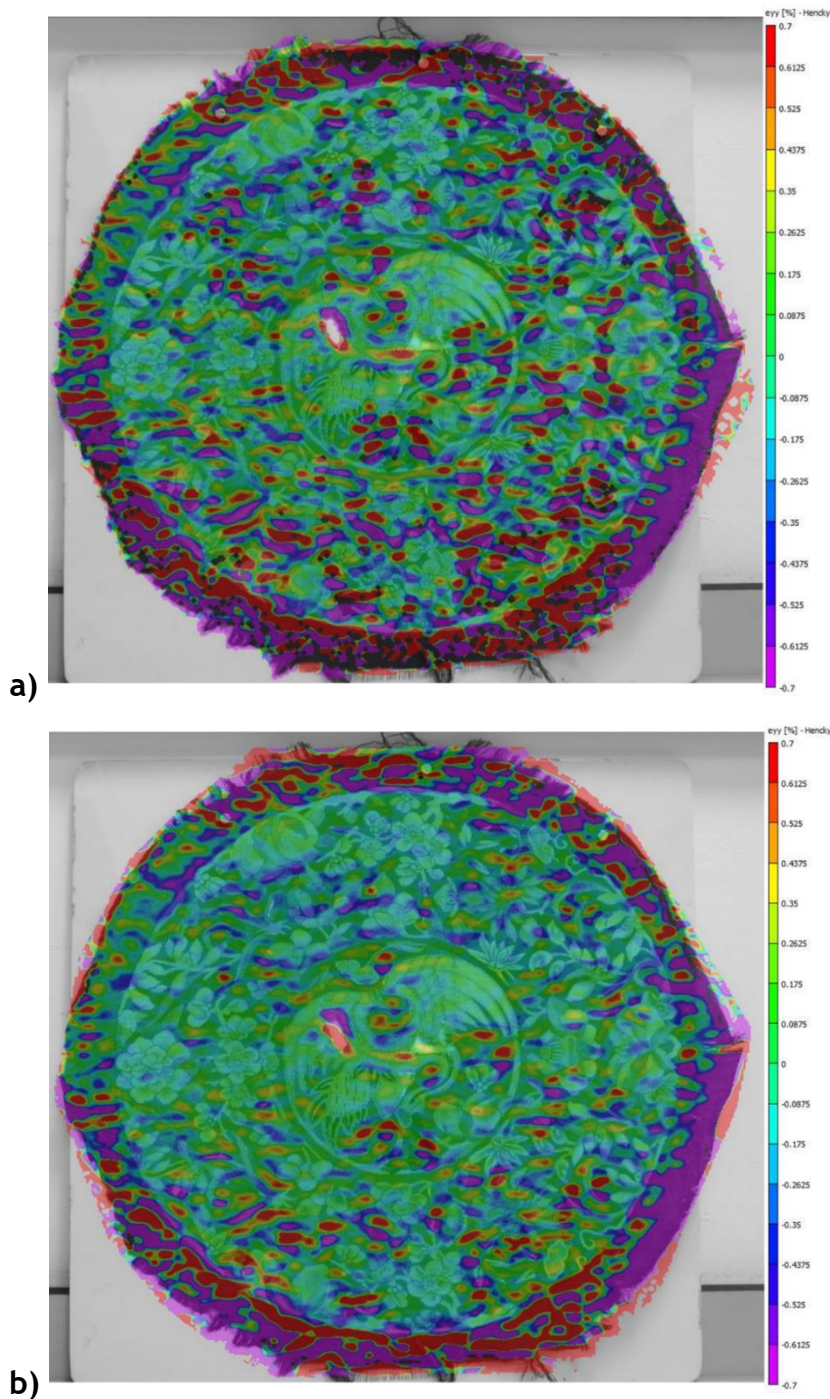


Figure 4.51. ϵ_{yy} [%] map of the *kesi* at the end of the 68-hour monitoring: a) 31 subset size, 5 step size; b) 61 subset size, 3 step size.

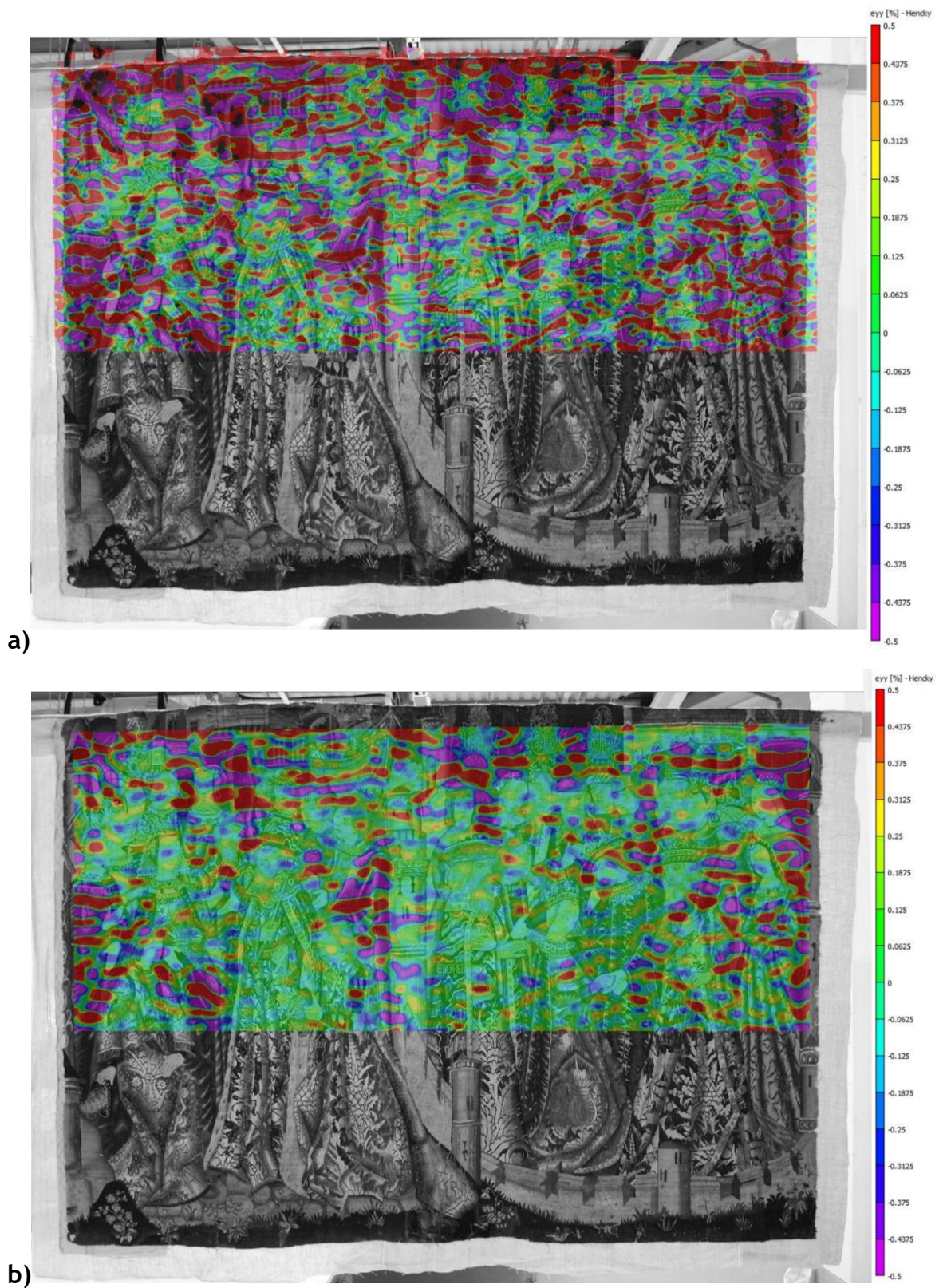


Figure 4.52. ϵ_{yy} [%] map of Florence tapestry at the end of the 100-hour monitoring: a) 31 subset size, 5 step size; b) 61 subset size, 3 step size.

However, differently from what was predicted by looking at the sigma maps, varying step and subset size did not significantly alter the calculation of the average strain. This is shown by the graphs in Figure 4.53 and Figure 4.54, where

are presented the longitudinal strain from the monitoring of the two tapestries with different DIC parameters. The trends of mean ϵ_{yy} , measured using varying subset and step sizes, are very similar and they almost overlap each other.

Therefore, it can be concluded that sigma values can be useful to estimate the suitability of patterns. Indeed, sigma maps efficiently identified where inaccurate *local* strain data would be calculated. On the other hand, sigma mapping was not helpful for defining the accuracy of *overall* strain data.

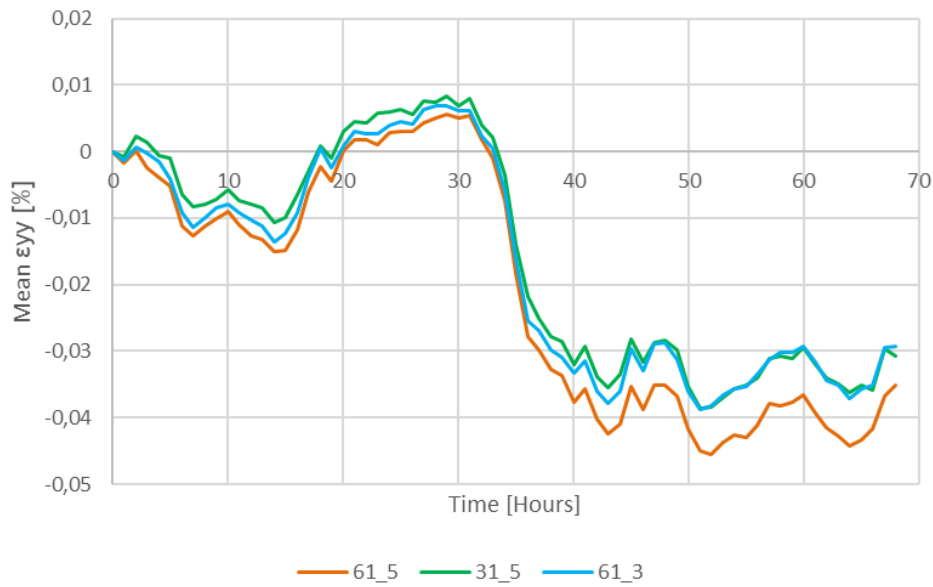


Figure 4.53. Mean ϵ_{yy} [%] calculated across the *kesî* when using different subset and step size.

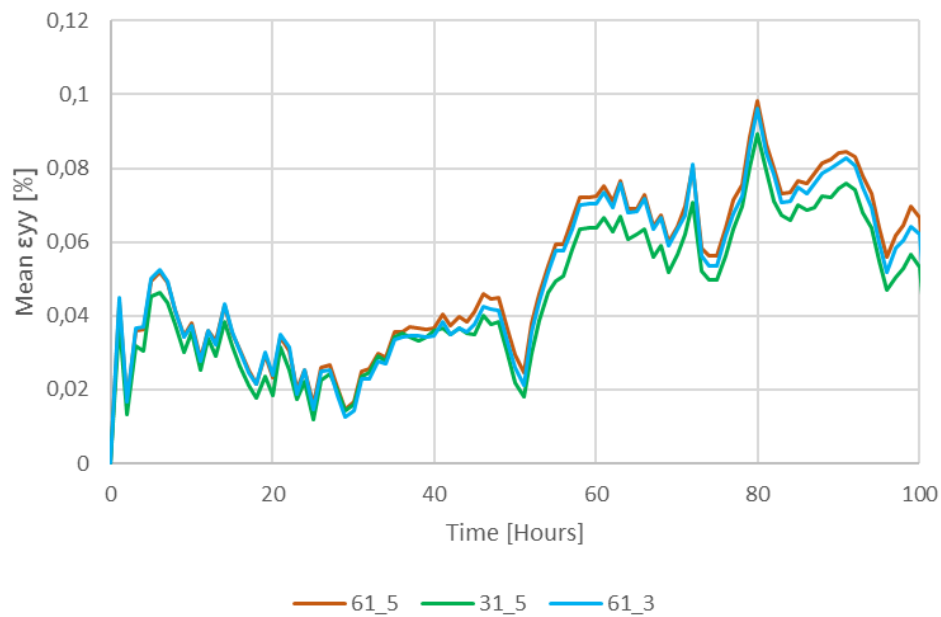


Figure 4.54. Mean ϵ_{yy} [%] calculated across *Florence* tapestry when using different subset and step size.

4.3.2.7 Notes on the mathematical relationship between strain and RH

As discussed in the previous sections, a linear relationship between strain and RH was noted in all the experiments. To better assess whether some differences on fatigue mechanism can be drawn by looking at the equations from the linear regressions, Table 4.4 is presented. Table 4.4 reports the slope, longitudinal strain versus RH, registered from the monitoring of each artwork.

Table 4.4. Slope from the linear fitting, ϵ_{yy} [%] versus RH [%], from the monitoring tests of the different artworks.

Case study	Slope
TapestryFragment_1	0.0090
TapestryFragment_2	0.0089
<i>Kesi</i>	0.0027
<i>Florence</i>	0.0099
<i>Unicorn tapestry</i>	0.0038

From Table 4.4 it is observed that, when considering the historic woollen tapestries, the slope did not show to vary significantly, ranging between 0.0089 (TapestryFragment_2) and 0.0099 (*Florence*). On the other hand, both the historic silk *kesi* and the contemporary tapestry showed a lower slope of 0.0027 and 0.0038 respectively. In such cases, the lower value can be linked to: I) the more contained hygroscopicity of silk threads composing the *kesi* and the lighter weight of the artwork (the latter limiting the effects of self-weight loading); II) the low level of degradation of the newly woven *Unicorn tapestry*.

As expressed in Section 2.2.1.2 when reviewing the work done in Southampton [61], these data are probably not able to build an empirical model for accurately predicting change in lengths due to humidity fluctuations. This seems unfeasible as many variables characteristic of each textile object, e.g. linked to the conservation history, may play a role in the equation. Nevertheless, from the results gathered it was interesting to note how major similarities and discrepancies could be related to the linear regression.

4.4 Conclusions

In this chapter, the feasibility of 2D DIC for monitoring strain across historic hangings was assessed. In general, the contactless technique was proved to be a suitable tool to track overall (globally averaged) displacement in all case studies. Importantly, the tests demonstrated that 2D DIC can be employed for studying larger areas of tapestries than those previously researched [1]. Moreover, the results from the experiment with the *kesi* demonstrated that the optical technique can be suitable for monitoring different types of textile objects, including light-weight silk artefacts affected by relatively small deformations. This is an important caveat, as originally in Southampton the approach was only addressed to the study of European woollen and heavy tapestries [2].

As better described below, the different experimental conditions used throughout the tests were helpful in delineating which parameters may affect the accuracy of DIC analysis. Furthermore, the outcomes gathered from the various tests were able to provide some new insights on the mechanical damage mechanisms affecting tapestries while on display.

4.4.1 Parameters affecting 2D DIC analysis

2D DIC was demonstrated to be a helpful tool to track strain across historic (and non-historic) hangings. Indeed, the high linearity between RH and strain (averaged from the entire surface of the objects) gave confidence to the outcomes. Nevertheless, some parameters were found to have an impact on strain calculation, namely:

- I) The figurative design. As expected, areas with a homogeneous pattern led to inaccurate ϵ_{yy} data, especially on a small-scale level (local strain).
- II) The image quality. When monitoring full-size tapestries of more than one m², the technique would probably be unable to provide accurate local data because of the low resolution of the acquired images. This means that, if damage propagation needs to be tracked across a specific area, the full-field DIC application should be avoided. In addition, it was observed that brightness is

crucial, especially in areas with homogeneous patterns, as it may impact greyscale contrast.

III) Out-of-plane displacements. These can be an issue when the monitored objects are hanging freely because of air circulation; however, they can be sometimes prevented by displaying tapestries against a wall/board.

IV) The subset size. Lowering the subset size was shown to increase the inaccuracy of local strain data (but not globally averaged data).

4.4.2 Mechanical damage mechanisms affecting tapestries when on display

After monitoring five different historic case studies, it was possible to distinguish three main processes determining the mechanical behaviour of tapestries when hung for display:

I) Time-dependent creep/uncrimping at the beginning of the display. When a full-size tapestry is hung after being in storage for a long time, or right after being woven, it elongates significantly during a limited time. The mechanism would mainly compromise weft threads, responsible for both the structure and the pictorial motif of the textile object. Interestingly, the time-dependent behaviour was shown to occur regardless of the application of conservation treatments like linen full support.

II) Fatigue and swelling. Due to the highly hygroscopic nature of wool and silk, tapestries are subjected to contraction and extension, in both horizontal and vertical direction, following humidity variations. This mechanism, that sometimes followed the time-dependent behaviour, proved to be the dominant one during most of the display, defining the overall changes in length in all the case studies examined. These changes are known to be reversible but, due to the constant cycling, may lead to damaging fretting process [10]. It is relevant to note that the case studies presented in this chapter were exposed to relatively low ranges of RH (with the only exception of the contemporary tapestry at Stirling). Because of this, it is important to underline that the negative impact of high RH on the mechanical behaviour could not be observed

through the tests. This represents a limit of the outcomes gathered, as high RH ranges, possibly frequent in historic houses, may lead to damaging shrinkage and structural modifications in wool artworks [10].

III) Creep-like behaviour across damaged areas. Although 2D DIC was found unsuitable to identify weaknesses before the occurrence of a visible defect in the weave structure, the optical method proved useful in describing how longitudinal (pseudo) strain may increase with time across damaged areas such as slits. In comparison to fatigue, the effects of creep should be expected to happen faster, to be more drastic and irreversible.

From a practical perspective, it is important to underline how these experiments clarified that the optical technique is likely to be unable to recognise mechanically fragile areas when they are still “invisible”. Through this, one of the research questions first asked by the group in Southampton is answered: DIC cannot indicate structural weaknesses before the occurrence of an evident defect [2]. This is especially true when considering limited time spans such as those reported in this chapter (up to 200 hours). Nevertheless, the non-invasive approach can be a helpful diagnostic tool for tracking time-dependent mechanisms across weak areas such as slits (calculation of pseudo local strain). As previously said, local data are likely to be less accurate than globally averaged ones, especially when the full-field approach is used on full-size woven hangings; nevertheless, they can provide useful qualitative information.

References

1. Khennouf, D., et al., *Assessing the Feasibility of Monitoring Strain in Historical Tapestries Using Digital Image Correlation*. Strain, 2010. **46**(1): p. 19-32.
2. Lennard, F., et al., *Strain monitoring of tapestries: results of a three-year research project*, in *ICOM-CC 16th Triennial Conference, Lisbon, 2011: Preprints*, J. Bridgland, Editor. 2012, International Council of Museums: Paris. p. 1-8.
3. Pan, B., *Digital image correlation for surface deformation measurement: historical developments, recent advances and future goals*. Measurement Science and Technology, 2018. **29**(8): p. 082001.
4. Sutton, M.A., H.W. Schreier, and J.-J. Orteu, *Image Correlation for Shape, Motion and Deformation Measurements*. 2009, New York: Springer Science+Business Media. 321 p.
5. Kammers, A.D. and S.J.E.M. Daly, *Digital image correlation under scanning electron microscopy: methodology and validation*. Experimental Mechanics, 2013. **53**(9): p. 1743-1761.
6. Sun, Z., J.S. Lyons, and S.R. McNeill, *Measuring Microscopic Deformations with Digital Image Correlation*. Optics and Lasers in Engineering, 1997. **27**(4): p. 409-428.
7. Salmanpour, A.H. and N. Mojsilovic, *Application of Digital Image Correlation for strain measurements of large masonry walls*, in *The 5th Asia Pacific congress on computational mechanics*. 2013: Singapore.
8. Ramos, T., et al., *2D and 3D digital image correlation in civil engineering-measurements in a masonry wall*. Procedia Engineering, 2015. **114**: p. 215-222.
9. Blaber, J., B. Adair, and A.J.E.M. Antoniou, *Ncorr: open-source 2D digital image correlation matlab software*. Experimental Mechanics 2015. **55**(6): p. 1105-1122.
10. Bratasz, L., et al., *Risk of Climate-Induced Damage in Historic Textiles*. Strain, 2015. **51**(1): p. 78-88.
11. Young, C., *Using DIC to develop an Experimental Methodology for Measuring Moisture Induced Fatigue in Panel Paintings*. 2015.
12. Gauvin, C., et al., *Image Correlation to Evaluate the Influence of Hygrothermal Loading on Wood*. Strain, 2014. **50**(5): p. 428-435.
13. Dupre, J.-C., et al., *Experimental study of the hygromechanical behaviour of a historic painting on wooden panel: devices and measurement techniques*. Journal of Cultural Heritage, 2020. **46**: p. 165-175.
14. Malesa, M., et al., *Application of digital image correlation (DIC) for tracking deformations of paintings on canvas*, in *Proceedings of the Optics for Arts, Architecture, and Archaeology III* 2011: Munich. p. 80840L.
15. Rodríguez-Vera, R., et al., *Digital image correlation method: a versatile tool for engineering and art structures investigations*, in *Proceedings of the Optics for Arts, Architecture, and Archaeology III*. 2011: Munich. p. 80119R.
16. Malowany, K., et al., *Application of 3D digital image correlation to track displacements and strains of canvas paintings exposed to relative humidity changes*. Applied Optics, 2014. **53**(9): p. 1739-1749.

17. Malowany, K., et al., *3D Digital Image Correlation for tracking displacements of canvas paintings with natural texture*, in *16th International Conference on Experimental Mechanics*. 2014: Cambridge, UK
18. Vilde, V., et al., *Digital image correlation for condition monitoring of lined painting*, in *ICOM Committee for Conservation. Triennial meeting, 18th, Copenhagen, Denmark, 2017: Preprints*, J. Bridgland, Editor. 2017, International Council of Museums: Paris.
19. Hinsch, K.D., et al., *Artwork monitoring by digital image correlation*, in *Lasers in the Conservation of Artworks*, K. Dickman, C. Fotakis, and J.F. Asmus, Editors. 2005, Springer-Verlag Berlin: Berlin. p. 459-467.
20. Zhao, X., et al., *Study of the quality of wood texture patterns in digital image correlation*. *Optik*, 2018. **171**: p. 370-376.
21. Wang, Z., et al., *Deformation Monitoring System Based on 2D-DIC for Cultural Relics Protection in Museum Environment with Low and Varying Illumination*. *Mathematical Problems in Engineering*, 2018. **2018**.
22. Pan, B., et al., *Two-dimensional digital image correlation for in-plane displacement and strain measurement: a review*. *Measurement Science and Technology*, 2009. **20**(6): p. 062001.
23. Giachetti, A., *Matching techniques to compute image motion*. *Image and Vision Computing*, 2000. **18**(3): p. 247-260.
24. Haddadi, H. and S. Belhabib, *Use of rigid-body motion for the investigation and estimation of the measurement errors related to digital image correlation technique*. *Optics and Lasers in Engineering*, 2008. **46**(2): p. 185-196.
25. Cooreman, S., et al., *Identification of mechanical material behavior through inverse modeling and DIC*. *Experimental Mechanics*, 2008. **48**(4): p. 421-433.
26. Lu, H. and P.D. Cary, *Deformation measurements by digital image correlation: Implementation of a second-order displacement gradient*. *Experimental Mechanics*, 2000. **40**(4): p. 393-400.
27. Pan, B., H. Xie, and Z. Wang, *Equivalence of digital image correlation criteria for pattern matching*. *Applied Optics*, 2010. **49**(28): p. 5501-5509.
28. Tong, W., *An Evaluation of Digital Image Correlation Criteria for Strain Mapping Applications*. *Strain*, 2005. **41**(4): p. 167-175.
29. Schreier, H.W. and M.A. Sutton, *Systematic errors in digital image correlation due to undermatched subset shape functions*. *Experimental Mechanics*, 2002. **42**(3): p. 303-310.
30. Bing, P., et al., *Performance of sub-pixel registration algorithms in digital image correlation*. *Measurement Science and Technology*, 2006. **17**(6): p. 1615-1621.
31. Dong, Y.L. and B. Pan, *A Review of Speckle Pattern Fabrication and Assessment for Digital Image Correlation*. *Experimental Mechanics*, 2017. **57**(8): p. 1161-1181.
32. Reu, P., *All about speckles: Speckle Size Measurement*. *Experimental Techniques*, 2014. **38**(6): p. 1-2.
33. Reu, P., *All about Speckles: Aliasing*. *Experimental Techniques*, 2014. **38**(5): p. 1-3.
34. Reu, P., *All about Speckles: Speckle Density*. *Experimental Techniques*, 2015. **39**(3): p. 1-2.
35. Reu, P., *All about Speckles: Contrast*. *Experimental Techniques*, 2015. **39**(1): p. 1-2.

36. Reu, P., *All about Speckles: Edge Sharpness*. Experimental Techniques, 2015. **39**(2): p. 1-2.
37. Lecompte, D., et al., *Quality assessment of speckle patterns for digital image correlation*. Optics and Lasers in Engineering, 2006. **44**(11): p. 1132-1145.
38. Hijazi, A. and C.J. Kahler, *Contribution of the Imaging System Components in the Overall Error of the Two-Dimensional Digital Image Correlation Technique*. Journal of Testing and Evaluation, 2017. **45**(2): p. 369-384.
39. Hijazi, A. and V. Madhavan, *A novel ultra-high speed camera for digital image processing applications*. Measurement Science and Technology, 2008. **19**(8): p. 085503.
40. Hain, R., C.J. Kähler, and C. Tropea, *Comparison of CCD, CMOS and intensified cameras*. Experiments in Fluids, 2007. **42**(3): p. 403-411.
41. Sutherland, H. *A low tech approach to high tech analysis*. in *New Perspectives: Contemporary Conservation Thinking and Practice*. Icon 2019 Conference. 2019. Belfast: Icon.
42. Yu, L. and B. Pan, *In-plane displacement and strain measurements using a camera phone and digital image correlation*. Optical Engineering 2014. **53**(5): p. 054107.
43. Pan, B., D. Wu, and Y. Xia, *An active imaging digital image correlation method for deformation measurement insensitive to ambient light*. Optics & Laser Technology, 2012. **44**(1): p. 204-209.
44. Ma, S., J. Pang, and Q. Ma, *The systematic error in digital image correlation induced by self-heating of a digital camera*. Measurement Science and Technology, 2012. **23**: p. 025403.
45. Pan, B., L. Yu, and D. Wu, *High-Accuracy 2D Digital Image Correlation Measurements with Bilateral Telecentric Lenses: Error Analysis and Experimental Verification*. Experimental Mechanics, 2013. **53**(9): p. 1719-1733.
46. Sutton, M.A., et al., *The effect of out-of-plane motion on 2D and 3D digital image correlation measurements*. Optics and Lasers in Engineering, 2008. **46**(10): p. 746-757.
47. Alsayednoor, J., et al., *Evaluating the use of digital image correlation for strain measurement in historic tapestries using representative deformation fields*. Strain, 2019. **55**(2): p. e12308.
48. Lava, P., et al., *Assessment of measuring errors in DIC using deformation fields generated by plastic FEA*. Optics and Lasers in Engineering, 2009. **47**(7): p. 747-753.
49. Lava, P., S. Cooreman, and D. Debruyne, *Study of systematic errors in strain fields obtained via DIC using heterogeneous deformation generated by plastic FEA*. Optics and Lasers in Engineering, 2010. **48**(4): p. 457-468.
50. Smith, M.J., T.H. Flowers, and F.J. Lennard, *Mechanical properties of wool and cotton yarns used in twenty-first century tapestry: Preparing for the future by understanding the present*. Studies in Conservation, 2015. **60**(6): p. 375-383.
51. Beingessner, A., *The Hunt of the Unicorn: Tapestry Copies Made for Stirling Castle, Scotland*, in *Art History and Visual Culture*. 2015, University of Guelph.
52. Ballard, M.W., *How backings work: the effect of textile properties on appearance in Lining and backing: the support of paintings, paper and textiles*. Papers delivered at the UKIC Conference, 7-8 November 1995.

- 1995, United Kingdom Institute for Conservation of Historic and Artistic Works: London. p. 34-39.
53. Strlič, M., et al., *Damage functions in heritage science*. Studies in Conservation, 2013. **58**(2): p. 80-87.
 54. <https://www.correlatedsolutions.com>.
 55. Khennouf, D., et al., *Application of digital image correlation to deformation measurement in textile*, in *Photomechanics 2008: International Conference on Full-Field Measurement Techniques and their Applications in Experimental Solid Mechanics*. 2008: Loughborough, UK.
 56. Duffus, P., *Manufacture, analysis and conservation strategies for historic tapestries*, in *Faculty of Engineering and Physical Sciences*. 2013, University of Manchester.
 57. Hutton, E. and J. Gartside, *The Moisture Regain of Silk i. Adsorption and Desorption of Water by Silk at 25° C*. Journal of the Textile Institute Transactions, 1949. **40**(3): p. T161-T169.
 58. Frame, K., et al., *Balancing Significance and Maintaining 'Sense of Place' in the Sustainable Display of Tudor Tapestries in the Great Hall, Hampton Court Palace*. Studies in Conservation, 2018. **63**: p. 87-93.
 59. Thickett, D., N. Luxford, and P. Lankester. *Environmental Management Challenges and Strategies in Historic Houses*. in *The artifact, its context and their narrative: multidisciplinary conservation in historic house museums* 2012. Los Angeles: ICOM-CC.
 60. Wood, J., et al., *Reconstruction of historical temperature and relative humidity cycles within Knole House, Kent*. Journal of Cultural Heritage, 2019. **39**.
 61. Dulieu-Barton, J.M., et al. *Long term condition monitoring of tapestries using image correlation*. in *Society for Experimental Mechanics (SEM) Annual Conference*. 2010. Indianapolis, USA.

5 Evaluation of sloping boards as a display method

Chapter 5 focuses on the study of sloping boards (also called slanted supports), an untraditional display method increasingly popular among museums in continental Europe. As mentioned in Chapter 1 and discussed more in detail in the introductory section of this chapter, sloping boards are preferred by some conservators and curators. They are considered a good alternative to the traditional vertical display since it is thought that they may retard the elongation of weft threads, and so reduce mechanical damage due to the self-weight loading. Few published works can be found on slanted supports [1, 2], and none that systematically examines, also from a scientific perspective, all advantages and disadvantages of such system. The first part of the chapter presents a literature review on the use of sloping boards and the few past experimental studies seeking to validate this approach. Furthermore, a review of past works dealing with fabric on fabric friction is presented in the first section.

The experimental work of the chapter aimed to investigate the usefulness of slanted supports for conservation purposes by considering two different factors that may contribute to strain reduction: friction and inclination. The coefficient of friction between common board-covering fabrics and tapestries (with and without cotton and linen for lining/support treatments) was measured using an inclined plane method. On the other hand, to assess the effects due to the inclination, 2D DIC (trialled in Chapter 4) was employed to monitor strain across wool rep mock-ups displayed on an uncovered support (low friction) slanted at different angles from the vertical. Lastly, strain across a historic tapestry fragment on a vertical wooden support half covered with cotton molton was monitored using DIC. This aimed to verify whether fabric on fabric adhesion/friction may be enough to limit overall extensions even at 0° from the vertical.

The experimental design of Chapter 5 is described in Table 5.1.

Table 5.1. Experimental design of Chapter 5.

Hypothesis	Case studies	Techniques	Methodological limits
Fabrics employed for covering sloping boards ensure a high level of friction when in contact with tapestries	Common covering fabrics (cotton molton, cotton domette, polyester felt, cotton veltet); 7 historic tapestry fragments with different weave structure; wool rep fabric; linen used for support treatments; cotton for lining treatments	Slanted plane method for measuring the coefficient of static friction (with and without added weight)	Not all variables playing a role in fabric/fabric friction are evaluated through the testing method (e.g. rate, asperity)
In case of no friction, only when tapestries are displayed at significant inclinations (e.g. 45° from the vertical) strain is successfully decreased	Wool rep mock-ups displayed at 0°, 5°, 45° from the vertical. A fixed load is added to speed up creep and a dotted pattern is applied on the surface to facilitate correlation	2D DIC (168-hour test per inclination)	The uncontrolled environmental conditions during testing can impede the comparison between results acquired at different inclinations
The high level of friction/adhesion between a tapestry and commonly employed board covering fabrics can limit strain even at 0° from the vertical	Historic tapestry fragment displayed on a vertical board half covered with cotton molton and half uncovered	2D DIC	The test can only last a limited amount of time (i.e. 340 hours), so long-term effects cannot be evaluated

5.1 Introduction

5.1.1 Origins and current diffusion of sloping boards for displaying tapestries

The use of slanted supports for displaying tapestries started in the 1990s thanks to André Brutillot who worked as a private textile conservator and at the Bayerisches National Museum (BNM) in Munich, Germany. Brutillot, now retired, did not thoroughly discuss his method in any (English) publication, from how it was first conceived to how it developed and improved. Nevertheless, Brutillot provided details of his approach at a conference held at the Metropolitan Museum of Art in 2009; the presentation was recorded and it can now be found on YouTube [3].

At the conference Brutillot examined his experience with slanted boards, underlining advantages and disadvantages. He started his speech by explaining why he first had had the idea of changing from the traditional vertical display to slanted supports. He thought of this new method when he got appointed to conserve, working alone and only 20 hours a week, highly damaged tapestries at the BNM. Due to the fragile conditions of the textile objects and the fact that they were expected to be on display for a long time once ready, Brutillot aimed to find a way to retard weft elongation. The need of conceiving a method that allowed tapestries to be on display for long periods and safely was essential. He acknowledged that the museum wanted to show them permanently as they were precious masterpieces, but he was also aware that originally the collection was not intended to be hung for long periods. This means that tapestries were designed and woven considering the structural strength as less important than the aesthetic appreciation. Therefore, Brutillot aimed to find a method able to compromise long-lasting display and supporting action. Besides these considerations, importantly, the treatment needed to be fast and minimally invasive, as he had a tight schedule.

The first boards prepared were made of wood and inclined by 5° from the vertical (no explanation was given for the choice of the angle). To prevent the historic hanging from sliding, from the beginning the importance of choosing a covering fabric for the board able to promote friction was highlighted. At first wool was considered, as Brutillot stated that the coefficient of friction between two textiles of the same material was expected to be higher than that between different ones, though he underlined he had no reference proving this. However, since wool is easily attacked by insects, other materials were preferred, namely: cotton molton, cotton babycord, polyester felt (also indicated with the term *fleece*) [3].

For the first time, in 1991 at the BNM a historic hanging was on display on a slanted board. From that moment on, different museums, especially in continental Europe, began to use this new display method, though few documented this with publications [4]. Examples portraying slanted supports in museums and galleries are shown in Figure 5.1. From the recent survey by Catic (2019) [5], it was highlighted that all the respondents working in Italy and

France sometimes opt for slanted supports, to reduce stress. Also among German conservators the use of sloping boards proved to be widespread (82% of interviewed people). On the other hand, only around one quarter of the respondents from British workshops claimed to employ this system (24%), specifically in the case of very fragile tapestries to reduce the amount of invasive treatments. However, from the survey it can be observed that French and Italian conservators do not change the type of treatment when they decide to use slanted supports, while 67% of German staff do. All the respondents using boards said they would cover them with fabrics to promote friction [5].



Figure 5.1. Slowing boards at the: a) Cluny Museum in Paris; b) Designmuseum Denmark in Copenhagen (profile).

Today, one of the most renowned examples using this display method is the Cluny Museum in Paris. There, the *Unicorn* set is currently presented on boards slanted at an angle varying from 2° to 5° from the vertical, as shown in Figure 5.1a [6, 7]. Some pieces of information on the design of the supports can be found in some reports in French [6, 8]. For instance, it is described that the boards are made of steel, with a surface made of aluminium, polyethylene and an isolating material [8]. The boards in the French museum are covered with a cotton needlecord fabric (“*velours bouclé de coton*”) [7].

5.1.2 Previous studies on the efficacy of sloping boards

When advocating for slanted supports, Brutillot underlines that they bring important and verifiable advantages, such as the decrease of: I) weft elongation; II) superficial waves; III) conservators' intervention; IV) dirt accumulation. To prove the validity of these points, Brutillot carried out some tests, as he explained at the American conference in 2009 [3].

To assess the ability of slanted supports in reducing strain (retardation of weft elongation), Brutillot measured the distance between the bottom edge of the board and that of some tapestries. He repeated the measurements weekly for at least five years, comparing tapestries displayed at 5° with one at only 1° from the vertical (while recording humidity and temperature). He noted that, in all the cases, the greatest elongation occurred within the first month of display (i.e. 5 mm when at 5°), then it remained stable for around five years. Another important observation was that textile objects on the supports slanted by 1° from the vertical elongated more than those at 5° (i.e. 10 mm in three months in the case of the display at 1°), as he expected. Thanks to this reduction in weft elongation, Brutillot decided to diminish the amount of conservation treatments [3]. It is important to underline that without more precise details on the methodology, it is difficult to properly evaluate the outcomes of these series of tests. For instance, how were the effects of fatigue separately evaluated from those linked to other time-dependent mechanical damage mechanisms like creep? How were the studied tapestries selected? How much did differences in the pre-existing condition of the objects under investigation affect the measurements?

When considering dust accumulation, Brutillot explained that this argument is often used against sloping boards, as one may think that the angle would make the surface dustier. However, he thinks that dust deposition is caused by air circulation and the different temperature between the front and the back of the object rather than the inclination of the support. In Brutillot's opinion, this is clearly shown when looking a tapestry with supporting straps on the back: the areas without lining, where air circulation is allowed, get dirty, while covered areas remain cleaner. Therefore, Brutillot suggested that sloping boards would avoid dust accumulation through impeding air from passing across the textile [3].

As remarked by Brutillot, another aspect of sloping boards often criticised is that they alter the original aesthetic, and this may affect the appreciation of tapestries design. Nevertheless, this point is in contrast with what he observed through some experiments assessing how people spent more time in front of tapestries on boards rather than those hung vertically [3]. Again, as no more specific pieces of information were given about the tests, it is difficult to properly examine the outcomes.

Besides Brutillot's own work, few other publications can be found on the assessment of slanted supports for displaying historic textiles [9], and more specifically tapestries [1, 2]. Barker in 2002 published an article where she discussed the usefulness starting from a mathematical model [1] (the same paper was also re-published in 2005 [10]). First, the author illustrates the forces acting on an object (tapestry) displayed on an inclined support. The reproduced graph is depicted in Figure 5.2.

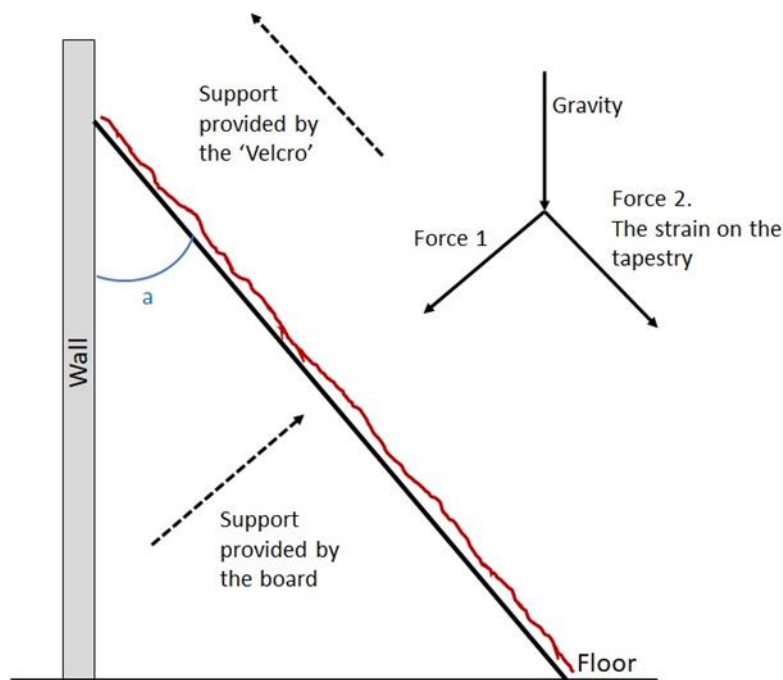


Figure 5.2. Forces acting on a tapestry displayed on a fabric-covered board. Reproduced from Barker [1].

From the model it can be measured that strain is reduced by only 0.4% with an inclination of 5° from the vertical. Also at greater angles the decrease in strain is still very much contained (-8.4% at 25° from the vertical).

In her theoretical analysis, Barker did not consider the impact of friction. Although the author mentioned the variable, no value for the fabric on fabric coefficient of static friction (μ_s) was given, and therefore its effects were not properly evaluated. In general, according to Barker, the level of fabric/fabric friction is not high enough to significantly affect the supporting action of the board [1].

On the other hand, Trosbach's master dissertation (unpublished, in German) focused more on the impact of friction on slanted supports' efficacy [2]. In this case, the author measured friction between one tapestry fragment and fabrics commonly employed in Germany for covering sloping boards, namely: cotton babycord; cotton molton; polyester felt (fleece), thick and thin variety. In addition, friction between these covering fabrics and two cotton textiles, sometimes used for conservation treatments, were measured. To calculate the coefficient of friction, a specific testing machine was designed and prepared. It consisted of a large board that, through an automated system, could be tilted at different angles at a fixed rate. The board was coated with one of the covering fabrics, while the tapestry sample (or one of the cotton fabrics), wrapped into a metal plate, was placed on top of the support while lying horizontally. Then the automated system was turned on, and the angle at which the textile object started to slip was recorded. The coefficient of friction was calculated from the tangent of the sliding angle, as it can be derived from Amontons' law (this is better discussed in the next Section). The outcomes showed that μ_s between the tapestry fragment and most of the covering fabrics was around 1.5. Only the thick polyester fleece led to a much greater μ_s , namely 3.3. Since a coefficient of static friction of 1.5 is relatively high, this already indicates how choosing an appropriate board-covering fabric in such display method is fundamental to increase the supporting action [2].

From the French report on the use of sloping boards at the Cluny Museum, it was stated that cotton needlecord was selected after some tests consisting of placing tapestry samples on small mock-up boards covered with different textiles. Although there are no details on the experiments, also in this case they confirmed the high level of friction and adhesion promoted by the fabrics under investigation [8].

5.1.3 Fabric on fabric friction: definition, how to measure it and what factors may influence it

Friction is defined as “the force resisting the relative lateral or tangential motion of solid surfaces, fluid layers or material elements in contact” [11]. When considering the interaction between two solid bodies, the phenomenon can be described by the dry or Coulomb friction model. Importantly, Coulomb distinguished two frictional forces: I) static friction; II) dynamic friction. The force of static friction, F_s , describes the force needed to move the object from lying still on a surface. Conversely, the force of dynamic, or kinetic, friction (F_R) represents the force once the body is moving, after overcoming the force of static friction.

Up to a certain level of approximation, reasonable in many case studies, both frictional forces can be calculated quite easily as they are proportional to the normal force [12], as expressed by equations 1 and 2 (also known as Amontons’ law):

$$F_s = \mu_s \times N \quad \text{Eq (1)}$$

$$F_R = \mu_K \times N \quad \text{Eq (2)}$$

where μ represents the coefficient of friction between the two solid bodies, and N the normal force. The coefficient of friction μ is indicated by a dimensionless scalar number and it is specific for each pairing of materials in contact. In many cases, like for instance for metallic surfaces, it is expected that frictional forces do not depend significantly on variables such as the contact area or roughness of the surface [12].

Figure 5.3 depicts the diagram of forces involved when considering an object sliding on an inclined plane, as in the case of a tapestry displayed on a slanted support.

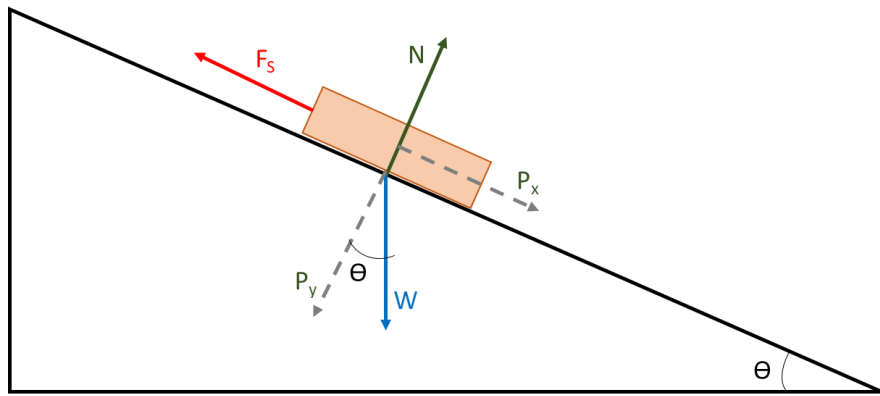


Figure 5.3. Object on an inclined plane and related applied forces.

Where:

- W = weight
- N = normal force
- F_s = static frictional force
- P_x = component of the weight of the object on the x axis.
- P_y = component of the weight of the object on the y axis.

From Figure 5.3, it can be determined that, when the object is sliding:

$$N = W \times \cos \theta \quad \text{Eq (3)}$$

Therefore, combining eq. 1 with eq. 3, it can be determined that:

$$F_s = \mu_s \times W \times \cos \theta \quad \text{Eq (4)}$$

From this, it can be derived that:

$$\mu_s = \tan \theta \quad \text{Eq (5)}$$

The equation just derived can be used to calculate the coefficient of friction using a slanted plane system [13]. In practice, the testing apparatus consists of a flat board that can be tilted at different angles. The surface of the board is covered with one of the pair of materials under investigation, while the other lies on top unfixed. During the measurement, the board moves progressively

from the initial horizontal position. Once the object starts to slide, the test finishes and the angle is recorded to calculate the coefficient of static friction from its tangent [2, 13-15].

This simple method is not the most widespread when looking at papers dealing with friction measurements and indicated by the standard [16]. However, it is sometimes employed, also when studying fabric/fabric friction, as it represents an easy-to-prepare and valid alternative to more elaborate tools [2, 13-15, 17]. Even when not opting for the slanted plane method, the testing machine needs to be specifically designed and built, as there are no ready-to-use devices. Often, the self-made tool is attached to the crosshead of a tensile tester and it is based on the principle of pulling the surface of a sled, covered with one fabric, against that of a horizontal plane, covered with the other fabric. The force needed for moving the sled is calculated by the load cell and it corresponds to the resistance frictional force [18, 19].

Past studies, using both methods described above, report that fabric on fabric frictional forces may vary greatly depending on the pairing textiles, however they are usually high, especially in the case of those made from natural fibres like wool ($\mu_s \geq 1$) [2, 14, 20]. This is evident when comparing fabric/fabric μ with that of other materials. For instance, μ_s of oak on oak ranges between 0.5 and 0.6, that of glass on glass is around 0.9, while in the case of hard steel on hard steel around 0.8 [21]. Usually the coefficient of dynamic friction is lower than the static one, as one may expect [14].

When considering fabrics, it should be noted that defining the coefficient of friction may be more complex than for other materials [22]. Indeed, it was found that in the case of many textiles, Coulomb's model and Amontons' law may not apply properly as some testing parameters can affect the measurements, namely: pressure [23]; normal force; tension [23-25]; tested area [24]; number of measurements [24]; speed [26]. Howell in 1953 identified the following relationship between friction (F) and normal force (N) [25, 27, 28]:

$$F = a N^n \quad \text{Eq (6)}$$

In Howell's equation, the proportionality between friction and normal force is defined by a , a coefficient that can be determined experimentally. On the other hand, n represents the fitting parameter linked to the deformation mechanism. In the specific case of $n = 1$, a corresponds to μ [25].

Wilson in his article dated 1963 [23] clarified more precisely, through both a theoretical and experimental approach, the influence of pressure, and the related contact area, on friction. He stated that the frictional force can be defined as:

$$F = C_1 + n \log P \quad \text{Eq (7)}$$

Where C_1 and n are variables, found to be characteristic of the type of textile. In particular, C_1 is linked to asperity (the higher the asperity, i.e. number of contacts between the materials, the higher C_1). From the tests, it was established that the fabrics under investigation could be divided in two groups: I) fabrics with a high n and a low C_1 , woven with yarns from continuous filaments; II) fabrics with a low n and high C_1 , woven with all/some spun yarns, or bulky yarns [23]. Wilson's work is important to prove how intrinsic properties of the material, like indeed the type of yarns, contribute to define the fabric/fabric frictional forces.

Nevertheless, the Wilson or Howell laws are an approximation of a more complex phenomenon that still needs to be fully defined, as also other variables are now known to partly determine fabric/fabric friction [29]. Indeed, more recently, studies analysed the influence of properties linked to the raw materials, weave meso-structure and yarns [20]. Factors like yarn hairiness [20], loop length, yarn linear density [30], yarn thickness, but also sample orientation [31], are demonstrated to have an impact on fabric on fabric friction.

5.1.4 Theoretical analysis of the role of inclination and friction

Prior to embarking on the experimental investigation, a theoretical analysis of the efficacy of sloping boards for reducing strain across tapestry-like materials is presented. The theoretical approach was elaborated within the context of the current project by Dr Philip Harrison, co-investigator. Differently from the model

provided by Barker [1], Harrison took into consideration the reciprocal influence of friction between covering fabric and a tapestry, as well as the inclination of the board. The observations drawn from the theoretical model were helpful to have a better, although still simplified, understanding of load distribution across a historic hanging displayed on a slanted support. Furthermore, such theoretical predictions were helpful to assess the reliability of the data gathered from the experimental work discussed in Section 5.3.2 and 5.3.3. In particular, this was relevant to verify the feasibility of 2D DIC for testing display/conservation approaches, as such application of the optical technique has not been extensively trialled before. A detailed description of the theoretical analysis can be found in the following publication from 2020 [32].

Figure 5.4 illustrates the load per unit of length (N) experienced by the top part of a 2m-long tapestry (areal density 1 kgm^{-2}) at different angles θ , and when considering different values of the coefficient of friction μ . The broad range of values selected reflects the variability observed when measuring μ in actual cases (Section 5.3.1). As expected, Figure 5.4 shows that the maximum line force experienced by the tapestry drops with both increasing inclination angle and at greater friction. When there is no friction, the load decreases are significant when sloping the board is at 45° , but very small for inclination angles of 5° from the vertical, or less. On the other hand, when examining a high μ of 1.5, the reductions are already significant at angles of 5° ($\approx 15\%$) and fall to complete reduction of the load at a display angle of about 34° . To reduce the load to 0 at smaller angles, such as 5° , μ would have to be close to 20. However, it is remarked that, as further discussed in Section 5.3.1.2, such high values of μ could not be fully explained using the Coulomb's model.

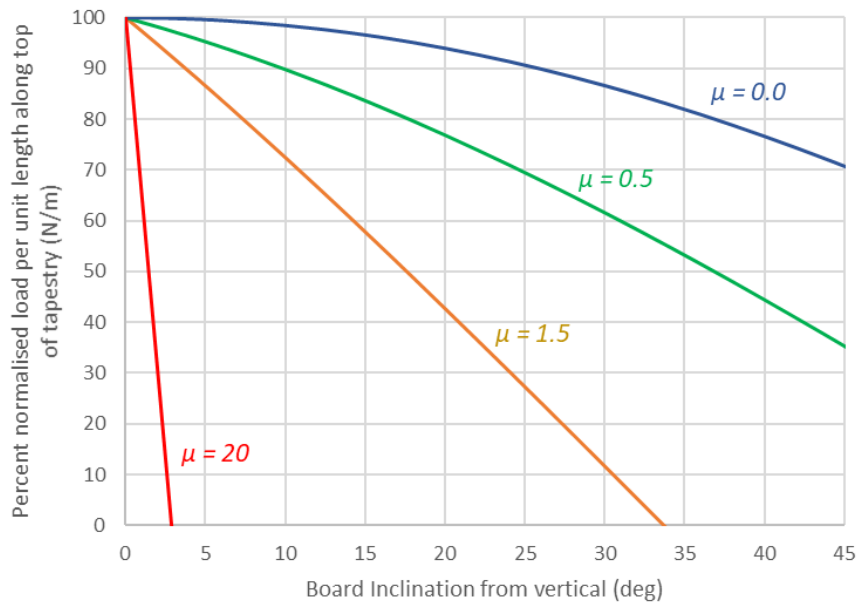


Figure 5.4. Line force per unit length acting along the top of the tapestry versus inclination angle of the display board with different coefficients of friction, normalised by the load at 0° of inclination.

Figure 5.5 depicts strain at various heights of the modelled tapestry when displayed at 5° from the vertical but experiencing different friction. In the graph, 2m corresponds to the top edge while 0m represents the bottom edge of the tapestry. Clearly, the higher the frictional force (and adhesion), the lower the strain experienced by the fabric; μ values of 20 or more lead to complete support (0 strain) in the tapestry.

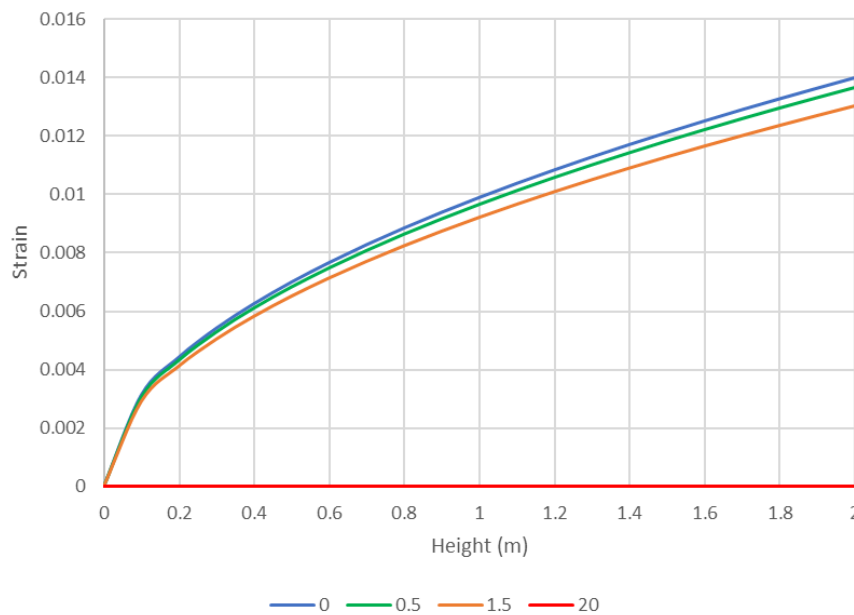


Figure 5.5. Strain versus height of the tapestry when displayed 5° from the vertical at different coefficient of friction: 0; 0.5; 1.5; 20.

These theoretical results can provide a basic understanding of the kind of loads and strains one might expect when hanging tapestries at different inclinations and level of friction. While the theory gave some enlightenment, this analysis did not consider the presence of heterogeneities (e.g. open slits) and only examined the effects of self-weight loading. In particular, the model described the load distribution that should be expected on a displayed woven hanging moving from a horizontal position, so in comparison to a distribution of 0 load. Other mechanical damage mechanisms like fatigue, discussed in Chapter 4, were not included in the theoretical analysis.

5.2 Materials and Methods

5.2.1 Friction measurements

The coefficient of static friction between tapestry fragments (with and without lining/support) and fabrics commonly employed for sloping boards was measured to assess the impact of this variable in reducing weft elongation (strain) when this display method is employed.






As indicated in Table 5.2, four different board-covering fabrics were selected for the tests: I) cotton molton; II) cotton domette; III) polyester felt; IV) cotton velvet. The textiles were chosen according to the responses from Catic's questionnaire [5] and Trosbach's work [2].




Table 5.2. Details of the board-covering fabrics tested.

Fabric type	Fibre	Weave	Supplier
Domette	Cotton	2:1 twill with brushed surface	NB: the quality of domette used in the testing is no longer available from this supplier https://www.naturstoff.de
Molton	Cotton	2:1 twill with brushed surface	Bio-Molton 160 https://www.whaleys-bradford.ltd.uk
Felt	Polyester	Non-woven, needle punched	Polyester felt (3mm; 120gsm) https://www.preservationequipment.com
Velvet	Cotton	Velvet, warp pile	Supplier: Naples NESP Obtained from https://www.mandors.co.uk

Six tapestry fragments were chosen to evaluate friction against the board-covering fabrics. Besides the historic samples, the newly woven wool rep fabric, used for the DIC strain monitoring experiments (as in described in Section 5.2.2), was tested. It should be noted that fragments Tap1 and Tap2 present, respectively, a cotton lining and a linen support stitched on the back. Friction of cotton and linen textiles on the board-covering fabrics was evaluated also separately, without any tapestry fragment attached. This was important as often these textiles can be found stitched on the back of historic hangings since they are used for conservation treatments such as support or lining/dust covering [33]. Details and images of the historic and non-historic fabrics are reported in Table 5.3.

Table 5.3. Details of the historic tapestry fragments, wool rep, linen and cotton fabrics tested against the board-covering fabrics to measure μ_s .

Sample Code	Dimensions [mm]	Thread count per cm (warp x weft)	Lining/support	Image
Tap1	225 x 200	7 x 27	Cotton, tightly woven tabby (plain weave)	
Tap2	300 x 240	5 x 16	Linen, tabby (plain weave)	
Tap3	210 x 90	8 x 32	-	
Tap4	150 x 105	7 x 27	-	
Tap5	908 x 950	5 x 17	-	

Tap6	925 x 270	8 x 30	-	
Wool Rep	200 x 200	23 x 8	-	
Cotton	200 x 200	.5 ⁵	-	
Linen⁶	200 x 200	17 x 17	-	

Tests were carried out using a simple inclined plane method, as described in Section 5.1.3. The technique consists of measuring the angle at which the sample under investigation (i.e. the tapestry fragment or the linen support/cotton lining fabric) starts to slide on a flat surface covered with the selected fabric (i.e. the board-covering textile). The value of the angle was read through a phone app (Multi Clinometer™). The coefficient of friction was calculated from the tangent of the mean value after 15 measurements of the sliding angle.

Two different variants of this procedure were followed: I) the sliding specimen was wrapped, prior to the test, around a glass plate (12 x 6 cm, 121 g); II) the sample was left without any weight. The second approach is thought to better replicate actual scenarios, as a tapestry being placed on a slanted support will

⁵ The weave is extremely fine and therefore thread count is difficult to quantify through a thread counter.

⁶ Corresponding to Linen B in Chapter 6, supplied by Claessens.

not present any extra load on its surface. However, previous studies calculating fabric/fabric friction with the slanted plane method, added an extra weight wrapped around the textile specimen, so as to apply a constant pressure on a defined area [2, 14]. As mentioned above, the coefficient of friction between fabrics is known to be influenced by factors like the applied load and the number of asperities [23, 25], so it was expected that the outcomes from the experiments using the two approaches would be different.

5.2.2 2D DIC strain monitoring: fixed-load experiments with non-historic samples on uncovered board slanted at different angles

Non-historic samples made with hand-woven wool rep fabric (by Context Weavers, see specifications in Section 3.1.2) were used to investigate the effects of displaying tapestry-like materials on uncovered board slanted at different angles. This allowed the study of strain reduction promoted by the inclination of slanted supports, when friction is neglectable. As mentioned in Chapter 3 and 4, the wool textile was selected to mimic the mechanical behaviour of historic hangings, although simplifying it, as also done in other studies [34].

For each test at a specific inclination, specimens 200 mm wide and 245 mm long were used. The samples presented a central horizontal open slit 50 mm wide to simulate the behaviour of a mechanically damaged textile object. One undamaged specimen was also monitored as reference. A cotton bag containing 100 g of lead weights was stitched at the bottom of all the samples to better match the load experienced near the top of a larger and heavier tapestries. The textiles were attached to the board using a wooden batten (covered with Velcro™, soft side) which in turn was fixed at the top edge of the display board via four bar clamps.

On the surface of the wool-rep samples a speckle pattern with dots of around 1 mm in diameter was artificially applied to ensure the DIC correlation algorithm could track the strains. The type of pattern was selected according to the results from the tests in Chapter 4. The speckle pattern was created by hand using both a Stabilo OHPen Universal Marker™ (Fine, black) and a Sharpie Permanent Marker™ (Fine, black). Figure 5.6 illustrates the monitoring set-up.



Figure 5.6. Set-up of wool rep specimens for the tests studying the effects of inclination. The open slits in the artificially damaged samples are indicated within the red dotted lines.

Each monitoring session lasted 168 hours, one week, during which a Canon camera was set up to take one picture per hour (details in Section 4.2.2). More precise information on the DIC analysis is reported in Section 4.2.2, including details on the post-processing calculation carried out through MATLAB. When comparing the results from different tests, the maximum strain registered across the area of interest was considered. Such value corresponds to the highest strain calculated in the specific region during the entire length of the experiment. It is underlined that a subset size of 61 and a step size of 5 were used throughout the analysis.

5.2.3 2D DIC strain monitoring of a historic tapestry fragment displayed on a half covered and half uncovered vertical board

Strain across a tapestry fragment was monitored through 2D DIC. The historic hanging was displayed for 340 hours on a wooden board placed at 0° from the vertical. The board, in the vertical direction, was left half uncovered while the other half was covered with cotton molton. The test aimed to verify whether frictional/adhesion forces originating from the contact of the surfaces of the two fabrics would be high enough to reduce strain when displayed vertically. The set-up is shown in Figure 5.7.

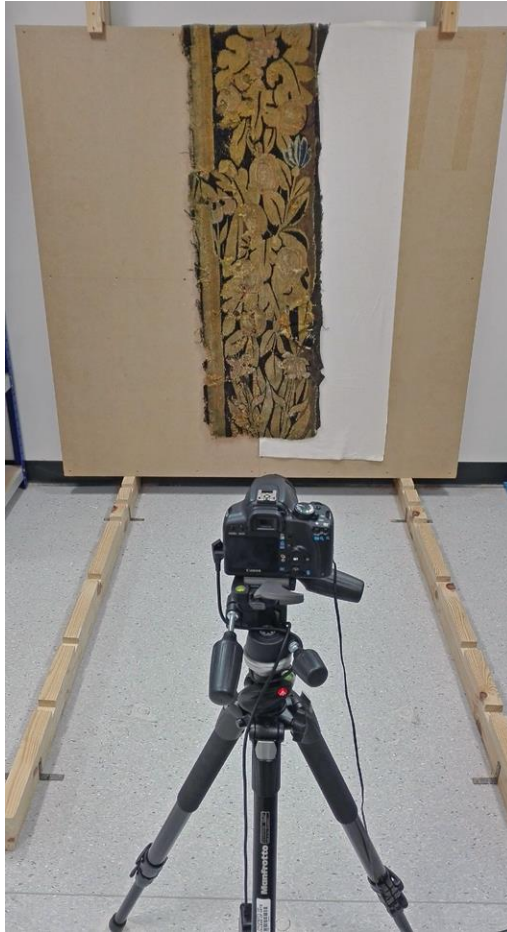


Figure 5.7. Monitoring set-up of the historic tapestry fragment displayed on a vertical wooden board, half uncovered, and half covered with cotton molton.

In Chapter 4, more detailed information on the fragment, DIC analysis and camera set-up can be found. Again, a subset size of 61 and a step size of 5 were chosen as fixed parameters.

5.3 Results and discussion

To evaluate the effectiveness of sloping boards as a display method for tapestries, tests were carried out to establish the role played by: I) fabric/fabric friction (measurements of μ_s); II) inclination (2D DIC strain monitoring).

5.3.1 The role of friction

First, the coefficient of static friction, μ_s , between tapestries and common covering fabrics was measured using a simple slanted plane method, with and without additional load.

5.3.1.1 Friction measurements: weighted specimens

Table 5.4 reports the angles at which the weighted samples, i.e. wrapped around the glass plate, started to slide from the board covered with cotton molton. The coefficient of static friction calculated from those angles are shown in Table 5.5. The data obtained agree with what was previously found by Trosbach [2]: the coefficient of static friction between the historic/newly woven fabrics and cotton molton was close to 1.5 (sliding angle between 57° and 62°). The only exception was Tap3, for which the μ_s was higher, around 3.2. It is important to remember that already a μ_s of 1.5 can be considered quite high in comparison to that of other materials (as discussed in Section 5.1.3), indicating the frictional force would oppose the sliding movement considerably.

Table 5.4. Angle [°] at which the weighted fabric samples (i.e. wrapped around a glass plate) started to slip from the board covered with cotton molton. The SD is also indicated (15 measurements per sample).

<i>Board covering fabric</i>	Cotton	Linen	Wool Rep	Tap3	Tap4
Cotton Molton	62.25 ± 3.58	56.98 ± 3.25	61.27 ± 3.45	72.87 ± 2.53	58.34 ± 1.02

Table 5.5. Coefficient of static friction between the weighted fabric samples and cotton molton.

<i>Board covering fabric</i>	Cotton	Linen	Wool Rep	Tap3	Tap4
Cotton Molton	1.90	1.54	1.82	3.24	1.62

5.3.1.2 Friction measurements: unweighted specimens

In Table 5.6 are reported the angles at which the tapestry fragments, without any extra load, started to slip from the board covered with the different fabrics under investigation. The fabric/fabric coefficients of friction derived from such measurements are recorded in Table 5.7, whenever possible. Indeed, in most of the cases the tapestry specimens only moved when inclining the plane at angles beyond the vertical, i.e. $\geq 90^\circ$ from the horizontal. This means that, when interpreting the results using a simple Coulomb friction model, the coefficient is effectively infinite (or at least very high) and so it cannot be calculated. Indeed, the tangent of an angle greater than 90° would correspond to a negative number. This suggests that Coulomb friction was not actually representative of

the slip behaviour of the textile, and so other forces were involved, and/or other variables affected the measurements. It is noted that measurements were carried out also between Tap3, Tap4 and the *uncovered* wooden board. As expected, in these cases the tapestry samples began to slide at lower angles, namely Tap3 at 48.79° ($\pm 4.04^{\circ}$), while Tap4 at 49.83° ($\pm 2.98^{\circ}$).

Although no values of μ_s can be drawn from most of the tests with unweighted specimens on the covered board, some more general observations on the interaction between the tapestry fragments and the four types of board-covering fabrics can be highlighted. Interestingly, it can be noted that the specimens slipped at the lowest angles when displayed on cotton velvet, namely between around 76° and 98° . Although these data are still very high and distant from following Coulomb's model, they point out that cotton velvet was the fabric promoting the least effective adhesion/friction. On the other hand, results from the measurements with cotton molton and domette were very similar and showed the greatest effects of adhesion/frictional forces: in both cases, the historic specimens started to slip at an inclination between 95° and 107° . In the case of polyester felt the results ranged more: Tap1 and Tap2, with cotton and linen respectively stitched on the back, slipped at lower angles (70° - 79°) than Tap3 and Tap4 (99° - 102°).

Molton and domette have a very similar weave structure, characterised by coarsely woven spun yarns, giving a texture with raised nap. Although also polyester felt and velvet have a textured surface with pile, molton and domette are less smooth. These intrinsic properties related to the type of weaving and finishing, together with other variables, may have contributed to the different levels of adhesion of the board-covering fabrics investigated.

Table 5.6. Angle [$^{\circ}$] at which the unweighted tapestry samples started to slip from the board covered with different textiles. The SD is also indicated (15 measurements per sample/covering fabric).

<i>Board covering fabric</i>	Tap1	Tap2	Tap3	Tap4	Tap5	Tap6
Cotton Molton	100.65 \pm 5.24	100.19 \pm 3.43	107.24 \pm 4.62	101.09 \pm 6.41	95.16 \pm 5.94	104.04 \pm 1.34

Cotton Domette	96.34 ± 2.93	100.21 ± 6.29	100.63 ± 4.67	107.19 ± 3.28	/ ⁷	/
Polyester Felt	70.05 ± 2.48	79.39 ± 3.17	99.07 ± 4.60	102.81 ± 6.63	/	/
Cotton Velvet	87.19 ± 1.53	97.50 ± 3.54	78.58 ± 3.29	75.59 ± 5.20	/	/

Table 5.7. Coefficient of static friction between the unweighted tapestry samples and the board-covering fabrics. Whenever the sign – is used, it indicates that the coefficient could not be calculated, as $\theta \geq 90^\circ$.

<i>Board covering fabric</i>	Tap1	Tap2	Tap3	Tap4	Tap5	Tap6
Cotton Molton	-	-	-	-	-	-
Cotton Domette	-	-	-	-	/	/
Polyester Felt	2.75	5.34	-	-	/	/
Cotton Velvet	20.37	-	4.95	3.89	/	/

By comparing the results from the friction measurements with and without extra load, the influence of variables such as contact area and pressure is evident. Indeed, whenever μ_s was calculated without wrapping the tapestry/textile specimens around the glass plate, its value was lower than those from the tests with the weights. This agrees with past studies [23, 25] and it shows the inability of Coulomb's model to properly describe the phenomenon. Nonetheless, it is not possible from this series of tests to clearly state which equation would better fit here to define the relationship between frictional force, normal force and coefficient of friction. Indeed, it should be highlighted that, besides normal force and contact area, other variables were noted to affect the measurements, such as the number of tests and the orientation of the textile sample. Namely, specimens were observed to slide at lower angles after that the measurement was repeated a few times, perhaps as the fabric surface became smoother.

The friction measurements without additional weight may suggest that, even without slanting the support, the level of friction/adhesion between board-

⁷ Measurement not done.

covering fabric and tapestries might be enough to impede the sliding of the historic textile, and thus promoting a certain strain reduction, even at 0° from the vertical. This could lead to an improvement of the display method, as this would mean that some benefits could be obtained even without inclining the support, and so without altering the aesthetic appreciation of the hanging design.

5.3.2 The role of inclination: fixed-load experiments with non-historic samples (uncovered board)

This series of tests aimed to study how much inclination of sloping boards may contribute to preventing damage propagation in fragile textiles. To do so, strain across wool rep mock-ups was monitored through 2D DIC. These experiments represent the first attempt of using the optical technique for evaluating conservation practices. Therefore, these tests were crucial for the project, since they sought to assess the feasibility of DIC as an evaluation tool for tapestry conservation methods.

It is important to underline that two types of DIC data are presented: I) strain averaged from the entire surface of the sample; II) local pseudo strain averaged from the damaged areas (i.e. open slits). As already highlighted in Chapter 4 through the different textile objects investigated, while the overall strain clearly shows the occurrence of fatigue mechanism, the pseudo strain calculated across slits depends less on the environmental conditions and more on time. Because of this, the pseudo strain data were expected to be more useful to define the efficacy of the inclination of the display method, as they would be more comparable and less dependent on the mutable RH. Therefore, this experimental approach mainly considered the efficacy of inclination in reducing creep-like behaviour rather than fatigue.

5.3.2.1 Display at 0° from the vertical

In this experiment the wool rep specimens were clamped at the top of the uncovered wooden board displayed vertically.

The strain map of the model samples with fixed-load after one week of monitoring is shown in Figure 5.8. The strain map points out the presence of

areas of high pseudo strain across the central open slit in the three damaged specimens (A, B, C). On the other hand, strain across the undamaged areas of the mock-ups, as well as the whole of sample D, appears to be more homogeneous. As expected, this indicates that the open slits were prime regions of damage propagation. It is important to note that the areas at the bottom of the specimens were not considered in the data analysis, as the high strain registered in these regions was most likely linked to errors from local out-of-plane displacement, caused by the stitched load. Similarly, the upper border of the samples was excluded from the DIC analysis as the shadow from the batten affected strain calculation.

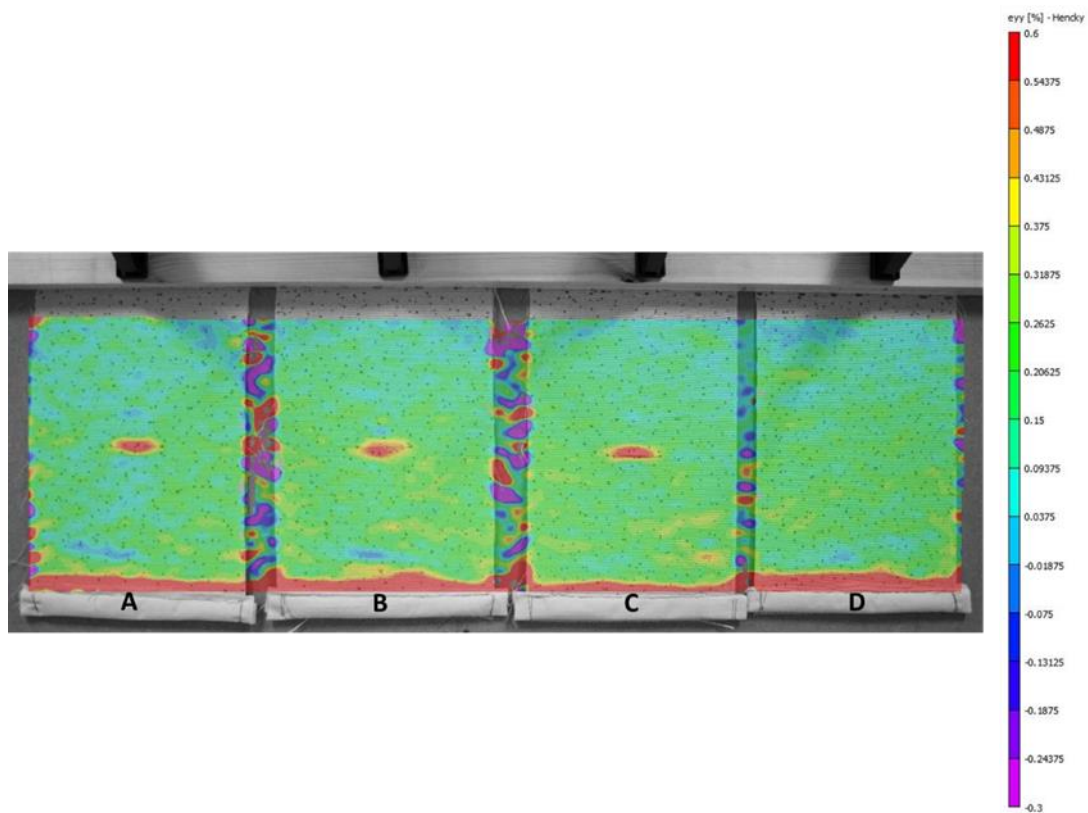


Figure 5.8. Longitudinal strain map of samples displayed at 0° from the vertical at the end of the 168-hour monitoring. Samples A, B, C have one central slit 50 mm wide, while sample D is undamaged.

Figure 5.9 depicts the overall strain averaged from the entire surface of the four samples during the 168 hours of monitoring. In addition, RH values are also plotted (dotted line). The data state that the overall strain greatly depended on the environmental conditions. For instance, it is clear that the drastic rise in humidity registered between the 25th and the 65th hours of monitoring (from around 27% to 48% of RH), caused a remarkable increase on the overall ϵ_{yy} . In

general, the analysis of the four samples gave comparable results. Sample D, without slits, showed to extend less than damaged samples B and C; however, it presented a longitudinal strain comparable to that of sample A. This can indicate that, as the specimens were mainly sound, this might have minimised the impact of the open slit on the overall ϵ_{yy} data, at least during the one-week test.

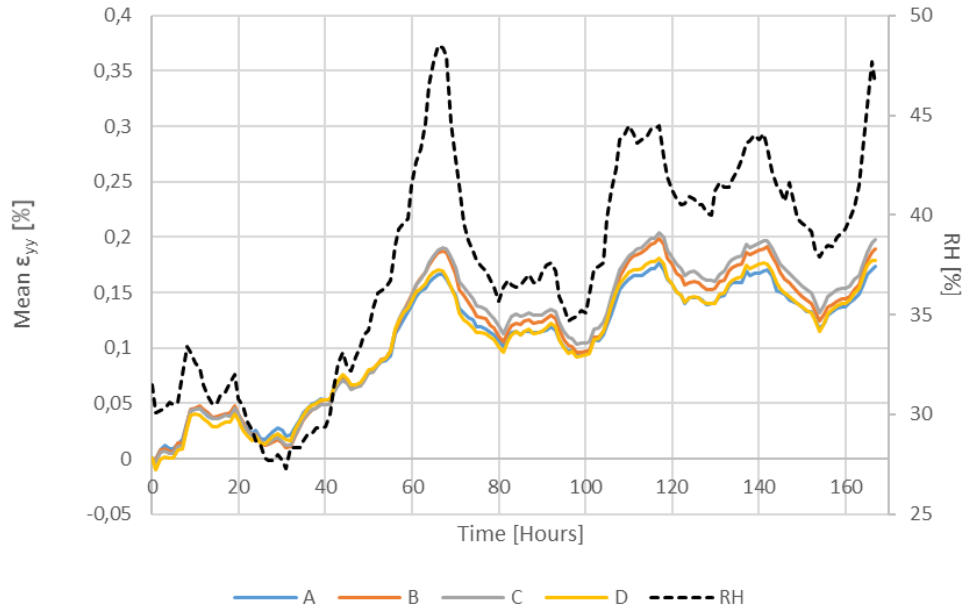


Figure 5.9. Overall ϵ_{yy} [%] of the damaged sample A, B and C and undamaged sample D during the 168-hour monitoring. RH [%] is indicated by the dotted line.

As previously mentioned, for the aim of this series of tests it is particularly important to consider the pseudo strain from the damaged areas. Figure 5.10 depicts the pseudo ϵ_{yy} from the areas across the slits in samples A, B and C. The data confirmed that the widening of the slits was the prime cause of weft elongation, and thus of mechanical damage propagation. This is evident since the pseudo strain was considerably higher than the overall strain in Figure 5.9. Besides being greater than the overall strain, pseudo ϵ_{yy} was also shown to be less affected by RH and to increase with time. This likely indicates the occurrence of creep (see discussion in Chapter 4). It should be underlined that humidity still had an impact on the pseudo strain, as again noted in the tests reported in the previous chapter. Indeed, the drastic rise in humidity between 25-65 hours corresponded to a steep growth in the pseudo ϵ_{yy} . Because of this, it may be difficult to directly compare the outcomes from tests where the

environmental conditions were remarkably different, as also the proper reading of the pseudo strain data would be compromised.

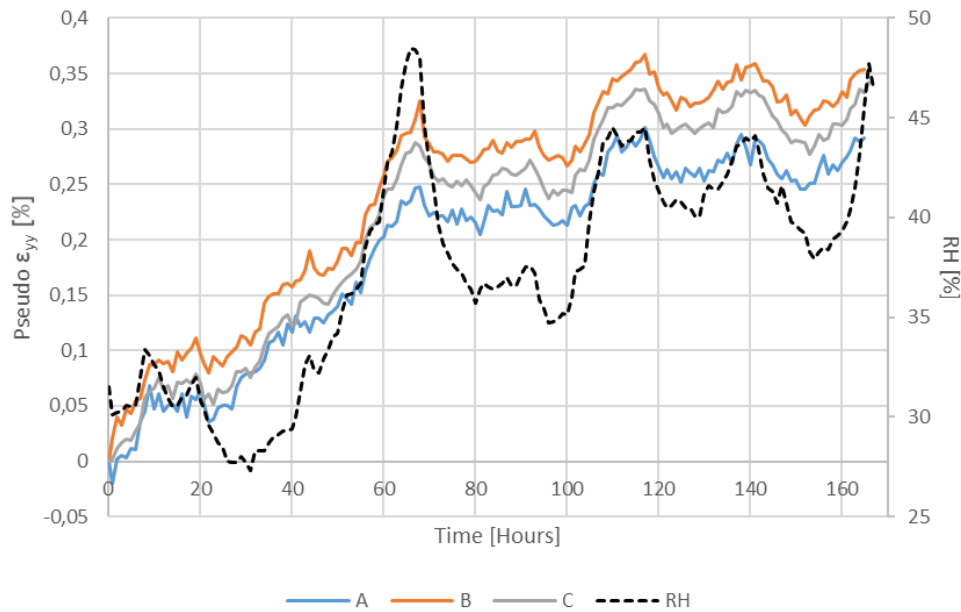


Figure 5.10. Pseudo ε_{yy} [%] across the damaged areas (open slits) of sample A, B and C. RH [%] is indicated by the dotted line.

5.3.2.2 Display at 5° from the vertical

Damaged wool rep samples were monitored while displayed on the uncovered board slanted at 5° from the vertical.

In Figure 5.11 the longitudinal strain averaged from the whole surface of the specimens is presented. Again, the occurrence of fatigue mechanism is evident, as the ε_{yy} data changed accordingly to the humidity fluctuations. However, it is important to underline that the environmental conditions did not differ significantly from the experiment at 0° from the vertical. Indeed, also in this case there was a steep rise in humidity: from the 85th to 115th hour, the humidity increased remarkably from 35% to 51%.

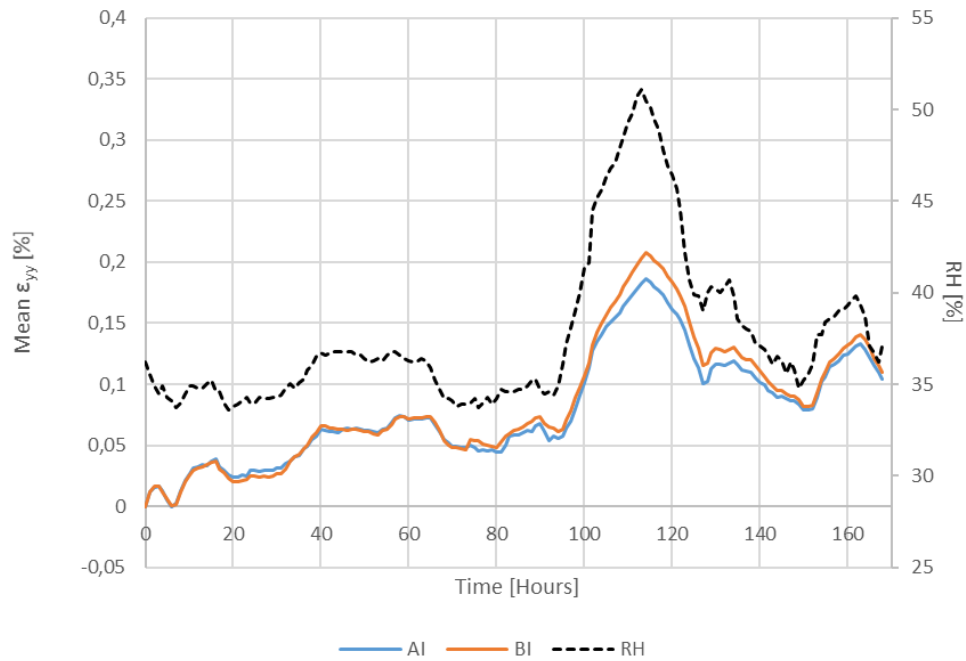


Figure 5.11. Overall ϵ_{yy} [%] of the damaged sample AI and BI during the 168-hour monitoring. RH [%] is indicated by the dotted line.

Figure 5.12 shows the pseudo strain across the slits, that progressively increased with time, even if partly affected by the humidity changes (in particular by the steep rise in humidity registered between 85-115 hours of monitoring).

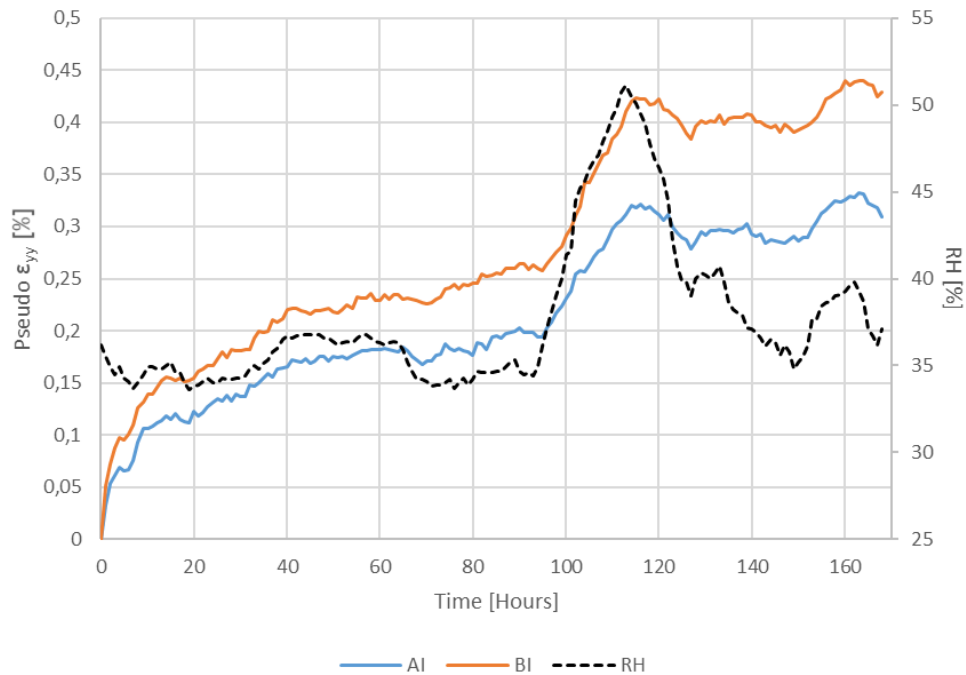


Figure 5.12. Pseudo ϵ_{yy} [%] across the damaged areas (open slits) of sample AI and BI. RH [%] is indicated by the dotted line.

5.3.2.3 Display at 45° from the vertical

Damaged wool rep mock-ups were displayed for one week on the uncovered board slanted at 45° from the vertical, while 2D DIC was used to monitor strain across the specimens.

The overall ϵ_{yy} averaged from the entire surface of the specimens is depicted in Figure 5.13. From Figure 5.13 the great influence of the variable environmental conditions can be stated. In comparison to the tests at 0° and 5° from the vertical, here the changes in RH were even more remarkable. Indeed, humidity greatly and quickly rose and decreased three times. However, it is interesting to note that, regardless of the more significant changes in the environmental conditions, especially during the first 40 hours of the test, the overall strain of samples at 45° from the vertical was more contained than that of specimens at 0° (Figure 5.9) and 5° (Figure 5.11).

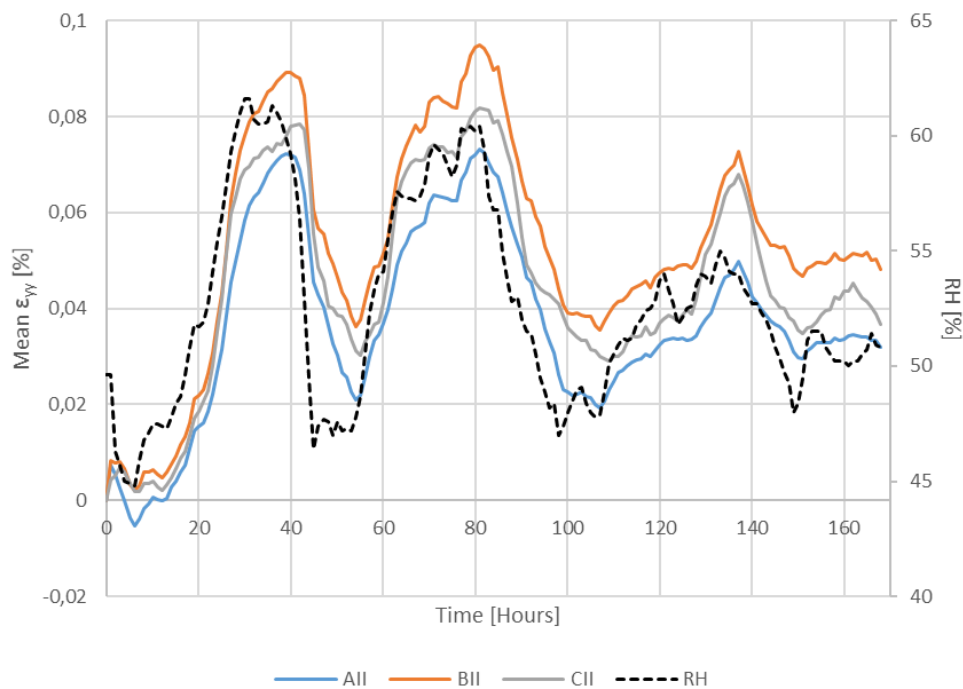


Figure 5.13. Overall ϵ_{yy} [%] of the damaged sample AII, BII and CII during the 168-hour monitoring. RH [%] is indicated by the dotted line.

The pseudo strain calculated across the open slits of the monitored specimens is illustrated in Figure 5.14. The influence of the humidity variations on the local strain is particularly evident when considering the data between the 15th and

30th hours of monitoring: RH rose from 47% to 60%, while the pseudo strain from 0.05% to 0.15%.

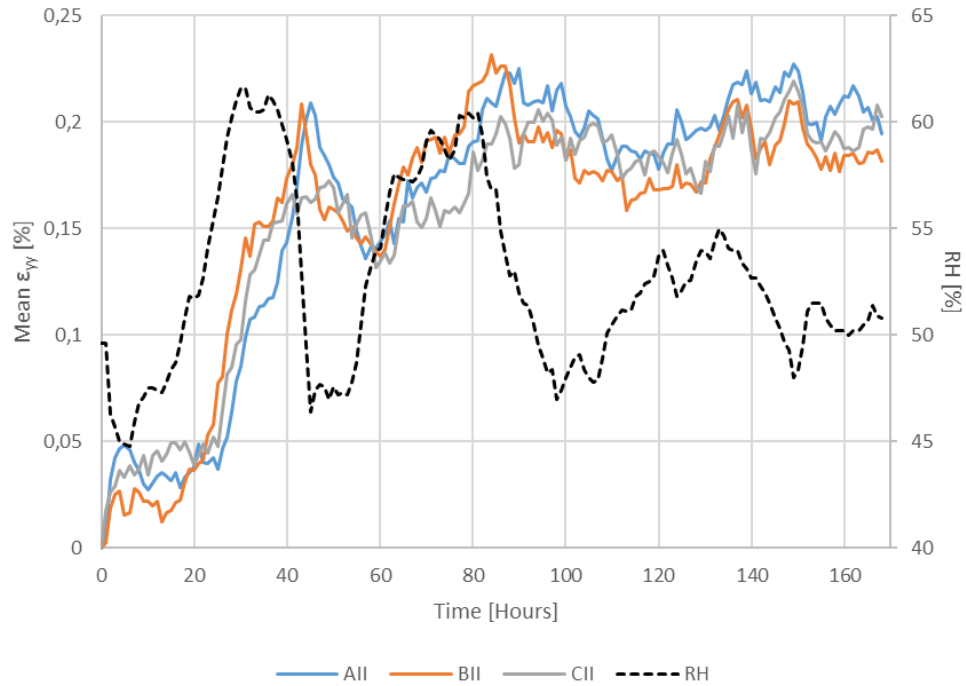


Figure 5.14. Pseudo ε_{yy} [%] across the damaged areas (open slits) of sample AII, BI and CII. RH [%] is indicated by the dotted line.

5.3.2.4 Discussion: comparison between the tests at different inclinations

The strain data from the tests in Section 5.3.2 are now compared to highlight whether inclining the board at different angles may prevent the elongation of structural weaknesses in tapestry-like textiles when friction is low. It should be pinpointed that the environmental conditions varied from experiment to experiment. Because of this, the partial but visible influence of humidity on the pseudo strain data is an important factor to consider when comparing the outcomes.

Figure 5.15 illustrates the maximum pseudo strain registered across the damaged areas of the specimens displayed at 0, 5 and 45 degrees from the vertical. The maximum pseudo strain represents the highest value registered across the area of interest (i.e. the region across the slit) during the 168 hours of monitoring. The graph shows that the difference between the samples at 0° and 5° is not statistically relevant, as the difference falls within the error (averaged data

from three damaged replicas of each experiment). This means that no strain reduction could be observed when moving the board from 0° to 5° from the vertical. On the other hand, the samples displayed at 45° elongated significantly less across the damaged areas compared to the other two inclinations, namely around 40% less.

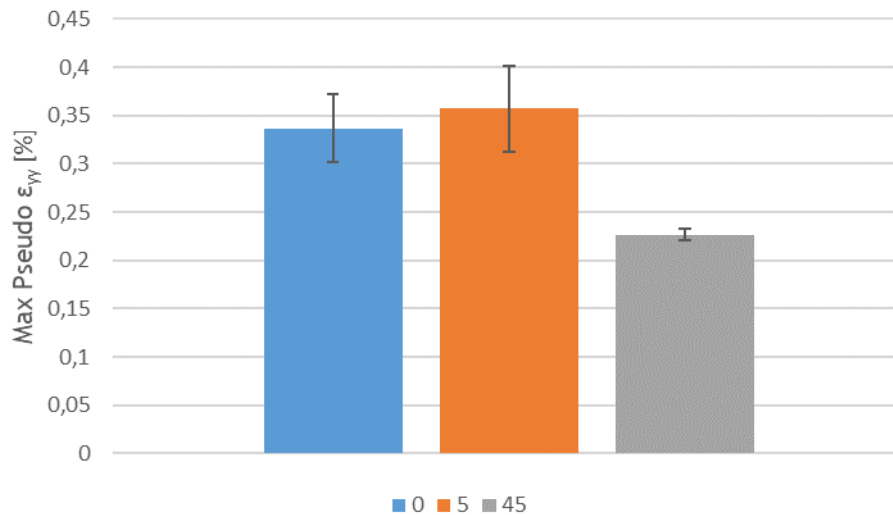


Figure 5.15. Maximum values of mean pseudo ϵ_{yy} [%] registered across the slits of the samples displayed at 0, 5, 45 degrees from the vertical for one week. The error bars indicate the SD, as three damaged replicas were tested for each inclination.

Figure 5.16 compares the trends of pseudo strain registered, during the 168-hour monitoring, across damaged samples displayed at 5° and 45° from the vertical. Although in both cases it can be noted that humidity partly affected the pseudo strain data, it is underlined that the wool rep mock-up at 45° from the vertical elongated considerably less than that at 5°. This is evident especially when considering the data from the first 80 hours of monitoring: while the local strain from the 5° specimens reached a value of around 0.2% over a period with stable RH, the 45° sample reached a similar value only during an intense initial rise in RH.

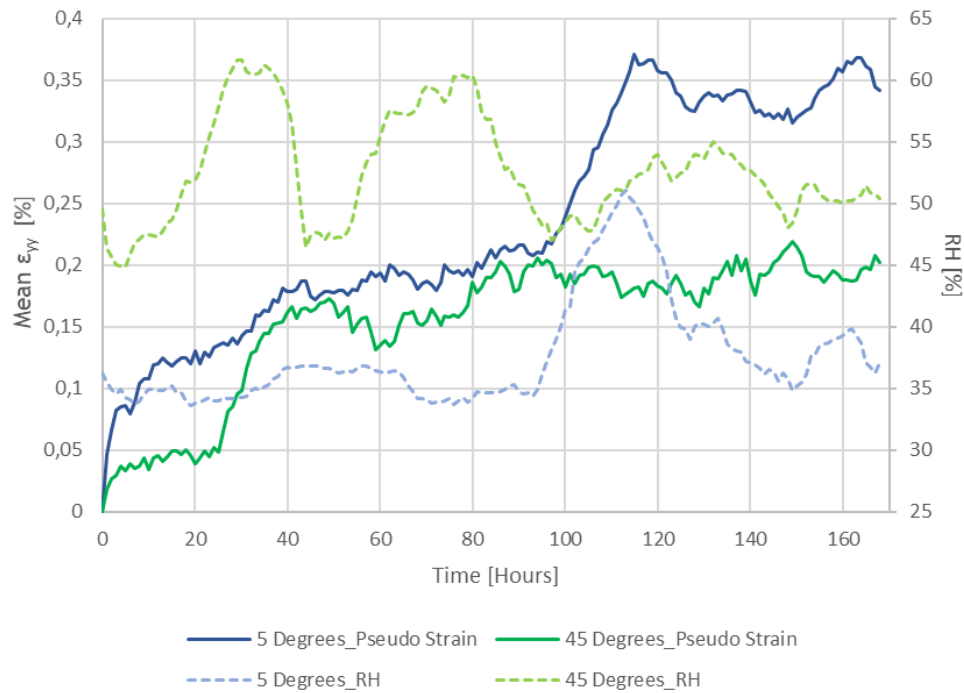


Figure 5.16. Pseudo ϵ_{yy} across the damaged areas of samples displayed at 5 and 45 degrees from the vertical (solid blue and green line) during the 168-hour monitoring tests. RH [%] variations are indicated by the dotted lines.

5.3.3 2D DIC strain monitoring of a historic tapestry fragment displayed on a half covered and half uncovered vertical board

This test aimed to verify the great effects of friction/adhesion from the interaction between tapestries and covering fabrics for slanted supports. Indeed, from the outcomes reported in Section 5.3.1 it was hypothesised that strain across a historic hanging could be reduced by displaying the textile on even a vertical support covered with fabrics like cotton molton. To better investigate this, 2D DIC was used to track displacements across a historic tapestry fragment displayed on the wooden board, half uncovered (to simulate the effects of a low friction surface) and half covered with cotton molton. Differently from the tests in Section 5.3.2, here the effects of the system were mainly evaluated considering the impact on overall ϵ_{yy} , determined by fatigue, rather than on local pseudo strain across damaged areas, due to creep.

Figure 5.17 shows the strain map of the historic tapestry fragment after 300 hours of hanging. In the map the weak areas, mainly open slits, are indicated as locations of high pseudo strain. As discussed in Chapter 4, but also in Section

5.3.2, the probable mechanical damage mechanism determining strain across open slits is time-dependent creep. It is noted that also on the bottom left corner of the tapestry alternating areas of high and low strain seem to be present. Unfortunately, this was due to a significant out-of-plane displacement that occurred during the monitoring. Because of this, only the ϵ_{yy} data from the top half of the tapestry were considered (area indicated by the dotted line), as the reliability of the results from the bottom half were negatively affected by the 3D movement of the textile object.

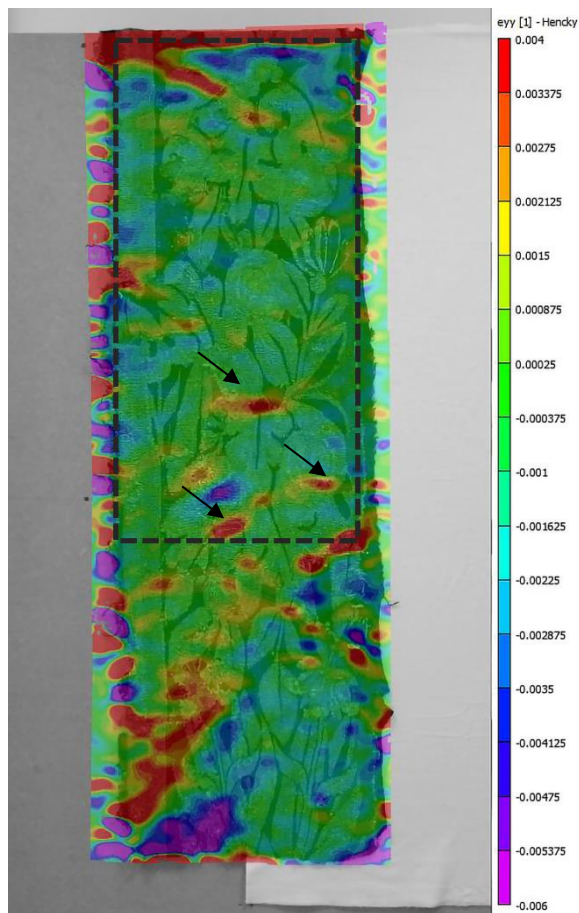


Figure 5.17. Longitudinal strain map of TapestryFragment_1 at the end of the 300-hour monitoring displayed on a vertical wooden board half uncovered and half covered with cotton molton. The arrows indicate open slits.

In Figure 5.18 the overall longitudinal strain data are reported, together with RH. Two lines indicating ϵ_{yy} fluctuations are shown: one depicts the data averaged from the area displayed on the uncovered board (blue line), the other from the remaining part directly in contact with the cotton molton (red line). By comparing the two graphs, the supporting effects of the covering fabric can be stated, as the area not in contact with cotton molton presented a greater strain

than the other. More specifically, the outcomes demonstrated that overall extensions, largely determined by RH fluctuations, were smoothed by the display on the fabric. Indeed, the part of the textile displayed on the wooden surface reached a maximum ϵ_{yy} of 0.05%, while that on cotton molton of 0.01% (at RH 58.5%). This may indicate that the level of adhesion/friction between the historic textile and the cotton fabric was high enough to reduce weft elongation due to fatigue, even without slanting the board. It is important to note that high pseudo strain was registered across open slits in contact with the molton, as shown in Figure 5.17. This demonstrates that the system was not completely effective in limiting creep across damaged areas.

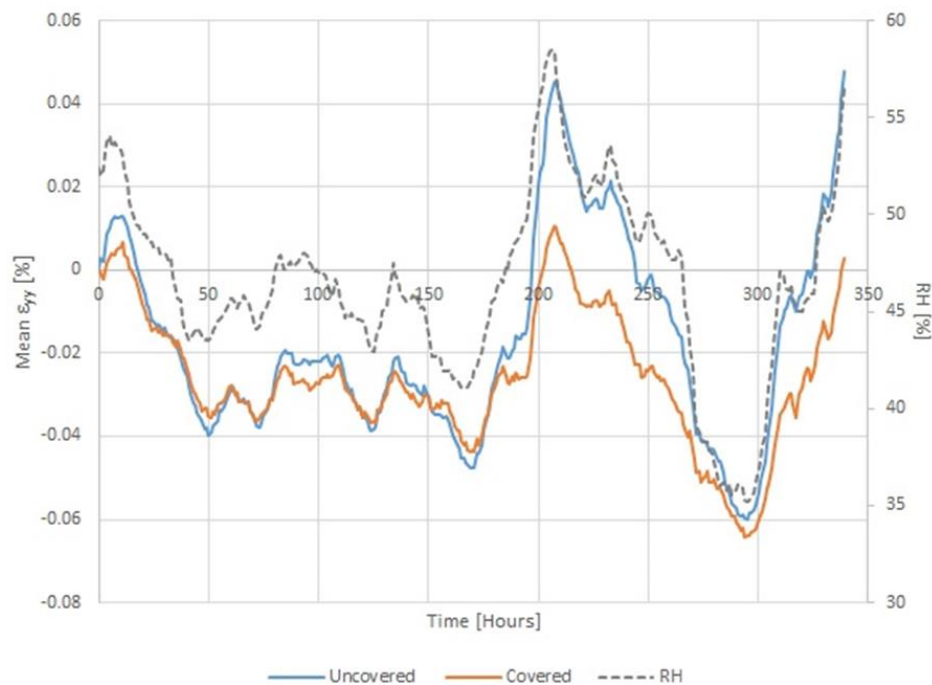


Figure 5.18. Mean ϵ_{yy} [%] across the area of the historic fragment in contact with the cotton molton (orange line), and the area in contact with the wooden surface of the board (blue line). RH [%] is indicated by the dotted line.

Even when considering the efficacy in preventing damage due to fatigue, the test only considered a limited time-lapse, therefore the long-term effects of such a system may differ from those here observed. For instance, it can be expected that eventually the adhesion with the covering fabric may fail because of the self-weight loading of the historic textile, as it is known that fabric on fabric frictional forces are affected by factors like pressure and contact area [23, 25]. Furthermore, the level of adhesion may vary from tapestry to tapestry

depending on the specific manufacturing/material properties of the object. For instance, woven hangings with large areas made of silk may adhere less than those entirely made of wool. In addition, it should be noted that often weak tapestries feature a linen fabric on their back, stitched by conservators as a support method. This would mean that the tapestry is not directly in contact with the highly “gripping” covering fabric, and thus the effects of adhesion with the smoother linen surface may be less evident. However, it is noted that outcomes reported in Paragraph 5.3.1.1 showed that also linen on cotton molton μ_s is high.

5.4 Conclusions

This chapter aimed to investigate the effects of sloping boards in retarding weft elongation and limiting the impact of mechanical damage mechanisms. The role of two variables, friction and inclination, were evaluated to assess why and how displaying tapestries on slanted supports could be beneficial.

First, the coefficient of static friction between commonly employed board-covering fabrics and tapestry/textile samples was measured using a slanted plane method, with and without additional load. The results showed that, in this situation, Coulomb’s model is not fully descriptive of the phenomenon, as the coefficient of friction (μ): I) it varies depending on the applied load and other factors related to the weave structure; II) in certain cases, it cannot be measured as the specimen started to slide at angles $> 90^\circ$. Nevertheless, it was observed that the interaction between the two fabrics led to great adhesion/friction. Perhaps, up to a certain level, this adhesion can be obtained even without slanting the board, and so while keeping it at the vertical position.

On the other hand, 2D DIC strain monitoring of wool rep samples displayed on a wooden board at different angles clarified that, without a proper board-covering fabric promoting adhesion and frictional forces, the use of slanted supports is not helpful in containing strain, particularly creep across damaged areas. This is true especially when considering small angles, like 5° from the vertical, as usually opted for this display method. The observations drawn upon the experimental work agreed with the theoretical analysis, conducted within the context of the current project, that modelled load distribution at the top of a

historic hanging when displayed at different angles and with different coefficients of friction. The good agreement between theoretical analysis (although not fully representative) and the DIC outcomes further validate the optical technique as a tool for studying the effects of conservation treatments, when a similar methodology is used.

Lastly, since the effects of adhesion/friction were greater than expected, 2D DIC was employed to monitor strain across a historic tapestry fragment displayed on a vertical board, half covered with cotton molton (high friction) and half uncovered (low friction). The test aimed to define whether strain can be reduced even without inclining the support, thanks to the forces from the interaction of the fabrics. The outcomes from the 340-hour experiment showed that the area of the tapestry in contact with the cotton fabric overall elongated less. This may indicate the positive effects of the covered vertical board in limiting length variations due to fatigue. However, it should be highlighted that the test lasted for a contained amount of time, so the long-term implications of the system are not known. Indeed, the usefulness of a vertical covered board may depend on factors like weave features and material properties, characteristic of each historic hanging. Furthermore, it should be remarked that no relevant positive impact of the approach was noted in limiting creep-like mechanisms affecting damaged areas.

From a practical perspective, the outcomes suggest that displaying a historic tapestry on a board, tilted at 5° from the vertical (or less) and covered with a fabric promoting high friction, could be useful in reducing weft elongation due to fatigue. A similar approach can be particularly helpful when the time for conservation is limited and the environmental conditions in the display location cannot be controlled. Nevertheless, the textile artwork would need to be structurally sound, as the system would be likely unable to entirely prevent the occurrence of time-dependent mechanical behaviours across damaged areas. This means that perhaps the display method should be used in combination with local treatments supporting evident structural weaknesses, as discussed in Chapter 6.

References

1. Barker, K., *Reducing the Strain: Is it worth displaying a large fragile textile at a slight angle?* Conservation news, 2002: p. 30.
2. Trosbach, G., *Physikalische Untersuchungen an historischen Tapisserien*, in *Fakultat fur Architektur*. 2002, Technische Universitat Munchen.
3. Brutillot, A. *Slant Boards for Display*. 2010; Available from: <https://www.youtube.com/watch?v=uDQSI1yJEs0&t=47s>.
4. Wild, C. and A. Brutillot, *The conservation of tapestries in Bavaria*, in *Tapestry Conservation: Principles and Practice*, F. Lennard and M. Hayward, Editors. 2006, Butterworth-Heinemann: Oxford. p. 177-184.
5. Catic, E.M., *A Research Project to Measure the Effectiveness of Stitching Methods when Stabilizing Weak Areas in Tapestries*. 2019, University of Glasgow.
6. Barnoud, P., L. Abécassis, and F. Magos, *Musée National De Cluny: Restauration et Muséographie de la Salle 13 Dite Salle De La Dame à la Licorne. Rapport de Présentation Description Sommaire des Travaux*. 2013.
7. E. Taburet-Delahaye, et al., *La Dame à la licorne, sa conservation et l'évaluation colorimétrique du nettoyage*. *Techne* 2015. 41: p. 87 - 93.
8. Elisabeth Taburet-Delahaye, et al. *Les coulisses de la scénographie, de la restauration et de l'installation des tapisseries de la Dame à la Licorne au musée national du Moyen Âge*. in *Conserver et presenter les tapisseries: du bilan sanitaire a la mise en valeur*. 2015.
9. Varoli-Piazza, R., R. Rosicarello, and M. Giorgi, *The use of photogrammetry in determining the correct method of displaying a textile artefact: the cowl of St. Francis of Assisi*, in *ICOM committee for conservation, 11th triennial meeting in Edinburgh, Scotland, 1996: Preprints*, J. Bridgland, Editor. 1996, James & James: London. p. 726-731.
10. Barker, K., *Reducing the Strain: Is it worth displaying a large fragile textile at a slight angle?* Newsletter of the ICOM Committee for Conservation, Working Group of Textiles, 2005: p. 4-6.
11. Behera, B.K. and P.K. Hari, *Friction and other aspects of the surface behavior of woven fabrics*, in *Woven Textile Structure*, B.K. Behera and P.K. Hari, Editors. 2010, Woodhead Publishing in association with The Textile Institute: Oxford; Cambridge; New Delhi. p. 230-242.
12. Popov, V.L., *Contact mechanics and friction: physical principles and applications*. 2010, Berlin: Springer. 362 p.
13. Rodriguez-Arias, H.A., *Low-cost automatic device for obtaining the coefficient of static friction*. IOP Conference Series: Materials Science and Engineering, 2019. 519: p. 012018.
14. Mercier, A.A., *Coefficient of friction of fabrics*. Bureau of Standards Journal of Research, 1930. 5: p. 243-246.
15. Thorndike, G.H. and L. Varley, *Measurement of the Coefficient of Friction between Samples of the Same Cloth*. Journal of the Textile Institute Proceedings, 1961. 52(6): p. P255-P271.
16. Standard, B., *BS EN 14882:2005 Rubber or plastic coated fabrics – Determination of the static and dynamic coefficient of friction*. 2005.

17. Harrison, P. and L.F. Gonzalez Camacho, *Deep draw induced wrinkling of engineering fabrics*. International Journal of Solids and Structures, 2021. 212: p. 220-236.
18. Kothari, V., N. Swani, and M. Gangal, *Frictional properties of woven fabrics*. Indian Journal of Fibre & Textile Research, 1991. 16: p. 251-256.
19. Ajayi, J.O. and H.M. Elder, *Comparative Studies of Yarn and Fabric Friction*. Journal of Testing and Evaluation, 1994. 22(5): p. 463-467.
20. Balci Kilic, G. and A. Okur, *Effect of yarn characteristics on surface properties of knitted fabrics*. 2019, SAGE Publications: London, England. p. 2476-2489.
21. Barrett, R.T., *Fastener design manual*. Vol. 1228. 1990: NASA, Scientific and Technical Information Division.
22. Hosseinali, F. and J.A. Thomasson, *Multiscale Frictional Properties of Cotton Fibers: A Review*. Fibers, 2018. 6(3): p. 49.
23. Wilson, D., *A Study of Fabric-on-Fabric Dynamic Friction*. Journal of the Textile Institute Transactions, 1963. 54(4): p. T143-T155.
24. Dreby, E.C., *A friction meter for determining the coefficient of kinetic friction of fabrics*. Journal of Research of the National Bureau of Standards, 1943. 31(4): p. 237.
25. Howell, H.G., *The Laws of Static Friction*. Textile Research Journal, 1953. 23(8): p. 589-591.
26. Hermann, D., et al., *Frictional study of woven fabrics: The relationship between the friction and velocity of testing*. Journal of Applied Polymer Science, 2004. 92(4): p. 2420-2424.
27. Howell, H.G., *The Laws of Friction*. Nature, 1953. 171(4344): p. 220-220.
28. Howell, H.G. and J. Mazur, *Amontons' Law and Fibre Friction*. Journal of the Textile Institute Transactions, 1953. 44(2): p. T59-T69.
29. Najjar, W., et al., *Analysis of frictional behaviour of carbon dry woven reinforcement*. Journal of Reinforced Plastics and Composites, 2014. 33(11): p. 1037-1047.
30. Ramkumar, S., G. Leaf, and S. Harlock, *A Study of the Frictional Properties of 1×1 Rib-knitted Cotton Fabrics*. Journal of the Textile Institute, 2000. 91: p. 374-382.
31. Allaoui, S., et al., *Influence of the dry woven fabrics meso-structure on fabric/fabric contact behavior*. Journal of Composite Materials 2012. 46(6): p. 627-639.
32. Costantini, R., et al., *Investigating mechanical damage mechanisms of tapestries displayed at different angles using 2D DIC*. The European Physical Journal Plus, 2020. 135(6): p. 515.
33. *Tapestry Conservation: Principles and Practice*. Butterworth-Heinemann series in conservation and museology, ed. F. Lennard and M. Hayward. 2006, Oxford: Butterworth-Heinemann. xxv, 247 p.
34. Lennard, F., et al., *Strain monitoring of tapestries: results of a three-year research project*, in *ICOM-CC 16th Triennial Conference, Lisbon, 2011: Preprints*, J. Bridgland, Editor. 2012, International Council of Museums: Paris. p. 1-8.

6 Evaluation of stitching and support methods

Chapter 6 investigates and compares the efficacy of different stitching techniques and support methods for the conservation of tapestries. To do so, a multi-analytical approach was used, involving both 2D DIC and uniaxial tensile testing. As discussed in Chapter 1, to prevent mechanical damage propagation in historic hangings, a broad range of approaches are used by textile conservators. Still nowadays, the choice of the type of treatment seems to be markedly influenced by subjective matters, such as where the workshop is based and by whom the staff was trained [1]. Therefore, the experiments presented in this chapter aimed to provide some objective data on various methods.

Among the different treatments in use, two stitching techniques, laid and brick couching were selected and studied by employing 2D DIC to track strain across differently conserved case studies. Brick and laid couching were chosen as they are the most widespread stitching techniques, building on previous research carried out at the CTCTAH [2-4] and elsewhere [5-7]. It should be reminded that these stitching methods intend to promote both structural stability and figurative continuity in damaged areas, in particular those where weft yarns are missing. Alongside laid and brick couching, the two main support approaches aiming to prevent damage propagation, full support of new fabric and with patches of fabric, were evaluated. After the strain monitoring, the tensile properties of the conserved specimens were researched. Similarly, two types of linen fabrics used by textile conservators in the UK for support treatments were also (uniaxially) tensile tested, to compare their mechanical behaviour with that of historic hangings, already discussed in Chapter 3. In addition, the tensile properties of Stabiltex™ were studied, as similar textiles made of synthetic fibres have also been (very rarely) used for supporting tapestries [8]. Investigating the mechanical properties of these materials is important as there are still some uncertainties regarding the type and reasons behind the choice of fabric [9, 10].

The experimental design of Chapter 6 is described in Table 6.1.

Table 6.1. Experimental design of Chapter 6.

Hypothesis	Case studies	Techniques	Methodological limits
The structural stability of damage in tapestries can be improved through the application of patch and full linen supports	Wool rep mock-ups differently conserved; one historic tapestry fragment first conserved with patches and later with a full support	2D DIC (for mock-ups and historic tapestry fragment); uniaxial tensile testing (for mock-ups)	Unstable environmental conditions limiting outcomes comparison; limited applicability of the results due to contained number of samples
The structural stability of damage in tapestries can be improved through laid and brick couching	Wool rep mock-ups differently conserved; one historic tapestry fragment conserved with brick and laid couching	2D DIC (for mock-ups and historic tapestry fragment); uniaxial tensile testing (for mock-ups)	Unstable environmental conditions limiting outcomes comparison; limited applicability of the results due to contained number of samples
Fabrics used for structural treatments in tapestries show desirable physical properties	Samples from 2 linen fabrics currently employed by conservators for support treatments (before and after washing); samples from 1 polyester fabric sometimes used for support treatments	Uniaxial tensile testing	Uncertainties regarding what should be considered as desirable by conservators

6.1 Materials and methods

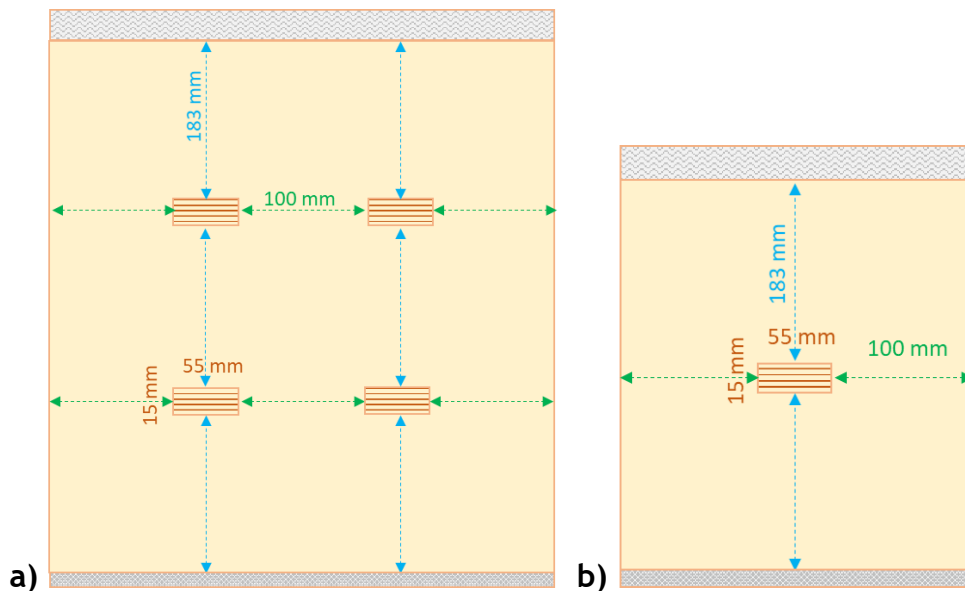
6.1.1 2D DIC monitoring of newly woven conserved samples

Hand-woven wool rep fabric provided by Context Weavers was employed for the preparation of mock-ups (for specifications see Section 3.1.2).⁸ The specimens varied, in the type of damage, sizes, and conservation treatments applied, depending on the specific aim of the test. Figure 6.1 schematically illustrates the three types of specimens used and the related artificial physical damage:

⁸ It is noted that, as specified in Chapter 3, the weft direction of the wool rep fabric is referred to as warp, and the warp as weft.

- I) Figure 6.1a: samples (650 x 410 mm) used to investigate both the influence of stitching and support techniques. Each sample presented four damaged areas (55 x \approx 15 mm) made of 12 bare warps.
- II) Figure 6.1b: samples (350 x 205 mm) used to investigate the influence of stitching techniques and the impact of spacing. Each sample presented one central damaged area (55 x \approx 15 mm) made of 12 bare warps.
- III) Figure 6.1c: samples (650 x 410 mm) used to investigate both the influence of stitching and support techniques. Each sample presented four damaged areas (55 x \approx 15 mm) made of 12 bare warps and other weak regions, like holes with missing weft and warp.

It should be noted that the 50 mm at the top of each sample were used to clamp the textile to the board, while, in the 20 mm at the bottom, a bag containing 100 g (for 350x205-mm samples) or 200 g (for 650x410-mm samples) of lead weights was added.



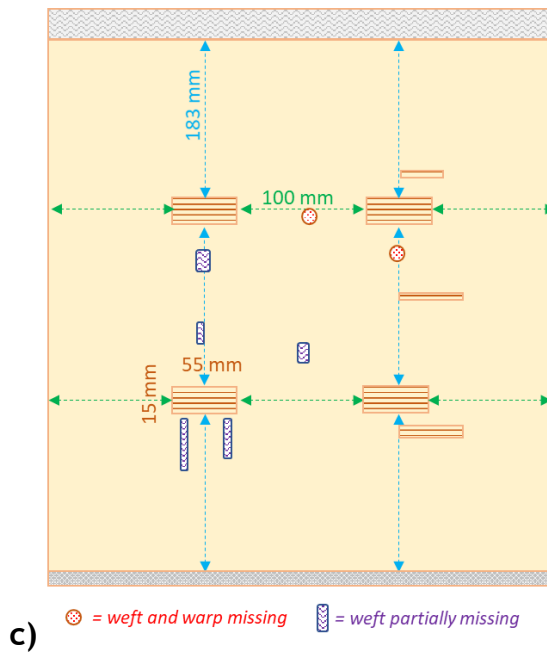


Figure 6.1. Wool rep mock-ups with artificial damage.

The mock-ups were conserved using different support and couching techniques to compare the diverse approaches, while limiting variables as much as possible at each stage. In particular, the two types of stitching techniques investigated were brick and laid couching. Examples of the two types of couching are provided in Figure 6.2 and Figure 6.3, while further information on the techniques can be found in Section 1.2.2 of Chapter 1. The stitches were carried out at different spacing, to observe how this would impact on strain in the area of damage. On the other hand, the two types of support treatment tested were full, depicted in Figure 6.4a, and patch, illustrated in Figure 6.4b. The samples used, and the related specifications, are provided in Table 6.2 and Table 6.3.

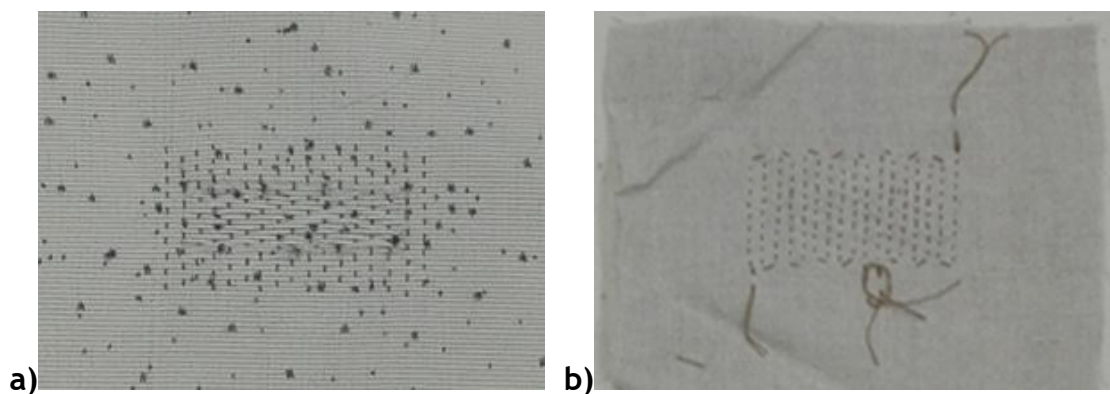


Figure 6.2. Damaged area on a wool rep sample conserved with brick couching, 4-mm spacing: a) front; b) back.

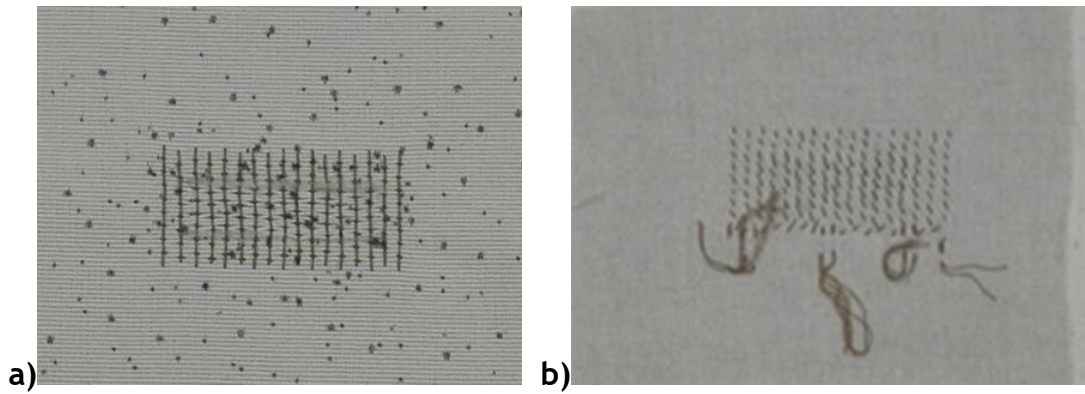


Figure 6.3. Damaged area on a wool rep sample conserved with laid couching, 4-mm spacing: a) front; b) back.

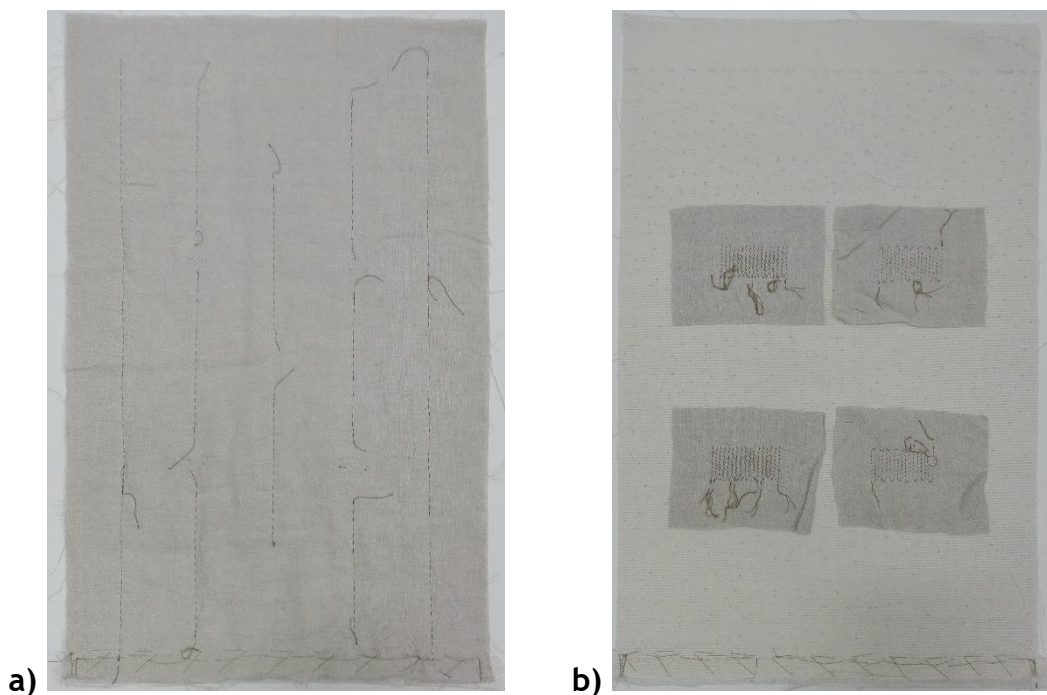


Figure 6.4. Back of wool rep mock-ups treated with: a) full support; b) patch support.

Table 6.2. Wool rep mock-ups used for testing the efficacy of support and stitching techniques. Samples AI-F are described by Figure 6.1a, samples G-I by Figure 6.1c (before conservation). Mock-ups DI/DII and G were left untreated and used as control samples. This aimed to highlight the impact of conservation strategies from the comparison with conserved samples.

Sample Code	Size [mm]	Damage	Support	Couching
AI/AII ⁹	650x410	4 damaged areas (12 bare warps each)	Full	Brick, laid (4-mm spacing)
B	650x410	4 damaged areas (12 bare warps each)	Patches	Brick, laid (4-mm spacing)

⁹ In case of samples AI/AII and DI/DII, two identical specimens were prepared as they were needed for two different tests.

C	650x410	4 damaged areas (12 bare warps each)	Full	Brick, laid (4-mm spacing)
DI/DII	650x410	4 damaged areas (12 bare warps each)	-	-
E	650x410	4 damaged areas (12 bare warps each)	Full	-
F	650x410	4 damaged areas (12 bare warps each)	Full	-
G	650x410	14 damaged areas (7 areas of bare warps, 2 areas of missing weft/warp, 5 areas of partially missing weft)	-	-
H	650x410	14 damaged areas (7 areas of bare warps, 2 areas of missing weft/warp, 5 areas of partially missing weft)	Patches, only on the back of the 4 main damaged areas	Brick (8-mm spacing)
I	650x410	14 damaged areas (7 areas of bare warps, 2 areas of missing weft/warp, 5 areas of partially missing weft)	Full	Brick (8-mm spacing)

Table 6.3. Wool rep mock-ups used for testing the influence of spacing in brick and laid couching. The samples are described by Figure 1b (before conservation). Da. was left untreated (control sample).

Sample Code	Size [mm]	Damage	Support	Couching / spacing
Br.1	350x205	1 damaged area (12 bare warps)	Full	Brick / 15-mm spacing
Br.2	350x205	1 damaged area (12 bare warps)	Full	Brick / 8-mm spacing
Br.3	350x205	1 damaged area (12 bare warps)	Full	Brick / 4-mm spacing
La.1	350x205	1 damaged area (12 bare warps)	Full	Laid / 15-mm spacing
La.2¹⁰	350x205	1 damaged area (12 bare warps)	Full	Laid / 8-mm spacing
Da.	350x205	1 damaged area (12 bare warps)	-	-

Usually full support requires a system of scrim and grid lines for being attached to a tapestry: scrim lines extend from top to bottom, while grid lines are shorter rows of stitches. In this study, when the specimens were conserved with a full

¹⁰ Since it was possible to monitor up to six samples at the same time, no sample with laid couching at 4-mm spacing was included in the experiment. Nonetheless, data on the efficacy of the 4-mm laid stitches were gathered from the monitoring of samples AI, AII, B and C.

support, this was applied in three different ways: I) without grid and scrim lines; II) with scrim lines 300 mm from each other and with grid lines between the areas of damage (20 mm distance between weak areas and grid lines); III) with scrim lines 300 mm from each other and with grid lines across the areas of damage. The distribution of grid lines when applied at a distance from the weak areas is shown in Figure 6.5a, while Figure 6.5b illustrates the grid lines system going across the damaged areas. In both cases, the grid lines consisted of running stitches. Table 6.4 records the three ways used for applying the full supports to the samples.

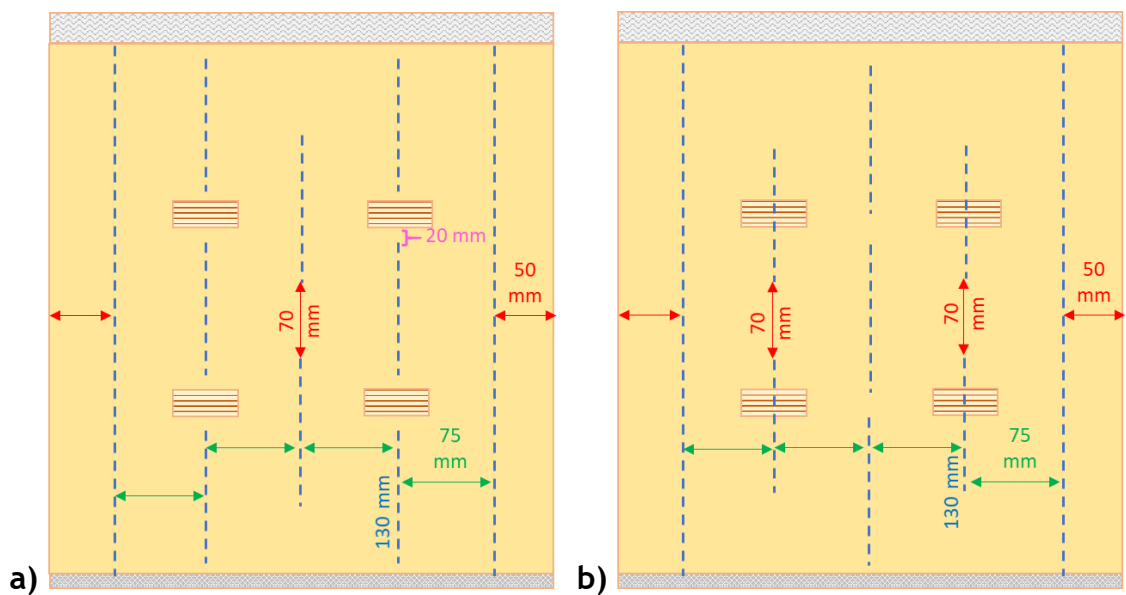


Figure 6.5. Wool rep mock-ups with full support applied on the back through scrim lines (at the edges of the samples) and grid lines (in the centre): a) grid lines far from the areas of damage (samples AI, AII, E, I); b) grid lines across the areas of damage.

Table 6.4. Grid lines systems used for attaching full supports to the samples.

Type of application of the full support	Samples applied
No grid lines	C
Grid lines far from the areas of damage	AI, AII, E, I
Grid lines across the areas of damage	F

All the experiments done, codes, aims and samples employed are listed in Table 6.5.

Table 6.5. Codes, objectives, and wool rep samples used in the experiments on the efficacy of stitching and support techniques.

Test Code	Treatments investigated and compared	Samples used
6.1	Full vs patch support; Brick vs laid couching	Al, B
6.2	Full support with scrim/grid lines vs full support without scrim/grid lines; Brick vs laid couching	All, C, DI
6.3	Full support with grid lines across the damage vs grid lines distant from the damage	DII, E, F
6.4	Full support with vs without couching	Al, E, F
6.5	Full vs patch support in highly damaged samples	G, H, I
6.6	Brick vs laid couching, at different spacing	Br.1, Br.2, Br.3, La.1, La.2, Da.

All the specifications of the materials used for conserving the mock-ups are reported in Table 6.6. It should be noted that, before the treatment, the linen fabric used for the support treatments (Linen B, see also Section 6.1.3.1), was washed in a washing machine, without any detergent and at 90°C. Then, it was applied in the warp direction with an extra allowance (also called “bag”) of 5 mm, meaning that for each 300mm-wide sample, a 305mm-wide linen fabric was stitched on the back. This is a common practice that aims to prevent the support fabric becoming too tight, although not all conservators agree with this approach [8].

Table 6.6. Materials used for conserving the wool rep samples.

Material	Description	Supplier
Wool Rep	Narrow ribbed rep	Context Weavers
Linen Fabric	Unprimed light weight linen scrim	Claessens (product's code OV10)
Thread for couching	Stranded cotton (2 threads were pulled from the 6-ply yarn)	Anchor
Thread for grid and scrim lines	Polyester yarn	Gütermann

All the conservation treatments on the wool rep samples were carried out by Prof Frances Lennard. It is underlined that the small number of mock-ups was largely determined by the high amount of time required for carrying out the treatments.

Following the procedure described in the previous chapter, the monitoring was conducted clamping the sample on a wooden board displayed vertically. A dotted speckle pattern was applied, following the procedure described in Section 5.2.2. At the same time, a camera was set to take one picture per hour during the entire length of each test (168 hours) and a data logger was placed next to the objects for recording the environmental conditions. Specifications on the camera settings, DIC analysis (subset size 61, step size 5) and data processing through MATLAB can be found in Section 4.2.2. It is underlined that, also in this case, both overall strain and pseudo strain across damaged/treated areas was measured.

6.1.2 2D DIC monitoring of a historic tapestry fragment after conservation

A historic tapestry fragment (details in Chapter 4, Section 4.2.1.2) was monitored for 200 hours using 2D DIC, after two successive conservation treatments. The test aimed to see if the results from the wool rep were also applicable to historic tapestry. The same materials as those employed for treating the mock-ups were used (Table 6.7). Strain distribution across the fragment, indicated with the code TapestryFragment_1, was studied also before conservation and the results were discussed in Section 4.3.2.1. As described in Chapter 4, before being treated, the textile object was in evident weak condition and showed different open slits, location of relatively high pseudo strain and therefore prone to a creep-like damage mechanism.

The first conservation treatment was applied only locally, and it consisted of small linen patches stitched on the back of some open slits. The patches were applied using brick couching, carried out at different spacing. The back of the fragment is depicted in Figure 6.6.

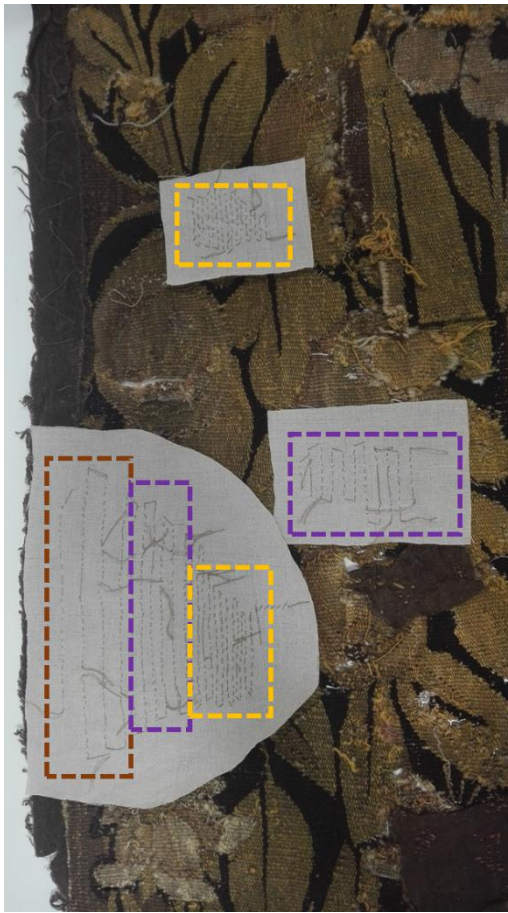


Figure 6.6. Detail of the back of TapestryFragment_1 after the first conservation treatment consisting of the application of three linen patches through brick couching in correspondence to weak areas. Brick couching was carried out at the following spacing: 3 mm (areas within yellow dotted line); 6 mm (areas within purple dotted line), 8 mm (area within brown dotted line).

After the first local treatment and strain monitoring, the tapestry was conserved again. The second time a full linen support was applied on the entire back of the fragment through a system of grid and scrim lines. As shown in Figure 6.7, the scrim lines were applied running from top to bottom of the external border, at 37 mm from vertical grid lines. On the other hand, 13mm-long grid lines were stitched leaving a 70-mm distance between each other in the vertical direction and 75 mm horizontally. It is important to note that usually the full support is not applied alongside the patches.



Figure 6.7. Back of TapestryFragment_1 after the second conservation treatment consisting of the application of a linen full support.

All the conservation treatments on TapestryFragment_1 were carried out by Prof Frances Lennard.

The DIC monitoring was carried out following the procedure reported in Section 4.2.2.

6.1.3 Uniaxial tensile testing

6.1.3.1 Fabrics for support treatments

One polyester fabric (Stabiltex™) and two types of linen fabrics currently in use by textile conservators (suppliers and details in Table 6.7), were uniaxially tensile tested to investigate their mechanical behaviour, and eventually to compare it to that of historic tapestries (Chapter 3, Section 3.2.1.1). Linen A is currently used by staff at Glasgow Museums for the conservation of tapestries, while Linen B is preferred by conservators at the National Trust and the Victoria

and Albert Museum. A fabric made of synthetic fibres was sometimes selected by Landi (Textile Conservation Consultancy) for supporting tapestries [11], but it is remarkably less widespread than linen [8, 10]. Magnified pictures of the supporting fabric are provided in Figure 6.8.

Table 6.7. Details of support fabrics.

Code	Areal density [kg/m ²]	Thickness ¹¹ [mm]	Weave count [yarn/cm] Weft x warp	Supplier
Linen_A	0.019	0.46	9x9	Whaleys (Bradford)
Linen_B Unwashed	0.020	0.25	17x17	Claessens (product's code OV10)
Linen_B Washed	0.017	0.25	17x17	Claessens (product's code OV10)
Polyester Stabiltex™	0.001	0.06	28x28	PlastOk

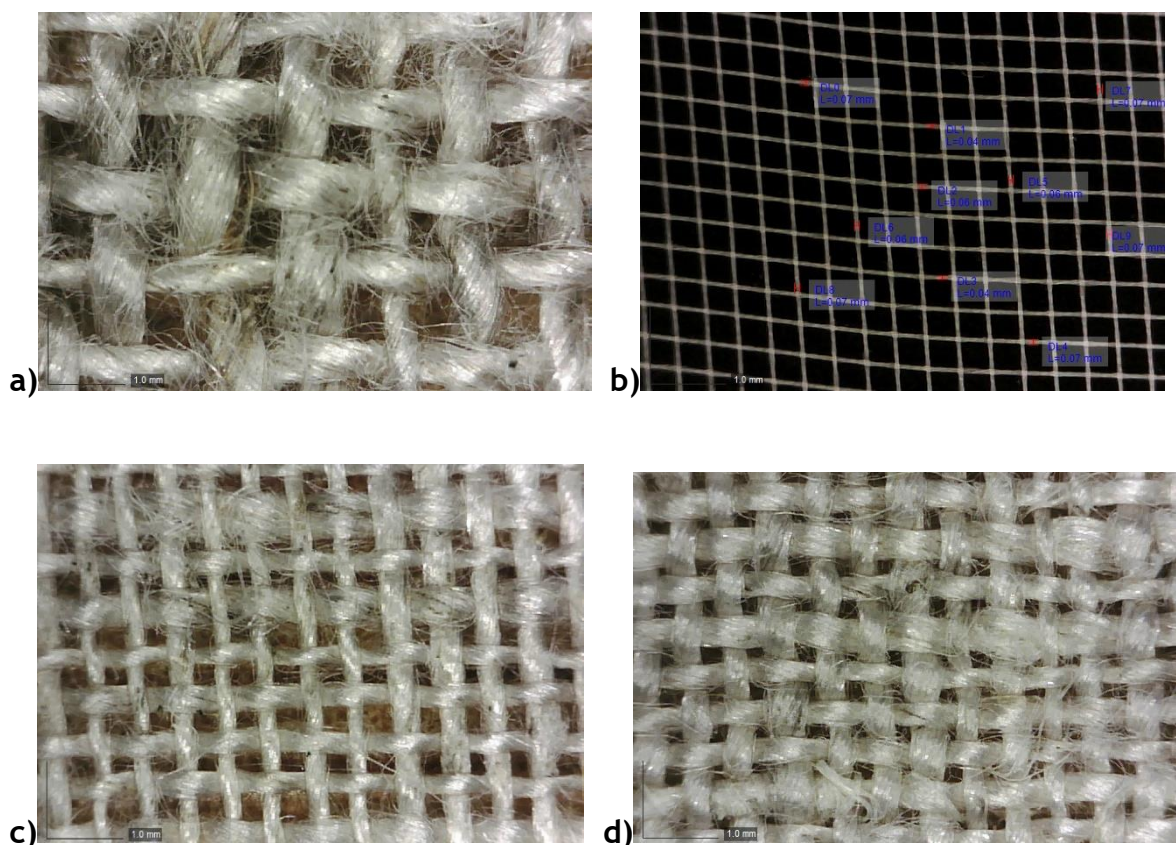


Figure 6.8. Weave structure (59x magnification) of: a) linen A; Stabiltex™ (annotated); linen B unwashed; linen B washed.

¹¹ The thickness of each specimen was measured, before the tensile test, with a digital micrometre (three measurements per specimens). The data reported in table represent the average thickness from all these measurements. The data were also confirmed by the optical analysis of the threads with the dino lite.

Uniaxial tensile testing was performed on the same equipment and with the same experimental conditions employed for studying historic samples and the wool rep fabric (Section 3.1.3). Five specimens, 200 x 50 mm, per linen type and weave orientation (warp and weft) were tested. The thickness of each specimen was calculated with a digital micrometre (average of three measurements at three different points).

6.1.3.2 Newly woven conserved samples

Uniaxial tensile testing was carried out on specimens cut from the stitched wool rep samples described in Section 6.1.1. The testing took place after the 2D DIC monitoring, so to gather more data on the efficacy of the different stitching and support techniques. The specimens (160 x 35 mm) were cut in the middle of the damaged area, as indicated by the example in Figure 6.9. To allow the specimens to be tested with the 1kN load cell, the width of the cross-sectional area was reduced to 35 mm. Since the weak areas were originally 55 mm wide, this means that the samples were cut in the middle of the region with bare warps, although with the repair stitches.

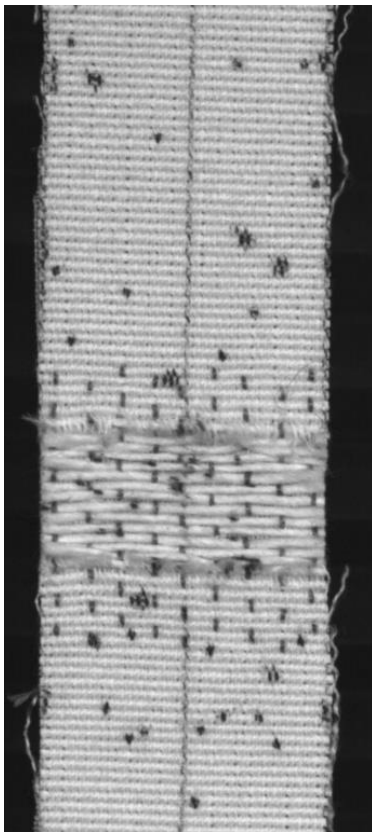


Figure 6.9. Specimen cut from sample A1.

The specimens, cut from the samples listed in Table 6.2 and Table 6.3, are shown in Table 6.8, together with the combination of treatments applied. For details on the equipment used and experimental conditions, see Section 3.1.3.

Table 6.8. Conserved wool rep specimens uniaxially tensile tested.

Specimen Code	Full Support	Patch Support	No Grid Lines	Far Grid Lines	Crossing Grid Lines	Brick Couching	Laid Couching
AI_B2	X			X		X 4 mm	
AI_L1	X			X			X 4 mm
AI_L2	X			X			X 4 mm
B_B1		X				X 4 mm	
B_L1		X					X 4 mm
C_B1	X		X			X 4 mm	
C_L1	X		X				X 4 mm
Br.2		X				X 8 mm	
Br.3		X				X 4 mm	
La.1							X 15 mm
La.2		X					X 8 mm

6.2 Results and discussion

6.2.1 2D DIC monitoring of newly woven conserved samples

2D DIC was used to evaluate the usefulness of brick and laid couching (with different spacing), patch and full support treatments (with different grid and scrim line systems) in reducing the strain across tapestry-like textiles when hung. Six monitoring tests were conducted and each experiment lasted 168 hours.

6.2.1.1 Full support vs patch support, brick vs laid couching (test 6.1)

One of the aims of this first test was to compare the effectiveness of a full support against that of a patch treatment. To do so, two wool rep samples, with four damaged areas each, were used: sample AI, with a full support on the back (grid lines between damage); sample B, with four patches on the back of the weak regions. Two out of four damaged areas of each sample were conserved using laid couching (right side), while the remaining were treated with brick couching (left side). This also aimed to compare the two stitching techniques.

Figure 6.10 shows a strain map at the end of the one-week monitoring of sample AI (full support) and sample B (patch support). From the strain maps no remarkable differences between the two samples can be observed, suggesting that the impact of two support techniques might have been very similar. In addition, Figure 6.10 shows no areas of higher strain in the samples, not even across the damage. This could indicate the success of both types of support and/or stitching techniques in preventing the elongation of the areas with bare warps. It is important to note that, from this test, it is not possible to distinguish the role of stitching from that of the support fabric in improving the mock-ups' structural stability. This is better addressed in experiment 6.4. It is noted that, since the surrounding areas of the specimens did not present any damage, they were expected to be already strong enough not to benefit from the support treatments.

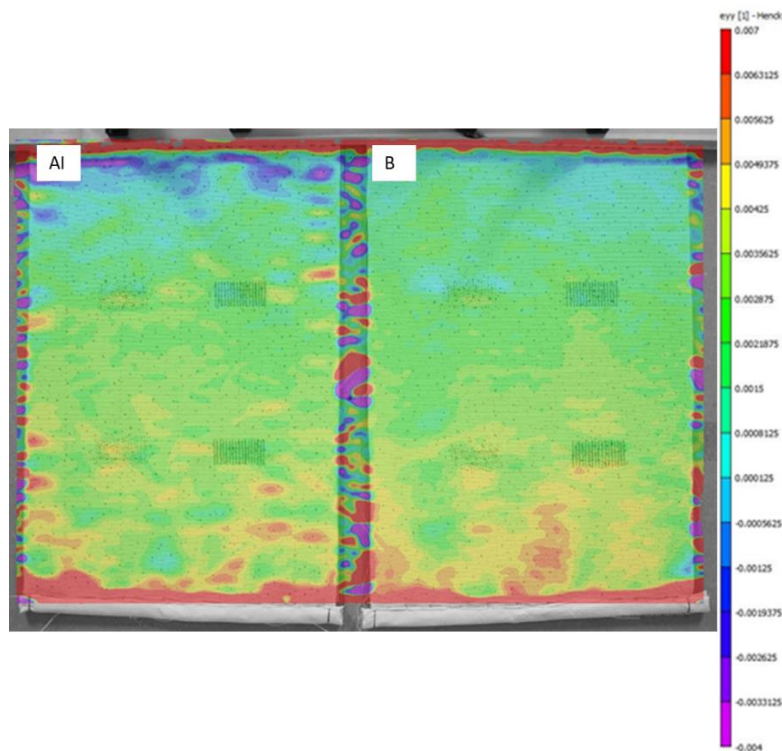


Figure 6.10. Strain map, ε_{yy} [%], of sample AI (full support, brick and laid couching) and sample B (patch support, brick and laid couching) at the end of the 168-hour monitoring.

Figure 6.11 presents the overall longitudinal strain data, together with the humidity. The graphs confirm the observations drawn by looking at the strain

maps: the trend and magnitude of ϵ_{yy} across the different samples is comparable, possibly stating a similar efficacy of patches and full support. From Figure 6.11 the linear relationship between humidity and strain fluctuations is also clear; as defined in Chapter 4, this indicates the occurrence of fatigue.

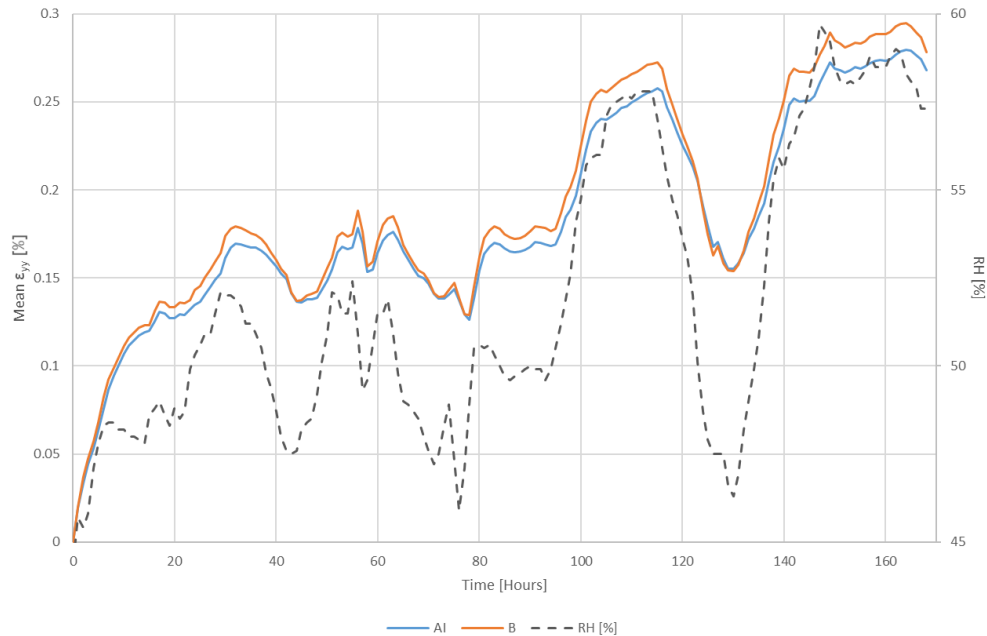


Figure 6.11. Mean ϵ_{yy} [%] of sample AI and sample B during the 168-hour monitoring. RH [%] is indicated by the dotted line.

When comparing the efficacy of brick and laid couching in more detail, the pseudo strain data measured across the weak areas is more helpful than the overall longitudinal strain. Indeed, a more time dependent behaviour, possibly creep, is expected to happen across the damaged areas, as they would tend to widen when left untreated, causing a relatively high local stain (Chapter 4). In this case, by looking at the pseudo strain data across the differently conserved areas (Figure 6.12 and Figure 6.13), the 2D DIC outcomes are not able to state whether one stitching technique, brick or laid, was more effective than the other. Indeed, as depicted in Figure 6.13, the error bars (SD) of the maximum pseudo strain overlap each other, so neither of the two couching techniques was more efficient than the other from a statistical point of view. However, by comparing Figure 6.11 and Figure 6.12, the data confirm the success of both conservation methods: the extension of the (treated) weak areas was around the same, or even less, than that across the entire surface of the samples. Therefore, it can be said that the treatments enabled the damaged areas to regain the physical strength lost. The fact that in general the 4-mm couching

seems to have partly impeded fatigue across the treated area (lower pseudo strain than overall strain) is further discussed in Section 6.2.1.6.

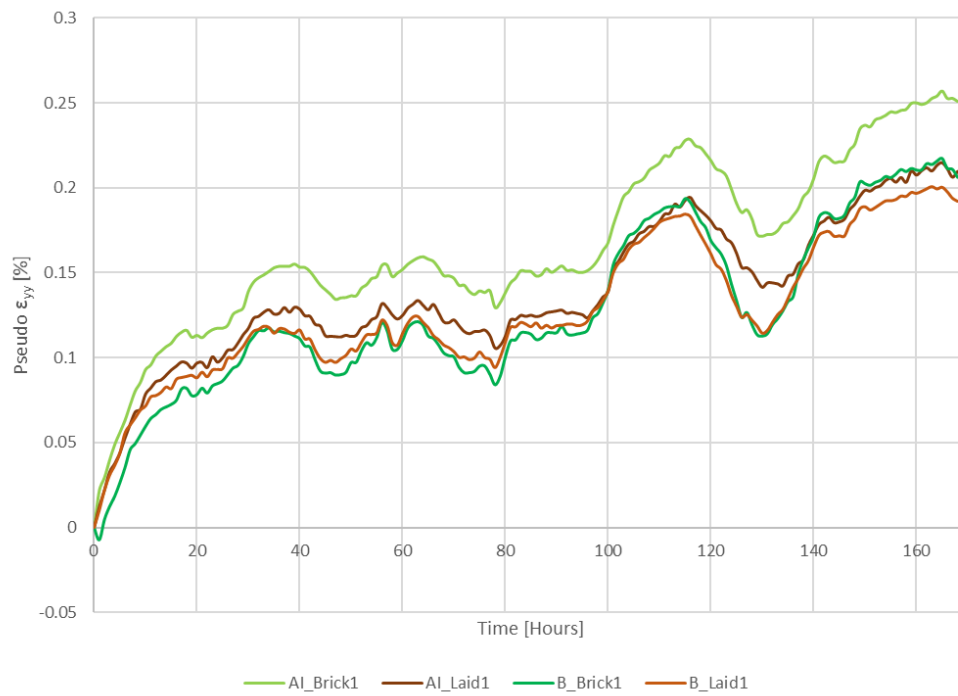


Figure 6.12. Pseudo ϵ_{yy} [%] across the damaged but conserved areas of sample AI.

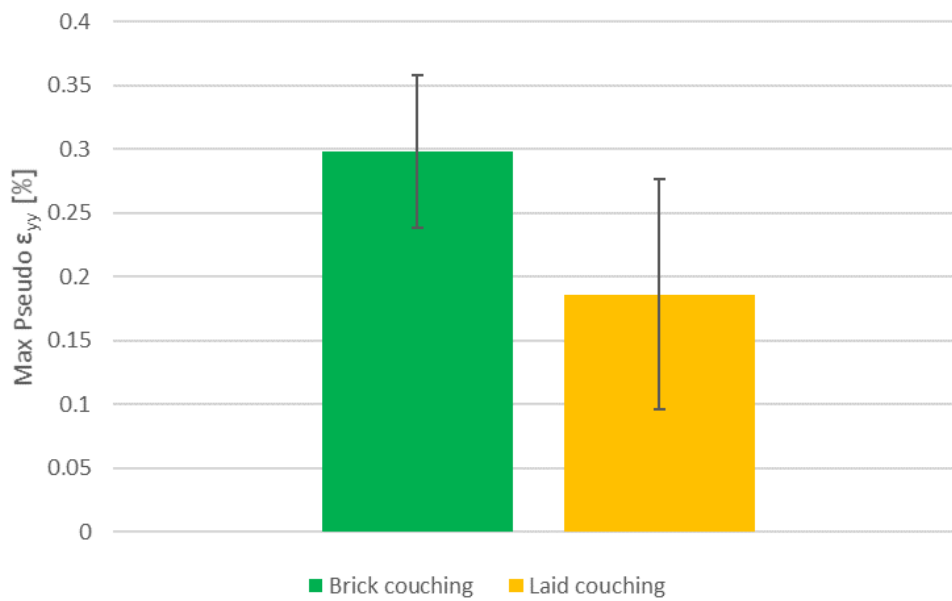


Figure 6.13. Maximum pseudo ϵ_{yy} [%] across areas of sample AI and B conserved with brick and laid coupling.

6.2.1.2 Full support with vs without grid lines, brick vs laid couching (test 6.2)

Experiment 6.2 investigated the effects of grid lines in full support treatments. Besides a non-conserved specimen (DI), two samples with a full support were used: All with grid lines 20 mm apart from the damaged area, and C without grid lines. The weak areas in mock-ups All and C were conserved using both brick and laid couching, so as to test the stitching techniques.

The strain map of the three samples after the one-week test is illustrated in Figure 6.14. As also observed for experiment 6.1, the strain map suggests the usefulness of the laid and brick couching in easing the strain around weak areas. Here it is even more evident thanks to the direct comparison with untreated sample DI: the damaged areas of specimen DI are marked as locations of high pseudo strain, in contrast to those conserved in specimens All and C.

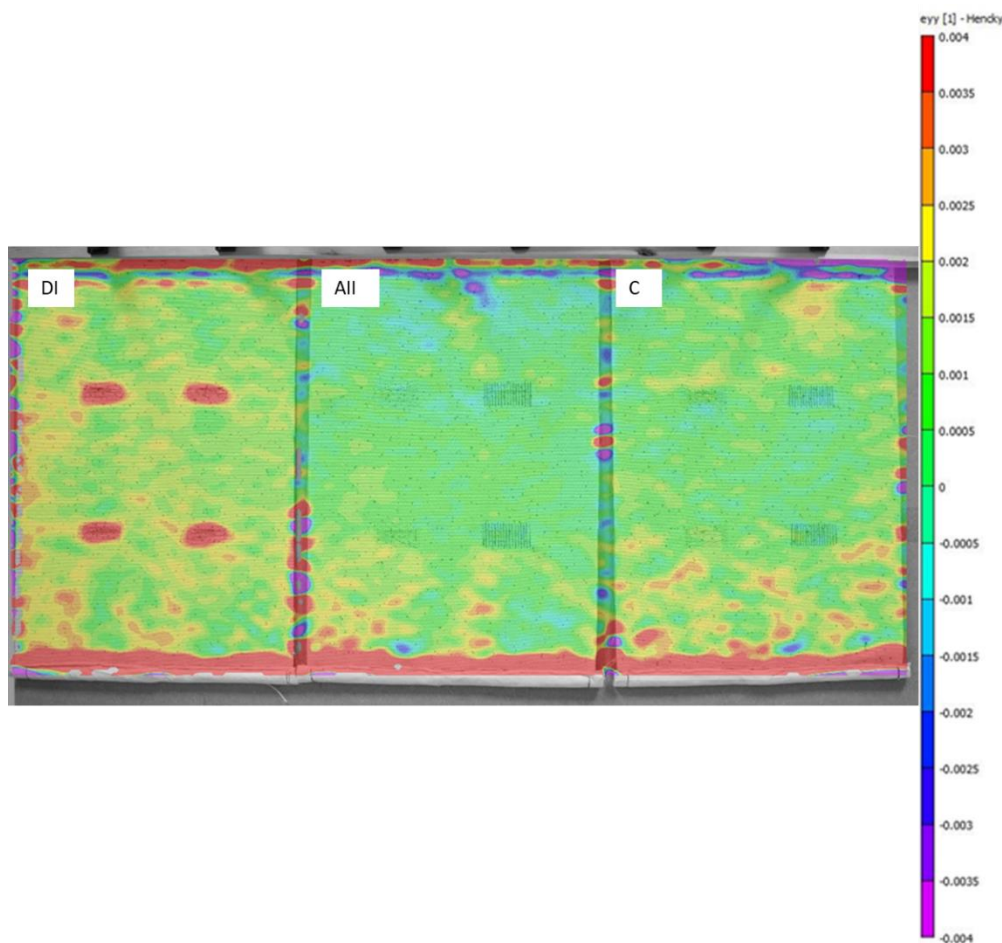


Figure 6.14. Strain map, ϵ_{yy} [%], of sample DI (no conservation), All (full support with grid lines, brick and laid couching) and sample C (full support without grid lines, brick and laid couching) at the end of the 168-hour monitoring.

The (overall) greater elongation of sample D is confirmed by the ε_{yy} [%] data in Figure 6.15, that also describe the occurrence of a fatigue mechanism thanks to the correlation with humidity variations. At the end of the one-week monitoring, after a steep rise in humidity levels (from 36.8% to 50.3% in the last 15 hours of monitoring), all samples reached the maximum elongation. However, the strain across untreated sample DI was around twice as much ($\approx 0.17\%$) as that in conserved samples All ($\approx 0.07\%$) and C ($\approx 0.10\%$). This suggests how effective the conservation treatments were in reducing strain, especially pseudo ε_{yy} associated with the opening of damaged areas as a result of creep behaviour (Figure 6.16). By looking at Figure 6.15 and Figure 6.16, it is interesting to note that negative strain (indicating contraction) took place in treated samples All and C, in opposition to non-conserved sample D, for which only positive values were recorded.

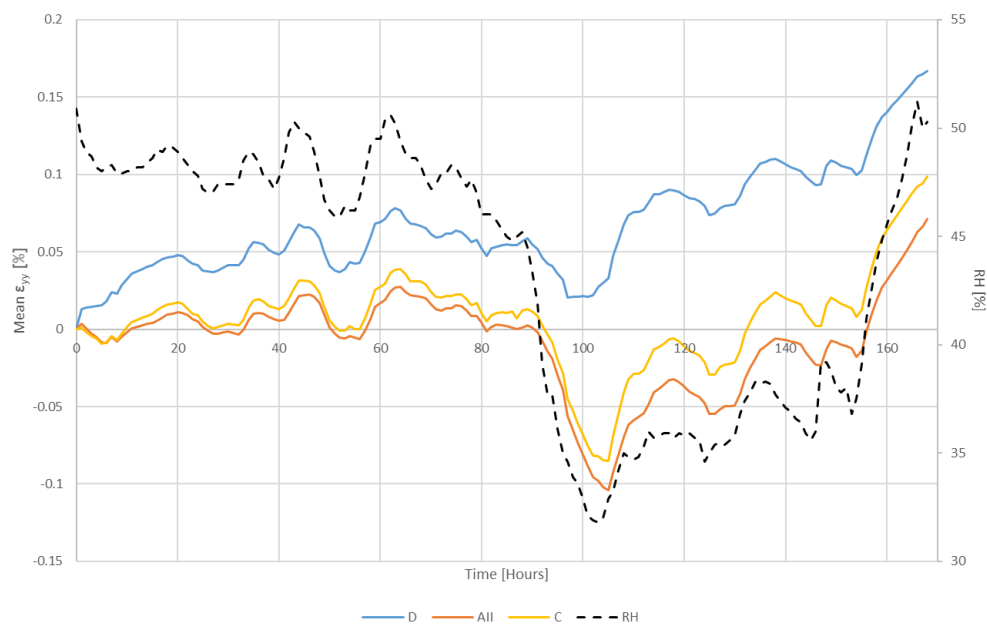


Figure 6.15. Mean ε_{yy} [%] of sample DI, All, and C during the 168-hour monitoring. RH [%] is indicated by the dotted line.

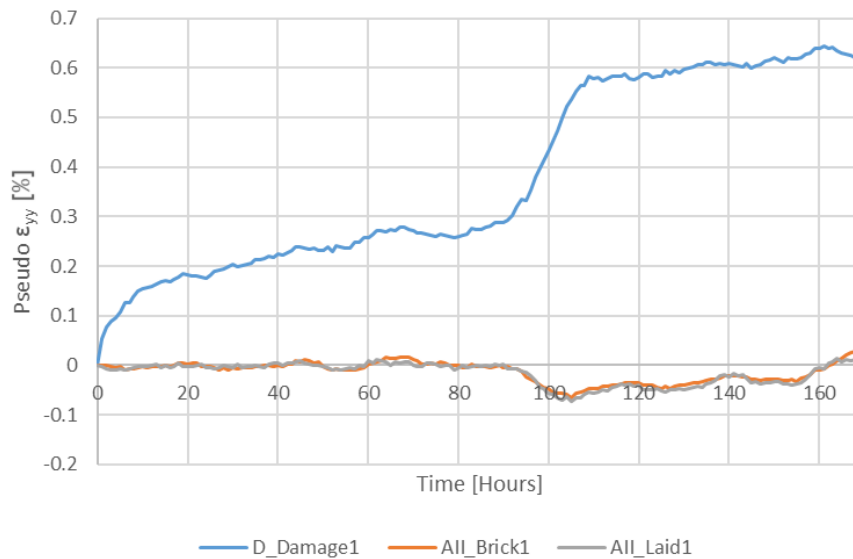


Figure 6.16. Pseudo ϵ_{yy} [%] across the damaged areas of sample D, and conserved areas of sample All.

Figure 6.17 reports the average maximum pseudo strain registered across the areas of samples All and C conserved with brick and laid couching, in contrast to those left untreated in sample DI. The average for each couching technique, and the related SD, was calculated from the four areas (two per sample) conserved with the same method. The results of Figure 6.17 seem to show a greater efficacy of the laid couching in preventing damage propagation (lower pseudo strain). Nonetheless, it is important to underline that the error range is relatively high, making the outcomes from the two techniques close.

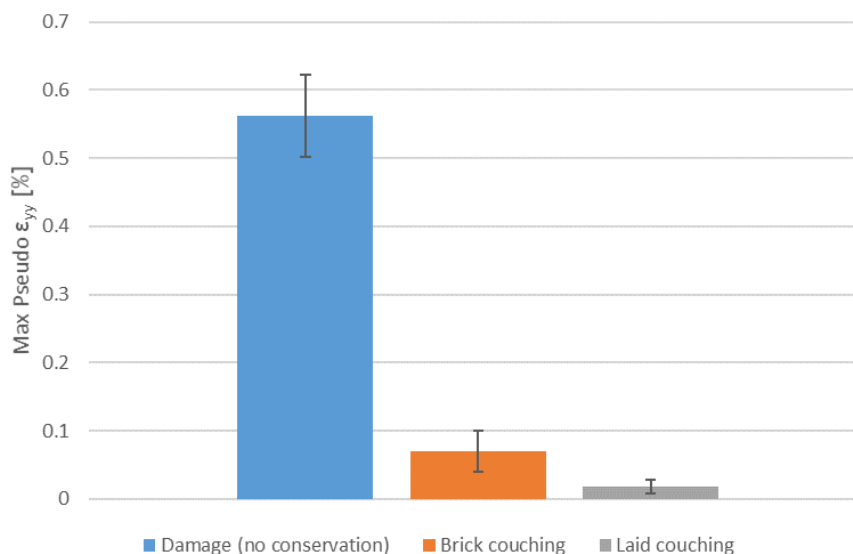


Figure 6.17. Maximum pseudo ϵ_{yy} [%] across the damaged/untreated areas of sample DI and the damaged/conserved areas of sample All and C.

6.2.1.3 Full support with grid lines across vs distant from damaged areas (test 6.3)

This test focused on the evaluation of grid lines used in full support treatments. To do so, two samples with different supporting line systems were monitored and the displacement analysed with 2D DIC. Both conserved specimens presented four damaged areas and a linen full support on the back. However, while in sample E grid lines were stitched at a distance from the damaged areas (20 mm), in sample F the lines were stitched through the centre of the weak regions. Alongside treated specimen E and F, sample DII, damaged but not conserved, was monitored as reference.

The strain across the three samples monitored for one week is depicted in Figure 6.18. It is clear that the greatest elongation was experienced by the weak areas of untreated sample DII and, less markedly, across structural weaknesses in sample E. On the other hand, strain on the entire surface of sample F appeared to be more homogeneous. All these observations suggest that the support treatment was effective in mitigating damage propagation, especially when grid lines were stitched across the slits. By comparing strain maps in Figure 6.18 with those in Figure 6.10 or Figure 6.14, it can be noted that weak areas appeared to be better stabilised by the combination of both grid lines and couching techniques. Indeed, while no high pseudo strain was noted across stitched areas (Figure 6.10 and Figure 6.14), damaged areas in samples E and F, treated with full support but no couching, present relatively high local ϵ_{yy} .

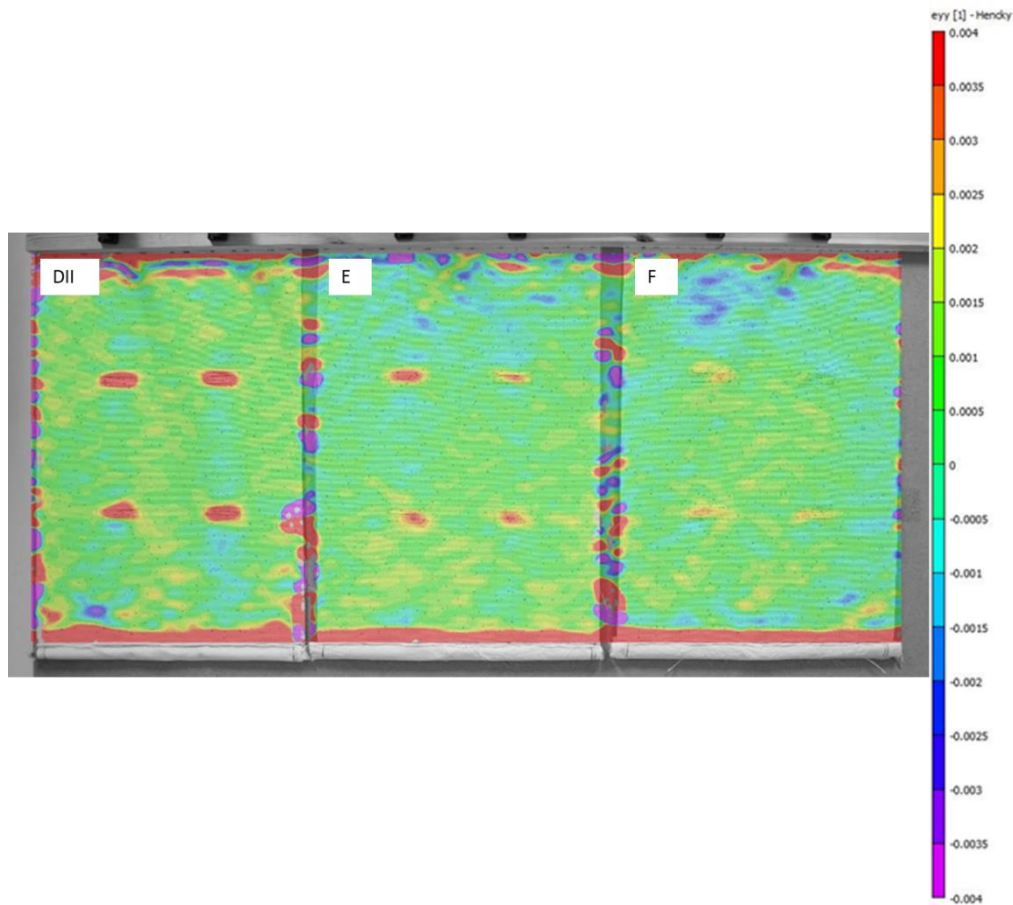


Figure 6.18. Strain map, ϵ_{yy} [%], of sample DII (no conservation), E (full support with grid lines at a distance from the damaged area) and sample F (full support with grid lines across the damaged area) at the end of the 168-hour monitoring.

Figure 6.19, by showing the overall strain data and RH [%], points out the effects of support treatments: sample DII was characterised by the greatest elongation when compared to samples E and F. The significant drops in RH during the test, especially from 54% to 35% RH (20-45 hours), caused significant contractions in samples E and F; on the other hand, overall ϵ_{yy} in sample DII was always positive. Average strain across specimen E appeared to be slightly higher than that across sample F, as expected.

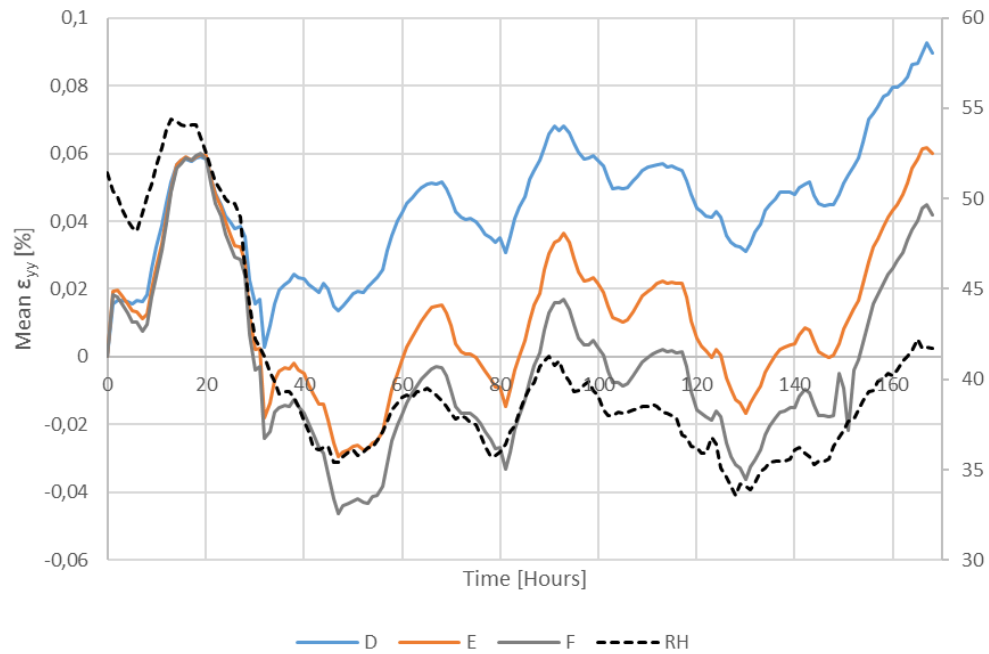


Figure 6.19. Mean ε_{yy} [%] of sample DII, E, and F during the 168-hour monitoring. RH [%] is indicated by the dotted line.

Figure 6.20 describes pseudo strain across damaged areas in the three different samples during the 168 hours of the test. The (average) maximum pseudo strain across the bare warps is shown in Figure 6.21. The outcomes confirm the usefulness of the full support treatments in minimising damage propagation in weak areas: untreated sample DII experienced a significantly greater elongation than the treated samples. However, it is pointed out that the pseudo ε_{yy} from the weak (treated) areas of samples E and F is greater than the overall strain in Figure 6.19. This confirms that the treatments were not effective enough to completely prevent damage propagation. Data in Figure 6.20 and Figure 6.21 also define the greater efficacy of the grid line system of sample F. Indeed, the (average) maximum pseudo strain across structural defects in sample F was around 0.16%, while in sample E was almost twice as much, around 0.30%. It is difficult from this test to establish whether the positive effects registered in sample E were due to the full support alone, or to its combination with grid lines distant from the slits.

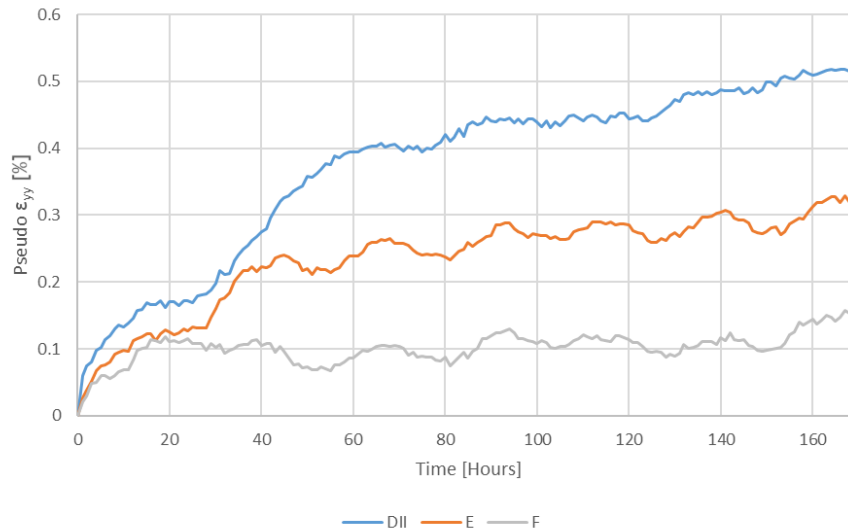


Figure 6.20. Pseudo ϵ_{yy} [%] across damaged areas of sample DII, E, and F during the 168 hours of monitoring.

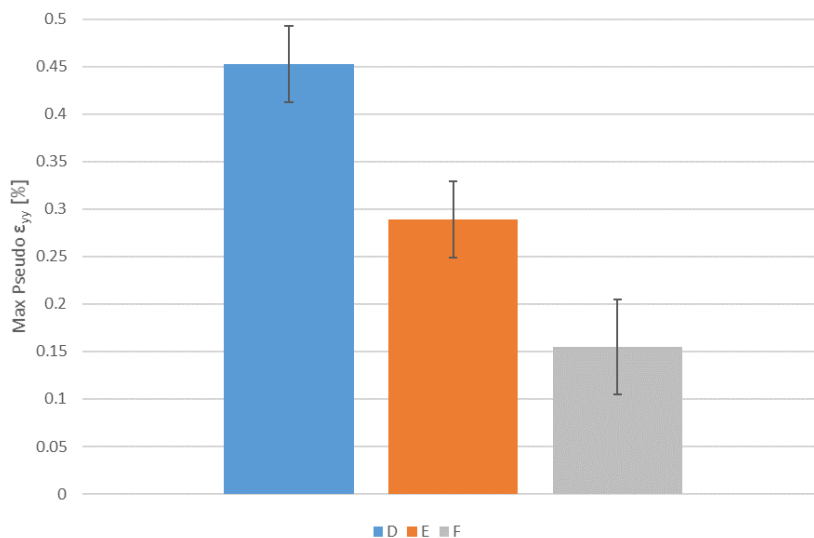


Figure 6.21. Maximum pseudo ϵ_{yy} [%] across the damaged areas of sample DII, E and F.

6.2.1.4 Full support vs brick/laid couching (test 6.4)

This experiment aimed to better distinguish the impact of full support treatments from that of couching techniques. To do so, specimens with and without couching, but all treated with full support, were employed. Namely, the samples used were: A1, full support with grid lines distant from the damaged areas, brick/laid couching; E, full support with grid lines distant from the damaged areas, no couching; F, full support with grid lines across the damaged areas, no couching. All the specimens had been used once before this test.

Figure 6.22 depicts strain across the three specimens. As noticed in the previous paragraph (6.2.1.3), the strain map highlights as regions of greater elongation the areas of weft loss in sample E, while ϵ_{yy} across specimens AI and F appeared to be more homogeneous.

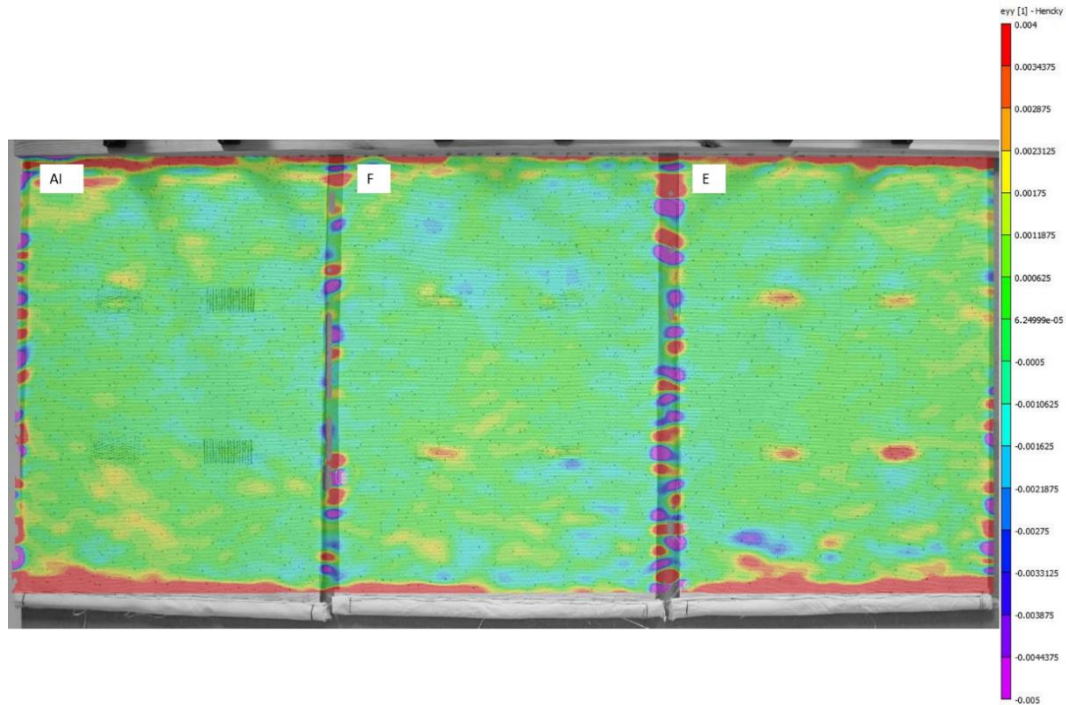


Figure 6.22. Strain map, ϵ_{yy} [%], of sample AI (full support, brick and laid couching), F (full support with grid lines across the damaged areas), E (full support with scrim lines distant from the damaged areas) at the end of the 168-hour monitoring.

Globally averaged strain across the three samples is described in Figure 6.23. Sample AI showed similar mean ϵ_{yy} of sample E, higher than the one of specimen F. This was unexpected: since sample AI presents, alongside the full support, laid and brick couching across the damaged areas, its overall strain was thought to be lower than mock-ups E and F, without couching. This unexpected result could be due to differences in the prior condition of the specimens, as they had been used for other tests before this experiment.

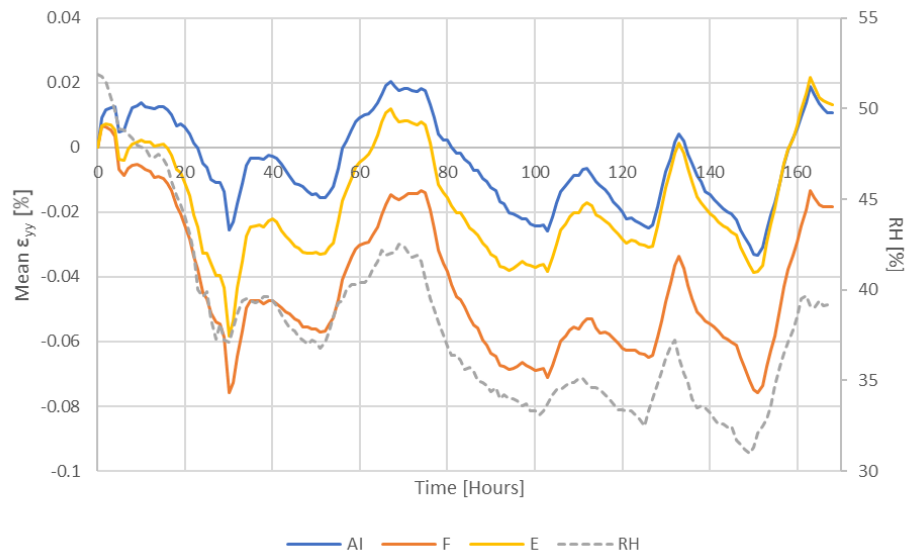


Figure 6.23. Mean ϵ_{yy} [%] of sample AI, F, and E during the 168-hour monitoring. RH [%] is indicated by the dotted line.

Figure 6.24 shows the overall pseudo strain across damaged areas in the three samples during the 168 hours of monitoring. The graphs outline the greatest effectiveness of the couching (both brick and laid) in preventing the opening of slits (sample AI), followed by the full support combined with grid lines across the damaged areas (sample F). Lastly, weak areas in sample E widened the most. The maximum pseudo strain values, described in Figure 6.25, confirm these observations. Again, in sample AI the areas conserved with laid couching possibly elongated less than those treated with brick couching, however the difference falls within the error range (Figure 6.25).

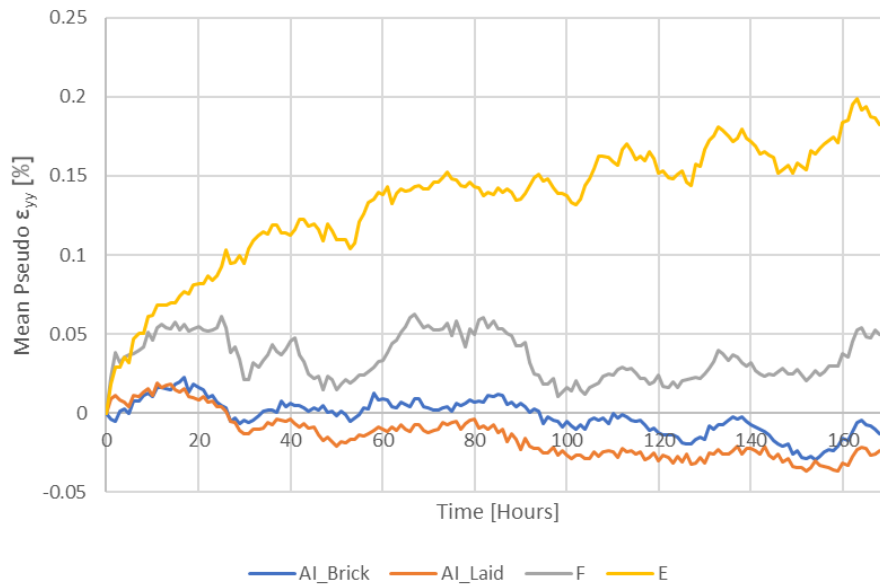


Figure 6.24. Pseudo ϵ_{yy} [%] across damaged areas of sample AI (blue line, brick couching; red line, laid couching), F (grey line), E (yellow line) during the 168 hours of monitoring.

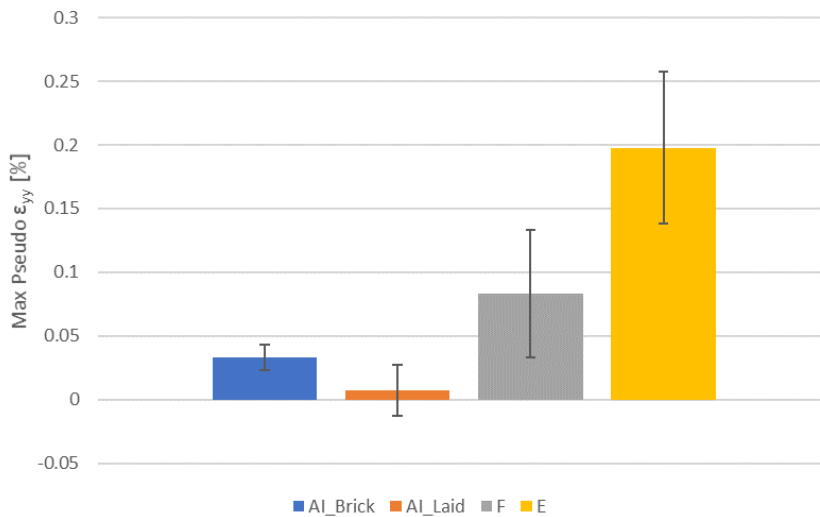


Figure 6.25. Maximum pseudo ϵ_{yy} [%] across the damaged areas of sample AI (conserved with brick and laid couching), E and F.

6.2.1.5 Full support vs patch support in highly damaged samples (test 6.5)

This test studied the different impact of a full and patch support in reducing the strain in a highly damaged tapestry-like material. Differently from the samples employed in the previous experiments (6.1-6.4), the mock-ups used here presented more extensive physical damage. This allowed us to observe whether the treatment, local (sample H, patch support) or full (sample I), can be effective in physically supporting different types of weak areas. Brick couching

was also used for the major damaged areas. Besides conserved specimens H and I, untreated sample G was also monitored as reference. In general, the samples employed here better describe actual scenarios, as historic hangings usually present more widespread, more pronounced, and a wider range of structural weaknesses than those in specimens A-I-F.

Figure 6.26 illustrates the strain map of the mock-ups at the end of the 160-hour monitoring.¹² It is evident that other weak regions than the four with 12 bare warps can be distinguished because of the high local strain linked to creep. In particular, the 50-mm horizontal slits on the right side of the mock-ups were clearly seen to widen during the monitoring, since they are indicated as locations of high ε_{yy} (Figure 6.26). As expected, this is especially evident from the strain maps of the untreated sample G, but also from those of sample H, with patch support. On the other hand, strain across specimen I, fully supported on the back, appears more homogeneous, possibly indicating the greater efficacy of this type of treatment.

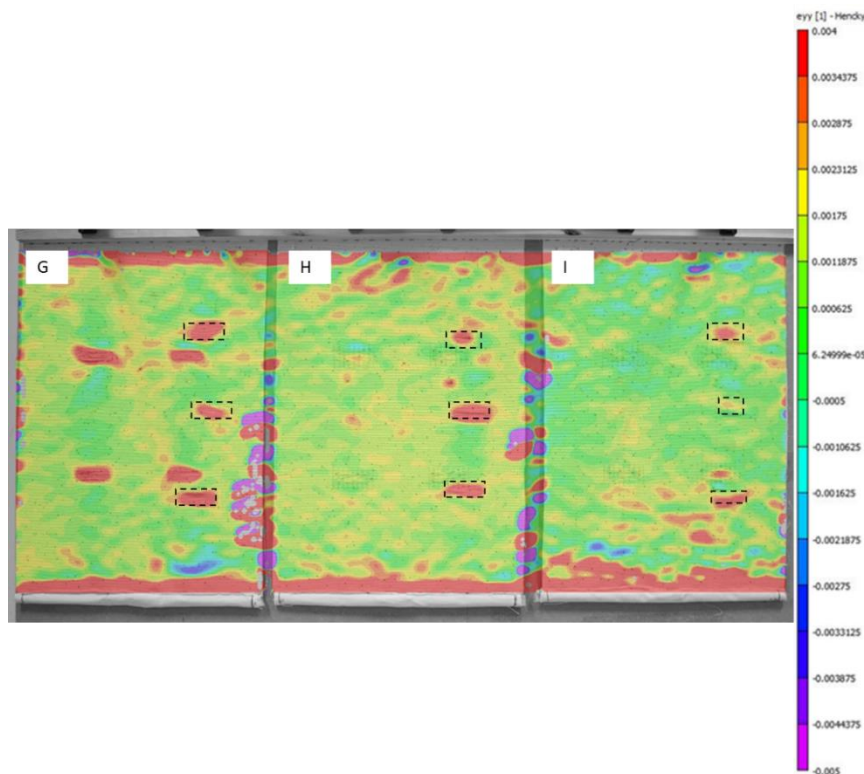


Figure 6.26. Strain map, ε_{yy} [%], of sample G (no conservation), H (patch support) and sample I (full support) after 160 hours of monitoring. The locations of particularly weak areas are marked within dotted lines.

¹² Although the test lasted 168 hours, unexpected out-of-plane displacements of the specimens occurred in the last 8 hours of monitoring, preventing the DIC analysis.

The mean overall ϵ_{yy} [%] across the three samples is plotted, together with RH and against time, in Figure 6.27. Figure 6.27 confirms the positive effects of the full support in reducing the global longitudinal strain: while mean ϵ_{yy} in sample H, with patches, was almost the same of that across non-conserved sample G, specimen I elongated less.

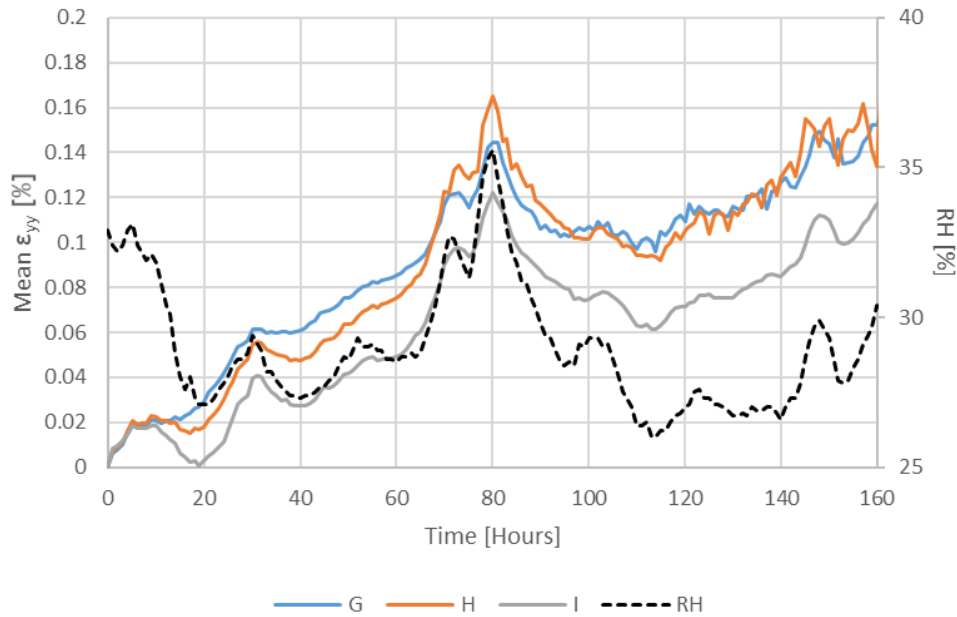


Figure 6.27. Mean ϵ_{yy} [%] of sample G, H, and I during the 160-hour monitoring. RH [%] is indicated by the dotted line.

Figure 6.28 and Figure 6.29 depict the data from the pseudo strain registered across the four damaged areas with 12 bare warps in the three specimens. From both figures, the success of the brick couching in preventing the opening of the slits is assessed. Indeed, the maximum pseudo strain across structural damage in untreated specimen G was shown to be remarkably greater ($\approx 0.65\%$) than that in conserved samples H ($\approx 0.15\%$) and I ($\approx 0.12\%$). The difference in the pseudo strains from specimens H and I falls within the error range, so it can be said that in both cases the weak areas were equally and successfully conserved through the brick couching.

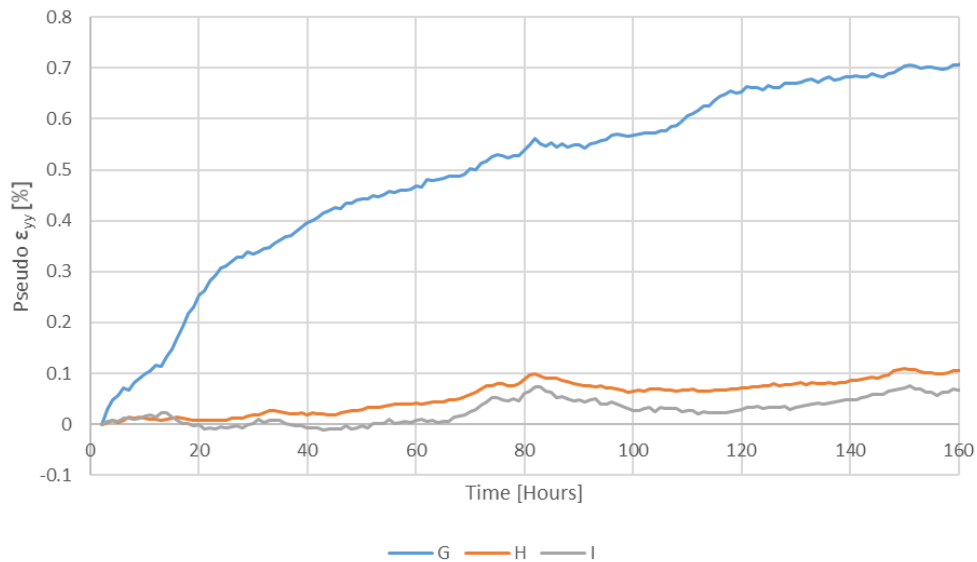


Figure 6.28. Pseudo ϵ_{yy} [%] across damaged areas (12 bare warps) of sample G, H, and I during the 160 hours of monitoring.

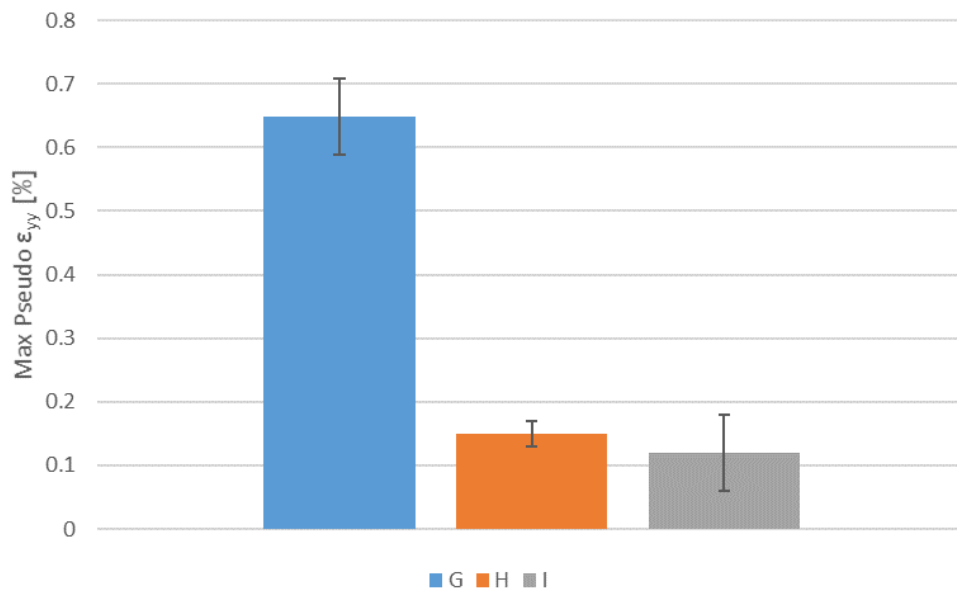


Figure 6.29. Maximum pseudo ϵ_{yy} [%] across the damaged areas (12 bare warps) of sample G, H and I.

When focusing on the results from the weak areas without couching (Figure 6.30), the greater efficacy of the full support in sustaining them and avoiding elongation is demonstrated. Indeed, patch support was ineffective whenever patches were not directly on the back of damage, as the max pseudo strain in sample H was around the same of that in untreated specimen G.

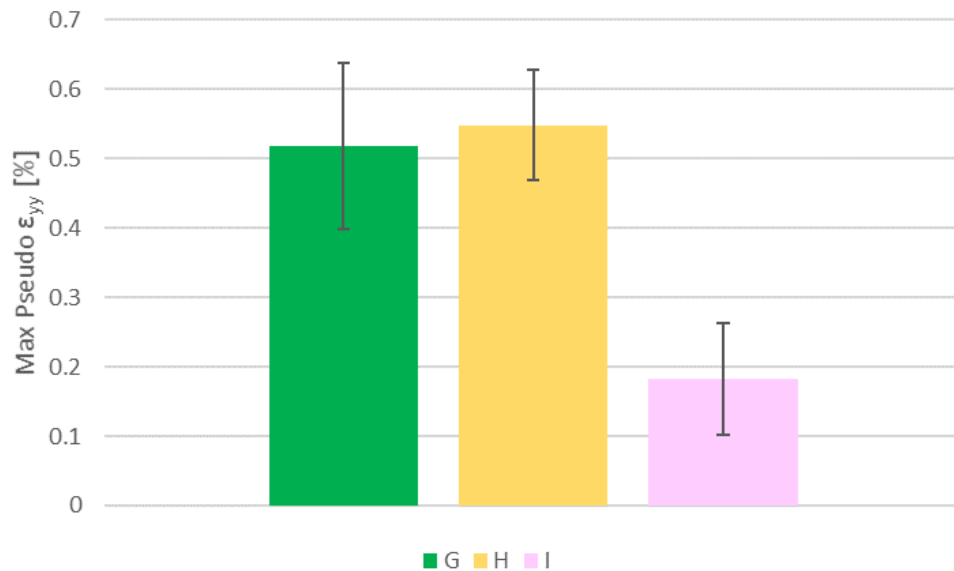


Figure 6.30. Maximum pseudo ϵ_{yy} [%] across the particularly damaged areas of sample G, H and I.

6.2.1.6 Different spacing (test 6.6)

Experiment 6.6 aimed to examine the impact of spacing in brick and laid couching. Five conserved samples were monitored: Br.1, brick couching, 15-mm spacing; Br.2, brick couching, 8-mm spacing; Br.3, brick couching, 4-mm spacing; La.1, laid couching, 15-mm spacing; La.2, laid couching, 8-mm spacing. In addition, untreated sample Da. was also tested as reference. Studying how spacing may impact strain across damage is important for different reasons: I) the number of stitches affects time and cost of the treatment; II) some conservators have been questioning whether close stitching excessively constrains the treated area [5]. The second point may raise the question of whether close spacing may be actually detrimental, as it may create different responses to RH and lead to local tension.

Figure 6.31 depicts the strain map of the six samples at end of the test. The central damaged area in specimen Da., the only one left untreated, is marked in red, expressing high longitudinal strain, and so elongation, due to a time-dependent mechanism. Contrarily to this, ϵ_{yy} across the five conserved specimens appears to be more homogeneous.

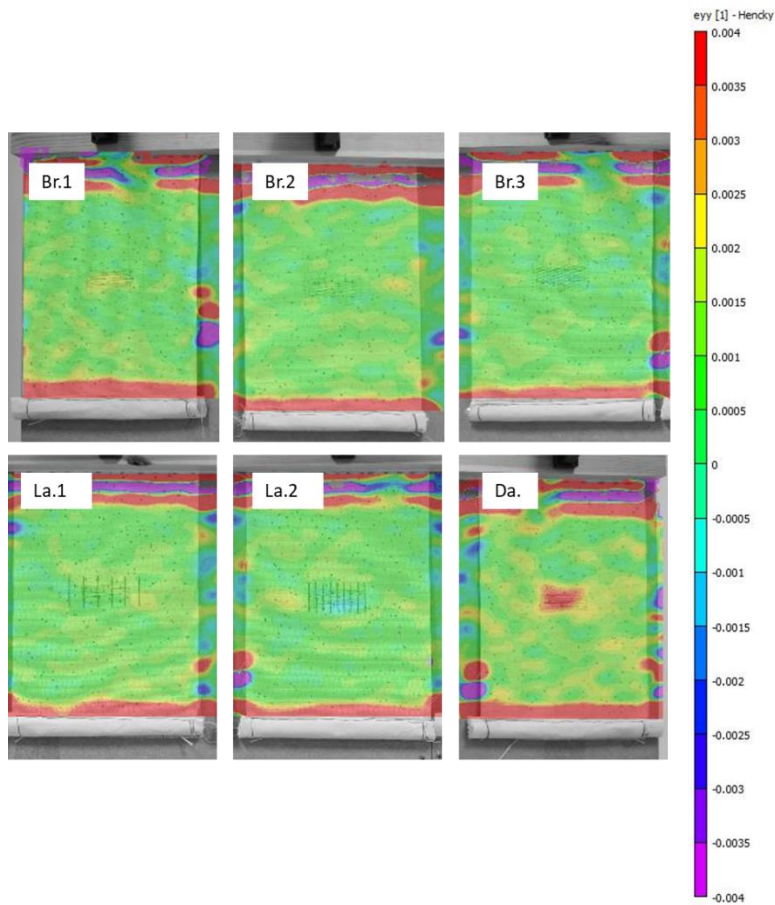


Figure 6.31. Strain map, ϵ_{yy} [%], after 168 hours of monitoring of sample: Br.1, Br.2, Br.3 (brick couching); La.1, La.2 (laid couching); Da. (no conservation).

The observations drawn from the strain maps can be further verified by the (overall) ϵ_{yy} data summarised in Figure 6.32: among the six samples, specimen Da. was the only one showing a distinctively higher strain than the others. In general, it can be noted that sample Br.3, with the closest stitches, was characterised by a more contained elongation than samples Br.1 and Br.2. Similarly, specimen La.2 (8-mm spacing) presented a lower strain than sample La.1 (15-mm spacing).

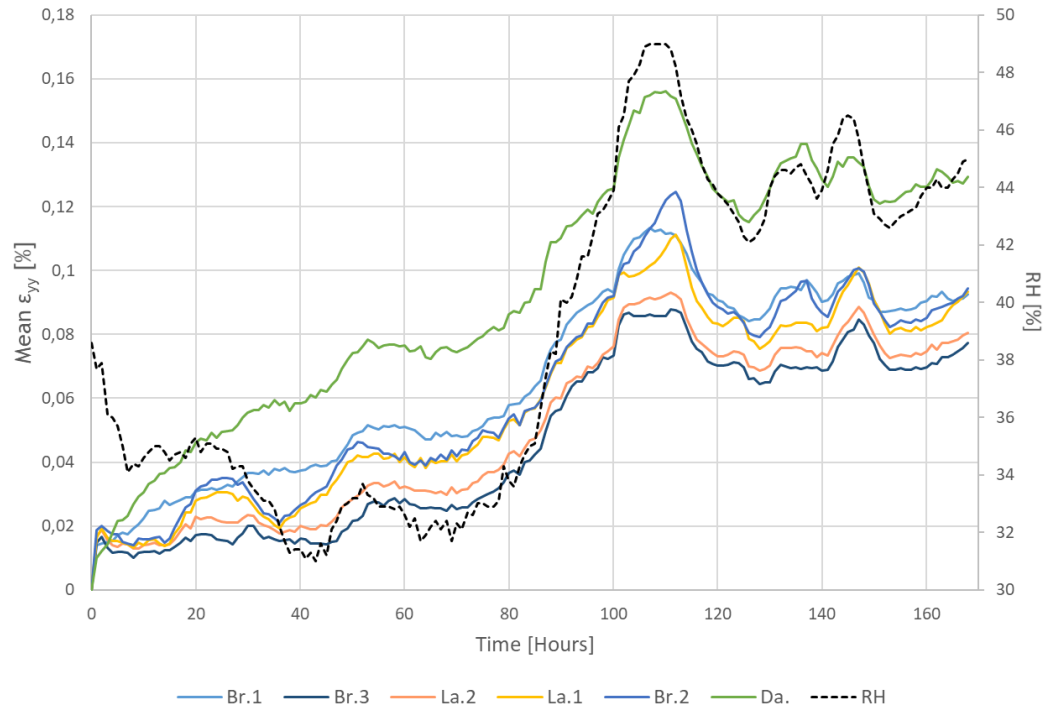


Figure 6.32. Mean ε_{yy} [%] during the 168-hour monitoring of sample: Br.1, Br.2, Br.3 (brick coupling); La.1, La.2 (laid coupling); Da. (no conservation). RH [%] is indicated by the dotted line.

Figure 6.33 illustrates the mean pseudo ε_{yy} measured across the damaged areas, conserved and non-conserved, of the six samples. The curves show a possible creep-like behaviour, affecting mostly the weak area in sample Da., without coupling. The greater extension of sample Da. is also confirmed by the maximum pseudo strain data reported in Figure 6.34. Furthermore, data in Figure 6.33 and Figure 6.34 seem to describe the impact of spacing in the coupling: close stitches (samples Br.3 and La.2) were more effective in preventing slits opening, when compared to more spaced coupling (specimens Br.1 and La.1). When the overall data (Figure 6.32) are compared against pseudo strain across treated areas (Figure 6.33), it is interesting to note that local ε_{yy} was lower than globally averaged strain in mock-ups with stitches at 8- and 4-mm spacing (see also discussion in Section 6.2.1.1). On the other hand, the specimens conserved with 15-mm brick and laid coupling have similar pseudo and overall strains. As an example, graphs plotting overall and pseudo ε_{yy} of Br.1 (15-mm spacing) and Br.2 (8-mm spacing) are provided in Figure 6.35. These observations could indicate that, when stitches were applied at lower distance than 15 mm, the treatment could have partly limited fatigue across the

conserved area. As previously mentioned, according to some conservators, such divergency in the response to RH between treated and untreated areas should be avoided. It is important to stress that only one specimen per type of couching-spacing was employed, so these outcomes should be regarded as indicative rather than statistically objective.

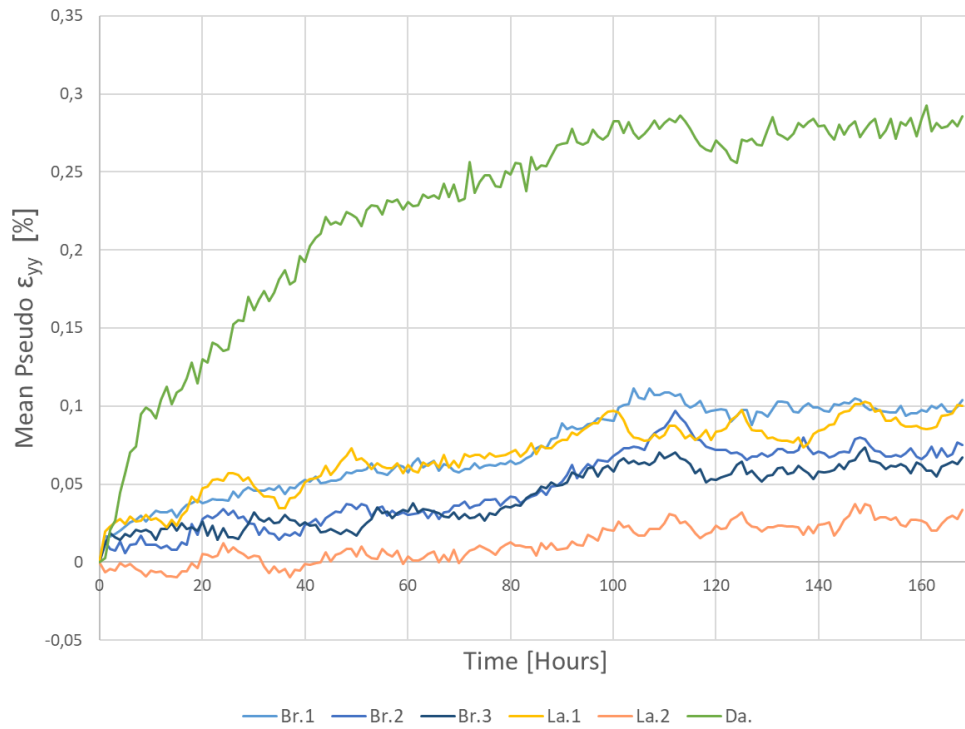


Figure 6.33. Pseudo ϵ_{yy} [%] across damaged areas of sample Br.1, Br.2, Br.3, La.1, La.2, Da. during the 168 hours of monitoring.

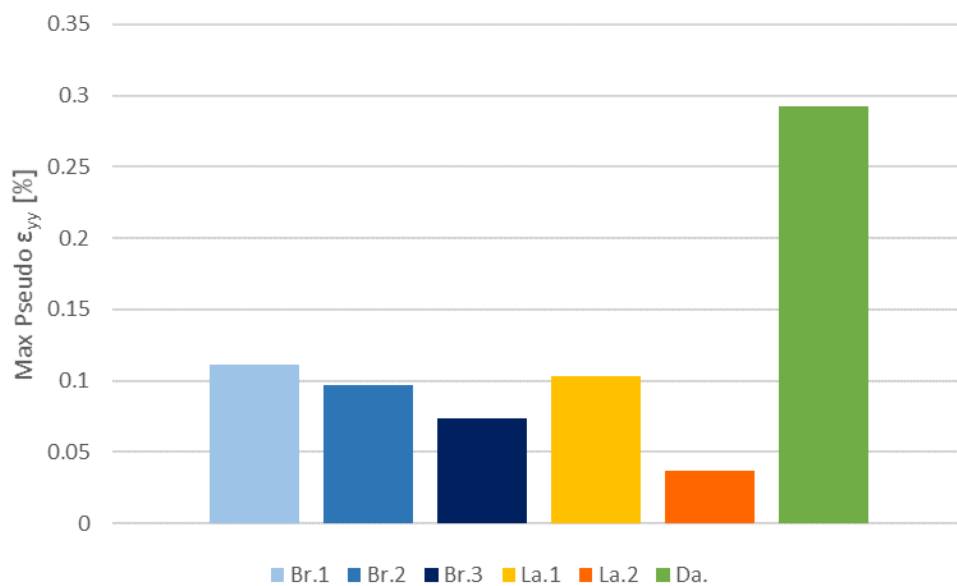


Figure 6.34. Maximum pseudo ϵ_{yy} [%] across the damaged areas of sample Br.2, Br.3, La.1, La.2, Da.

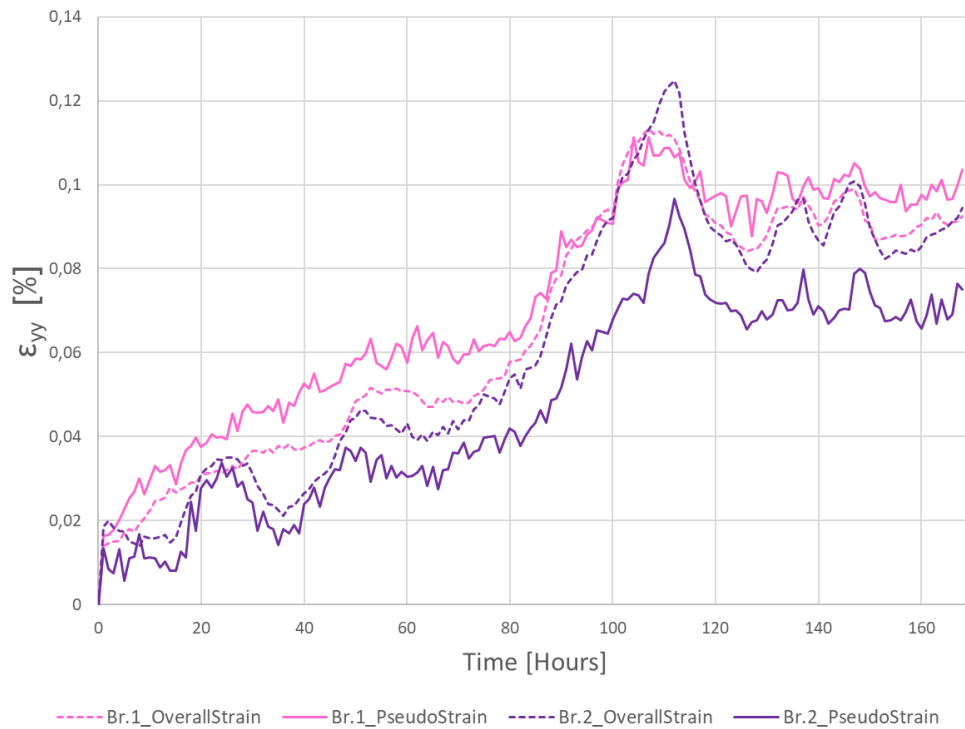


Figure 6.35. Mean and pseudo ε_{yy} [%] of sample Br.1 (15-mm spacing) and Br.2 (8-mm spacing) during the 168 hours of monitoring.

6.2.1.7 Summary and discussion

From the tests described in Section 6.2.1 on wool rep mock-ups the following general observations on the efficacy of different stitching and support techniques for tapestries can be drawn:

- Strain across weak areas (i.e. bare warps), possibly linked to a time-dependent creep behaviour, can be successfully reduced by both support treatments alone (full and patch), and, even more greatly, when in combination with couching techniques (brick and laid). Results showed that the extension across fully conserved areas was similar to that across the undamaged fabric, indicating a successful regain in strength.
- Full support treatments proved to be more effective than patches, when damage across the textiles was extensive. On the other hand, when the two types of treatment were applied on the back of more sound specimens (thus the patches were directly behind the few weak areas), both support methods were shown to be equally useful in preventing damage propagation, at least at the tested loads.

- Grid lines used for full supports contributed to reducing strain across weak areas when they overlapped them. On the other hand, when the lines were farther away from the mechanical defects (20 mm), their presence did not seem to contribute to the strain reduction.
- No statistically significant difference between brick and laid couching was noted. In general, structural weaknesses conserved with laid couching appeared to be better supported than those treated with brick couching, however the strain difference was within or close to the error range. Therefore, even if laid couching might have been more effective than brick couching, the dissimilarity was too subtle to be consistently revealed through 2D DIC.
- Indicatively, the impact of spacing on the efficacy of brick and laid couching was noted: the smaller the distance between the stitches, the lower the local pseudo strain.

It should be noted that these general conclusions were drawn by looking at each test individually, as the quantitative data were greatly affected by the environmental conditions and this prevented a proper overall comparison, from a quantitative perspective.

The findings are in good agreement with the previous research by Asai et al. on the evaluation of support techniques, stabilising lines and couching on unaged tapestry-like samples by using tensile testing [5]. In particular, Asai et al. also reported that the physical strength of weak areas can be completely restored when using couching and support treatments, especially when these are combined. In addition, the research team also proved the usefulness of stabilising (grid) lines, in particular when they are close to the damage [5]. Regarding the similar positive impact of brick and laid couching, this was also observed by Nilsson, although her work focused on artificially aged silk samples [12]. The agreement with previous studies is particularly significant since, in this project, 2D DIC was used for the first time as a tool for evaluating conservation treatments, therefore the reliability of the results could not be ensured *a priori*.

On the other hand, some differences can be noted when comparing the data with those reported by Catic's work [2], partly conducted within the context of the current project. Catic followed the same methodology here presented (i.e. same materials, same type of damage, same stitching techniques and similar DIC set-up), however the treatments, especially the brick couching, were reported to be less effective in minimising elongation. This can be due to the conservators who treated the mock-ups: while Prof Lennard conserved the specimens for this study, CTC students carried out those in Catic's research. It is likely, as the support stitching is carried out by hand, that there will be variations from one individual to another, reflecting differences in training, experience and technique. In addition, it should be noted that the DIC analysis in Catic's work presented some issues that might have affected some of the outcomes (e.g. use of two different cameras with different settings) [2].

6.2.2 2D DIC monitoring of a historic tapestry fragment after conservation

2D DIC was employed to monitor strain across TapestryFragment_1, already studied in Chapter 4 before conservation. This test aimed to investigate the effects of conservation strategies when applied on actual tapestries, affected by more extensive and complex damage processes than the wool rep mock-ups in Section 6.2.1. The fragment was treated twice: first, it was conserved by applying some local linen patches with brick couching at different spacing; later, a full linen support was stitched on the back through grid and scrim lines. The two monitoring tests were carried out at the end of each treatment and they both lasted 200 hours.

The strain map of the fragment at the end of the first treatment is presented in Figure 6.36. The conserved areas are highlighted in yellow, while the pre-existing open slits left untreated are marked by the blue dotted line. Slit 5 is not indicated since it underwent some uncontrolled structural modifications between the different tests, impeding a correct comparison before and after treatment. Already from the strain map, the impact of the linen patches and brick couching in diminishing damage propagation can be observed. Indeed, the conserved areas show lower local pseudo strain than the untreated ones.

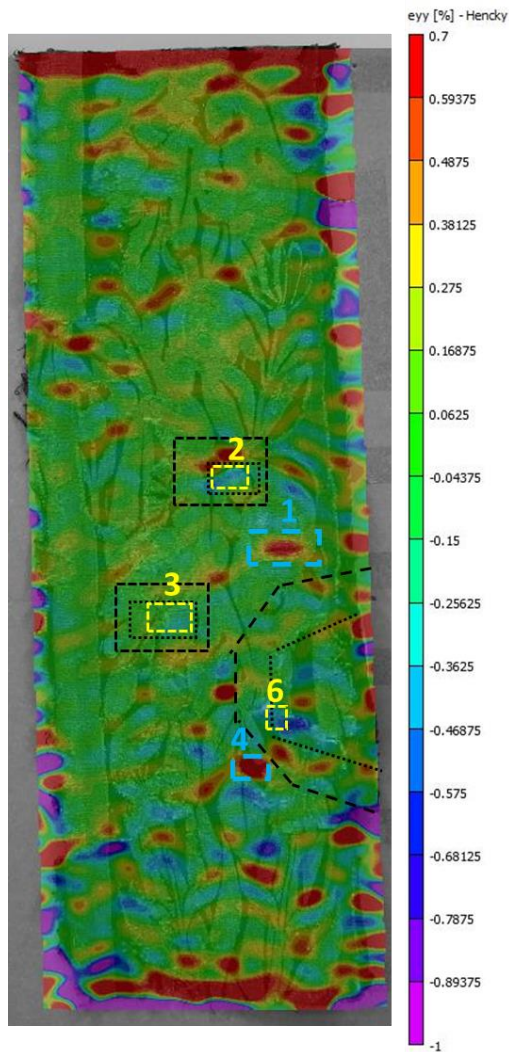


Figure 6.36. Strain map, ε_{yy} [%], of TapestryFragment_1 at the end of the 200-hour monitoring after the first conservation treatment (application of patches through couching). The conserved areas are highlighted in yellow, while those left untreated in blue. The location of the patches is indicated by the thick black dotted line, while that of brick couching by the fine black dotted line.

The local strain data from the areas of interest (treated and untreated), presented in Figure 6.37, confirm the effect of the patches and couching: Slit1 and Slit4 enlarged significantly more than the conserved slits. In general, it is observed that the pseudo strain across the treated areas was similar, or even lower, than globally averaged strain, plotted in Figure 6.38. On the other hand, pseudo strain across non-conserved areas, Slit1 and Slit4, was remarkably greater than mean ε_{yy} . Namely, while overall strain reached a maximum of 0.05% (at 52.5% RH), pseudo strain across Slit1 and Slit4 was 0.21% and 0.29%, respectively. This means that a creep-like behaviour determined the widening of the two untreated slits, that extended up to six times the increase in length registered for the overall tapestry.

When comparing the data calculated across stitched Slit2 (3-mm spacing), Slit6 (3-mm spacing) and Slit3 (6-mm spacing), it is noted that Slit2 showed the highest extension. The fact that the area treated with brick couching at 3-mm spacing (Slit2) extended more than that at 6-mm spacing (Slit3) is counterintuitive, also considering the outcomes reported in Section 6.2.1. However, it is worth noting that above Slit2 an area of high pseudo strain was registered (Figure 6.36), not observed before conservation (Chapter 4, Section 4.3.2.1). Although further investigation is needed to clarify this point and to exclude the occurrence of local strain miscalculation, it could be thought that Slit2 was negatively affected by the damage propagation occurring in the neighbouring area.

It is underlined that Slit6 only indicates the open slit affected by the application of the patch (same area monitored before conservation, Chapter 4), while Patch_Slit6 refers to the entire part of the tapestry covered by the patch. It is highlighted that pseudo ϵ_{yy} in the two areas is different (Figure 6.37). Perhaps, the stitching across the small area of Slit6 determined some tension, excessively impeding the textile to move. In general, it is important to point out that local strain data may be less accurate from a quantitative perspective than globally averaged ones. This is particularly true when monitoring historic textiles (no speckle pattern). Therefore, errors in displacement calculation may prevent a proper (quantitative) reading of the local data.

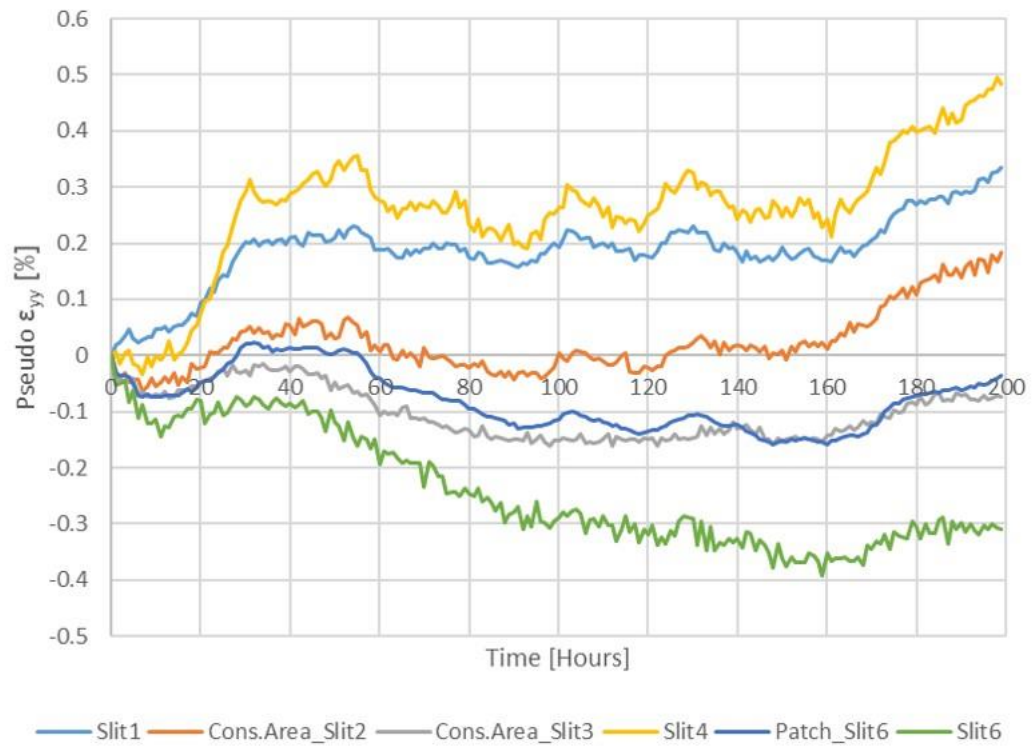


Figure 6.37. Pseudo ε_{yy} [%] across damaged areas of TapestryFragment_1 during the 200-hour monitoring after the first conservation treatment (application of patches though couching).

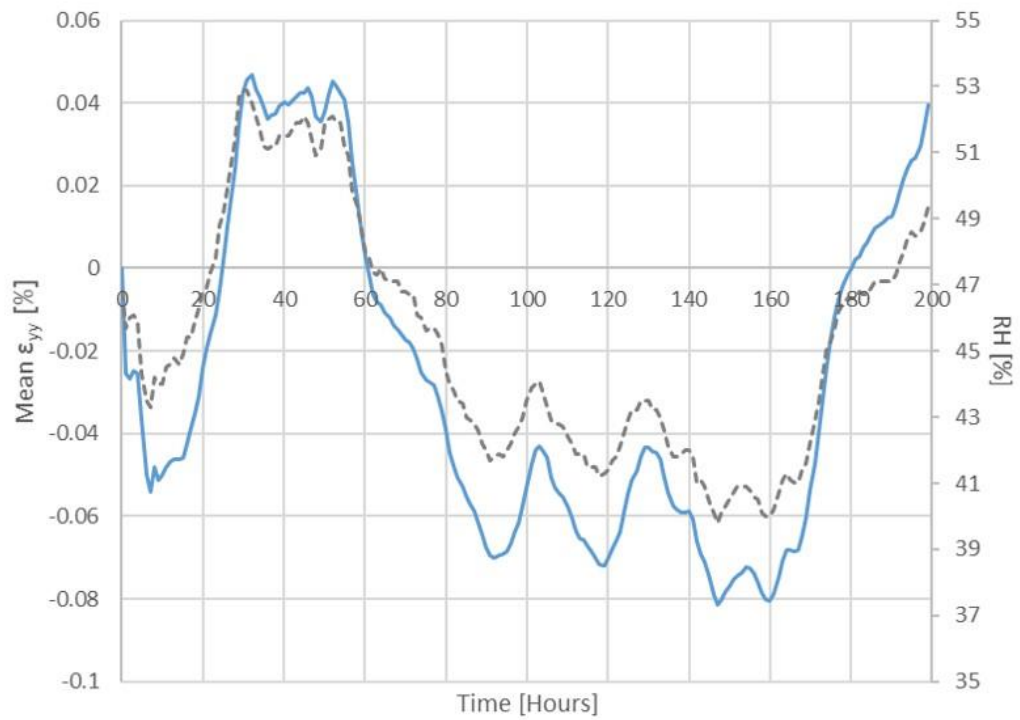


Figure 6.38. Mean ε_{yy} [%] during the 200-hour monitoring TapestryFragment_1 after the first conservation treatment. RH [%] is indicated by the dotted line.

Importantly, the second treatment, which affected the entire back of the fragment, resulted in limiting the extension across Slit1 and Slit4, not treated with patches and couching in the first phase of conservation. This can be observed from the strain map at the end of the monitoring, illustrated in Figure 6.39: local pseudo strain across all the slits is less evident.

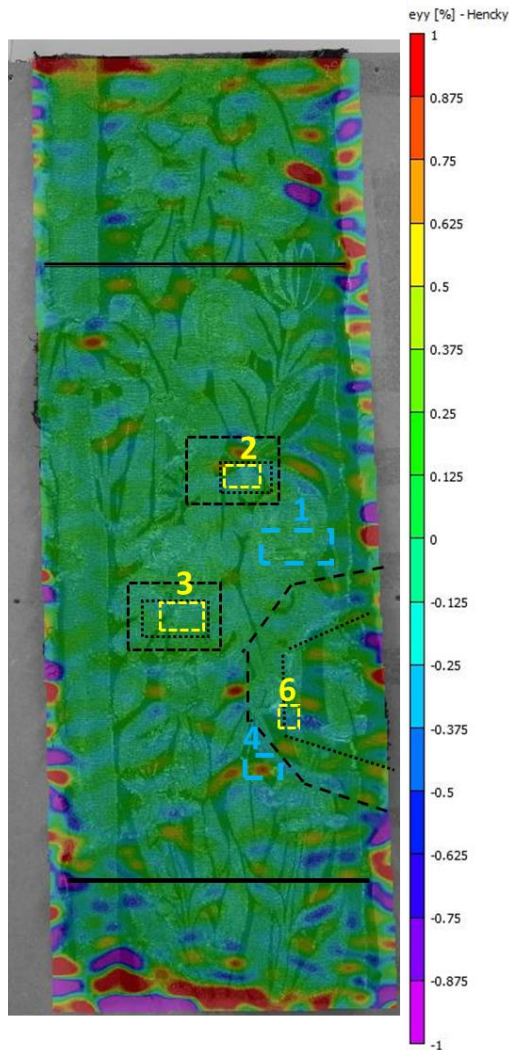


Figure 6.39. Strain map ϵ_{yy} [%] of TapestryFragment_1 at the end of the 200-hour monitoring of TapestryFragment_1 after the second conservation treatment (application of full support). The area treated with full support is indicated by the horizontal black lines.

The efficacy of the full support in containing the widening of the open slits is also revealed by the pseudo strain data, shown in Figure 6.40. Indeed, pseudo strain across Slit1 was shown to be efficiently contained thanks to the application of the full linen support on the back. Interestingly, pseudo ϵ_{yy} registered across Slit1 was around the same as that across Slit2, Slit3, and Slit6, already conserved with patches. When considering Slit4, this was shown to widen

the most. Although it can be said that the treatment was not completely effective in preventing the occurrence of creep, from comparison between data in Figure 6.37 and Figure 6.40 it is delineated that the application of the support partly contained the damage mechanism. These observations on the usefulness of support techniques agree with what was indicated by the DIC strain monitoring of wool rep mock-ups: patch support may effectively prevent damage propagation, but when weaknesses are widespread, full support can represent a better option.

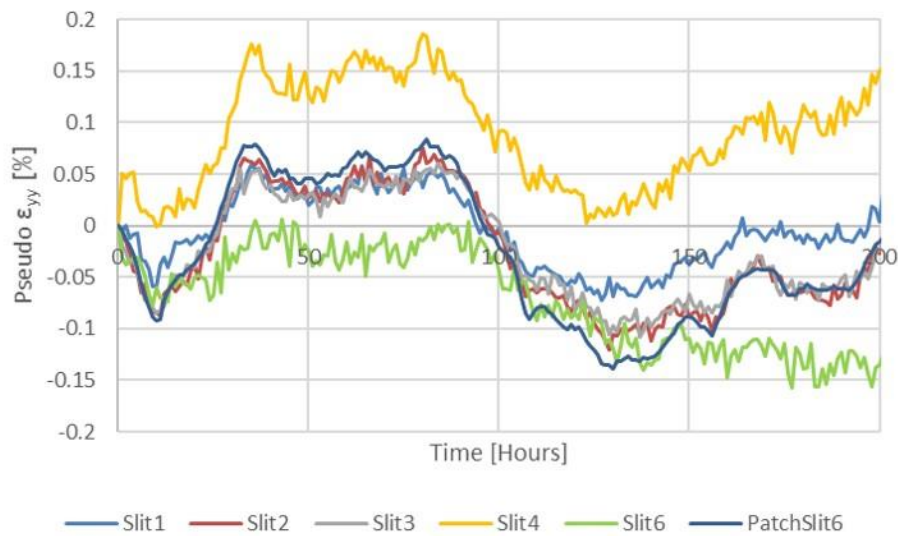


Figure 6.40. Pseudo ϵ_{yy} [%] across damaged areas of TapestryFragment_1 during the 200 hours of monitoring after the first conservation treatment (application of full support).

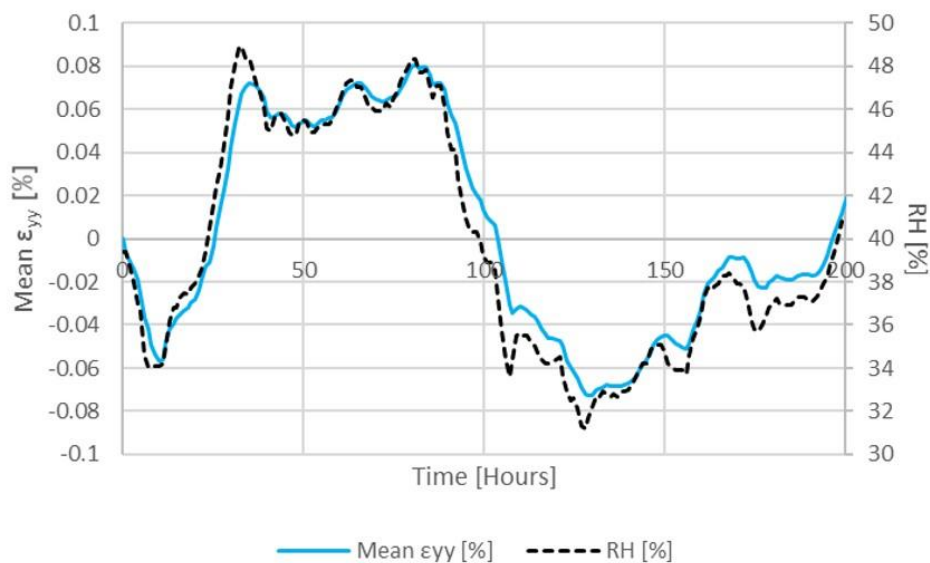


Figure 6.41. Mean ϵ_{yy} [%] during the 200-hour monitoring TapestryFragment_1 after the second conservation treatment. RH [%] is indicated by the dotted line.

6.2.3 Uniaxial tensile testing: fabrics for support treatments

6.2.3.1 Linen fabrics

Uniaxial tensile testing was carried out on two different linen fabrics currently used by textile conservators in the UK for full and patch support treatments on tapestries. Linen B (by Claessens), which has a higher thread count than Linen A (by Whaleys) and was employed to conserve the samples monitored in the previous sections, was tested before and after the pre-treatment. The pre-treatment consisted of washing the fabric at 90 °C in a machine. The objectives of the experiment were to better define physical properties, namely ultimate tensile strength and Young's modulus, of these conservation materials and eventually relate the results with those from the mechanical characterisation of historic fragments reported in Chapter 3.

Typical stress-strain curves of the two washed linen fabrics are shown in Figure 6.42 (weft direction) and Figure 6.43 (warp direction). Similarly, representative curves of unwashed Linen B are illustrated in Figure 6.44 (weft direction) and Figure 6.45 (warp direction). All the graphs describe a similar mechanical behaviour: the occurrence of slack and de-crimping regions, followed by a linear section indicating the elastic behaviour (from which the Young's modulus was calculated), eventually interrupted by the failure of the specimen.

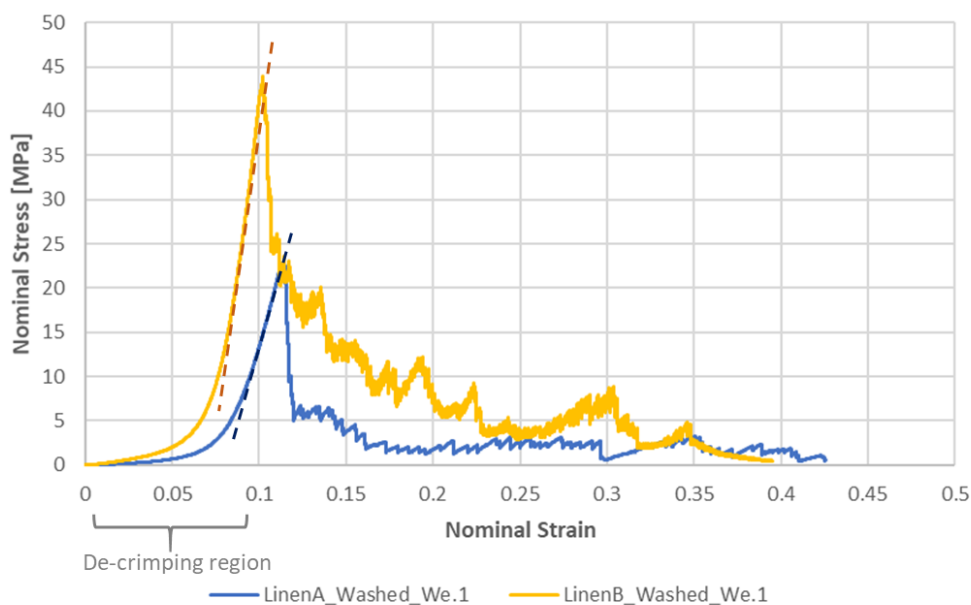


Figure 6.42. Stress-strain curves of specimens from washed Linen A (blue line) and washed Linen B (yellow line) tested in the weft direction.

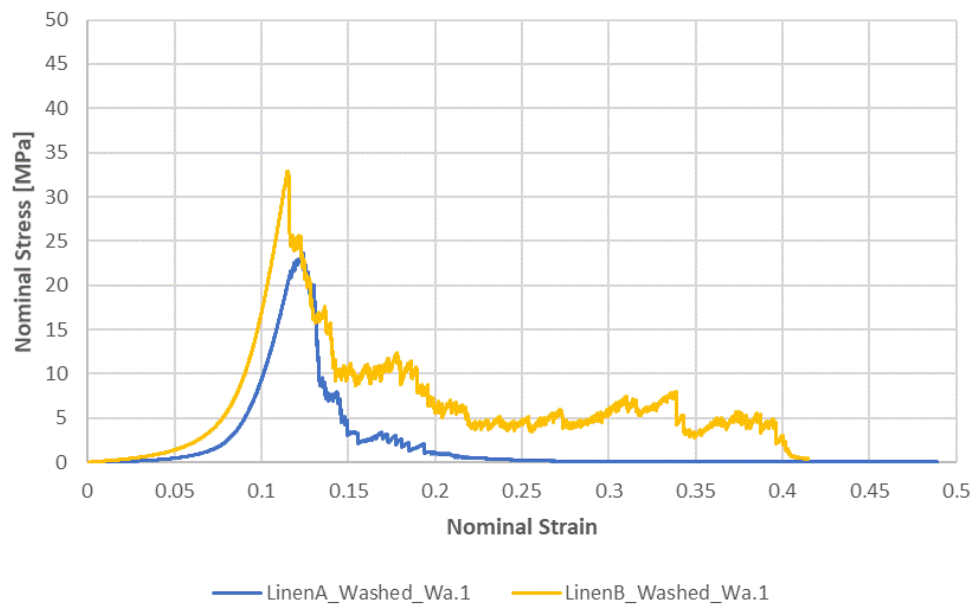


Figure 6.43. Stress-strain curves of specimens from washed Linen A (blue line) and washed Linen B (yellow line) tested in the warp direction.

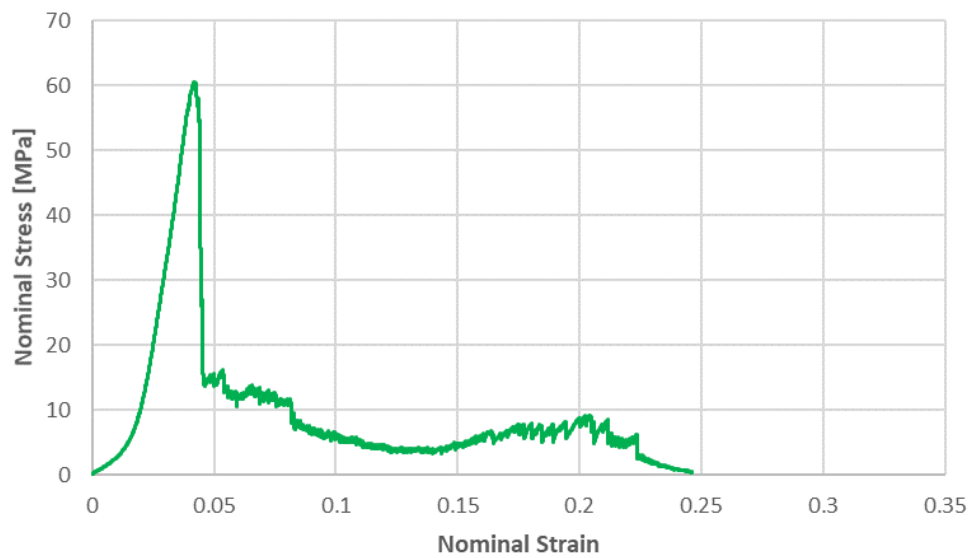


Figure 6.44. Stress-strain curve of specimen from unwashed Linen B in the weft direction.

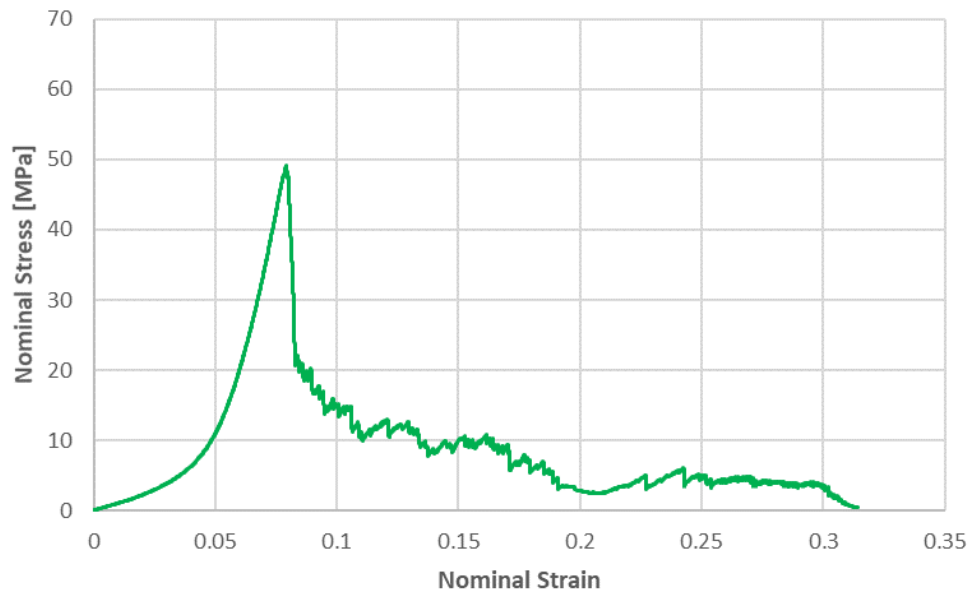


Figure 6.45. Stress-strain curve of specimen from unwashed Linen B in the warp direction.

Table 6.9 summarised the tensile properties of the two linen fabrics investigated. From the data reported, it can be pointed out that the slack and crimp-removal regions ended at a nominal strain between 0.02 and 0.09. The unwashed Linen B showed the lowest extension before the occurrence of the Hookean region; on the opposite, washed Linen A and B presented similar strain at the end of the crimp (in both cases, higher in the warp direction).

Table 6.9. Uniaxial tensile properties of the two linen fabrics (the SD is also indicated, average of five measurements per direction).

Fabric / Direction / Pre-treatment	Strain at the End of the Crimp	Young's Modulus [MPa]	Stress at Failure [MPa]	Strain at Failure
Linen A / Warp / Washed	0.090 ± 0.002	581.51 ± 30.04	24.42 ± 0.81	0.012 ± 0.003
Linen A / Weft / Washed	0.074 ± 0.005	570.43 ± 15.55	21.55 ± 0.95	0.010 ± 0.009
Linen B / Warp / Unwashed	0.058 ± 0.002	1470.0 ± 137.46	47.37 ± 5.13	0.080 ± 0.001
Linen B / Weft / Unwashed	0.021 ± 0.002	2460.40 ± 40.97	58.98 ± 1.83	0.041 ± 0.002
Linen B / Warp / Washed	0.087 ± 0.010	1164.6 ± 164.25	37.31 ± 5.05	0.105 ± 0.012
Linen B / Weft / Washed	0.071 ± 0.009	1523.8 ± 203.68	43.93 ± 6.60	0.090 ± 0.008

When comparing the two washed fabrics, Linen B presented a greater Young's modulus than Linen A, in both warp and weft direction, as indicated by data in Table 6.9 and in Figure 6.46. It can be noted that the modulus of Linen B in the warp direction was lower (1164.60 MPa) than that in the weft direction (1523.80 MPa). On the other hand, Linen A seemed to show a more isotropic behaviour, as the modulus in both directions was around 575 MPa. Differences in stiffness between warp and weft of linen fabrics have been reported by other studies investigating similar materials used in painting conservation [13-15]. The studies indicate that usually the weft direction is stiffer than the warp, and this can be due to the manufacturing process [13]. It is important to underline that in tapestry conservation the linen would be used so that the warp direction hangs vertically and takes the weight of the object.

Considering the effects of the pre-treatment, the data in Figure 6.46 state that the washing of Linen B caused a decrease in the modulus.

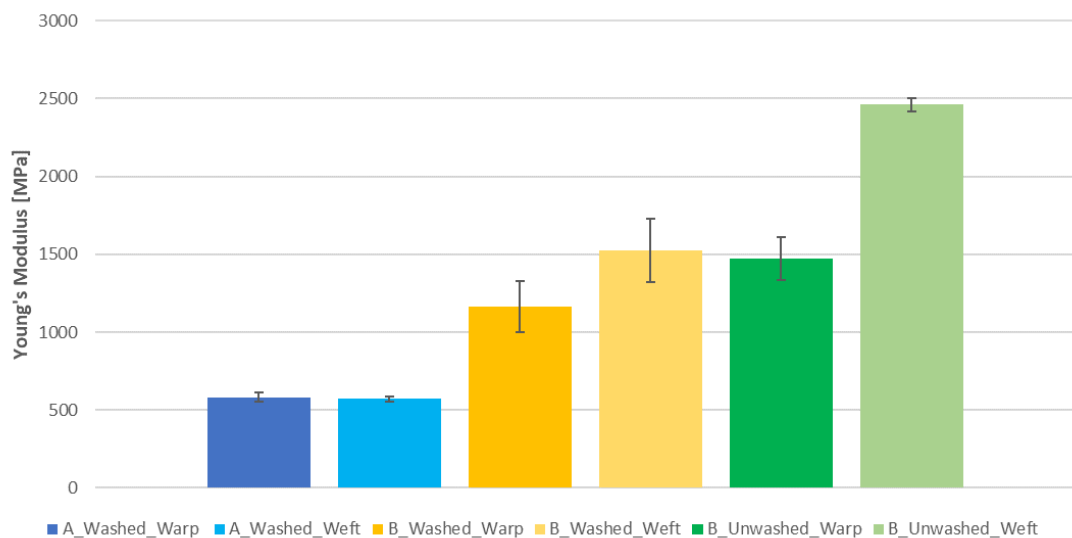


Figure 6.46. Young's modulus of the washed Linen A, washed Linen B, unwashed Linen B.

Besides showing a greater “stiffness”, washed Linen B had a higher breaking stress, and thus tensile strength, than washed Linen A (Figure 6.47). This is true for both the warp and weft direction. Probably, the higher thread count of Linen B may have contributed to this.

As observed for the Young's modulus, the tensile strength of washed Linen B was lower than the unwashed fabric.

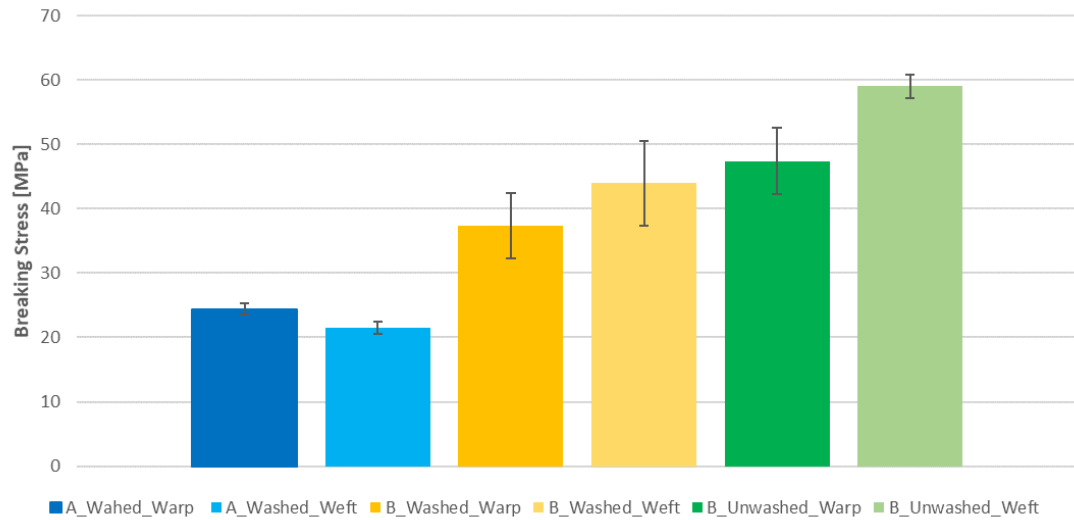


Figure 6.47. Breaking stress of washed Linen A, washed Linen B, unwashed Linen B.

Strain at failure of the two washed linen fabrics (Figure 6.48) ranged between 0.009 and 0.012. In both cases, specimens tested in the warp direction elongated more than those in the weft direction.

It is observed that the pre-treatment of Linen B caused an increase in the elongation at break, especially in the weft direction as a growth of almost 50% was registered. This indicates that the washed linen fabric is likely more elastic than the same unwashed textile. Similarly, also strain at the end of the crimp raised after the washing of Linen B (Table 6.9). This is in agreement with previous studies, as further discussed in Section 6.2.3.3 [8].

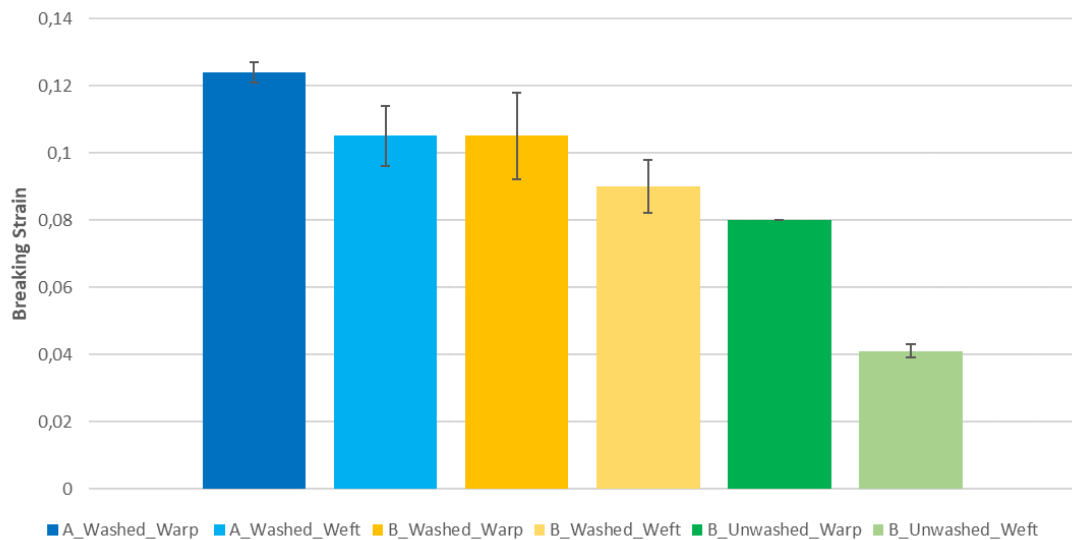


Figure 6.48. Breaking strain of washed Linen A, washed Linen B, unwashed Linen B.

6.2.3.2 Polyester Stabiltex™

In addition to the two linen fabrics, polyester Stabiltex™ was uniaxially tensile tested. Synthetic materials as polyester and polypropylene fabrics have also been (rarely) reported as an option for supporting tapestries [8, 10, 11].

Typical stress-strain curves in both warp and weft direction of polyester Stabiltex™ are illustrated in Figure 6.49. It is evident that the mechanical response of the synthetic fibre is remarkably different from that of linen, as the curve presents two distinctive regions before the failure. The first part of the graphs represents the elastic (Hookean) region, where the elongation is directly proportional to the stress and from which the Young's modulus was calculated. However, the elastic behaviour of the fabric is interrupted from the yield point on, that indeed marks the start of plastic deformations. Before failure takes place, the non-elastic region presents an inflection, particularly evident in the weft-direction curve of Figure 6.49. This is due to the re-arrangement of the molecular structure of the material, that eventually grows in resistance. In the region before the inflection, amorphous tie chains, characteristic of polyester materials, stretch (strain softening). After this, the chains are taut and started to be deformed (strain hardening) [16, 17].

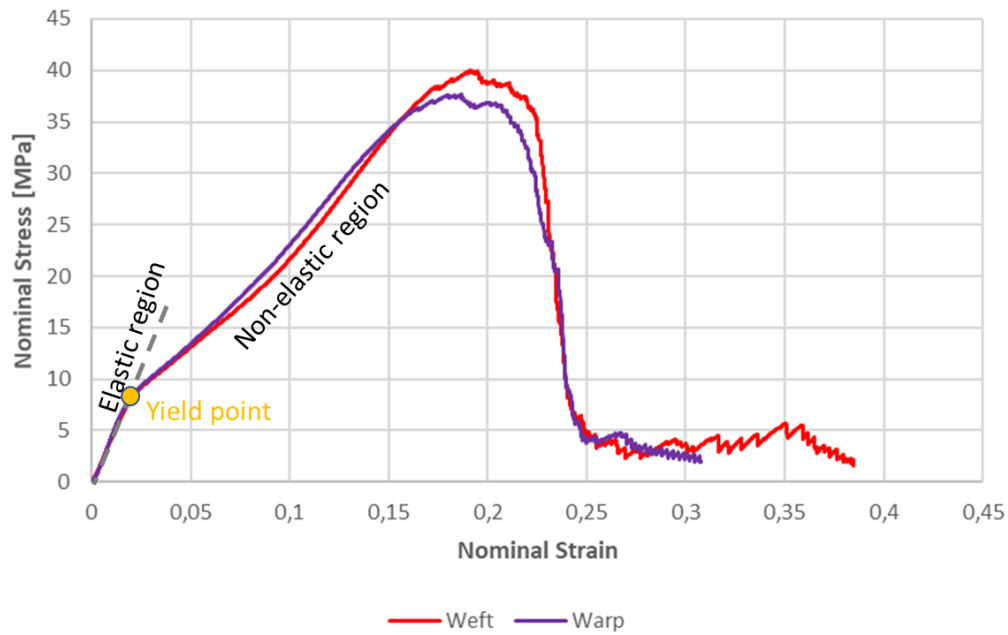


Figure 6.49. Stress-strain curves of polyester Stabiltex™ in the weft and warp direction.

The data from the uniaxial tensile testing of the polyester fabric are reported in Table 6.10. The properties do not vary remarkably from the warp to the weft direction. In both directions, the yield point occurred at a nominal strain of between 0.018-0.019, and specimens failed between 0.16-0.18 strain. The Young's modulus is around 416 MPa in the weft direction, and 470 MPa in the warp direction. This indicates a lower “stiffness” than that of the linen fabrics tested in the previous section, especially of Linen B. On the other hand, the stress at failure of the synthetic textile (37-39 MPa) describes a strength similar to washed Linen B, and even greater than that of washed Linen A.

Table 6.10. Uniaxial tensile properties of the polyester Stabiltex™ (the SD is also indicated, average of five measurements per direction).

Direction	Strain at the Yield Point	Young's Modulus [MPa]	Stress at Failure [MPa]	Strain at Failure
Weft	0.019 ± 0.001	416.11 ± 17.29	39.58 ± 0.74	0.18 ± 0.004
Warp	0.018 ± 0.001	470.39 ± 34.81	37.26 ± 1.94	0.16 ± 0.013

6.2.3.3 Discussion: comparison between the tensile properties of fabrics for support treatments and historic tapestries

The data presented in the previous section are now compared with those obtained from the uniaxial tensile testing of historic tapestry fragments

presented in Paragraph 3.2.1.1. The observations from the comparison are then discussed considering previous studies on the evaluation, from a mechanical perspective, of support treatments in conservation.

As expected, the overall shape of the stress-strain curves of linen and tapestry samples were significantly different. In general, the two linen fabrics were considerably less flexible than the historic hangings, as they showed a Young's modulus even one hundred times higher than that of tapestries. At the same time, Linen A and Linen B presented a greater tensile strength than the tapestry specimens, especially when the latter had a low thread count and were in evident poor condition. Similar considerations could be made for Stabiltex™ as, also in the case of the synthetic fabric, the material was shown to be greatly stiffer and stronger than the actual tapestry specimens. Overall, the polyester textile proved to differ from the linen samples in the general mechanical behaviour because of the presence of a non-elastic region after the yield point and the consequently much greater strain at failure. It should be noted that all these observations are not only valid for the comparison between support fabrics and historic tapestries, but also between the conservation materials and wool rep. Indeed, linen and polyester fabrics are also stronger and stiffer than the newly woven tapestry-like material (especially in the weft hanging direction).

Both the lower flexibility (up to a certain extent) and higher tensile strength of conservation materials are desirable qualities, as they would increase the ability to, fully or partially, support weak areas in historic textiles. Indeed, the same parameters are considered when evaluating linings for paintings, e.g. [18]. However, in painting conservation, the mechanical behaviour is even more complex due to the wider range of constituent materials, related physical behaviour, pre-treatment of the lining (i.e. stretching), and application system (i.e. type of adhesive) [13-15, 18, 19]. For instance, Young et. al in [19] state that the stiffness of the lining fabrics drops once they are stretched for the application, and this may negatively affect the efficacy of the support. Indeed, loads are proportionately distributed between lining and painting according to their stiffness, at least when they are strictly bonded and the adhesive has a contained shear movement: the most flexible will take the lowest amount of load [19]. In the case of tapestries, stretching and adhesive type are not

relevant variables, as the fabric is directly stitched to the back of the artwork. Another mechanical property critical for paintings but less for tapestries conservation is isotropy: paintings (on canvas) are tensioned biaxially as they are prepared and displayed on a stretcher, so the lining treatment aims to support evenly both vertical and horizontal direction. On the other hand, support treatments for tapestries aim to prevent damage caused by the self-weight loading acting in the weft vertical direction. Because of this, in the current study textile specimens were uniaxially, and not biaxially, tensile tested.

The results in Section 6.2.3.1 highlighted that the tensile properties of linen are affected by the preparation of the fabric. Before the current study, Hofenk de Graaff et al. also studied the effects of pre-treatment (i.e. washing and drying) and environmental factors (i.e. heat and humidity) on the tensile strength and breaking elongation of linen and cotton fabrics used for supporting tapestries [9]. The data showed that the pre-treatment can weaken the fabrics (especially linen) and that the impact of ageing conditions was similar on both type of cellulosic material. In addition, the research group investigated the dimensional changes of linen and cotton, and two woollen tapestry fragments, due to fluctuations in relative humidity and temperature (measured through a thermo-hygrograph). Although the outcomes stated that treated fabrics and the tapestries behaved similarly, the tests were not considered fully representative. Factors like the lack of replicas, the testing methods (e.g. the modified thermo-hygrograph), as well as the lack of some results (e.g. no indications on stiffness), partly affected the accuracy of the study, as already mentioned by the authors. Overall the research concluded that it is difficult to indicate which fabric, linen and cotton, should be employed, as the tensile properties greatly depend on variables like density [9].

When comparing the synthetic and the natural fabrics tested in section 6.2.2, it should be pointed out that Stabiltex™ was introduced for textile conservation treatments not only for its strength, but also for its durability and contained moisture regain [20, 21]. However, in the conservation field, the polyester fabric has been usually employed for supporting fragile textiles in combination with adhesive [21-23]. Since neither durability nor moisture regain were evaluated in this study, they cannot be here considered. Nevertheless, it is relevant to note

that the use of synthetic fabrics (both polyester and polypropylene) as support for historic hangings is very limited [8, 10, 11]. In the most recent questionnaire no respondent claimed to employ other materials than linen (the preferred one) and cotton [2]. Overall, the experiments reported in this chapter are not able to surely state whether Stabiltex™ is a better or worse option than linen for supporting tapestries. Nevertheless, the uniaxial tensile testing of the conservation material and historic hangings can be used as a starting point for further research.

In general, as stated by Young, characterising the mechanical behaviour of conservation materials used for structural treatments is a crucial but initial step of a longer evaluation process [13]. Indeed, when all the materials tested show desirable qualities, as in this case, to decide which one will give the best long-term results in the continuous interaction with the artwork is particularly complex. This is especially true in the context of the current research, as textile conservators still do not agree on the reasons behind treatments' choice (e.g. should the support fabric *restrict* or *allow* fatigue? [10]), impeding our ability clearly establish what is indeed desirable in the long term.

6.2.4 Uniaxial tensile testing: newly woven conserved samples

Conserved specimens were uniaxially tensile tested to compare the mechanical strength. Through this, the observations drawn from the DIC strain monitoring of the same samples reported in Paragraph 6.2.1 were further verified.

The graph in Figure 6.50 illustrates the stress-strain curves of specimens Al_B2 and C_B1, both conserved with brick couching and full support. Figure 6.51 shows the trend of specimens Al_L1 and C_L1, also with a linen support on the entire back but then treated with laid couching. Although the specimens presented a complex structure and different materials, namely the wool rep, the linen and threads for the stitching, the curves mainly resembled those from the characterisation of the support fabric (Figure 6.43). This suggests that the mechanical response was greatly determined by the linen on the back.

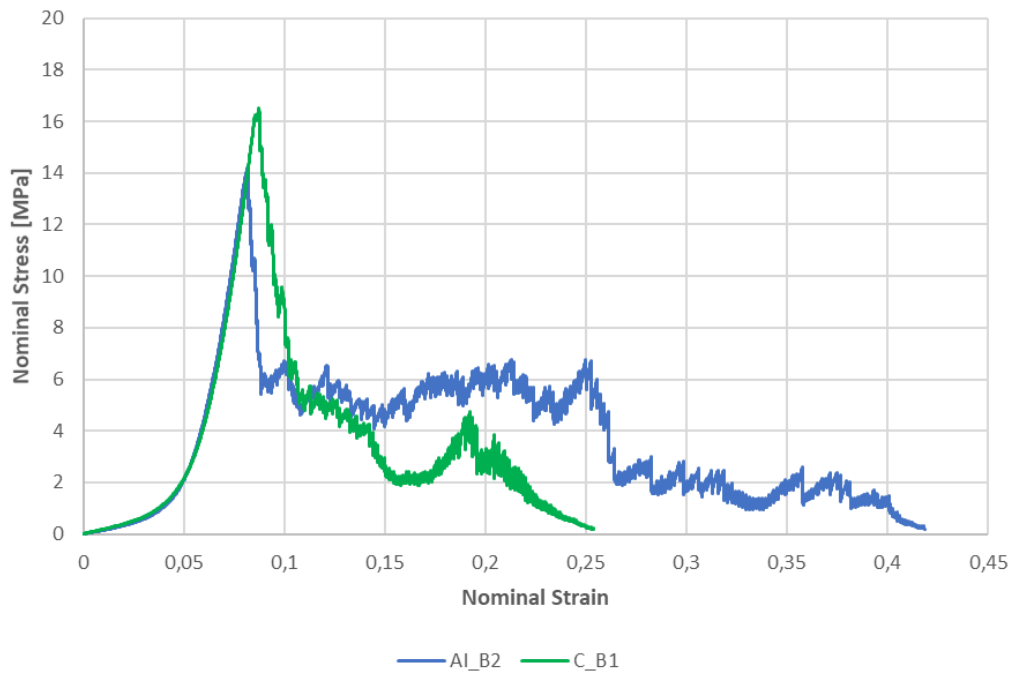


Figure 6.50. Stress-strain curve of specimen AI_B2 (full support, grid lines far from areas of damage, 4-mm brick coupling) and C_B1 (full support, no grid lines, 4-mm brick coupling).

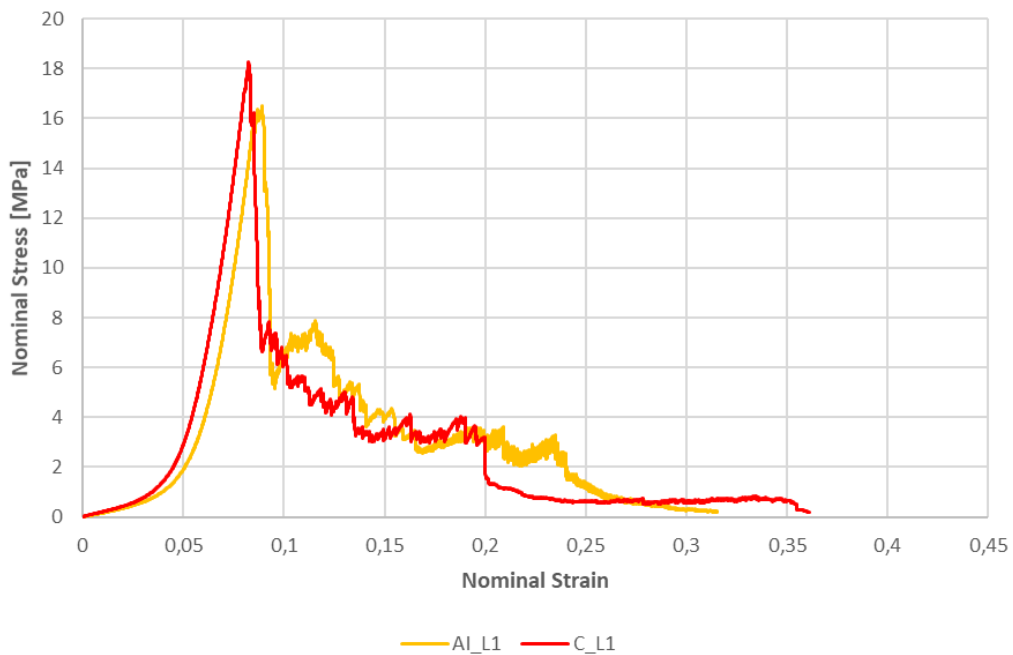


Figure 6.51. Stress-strain curve of specimen AI_L1 (full support, grid lines far from areas of damage, 4-mm laid coupling) and C_L1 (full support, no grid lines, 4-mm laid coupling).

Typical failure mechanism of specimens with full support and coupling across the area with bare warps is represented in Figure 6.52: the wool rep fabric and

the stitches were torn apart at lower loads than the linen fabric, that was indeed the last material to break down.

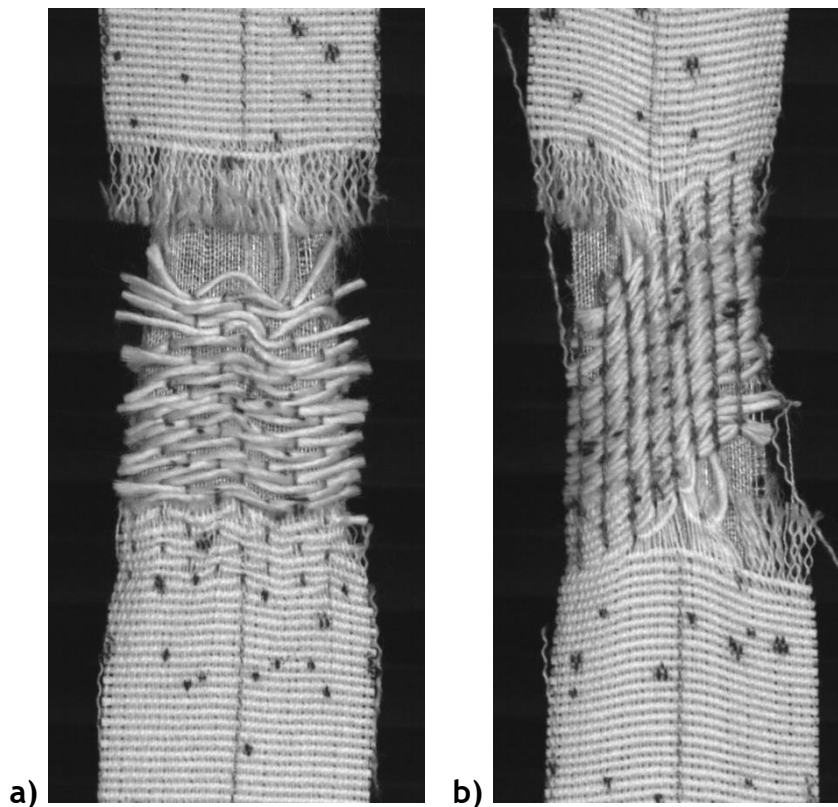


Figure 6.52. Specimen AI_B2 (a) and C_L1 (b) during the uniaxial tensile testing.

The dominating impact of linen fabric in defining the tensile properties of the fully supported specimens can be also assessed by considering the stress-strain curves of the samples with patches on the back of the damaged areas (Figure 6.53 and Figure 6.54). The graphs, representing patch support in combination with brick (Figure 6.53) and laid couching (Figure 6.54), show that the specimens with only local treatments failed at much lower stress and had lower moduli than those with the linen fabric on the entire back (Figure 6.50 and Figure 6.51). From the same graphs, the impact of the spacing can also be observed: the larger the space between stitches, the weaker the specimens.

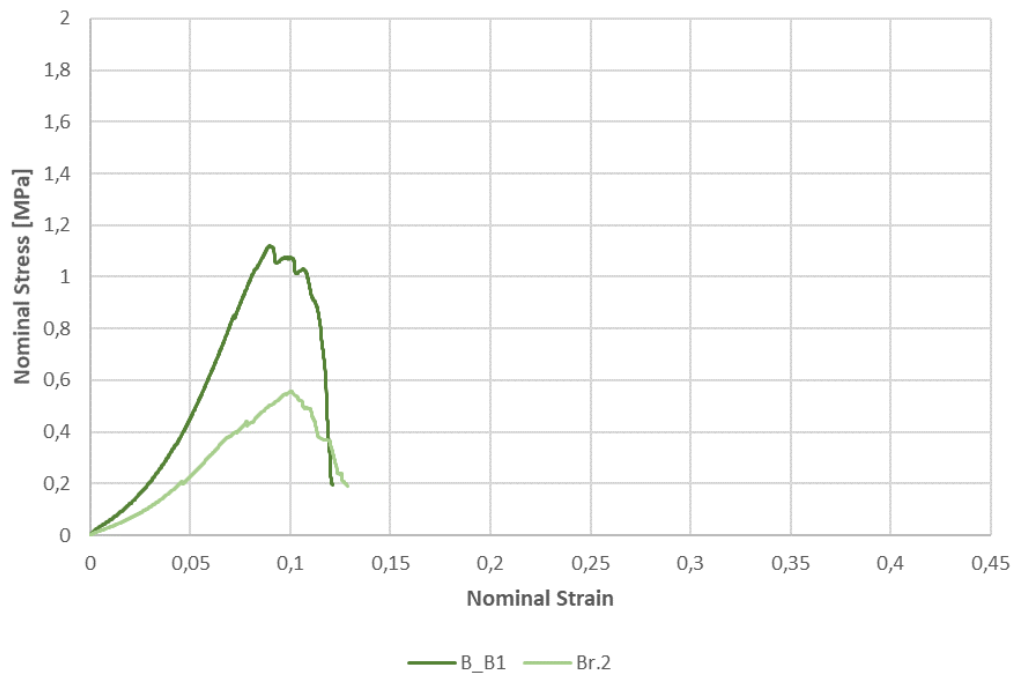


Figure 6.53. Stress-strain curves of specimen B_B1 (patch support, 4-mm brick couching), Br.2 (patch support, 8-mm brick couching).

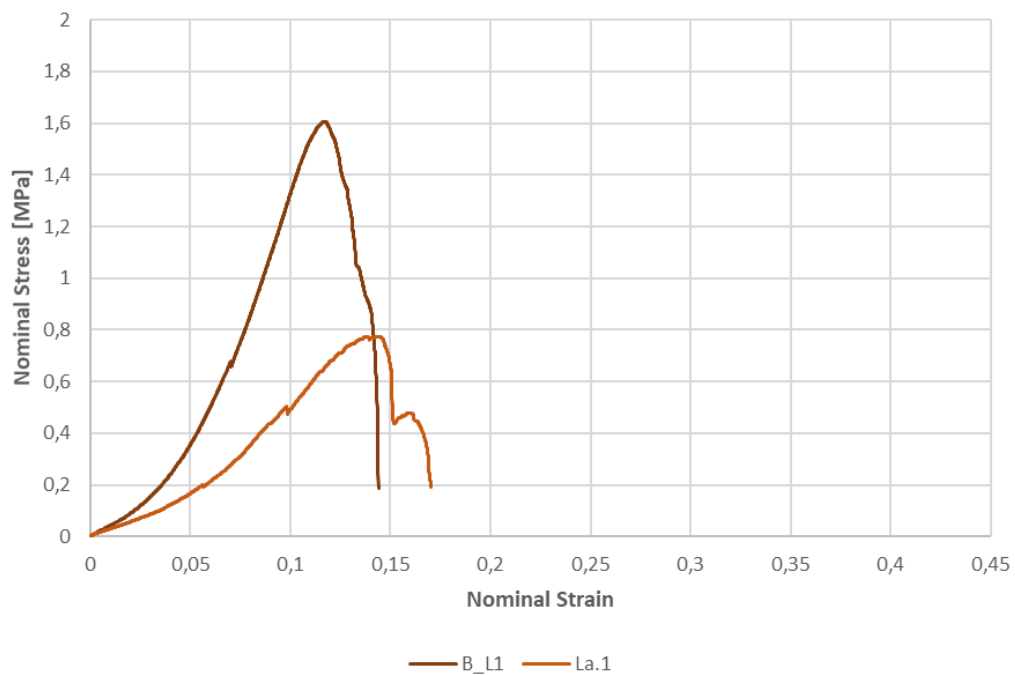


Figure 6.54. Stress-strain curves of specimen B_L1 (patch support, 4-mm laid couching), La.1 (patch support, 15-mm laid couching).

The data on the tensile properties of the tested specimens are reported in Table 6.11. By comparing the mechanical properties of specimens with the same couching treatments but with different support methods, full (from samples Al and C) and patch (from samples B, Br., La.), the difference is significant, as

already anticipated by the analysis of the stress-strain curves. Specimens with the linen fabric on the entire back were remarkably stronger and with a higher Young's modulus than those with the linen textile only covering the damaged area. Perhaps the 2D DIC strain monitoring tests in section 6.2.1 were unable to pinpoint differences in stain reduction between patch and full support as the samples were exposed to lower loads and the sound part was big enough to minimise the impact of the treatments.

When considering the effects of the two couching techniques from the data in Table 6.11, it can be stated that the specimens treated with laid couching were stronger and had higher moduli than those with brick couching. This confirms the preliminary observations drawn from the 2D DIC monitoring tests reported in Section 6.2.1 on the greater ability of laid couching in carrying the load from weak areas. In addition, as already observed from the analysis of stress-strain curves and the DIC monitoring, it is verified that the spacing of the couching affected strength and modulus of specimens. Interestingly, when considering samples with patches, there is not a significant difference between 4-mm laid couching (B_L1) and 8-mm laid couching (La.2). On the contrary, in the case of the brick couching, the specimen with the 8-mm spacing (Br.2) was significantly weaker than those with the 4-mm spacing (B_B1, Br.3).

Table 6.11. Uniaxial tensile properties of specimens conserved with different support and stitching techniques.

Sample code	Strain at the end crimp	Young's modulus [MPa]	Stress at failure [MPa]	Strain at failure
AI_B2	0.060	463.05	13.50	0.080
AI_L1	0.065	529.48	15.68	0.085
AI_L2	0.060	539.70	14.26	0.075
B_B1	0.040	17.33	0.99	0.080
B_L1	0.060	21.28	1.44	0.105
C_B1	0.065	513.13	15.98	0.085
C_L1	0.060	542.53	16.81	0.080
Br.2	0.040	6.90	0.50	0.090
Br.3	0.055	20	1.18	0.090
La.1	0.060	7.77	0.68	0.120
La.2	0.065	20.15	1.44	0.110

6.3 Conclusions

In this chapter objective data on the usefulness of couching and support techniques to prevent the propagation of mechanical damage in tapestries were provided. To do so, wool rep mock-ups were artificially damaged and then conserved using different couching techniques (brick and laid) and support methods (full, with different grid lines systems, and patches). To investigate the impact of the different approaches, strain across the samples was monitored through 2D DIC. Then, specimens were cut from the conserved samples and uniaxially tensile tested to study the mechanical behaviour. The tensile properties of fabrics employed for supporting tapestries, i.e. linen and polyester textiles, were also assessed. This aimed to provide a better understanding on how load is successfully transferred from weak areas in tapestries to the conservation material.

By combining the observations from the 2D DIC strain monitoring and the tensile tests, it can be deduced that:

- The support fabric plays a fundamental role in determining the mechanical response of conserved specimens. When a linen full support is applied on woollen tapestry-like textiles, the mechanical behaviour is significantly altered. The strength and stiffness of the supported tapestry may be even greater than those of the unaged material. The impact of patches applied on the back of weak areas, in combination with couching, appears to be more contained, although still successful in preventing damage propagation. This may be true especially at loads experienced in normal conditions and for relatively sound historic hangings.
- Both couching techniques, in combination with support methods, are effective in avoiding the failure of weak areas of weft loss. In general, brick couching seemed to improve less the strength than laid couching, although the difference observed was not significant. On the other hand, the space between the stitches may affect the success of the treatment.

It is important to remember that, from the conservators' perspective, several aspects should be taken into consideration when deciding how to treat a

tapestry. In general, the soundness of the historic object seems to primarily determine conservators' decisions. For instance, when choosing the support method, many workshops may already opt for full support only for tapestries in evident weak conditions [2, 10]. However, besides this, factors like time and cost also influence the choice of the treatment [10]. Therefore it should be highlighted that the observations drawn in this chapter on the usefulness of conservation approaches only consider one aspect of a more complex decision-making process.

From a methodological perspective, the combination of analytical techniques employed here, 2D DIC and tensile testing, was proved to be useful in providing some insights on the mechanical behaviour of conserved textiles. While this work represents the first extensive trial of DIC within the field of textile conservation, tensile testing has been employed before for evaluating treatments, also in the case of tapestries [5]. Due to the uncertainty on the accuracy of DIC results, it was necessary to include the more established tensile testing method. The destructive technique showed that confidence can be given to DIC, although sometimes the optical method was unable to clearly highlight differences in the treatments' ability to reduce strain. For instance, the tensile testing proved the greater ultimate tensile strength of samples treated with laid couching than those conserved with brick couching. Of course, this largely depends on the fact that the stress experienced by tensile tested samples was significantly higher than that in fixed-load experiments. Because of this, the contribution from the DIC analysis can be critical as the contactless method allows the monitoring of damage propagation in actual cases, considering realistic load distributions.

References

1. *Tapestry Conservation: Principles and Practice*. Butterworth-Heinemann series in conservation and museology, ed. F. Lennard and M. Hayward. 2006, Oxford: Butterworth-Heinemann. xxv, 247 p.
2. Catic, E.M., *A Research Project to Measure the Effectiveness of Stitching Methods when Stabilizing Weak Areas in Tapestries*. 2019, University of Glasgow.
3. Benson, S.J., F. Lennard, and M.J. Smith, 'Like-With-Like': A Comparison of Natural and Synthetic Stitching Threads used in Textile Conservation, in *ICOM Committee for Conservation (ICOM-CC). Triennial meeting, 17th, Melbourne, Australia, 2014: Preprints*, J. Bridgland, Editor. 2014, The International Council of Museums: Paris.
4. Sutherland, H. and F. Lennard, "Each to their own"? An investigation into the spacing of laid-thread couching as used in textile conservation. Newsletter of the ICOM Committee for Conservation, Working Group of Textiles, 2017. 39.
5. Asai, K., et al., *Tapestry conservation traditions: an analysis of support techniques for large hanging textiles*, in *15th Triennial Conference New Delhi*. 2008: New Delhi. p. 967-975.
6. Schön, M., *The Mechanical and Supporting effect of stitches in Textile Conservation*. 2017, Göteborgs Universitet.
7. Nilsson, J., *Ageing and conservation of silk*. 2015, University of Gothenburg.
8. Hofenk de Graaff, J.H., *Tapestry Conservation: Support Methods and Fabrics*. 1997.
9. Hofenk de Graaff, J.H., F. Boersma, and W.G.T. Roelofs, *Tapestry Conservation (Part III Scientific Research 'Linen versus Cotton')*. 1998.
10. Duffus, P., *Manufacture, analysis and conservation strategies for historic tapestries*, in *Faculty of Engineering and Physical Sciences*. 2013, University of Manchester.
11. Landi, S., *A description and evaluation of a conservation system for tapestries*, in *Tapestry Conservation: Principles and Practice*, F. Lennard and M. Hayward, Editors. 2006, Butterworth-Heinemann: Oxford. p. 108-112.
12. Nilsson, J., et al., *Evaluation of stitched support methods for the remedial conservation of historic silk costumes*. e-conservation Journal, 2015(3).
13. Young, C.R.T., *Measurement of the Biaxial Tensile Properties of Paintings on Canvas*, in *Department of Mechanical Engineering*. 1996, Imperial College, University of London.
14. Mecklenburg, M.F., *Some aspects of the mechanical behavior of fabric supported paintings*, in *The Mechanics of Art Materials and Its Future in Heritage Science*, D.V. Rogala, et al., Editors. 2019, Smithsonian Institution Scholarly Press: Washington D.C. p. 107-129.
15. Andersen, C.K., *Lined canvas paintings: Mechanical properties and structural response to fluctuating relative humidity, exemplified by the collection of Danish Golden Age paintings at Statens Museum for Kunst (SMK)*. 2013, Centre for Art Technological Studies and Conservation, Statens Museum for Kunst, Royal Academy of Fine Arts.

16. Gonzalez-Chi, P., L. May-Hernández, and J. Carrillo, *Polypropylene Composites Unidirectionally Reinforced with Polyester Fibers*. Journal of Composite Materials, 2004. **38**: p. 1521-1532.
17. Militký, J., *Tensile failure of polyester fibers*, in *Handbook of Properties of Textile and Technical Fibres*, A.R. Bunsell, Editor. 2018, Woodhead Publishing. p. 421-514.
18. Ackroyd, P., *The structural conservation of canvas paintings: changes in attitude and practice since the early 1970s*. Studies in Conservation, 2002. **47**(sup1): p. 3-14.
19. Young, C., R. Hibberd, and P. Ackroyd, *An investigation into the adhesive bond and transfer of tension in lined canvas paintings*, in *ICOM Committee for Conservation. Triennial meeting, 13th, Rio de Janeiro, Brazil, 2002: Preprints*. 2002, James & James: London. p. 370-378.
20. Knutson, T. and M.W. Ballard, *Dyeing Polyester: Disperse Dyes for Textile Conservation Work*, in *20th Century Materials, Testing and Textile Conservation, 9th Symposium*. 1989.
21. Hillyer, L., Z. Tinker, and P. Singer, *Evaluating the use of adhesives in textile conservation: Part I: An overview and surveys of current use*. The Conservator, 1997. **21**(1): p. 37-47.
22. Gentle, N., *The examination and conservation of two Indian textiles*. The conservator, 1993. **17**(1): p. 19-25.
23. Karsten, I.F. and N. Kerr, *The Properties and Light Stability of Silk Adhered to Sheer Silk and Polyester Support Fabrics with Poly(Vinyl Acetate) Copolymer Adhesives*. Studies in Conservation, 2002. **47**(3): p. 195-210.

7 Conclusions and future research

This thesis aimed to extend the knowledge on the degradation and preservation of historic tapestries. The research was carried out within the context of the project *From the Golden Age to the Digital Age: Modelling and Monitoring Historic Tapestries*, involving the Centre for Textile Conservation and Technical Art History and the School of Engineering of the University of Glasgow. The work was conducted through a multi-analytical approach combining textile conservation, analytical chemistry, and mechanical engineering. The cross-disciplinary nature of the work and the variety of diagnostic tools employed allowed the characterisation, and the understanding, of the mechanical behaviour of tapestries both on a small-scale level and from a macroscopic perspective. Moreover, the use of well-established techniques benefitted the assessment of more novel methods. Innovative aspects investigated and achieved goals include:

- Comparative investigation of factors affecting the physical and chemical durability of tapestries (Chapter 3).
- Improvement of the analytical approach, involving digital image correlation (DIC), to be used when monitoring strain across historic hangings to study mechanical damage mechanisms occurring during display (Chapter 4).
- Comprehensive study on the efficacy of sloping boards as a display method for tapestries, evaluating the role of fabric/fabric friction and inclination in decreasing strain (Chapter 5).
- Objective investigation, through DIC and uniaxial tensile testing, of the mechanical behaviour of bespoke mock-ups when using different conservation strategies for supporting weak areas in tapestries (Chapter 6).

More specifically, from this work the following conclusions can be drawn:

Factors affecting the structural stability of tapestries on a small-scale level

The tensile properties of small-scale fragments from various historic tapestries were shown to vary on the basis of different parameters, associated with both the geometry of the weave and chemical features, that were here connected for the first time. Chemical degradation, measured by attenuated total reflectance Fourier transform infrared spectroscopy (ATR-FTIR) in wool samples considering the level of cysteic acid (CA) formed from cystine oxidation, leads to a certain loss in strength. Processes behind this alteration of chemical and physical features were shown to be likely associated to the exposure to environmental factors. In particular, it could be thought that humidity, temperature and/or pollutants may play a role, as the warp threads, undyed and unexposed to light, were also affected. This builds on the knowledge from past studies, and namely from the Monitoring of Damage of Historic Tapestries (MODHT) project, as spectroscopic investigation previously focused on historic weft threads and on the effects of light. Some dyeing processes and materials, e.g. tannins, were shown to have a possible, but partial, impact on wool chemical degradation, although only a limited number of coloured weft threads was analysed. Interestingly, it was noted that, despite the great chemical degradation, textile samples may still preserve a good tensile strength thanks to the great fineness of the weave.

Feasibility of 2D DIC for monitoring strain across tapestries and defining mechanical damage mechanisms

2D DIC was proved to be successful in monitoring overall displacements across tapestries, with different figurative designs, fibres, and sizes. Overall strain data, averaged from the entire surface of the textile, was shown to be useful in defining fatigue, as well as time-dependent mechanisms causing a significant elongation of weft threads when the object is first hung for the display. Importantly, such mechanical mechanisms were identified also when full-size tapestries were studied, indicating a broader applicability of the technique than was established before. Nevertheless, it was clear that when monitoring large tapestries with an area of more than one m², local strain data were likely to be inaccurate and unable to provide information on structural weaknesses. On the other hand, when the monitored area was reduced, the increased resolution of

the images sometimes enabled the tracking of the propagation of local damage, such as the widening of open slits due to creep-like behaviours. It is important to underline that, even when the monitored area was limited, no damage was detected before the occurrence of a visible defect in the weave.

From these observations, it can be concluded that 2D DIC can be a helpful tool for a non-invasive and *in situ* assessment of strain distribution across historic textile objects while hanging. Nevertheless, when the objective of the experiment is to define the mechanical degradation occurring in a specific area, the full-field approach should be avoided. For instance, when the propagation of an evident defect needs to be tracked over time (e.g. for assessing the helpfulness of a local conservation treatment), the monitored area should be restricted to the few cm² of interest.

Evaluation of display methods and conservation strategies

It was shown that the helpfulness of sloping boards in limiting overall strain across tapestries greatly depends on the covering fabrics, and that those currently in use for such systems may be effective in preventing extensions/contractions caused by humidity fluctuations. However, sloping boards would probably be unable to contain strain across evident damaged areas. Since the inclination was observed to play a more marginal role than friction/adhesion, covered boards inclined at lower angles than 5° could be employed for displaying structurally sound tapestries. This can help in smoothing fatigue, although the long-term effects of this approach are not known, and the adhesion/friction mechanism was not fully explained.

Moving to treatments aiming to improve the structural stability of tapestries, full and patch supports were shown to be similarly effective in carrying load from damaged areas, when wool rep mock-ups were tested. However, from the outcomes it can be stated that, when weaknesses are widespread across the surface of the woven hanging, full support is a more effective option. From the data gathered, laid and brick couching have demonstrated a similar positive impact when conserving areas of weft loss, although effects may vary depending on spacing.

From a practical perspective, it is thought that the combined use of sloping boards (inclination $\leq 5^\circ$ from the vertical) and local support linen patches could be a valuable option to help preserving historic hangings, although only when they are in good condition. Advantages of this approach would be the limited amount of time and material for the conservation treatment, as well as the possibility of leaving the back of the artwork available for future research. Although the application of a full support may impede further study of the original materials on the back, as the treatment is difficult to reverse, the presence of a textile barrier (perhaps also represented by a lining) between the tapestry and the wall may be beneficial. Indeed, this can help in retarding degradation processes in fibres, such as those promoted by humidity.

7.1 Future research

Based on the conclusions drawn from the current study, the following areas of future research are identified:

- More detailed study of the chemical degradation processes behind the formation of CA in wool threads from tapestries, defining the related responsibility of environmental factors, and in particular of humidity.
- More extended and more numerous long-term *in situ* monitoring tests of historic tapestries to better understand the actual structural risk caused by high levels of RH and fretting fatigue. Extended experiments can be helpful to delineate if and when the variation in length due to RH fluctuations may lead to irreversible changes. This can be useful also for textile conservators who need to establish the objectives of the treatments (i.e. should the artwork be allowed to move, or should it be constrained?).
- Evaluation of the long-term effects on strain when displaying a tapestry on a vertical board covered with cotton molton, or a similar fabric. In addition, further analysis is needed to provide a more accurate definition of the friction and adhesion process occurring between tapestries and the covering fabric of boards.

- Further application of 2D DIC for validating conservation approaches, possibly carrying out tests directly on historic hangings. A relevant aspect to further investigate can be establishing the minimum spacing between couching stitches to ensure long-term structural stability. In addition, further tests should be carried out to verify whether very close conservation stitches may negatively impact the treated areas (through an increase in tension).

Appendix – Technical notes

Attenuated total reflectance Fourier transform infrared spectroscopy

Fourier transform infrared spectroscopy (FTIR) is a common absorption technique for identifying and characterising a wide range of organic and inorganic materials within artworks [1]. Broadly speaking, the technique relies on the ability of the infrared (IR) radiation of leading molecular bonds, in distinctive functional groups, to vibrate once absorbed. Since each functional group absorbs only specific frequencies of the incident IR radiation, by detecting the ranges absorbed, the groups can be identified. Eventually, by recognising the various chemical groups, it can be possible to qualitatively define molecular structures and so the chemical composition of the sample analysed [2].

In the case of attenuated total reflectance (ATR) FTIR, samples are irradiated with radiation in the mid-IR region, which ranges between 4000 cm^{-1} and 400 cm^{-1} . Importantly, when the ATR approach is used the sample, or object, is placed against a specific crystal and clamped. The ATR approach allows some advantages, such as: no samples preparation is required; in some cases, no sample is needed, allowing a non-destructive analysis (depending on the object size and its surface flatness). One of the possibly crucial limits of ATR-FTIR is that it only enables the investigation of the surface, as the penetration depth of the radiation is limited to maximum of around $2\text{ }\mu\text{m}$, depending on the crystal [1, 3]. Besides, in some cases it can be difficult to properly define the composition when complex mixture of materials is present [4]. Both circumstances are not relevant considering the objectives and case studies of the current work.

High performance liquid chromatography coupled with photodiode array detector

Like all chromatographic techniques, high performance liquid chromatography (HPLC) enables the separation of different chemical components within a mixture. Fundamental element in a HPLC instrument is the column, usually made of stainless steel. Importantly, the column is covered with a so-called stationary phase, designed to have a specific chemical affinity with the analytes.

When HPLC is conducted, the sample is in the form of a small volume of solution which contains, as a mixture, the solubilised analytes. During the analysis, part of the solution is injected and allowed to pass through the column together with specific solvents. The solvents (mobile phase), mixed at different % during the analysis, are pumped at high pressure. While passing through the column, the components in the sample interact with the stationary and mobile phase, and, depending on chemical properties, they show a different chemical attraction. Based on the characteristic affinity, each component is retained in the column for a specific amount of time, enabling the original mixture to be effectively separated. Since the time at which the compound is eluted from the column and it reaches the detector depends on its chemical structure, the retention time (RT) is one of the variables to be considered when identifying the component.

When analysing dyes in historic artworks, in the last decades HPLC has been usually coupled with the photodiode array detector (PDA). The PDA detector allows to measure the radiation absorbed, in the UV-Vis range (\approx 250-750 nm), by each compound previously separated. Since when studying dyes (some of the) components of interests are coloured, this means that they absorb characteristic wavelengths in the UV-Vis range. The absorbance spectrum of each component, provided by the PDA detector, represents another distinctive feature that can lead to the chemical identification [5, 6].

Within the context of the current work, UHPLC-PDA was employed. Differently from traditional HPLC, ultra HPLC enables to obtain a higher resolution and sensitivity, meaning that smaller samples can be analysed. Besides, lower volumes of solvents are needed for the UHPLC application [7].

Before the actual chromatographic analysis, when characterising dyes from historic textile samples, a crucial step is represented by the extraction method for solubilising the components from the threads. Depending on the analytes expected, the pre-treatment should be selected carefully [5].

References

1. Thickett, D. and B. Pretzel, *FTIR surface analysis for conservation*. Heritage Science, 2020. **8**(1): p. 5.
2. Derrick, M., D. Stulik, and J.M. Landry, *Infrared Spectroscopy in Conservation Science*. Scientific Tools for Conservation. 1999, Los Angeles: Getty Conservation Institute. x, 235 p.
3. Smith, M., K. Thompson, and F. Lennard, *A literature review of analytical techniques for materials characterisation of painted textiles-Part 2: spectroscopic and chromatographic analytical instrumentation*. Journal of the Institute of Conservation, 2017. **40**(3): p. 252-266.
4. Izzo, F.C., *20th Century Artists' Oil Paints: A Chemical-Physical Survey*. 2009-2010, Università Ca' Foscari Venezia.
5. Degano, I. and J. La Nasa, *Trends in High Performance Liquid Chromatography for Cultural Heritage*. Topics in Current Chemistry, 2016. **374**(2): p. 20.
6. Skoog, D.A., et al., *Fondamenti di Chimica Analitica*. 2009, Città di Castello: EdiSES. 1051 p.
7. Troalen, L.G., *Historic Dye Analysis: Method Development And New Applications In Cultural Heritage*, in *School Of Chemistry*. 2013, University Of Edinburgh.

Complete bibliography

1964 Delft conference on the conservation of textiles: collected preprints. London: IIC; 1964. 153 p.

Ackroyd P. The structural conservation of canvas paintings: changes in attitude and practice since the early 1970s. *Stud Conserv.* 2002;47(sup1):3-14.

Acts of the Tapestry Symposium, November 1976. San Francisco: Fine Arts Museums of San Francisco; 1979. 223 p.

Ajayi JO, Elder HM. Comparative Studies of Yarn and Fabric Friction. *Journal of Testing and Evaluation.* 1994;22(5):463-7.

Allaoui S, Hivet G, Wendling A, Ouagne P, Soulat D. Influence of the dry woven fabrics meso-structure on fabric/fabric contact behavior. *Journal of Composite Materials* 2012;46(6):627-39.

Alsayednoor J, Harrison P, Dobbie M, Costantini R, Lennard F. Evaluating the use of digital image correlation for strain measurement in historic tapestries using representative deformation fields. *Strain.* 2019;55(2):e12308.

Andersen CK. Lined canvas paintings: Mechanical properties and structural response to fluctuating relative humidity, exemplified by the collection of Danish Golden Age paintings at Statens Museum for Kunst (SMK): Centre for Art Technological Studies and Conservation, Statens Museum for Kunst, Royal Academy of Fine Arts; 2013.

Appel WD, Jessup DA. Accelerated ageing test for weighted silk. *Journal of Research of the National Bureau of Standards.* 1935;15:601-8.

Asai K, Biggs E, Ewer P, Hallet K. Tapestry conservation traditions: an analysis of support techniques for large hanging textiles. 15th Triennial Conference New Delhi; New Delhi 2008. p. 967-75.

Badillo-Sanchez D, Chelazzi D, Giorgi R, Cincinelli A, Baglioni P. Understanding the structural degradation of South American historical silk: A Focal Plane Array (FPA) FTIR and multivariate analysis. *Scientific reports.* 2019;9(1):1-10.

Balci Kilic G, Okur A. Effect of yarn characteristics on surface properties of knitted fabrics. London, England: SAGE Publications; 2019. p. 2476-89.

Ballard MW, Koestler RJ, Indictor N. Weighted silks observed using energy dispersive X-ray spectrometry. *Scanning electron microscopy.* 1986(II):499-506.

Ballard MW. Hanging Out Strength, Elongation and Relative Humidity: Some Physical Properties of Textile Fibers. In: Bridgland J, editor. ICOM committee for conservation, 11th triennial meeting in Edinburgh, Scotland, 1996: Preprints. II. London: James & James; 1996. p. 665-9.

Ballard MW. How backings work: the effect of textile properties on appearance Lining and backing: the support of paintings, paper and textiles Papers delivered at the UKIC Conference, 7-8 November 1995. London: United Kingdom Institute for Conservation of Historic and Artistic Works; 1995. p. 34-9.

Band J. The survival of Henry VIII's History of Abraham tapestries: an account of how they were perceived, used and treated over the centuries. In: Lennard F, Hayward M, editors. *Tapestry Conservation: Principles and Practice.* Oxford: Butterworth-Heinemann; 2006. p. 20-7.

Barker K. Reducing the Strain: Is it worth displaying a large fragile textile at a slight angle? *Conservation news.* 2002:30.

Barker K. Reducing the Strain: Is it worth displaying a large fragile textile at a slight angle? *Newsletter of the ICOM Committee for Conservation, Working Group of Textiles.* 2005:4-6.

Barnett R, Blohm AA, Colburn K, Kane T, Sato M, Zaharia F. Tapestry conservation at the Metropolitan Museum of Art. In: Lennard F, Hayward M, editors. *Tapestry Conservation: Principles and Practice*. Oxford: Butterworth-Heinemann; 2006. p. 155-62.

Barnoud P, Abécassis L, Magos F. Musée National De Cluny: Restauration et Muséographie de la Salle 13 Dite Salle De La Dame à la Licorne. Rapport de Présentation Description Sommaire des Travaux. 2013.

Barrett RT. Fastener design manual: NASA, Scientific and Technical Information Division; 1990.

Batcheller J, Hacke AM, Mitchell R, Carr CM. Investigation into the nature of historical tapestries using time of flight secondary ion mass spectrometry (ToF-SIMS). *Applied Surface Science*. 2006;252(19):7113-6.

Behera BK, Hari PK. Friction and other aspects of the surface behavior of woven fabrics. In: Behera BK, Hari PK, editors. *Woven Textile Structure*. Oxford; Cambridge; New Delhi: Woodhead Publishing in association with The Textile Institute; 2010. p. 230-42.

Beingessner A. The Hunt of the Unicorn: Tapestry Copies Made for Stirling Castle, Scotland: University of Guelph; 2015.

Benson SJ, Lennard F, Smith MJ. 'Like-With-Like': A Comparison of Natural and Synthetic Stitching Threads used in Textile Conservation. In: Bridgland J, editor. *ICOM Committee for Conservation (ICOM-CC) Triennial meeting, 17th, Melbourne, Australia, 2014: Preprints*. Paris: The International Council of Museums; 2014.

Bilson T, Howell D, Cooke B. Mechanical Aspects of Lining 'Loose Hung' Textiles. Fabric of an exhibition: an interdisciplinary approach Preprints Ottawa: Canadian Conservation Institute; 1997. p. 63-9.

Bing P, Hui-min X, Bo-qin X, Fu-long D. Performance of sub-pixel registration algorithms in digital image correlation. *Measurement Science and Technology*. 2006;17(6):1615-21.

Blaber J, Adair B, Antoniou AJEM. Ncorr: open-source 2D digital image correlation matlab software. *Experimental Mechanics* 2015;55(6):1105-22.

Böttiger J. Les tapisseries des châteaux royaux de Suède: expériences et conseils. Uppsala: Almqvist & Wiksells Boktryckeri; 1937.

Bratasz L, Lukomski M, Klisinska-Kopacz A, Zawadzki W, Dzierzega K, Bartosik M, et al. Risk of Climate-Induced Damage in Historic Textiles. *Strain*. 2015;51(1):78-88.

Breeze CM. A Survey of American Tapestry Conservation Techniques: American Textile History Museum 2000.

Bruni S, De Luca E, Guglielmi V, Pozzi F. Identification of Natural Dyes on Laboratory-Dyed Wool and Ancient Wool, Silk, and Cotton Fibers Using Attenuated Total Reflection (ATR) Fourier Transform Infrared (FT-IR) Spectroscopy and Fourier Transform Raman Spectroscopy. *Appl Spectrosc*. 2011;65(9):1017-23.

Brutillot A. Conservation of a fifteenth-century tapestry from Franconia. In: Grimstad K, editor. *The Conservation of Tapestries and Embroideries*. Marina del Rey: The Getty Conservation Institute; 1989. p. 75-9.

Brutillot A. Slant Boards for Display 2010. Available from: <https://www.youtube.com/watch?v=uDQSI1yJE0&t=47s>.

Bryson WM, McNeil SJ, McKinnon AJ, Rankin, DA. The Cell Membrane Complex of Wool. Wool Research Organisation of New Zealand; 1992.

Calia A, Lettieri M, Quarta G. Cultural heritage study: Microdestructive techniques for detection of clay minerals on the surface of historic buildings. *Applied Clay Science*. 2011;53(3):525-31.

- Campanella L, Casoli A, Colombini MP, Marini Bettolo R, Matteini M, Migneco LM, et al. *Chimica per l'arte*. Ozzano Emilia: Zanichelli; 2007. 490 p.
- Campbell TP, Ainsworth MW, White B. *Tapestry in the Renaissance: art and magnificence*. London; New York; New Haven: Metropolitan Museum of Art; 2002. 594 p.
- Campbell TP. *Henry VIII and the art of majesty: tapestries at the Tudor Court*. New Haven; London: Yale University Press; 2007. xviii, 419 p.
- Cardon D. *Le monde des teintures naturelles*. Paris: Belin; 2003. 783 p.
- Cariati F, Rampazzi L, Toniolo L, Pozzi A. Calcium Oxalate Films on Stone Surfaces: Experimental Assessment of the Chemical Formation. *Stud Conserv*. 2000;45:180-8.
- Carò F, Chiostrini G, Cleland E, Shibayama N. Redeeming Pieter Coecke van Aelst's Gluttony Tapestry: Learning from Scientific Analysis. *Metropolitan Museum Journal*. 2014;49:151-64.
- Carr CM, Lewis DM. An FTIR spectroscopic study of the photodegradation and thermal degradation of wool. *Journal of the Society of Dyers and Colourists*. 1993;109(1):21-4.
- Catic EM. *A Research Project to Measure the Effectiveness of Stitching Methods when Stabilizing Weak Areas in Tapestries*: University of Glasgow; 2019.
- Chahardoli Z, Vanden Berghe I, Rocco M. Twentieth century Iranian carpets: investigation of red dye molecules and study of traditional madder dyeing techniques. *Heritage Science*. 2019;7.
- Church JS, Millington KR. Photodegradation of wool keratin: Part I. Vibrational spectroscopic studies. *Biospectroscopy*. 1996;2(4):249-58.
- Clarke A, Hartog F. The cost of tapestry conservation. In: Barnett J, Cok S, editors. 'The Misled Eye...' Reconstruction and Camouflage Techniques in Tapestry Conservation; Amsterdam: TRON; 1996. p. 69-72.
- Clementi C, Miliani C, Romani A, Santamaria U, Morresi F, Mlynarska K, et al. In-situ fluorimetry: a powerful non-invasive diagnostic technique for natural dyes used in artefacts. Part II. Identification of orcein and indigo in Renaissance tapestries. *Spectrochimica Acta Part A: Molecular and Biomolecular Spectroscopy*. 2009;71(5):2057-62.
- Comite V, Fermo P. The effects of air pollution on cultural heritage: The case study of Santa Maria delle Grazie al Naviglio Grande (Milan). *The European Physical Journal Plus*. 2018;133(12):556.
- ervazione e restauro dei tessili: Convegno internazionale. 1980; Como. Milano: Edizioni C.I.S.S.T.; 1982.
- Cook JG. *Handbook of textile fibres*. 5th ed. Cambridge: Woodhead Publishing Limited; 2001. 205 p.
- Cooreman S, Lecompte D, Sol H, Vantomme J, Debruyne D. Identification of mechanical material behavior through inverse modeling and DIC. *Experimental Mechanics*. 2008;48(4):421-33.
- Costantini R, Lennard F, Alsayednoor J, Harrison P. Investigating mechanical damage mechanisms of tapestries displayed at different angles using 2D DIC. *The European Physical Journal Plus*. 2020;135(6):515.
- Costantini R, Shibayama N, Carò F. Logwood blue: dyeing, fading and the possible marker compound for the HPLC-PDA identification by a mild extraction. *Dye in History and Archaeology* 37; 2018; Lisbon.
- Cousens S. The Conservation Treatment of a Heavily Restored Fragment of a Hercules Tapestry: a Method of Approach. In: Barnett J, Cok S, editors. 'The Misled Eye...' Reconstruction and Camouflage Techniques in Tapestry Conservation; Amsterdam: TRON; 1996. p. 132-5.

- Cuoco G, Mathe C, Archier P, Vieillescazes C. Characterization of madder and garancine in historic French red materials by liquid chromatography-photodiode array detection. *Journal of Cultural Heritage* 2011;12:98-104.
- Cussell S. Tapestry conservation techniques at Chevalier Conservation. In: Lennard F, Hayward M, editors. *Tapestry Conservation: Principles and Practice*. Oxford: Butterworth-Heinemann; 2006. p. 145-52.
- da Costa AC, Correa F, Sant'Anna G, de Carvalho S, Santos F, Lutterbach M. Scanning Electron Microscopic Characterization of Iron-Gall Inks from Different Tannin Sources - Applications for Cultural Heritage. *Chemistry and Chemical Technology*. 2014;8:423-30.
- Davidson RS. The photodegradation of some naturally occurring polymers. *Journal of Photochemistry and Photobiology B*. 1996;33:3-25.
- De Boeck J, De Bruecker M, Carpentier C, Housiaux K. The treatment of two sixteenth-century tapestries at the Institut Royal du Patrimoine Artistique. In: Grimstad K, editor. *The Conservation of Tapestries and Embroideries*. Marina del Rey: The Getty Conservation Institute; 1989. p. 113-7.
- De Luca E, Poldi G, Redaelli M, Zaffino C, Bruni S. Multi-technique investigation of historical Chinese dyestuffs used in Ningxia carpets. *Archaeological and Anthropological Sciences*. 2016;9(8):1789-98.
- Degani L, Riedo C, Chiantore O. Identification of natural indigo in historical textiles by GC-MS. *Analytical and Bioanalytical Chemistry*. 2015;407(6):1695-704.
- Degano I, Łucejko JJ, Colombini MP. The unprecedented identification of Safflower dyestuff in a 16th century tapestry through the application of a new reliable diagnostic procedure. *Journal of Cultural Heritage*. 2011;12(3):295-9.
- Degano I, Mattonai M, Sabatini F, Colombini MP. A Mass Spectrometric Study on Tannin Degradation within Dyed Woolen Yarns. *Molecules*. 2019;24(12):2318.
- Degano, I, La Nasa J. Trends in High Performance Liquid Chromatography for Cultural Heritage. *Topics in Current Chemistry*. 2016;374(2),20.
- Derrick M, Stulik D, Landry JM. *Infrared Spectroscopy in Conservation Science*. Los Angeles: Getty Conservation Institute; 1999. x, 235 p.
- Diehl JM. The workshop for the restoration of ancient textiles, Haarlem. Delft Conference on the Conservation of Textiles. London: IIC; 1964. p. 105-8.
- Dolcini L. The tapestries of the Sala dei Duecento in the Palazzo Vecchio. In: Grimstad K, editor. *The Conservation of Tapestries and Embroideries*. Marina del Rey: The Getty Conservation Institute; 1989. p. 81-7.
- Dong YL, Pan B. A Review of Speckle Pattern Fabrication and Assessment for Digital Image Correlation. *Experimental Mechanics*. 2017;57(8):1161-81.
- Dreby EC. A friction meter for determining the coefficient of kinetic friction of fabrics. *Journal of Research of the National Bureau of Standards*. 1943;31(4):237.
- Duffus P. *Manufacture, analysis and conservation strategies for historic tapestries*: University of Manchester; 2013.
- Dulieu-Barton JM, Dokos L, Eastop D, Lennard F, Chambers AR, Sahin M. Deformation and strain measurement techniques for the inspection of damage in works of art. *Reviews in Conservation* 2005;6:63-73.

- Dulieu-Barton JM, Khennouf D, Chambers AR, Lennard FJ, Eastop DD. Long term condition monitoring of tapestries using image correlation. Society for Experimental Mechanics (SEM) Annual Conference; 2010 7-10 June 2010; Indianapolis, USA.
- Dulieu-Barton JM, Sahin M, Lennard FL, Eastop DD, Chambers AR. Assessing the feasibility of monitoring the condition of historic tapestries using engineering techniques. *Key Engineering Materials*. 2007;347:187-92.
- Dulieu-Barton JM, Ye C-C, Chambers AR, Lennard FL, Eastop DD. Optical fibre sensors for monitoring damage in historic tapestries. XIth International Congress on Experimental and Applied Mechanics; 2008 2-5 June 2008; Orlando, USA.
- Dupre J-C, Jullien D, Uzielli L, Hesser F, Riparbelli L, Gauvin C, et al. Experimental study of the hygromechanical behaviour of a historic painting on wooden panel: devices and measurement techniques. *Journal of Cultural Heritage*. 2020;46:165-75.
- Dyer JM, Bringans SD, Bryson WG. Characterisation of photo-oxidation products within photoyellowed wool proteins: tryptophan and tyrosine derived chromophores. *Photochemical & Photobiological Sciences*. 2006;5(7):698-706.
- E. Taburet-Delahaye, R. Déjean, D. de Reyer, Nowik W. La Dame à la licorne, sa conservation et l'évaluation colorimétrique du nettoyage. *Technique* 2015;41:87 - 93.
- Elisabeth Taburet-Delahaye, Béatrice de Chancel-Bardelot, Alain Decouche, Déjean R. Les coulisses de la scénographie, de la restauration et de l'installation des tapisseries de la Dame à la Licorne au musée national du Moyen Âge. *Conserver et présenter les tapisseries: du bilan sanitaire à la mise en valeur*; 2015.
- Falcão L, Araújo ME. Tannins characterization in historic leathers by complementary analytical techniques ATR-FTIR, UV-Vis and chemical tests. *Journal of Cultural Heritage*. 2013;14:499-508.
- Feller RL. *Accelerated Aging: Photochemical and Thermal Aspects*. United States of America: The J. Paul Getty Trust; 1994.
- Ferreira ES, Hulme AN, McNab H, Quye A. The natural constituents of historical textile dyes. *Chemical Society Reviews*. 2004;33(6):329-36.
- Fiette A. Tapestry restoration: An historical and technical survey. *The Conservator*. 1997;21(1):28-36.
- Finch K. Evolution of tapestry repairs: a personal experience. *Seminaire international la restauration et la conservation des tapisseries*; Paris: IFROA; 1984. p. 125-32.
- Finch K. Problems of tapestry preservation. *Tecniche di conservazione degli arazzi: tre giornate di studio Firenze 18-20 Settembre 1981*; Firenze: Leo S. Olschki; 1986. p. 39-45.
- Finch K. Tapestries: conservation and original design. In: Grimstad K, editor. *The Conservation of Tapestries and Embroideries*. Marina del Rey: The Getty Conservation Institute; 1989. p. 67-74.
- Five centuries of tapestry from the Fine Arts Museums of San Francisco. Bennett AG, editor. San Francisco: Fine Arts Museums of San Francisco; 1992. 329 p.
- Flowers TH, Smith MJ, Brunton J. Colouring of Pacific barkcloths: identification of the brown, red and yellow colourants used in the decoration of historic Pacific barkcloths. *Heritage Science*. 2019;7(2):1-15.
- Foskett S. A Brief History of the Maintenance and Care of Tapestries. In: Cleland E, Karafel L, editors. *Tapestries from the Burrell Collection*. London: Philip Wilson Publishers; 2017. p. 27-33.
- Frame K, Vlachou-Mogire C, Hallett K, Takami M. Balancing Significance and Maintaining 'Sense of Place' in the Sustainable Display of Tudor Tapestries in the Great Hall, Hampton Court Palace. *Stud Conserv*. 2018;63:87-93.

- Franceschi VR, Nakata PA. Calcium Oxalate in Plants: Formation and Function. *Annual review of plant biology*. 2005;56(1):41-71.
- Francis K, Fredette T, Halvorson B, Windsor D. Tapestries on long-term view at the Isabella Stewart Gardner Museum: a synthesis of treatment options. In: Lennard F, Hayward M, editors. *Tapestry Conservation: Principles and Practice*. Oxford: Butterworth-Heinemann; 2006. p. 163-70.
- Franses J. *Tapestries and their mythology*. London: John Gifford Ltd.; 1973. 160 p., 18 p. of plates.
- Freeman MB. *The Unicorn Tapestries*. Lausanne: The Metropolitan Museum of Art; 1983. 244 p. p.
- Fusek J. An attempt to regain the original colour and structure of an old tapestry. *Stud Conserv*. 1964;9(sup1):109-12.
- Fuster López L, Mecklenburg M, Yusa Marco DJ, Vicente Palomino S, Batista dos Santos AF. Effects of mordants on the mechanical behaviour of dyed silk fabrics: preliminary tests on cochineal dyestuffs. *Arché*. 2007;2:115-20.
- Garside P, Lahlil S, Wyeth P. Characterization of Historic Silk by Polarized Attenuated Total Reflectance Fourier Transform Infrared Spectroscopy for Informed Conservation. *Appl Spectrosc*. 2005;59(10):1242-7.
- Gauvin C, Jullien D, Doumalin P, Dupré JC, Gril J. Image Correlation to Evaluate the Influence of Hygrothermal Loading on Wood. *Strain*. 2014;50(5):428-35.
- Geijer A. Treatment and Repair of Textiles and Tapestries. *Stud Conserv*. 1961;6(4):144-7.
- Gentle N. The examination and conservation of two Indian textiles. *The conservator*. 1993;17(1):19-25.
- Giachetti A. Matching techniques to compute image motion. *Image and Vision Computing*. 2000;18(3):247-60.
- Gilbert AS. IR Spectral Group Frequencies of Organic Compounds. In: Lindon JC, editor. *Encyclopedia of Spectroscopy and Spectrometry*: Academic Press; 2000. p. 1035-47.
- Gonzalez-Chi P, May-Hernández L, Carrillo J. Polypropylene Composites Unidirectionally Reinforced with Polyester Fibers. *Journal of Composite Materials*. 2004;38:1521-32.
- Grau-Bové J, Strlič M. Fine particulate matter in indoor cultural heritage: a literature review. *Heritage Science*. 2013;1(1):8.
- Hacke AM. *Investigation into the Nature and Ageing of Tapestry Materials*: University of Manchester 2006.
- Hacke M, Hutchings C, Hallett K, Carr CM. Investigation into the Nature and Degradation of Historical Wool Tapestries. 11th International Wool Textile Research Conference; 2005; Leeds, UK.
- Hacke M. Weighted silk: history, analysis and conservation *Stud Conserv*. 2008;53(sup2):3-15.
- Haddadi H, Belhabib S. Use of rigid-body motion for the investigation and estimation of the measurement errors related to digital image correlation technique. *Optics and Lasers in Engineering*. 2008;46(2):185-96.
- Hain R, Kähler CJ, Tropea C. Comparison of CCD, CMOS and intensified cameras. *Experiments in Fluids*. 2007;42(3):403-11.

- Hallett K, Howell D. Size exclusion chromatography of silk: inferring the tensile strength and assessing the condition of historic tapestries. In: Verger I, editor. ICOM Committee for Conservation Triennial meeting, 14th, The Hague, Netherlands, 2005: Preprints. II. London: James & James/Earthscan; 2005. p. 911-9.
- Halpine SM. An Improved Dye and Lake Pigment Analysis Method for High-Performance Liquid Chromatography and Diode-Array Detector. *Stud Conserv.* 1996;41(2):76-94.
- Han J, Wanrooij J, van Bommel M, Quye A. Characterisation of chemical components for identifying historical Chinese textile dyes by ultra high performance liquid chromatography - photodiode array - electrospray ionisation mass spectrometer. *Journal of Chromatography A.* 2017;1479:87-96.
- Han J. The historical and chemical investigation of dyes in high status Chinese costume and textiles of the Ming and Qing dynasties (1368-1911): University of Glasgow; 2016.
- Harrison P, Gonzalez Camacho LF. Deep draw induced wrinkling of engineering fabrics. *International Journal of Solids and Structures.* 2021;212:220-36.
- Hayward M. Fit for a king? Maintaining the early Tudor tapestry collection. In: Lennard F, Hayward M, editors. *Tapestry Conservation: Principles and Practice.* Oxford: Butterworth-Heinemann; 2006. p. 13-9.
- Hearle JWS. A critical review of the structural mechanics of wool and hair fibres. *International Journal of Biological Macromolecules.* 2000;27:123-38.
- Hefford W. Bread, brushes and broom: aspects of tapestry restoration in England, 1660-1760. In: Bennett A, editor. *Acts of the Tapestry Symposium; San Francisco Fine Arts Museums of San Francisco;* 1979. p. 65-75.
- Hermann D, Ramkumar SS, Seshaiyer P, Parameswaran S. Frictional study of woven fabrics: The relationship between the friction and velocity of testing. *Journal of Applied Polymer Science.* 2004;92(4):2420-4.
- Hijazi A, Kahler CJ. Contribution of the Imaging System Components in the Overall Error of the Two-Dimensional Digital Image Correlation Technique. *Journal of Testing and Evaluation.* 2017;45(2):369-84.
- Hijazi A, Madhavan V. A novel ultra-high speed camera for digital image processing applications. *Measurement Science and Technology.* 2008;19(8):085503.
- Hillyer L, Tinker Z, Singer P. Evaluating the use of adhesives in textile conservation: Part I: An overview and surveys of current use. *The Conservator.* 1997;21(1):37-47.
- Hinsch KD, Gulker G, Hinrichs H, Joost H. Artwork monitoring by digital image correlation. In: Dickman K, Fotakis C, Asmus JF, editors. *Lasers in the Conservation of Artworks. Springer Proceedings in Physics.* 100. Berlin: Springer-Verlag Berlin; 2005. p. 459-67.
- Hofenk de Graaff JH, Boersma F, Roelofs WGT. Tapestry Conservation (Part III Scientific Research 'Linen versus Cotton'). 1998.
- Hofenk de Graaff JH. Tapestry Conservation: Support Methods and Fabrics. 1997.
- Hosseinali F, Thomasson JA. Multiscale Frictional Properties of Cotton Fibers: A Review. *Fibers.* 2018;6(3):49.
- Howell D. Some Mechanical Effects of Inappropriate Humidity on Textiles. In: Bridgland J, editor. ICOM committee for conservation, 11th triennial meeting in Edinburgh, Scotland, 1996: Preprints. II. London: James & James; 1996. p. 692-7.
- Howell HG, Mazur J. Amontons' Law and Fibre Friction. *Journal of the Textile Institute Transactions.* 1953;44(2):T59-T69.

Howell HG. The Laws of Friction. *Nature*. 1953;171(4344):220-.

Howell HG. The Laws of Static Friction. *Textile Research Journal*. 1953;23(8):589-91.

<https://www.correlatedsolutions.com>

Hulme AN, McNab H, Pegg DA, Quye A. The chemical characterisation by HPLC-PDA and HPLC-ESI-MS of unaged and aged fibre samples dyed with sawwort (*Serratula tinctoria* L.). *Dyes in History and Archaeology*. 2017:374-82.

Hunter GL. *The practical book of tapestries*. Philadelphia: J. B. Lippincott Company; 1925. 302 p.

Huson MG. Properties of wool. In: Bunsell AR, editor. *Handbook of properties of textile and technical fibres*: Elsevier Ltd; 2018. p. 59-103.

Hutchison RB. Gluttony and Avarice: two different approaches. In: Grimstad K, editor. *The Conservation of Tapestries and Embroideries*. Marina del Rey: The Getty Conservation Institute; 1989. p. 89-94.

Hutton E, Gartside J. The Moisture Regain of Silk i. Adsorption and Desorption of Water by Silk at 25° C. *Journal of the Textile Institute Transactions*. 1949;40(3):T161-T9.

Ioele M, Sodo A, Casanova Municchia A, Ricci MA, Russo AP. Chemical and spectroscopic investigation of the Raphael's cartoon of the School of Athens from the Pinacoteca Ambrosiana. *Applied Physics A*. 2016;122(12):1045.

Izzo FC. *20th Century Artists' Oil Paints: A Chemical-Physical Survey*: Università Ca' Foscari Venezia; 2009-2010.

Jones DC, Carr CM, Cooke WD. Investigating the Photo-Oxidation of Wool Using FT-Raman and FT-IR Spectroscopies. *Textile Research Journal*. 1998;68(10):739-48.

Kajitani N. Conservation maintenance of tapestries at the Metropolitan Museum of Art. In: Grimstad K, editor. *The Conservation of Tapestries and Embroideries*. Marina del Rey: The Getty Conservation Institute; 1989. p. 53-66.

Kammers AD, Daly SJEM. Digital image correlation under scanning electron microscopy: methodology and validation. *Experimental Mechanics*. 2013;53(9):1743-61.

Karapanagiotis I, Lakka A, Valianou L, Chrysoulakis Y. High-performance liquid chromatographic determination of colouring matters in historical garments from the Holy Mountain of Athos. *Microchimica Acta*. 2007;160(4):477-83.

Karapanagiotis I, Mantzouris D, Kamaterou P, Lampakis D, Panayiotou C. Identification of materials in post-Byzantine textiles from Mount Athos. *Journal of Archaeological Science*. 2011;38(12):3217-23.

Karapanagiotis I, Minopoulou E, Valianou L, Daniilia S, Chrysoulakis Y. Investigation of the colourants used in icons of the Cretan School of iconography. *Analytica Chimica Acta*. 2009;647(2):231-42.

Karsten IF, Kerr N. The Properties and Light Stability of Silk Adhered to Sheer Silk and Polyester Support Fabrics with Poly(Vinyl Acetate) Copolymer Adhesives. *Stud Conserv*. 2002;47(3):195-210.

Khenouf D, Dulieu-Barton JM, Chambers AR, Lennard FJ, Eastop DD. Application of digital image correlation to deformation measurement in textile. *Photomechanics 2008: International Conference on Full-Field Measurement Techniques and their Applications in Experimental Solid Mechanics*; 7-9 July 2008; Loughborough, UK2008.

Khenouf D, Dulieu-Barton JM, Chambers AR, Lennard FJ, Eastop DD. Assessing the Feasibility of Monitoring Strain in Historical Tapestries Using Digital Image Correlation. *Strain*. 2010;46(1):19-32.

Kirby J, van Bommel M, Verhecken A, Spring M, Vanden Berghe I, Stege H, et al. Natural colorants for dyeing and lake pigments: practical recipes and their historical sources. London: Archetype Publications Ltd in association with CHARISMA; 2014. 114 p.

Kissi N, Curran K, Vlachou-Mogire C, Fearn T, McCullough L. Developing a non-invasive tool to assess the impact of oxidation on the structural integrity of historic wool in Tudor tapestries. *Heritage Science*. 2017;5(49).

Knutson T, Ballard MW. Dyeing Polyester: Disperse Dyes for Textile Conservation Work. 20th Century Materials, Testing and Textile Conservation, 9th Symposium 1989.

Koperska MA, Łojewski T, Łojewska J. Evaluating degradation of silk's fibroin by attenuated total reflectance infrared spectroscopy: Case study of ancient banners from Polish collections. *Spectrochimica Acta Part A: Molecular and Biomolecular Spectroscopy*. 2015;135:576-82.

Koperska MA, Pawcenis D, Bagniak J, Zaitz MM, Missori M, Łojewski T, et al. Degradation markers of fibroin in silk through infrared spectroscopy. *Polymer Degradation and Stability*. 2014;105:185-96.

Kothari V, Swani N, Gangal M. Frictional properties of woven fabrics. *Indian Journal of Fibre & Textile Research*. 1991;16:251-6.

Landi S. A description and evaluation of a conservation system for tapestries. In: Lennard F, Hayward M, editors. *Tapestry Conservation: Principles and Practice*. Oxford: Butterworth-Heinemann; 2006. p. 108-12.

Lava P, Cooreman S, Coppieters S, De Strycker M, Debruyne D. Assessment of measuring errors in DIC using deformation fields generated by plastic FEA. *Optics and Lasers in Engineering*. 2009;47(7):747-53.

Lava P, Cooreman S, Debruyne D. Study of systematic errors in strain fields obtained via DIC using heterogeneous deformation generated by plastic FEA. *Optics and Lasers in Engineering*. 2010;48(4):457-68.

Lech K, Fornal E. A Mass Spectrometry-Based Approach for Characterization of Red, Blue, and Purple Natural Dyes. *Molecules*. 2020;25(14):3223.

Lecompte D, Smits A, Bossuyt S, Sol H, Vantomme J, Van Hemelrijck D, et al. Quality assessment of speckle patterns for digital image correlation. *Optics and Lasers in Engineering*. 2006;44(11):1132-45.

Leeder JD, Bishop DG, Jones LN. Internal Lipids of Wool Fibers. *Textile Research Journal*. 1983;53(7):402-7.

Lennard F, Dulieu-Barton JM. Quantifying and visualizing change: Strain monitoring of tapestries with digital image correlation. *Stud Conserv*. 2014;59(4):241-55.

Lennard F, Eastop D, Dulieu-Barton J, Chambers A, Khenouf D, Ye C-C, et al. Strain monitoring of tapestries: results of a three-year research project. In: Bridgland J, editor. *ICOM-CC 16th Triennial Conference, Lisbon, 2011: Preprints*. Paris: International Council of Museums; 2012. p. 1-8.

Lennard F, Eastop D, Ye CC, Dulieu-Barton JM, Chambers AR, Khenouf D. Progress in strain monitoring of tapestries. In: Bridgland J, editor. *ICOM Committee for Conservation Triennial meeting, 15th, New Delhi, India, 2008. II: Allied Publishers Pvt. Ltd.; 2008. p. 843-8.*

Lennard F. Methods of infilling areas of loss. In: Lennard F, Hayward M, editors. *Tapestry Conservation: Principles and Practice*. Oxford: Butterworth-Heinemann; 2006. p. 138-44.

Lennard F. Preserving image and structure: tapestry conservation in Europe and the United States. *Stud Conserv.* 2013;51(sup1):43-53.

Lewis DM. Damage in wool dyeing. *Review of Progress in Coloration and Related Topics.* 1989;19(1):49-56.

Lion V, Cussell S. The tapestry imposes its own treatment. In: Barnett J, Cok S, editors. 'The Misled Eye...' Reconstruction and Camouflage Techniques in Tapestry Conservation; Amsterdam: TRON; 1996. p. 81-90.

Lodewijks J. The Use of Synthetic Material for the Conservation and Restoration of Ancient Textiles. *Stud Conserv.* 2014;9(sup1):79-85.

Lu H, Cary PD. Deformation measurements by digital image correlation: Implementation of a second-order displacement gradient. *Experimental Mechanics.* 2000;40(4):393-400.

Lugtigheid R. The eye deceived: camouflage techniques used at the Werkplaats tot Herstel van Antiek Textiel in Haarlem. In: Barnett J, Cok S, editors. 'The Misled Eye...' Reconstruction and Camouflage Techniques in Tapestry Conservation; Amsterdam: TRON; 1996. p. 59-67.

Luxford N, Thickett D, Wyeth P. Applying preventive conservation recommendations for silk in historic houses. *Proceedings of the joint interim conference multidisciplinary conservation: a holistic view for historic interiors*; Rome: ICOM-CC; 2010.

Luxford N. Reducing the Risk of Open Display: Optimising the Preventive Conservation of Historic Silks: University of Southampton; 2009.

Luxford N. Silk durability and degradation. In: Annis PA, editor. *Understanding and improving the durability of textiles.* Oxford; Philadelphia: Woodhead Publishing; 2012. p. 205-32.

Ma S, Pang J, Ma Q. The systematic error in digital image correlation induced by self-heating of a digital camera. *Measurement Science and Technology.* 2012;23:025403.

Maes Y. The conservation/restoration of the sixteenth-century tapestry *The Gathering of the Manna*. In: Grimstad K, editor. *The Conservation of Tapestries and Embroideries.* Marina del Rey: The Getty Conservation Institute; 1989. p. 103-12.

Malesa M, Malowany K, Tymińska-Widmer L, Kwiatkowska EA, Kujawińska M, Rouba BJ, et al. Application of digital image correlation (DIC) for tracking deformations of paintings on canvas. *Proceedings of the Optics for Arts, Architecture, and Archaeology III Munich 2011.* p. 80840L.

Malowany K, Chrzanowska J, Kujawińska M, Targowski P, Tymińska-Widmer L, Rouba BJ. 3D Digital Image Correlation for tracking displacements of canvas paintings with natural texture. *16th International Conference on Experimental Mechanics*; Cambridge, UK 2014.

Malowany K, Tyminska-Widmer L, Malesa M, Kujawinska M, Targowski P, Rouba BJ. Application of 3D digital image correlation to track displacements and strains of canvas paintings exposed to relative humidity changes. *Appl Opt.* 2014;53(9):1739-49.

Manhita A, Balcaen L, Vanhaecke F, Ferreira T, Candeias A, Dias CB. Unveiling the colour palette of Arraiolos carpets: Material study of carpets from the 17th to 19th century period by HPLC-DAD-MS and ICP-MS. *Journal of Cultural Heritage.* 2014;15(3):292-9.

Manhita A, Santos V, Vargas H, Candeias A, Ferreira T, Dias CB. Ageing of brazilwood dye in wool - a chromatographic and spectrometric study. *Journal of Cultural Heritage.* 2013;14(6):471-9.

Marko K. Experiments in Supporting a Tapestry Using the Adhesive Method. *The Conservator.* 1978;2(1):26-9.

Marko K. Tapestry conservation - a confusion of ideas. *Lining and Backing: the Support of Paintings, Paper and Textiles.* London: UKIC; 1995. p. i-iv.

- Marko K. Textiles in trust. London: Archetype Publications in association with the National Trust; 1997. xiii, 199 p., 24 p. of plates.
- Marko K. Two case histories: a seventeenth-century Antwerp tapestry and an eighteenth-century English Soho tapestry. In: Grimstad K, editor. *The Conservation of Tapestries and Embroideries*. Marina del Rey: The Getty Conservation Institute; 1989. p. 95-101.
- Marko K. *Woven Tapestry: Guidelines for Conservation*: Archetype Publications Limited; 2020.
- Mathisen SA. An Excess of Metal Threads: the Techniques Used in Conservation of the Tapestry Entitled 'The Bridal Chamber of Herse'. In: Barnett J, Cok S, editors. 'The Misled Eye...' Reconstruction and Camouflage Techniques in Tapestry Conservation; Amsterdam: TRON; 1996. p. 73-80.
- Máximo Rocha P, D'Ayala D, Vlachou-Mogire C. Methodology for tensile testing historic tapestries. *IOP Conference Series: Materials Science and Engineering*. 2018;364:012003.
- May E, Jones M, Ebooks Corporation L, Royal Society of C. *Conservation science: heritage materials*. Cambridge: Royal Society of Chemistry; 2006.
- Mecklenburg MF. Some aspects of the mechanical behavior of fabric supported paintings. In: Rogala DV, DePriest PT, Charola AE, Koestler RJ, editors. *The Mechanics of Art Materials and Its Future in Heritage Science*. Washington D.C.: Smithsonian Institution Scholarly Press; 2019. p. 107-29.
- Mercier AA. Coefficient of friction of fabrics. *Bureau of Standards Journal of Research*. 1930;5:243-6.
- Militký J. Tensile failure of polyester fibers. In: Bunsell AR, editor. *Handbook of Properties of Textile and Technical Fibres*: Woodhead Publishing; 2018. p. 421-514.
- Miller JER, Barbara M. Degradation in Weighted and Unweighted Historic Silks. *Journal of the American Institute for Conservation*. 1989;28(2):97-115.
- Milligan B. The Degradation of Automotive Upholstery Fabrics by Light and Heat. *Review of Progress in Coloration and Related Topics*. 1986;16(1):1-7.
- Millington KR, Church JS. The photodegradation of wool keratin II. Proposed mechanisms involving cystine. *Journal of Photochemistry and Photobiology B: Biology*. 1997;39(3):204-12.
- Millington KR. Photoyellowing of wool. Part 1: Factors affecting photoyellowing and experimental techniques. *Coloration Technology*. 2006;122(4):169-86.
- Millington KR. Photoyellowing of wool. Part 2: Photoyellowing mechanisms and methods of prevention. *Coloration Technology*. 2006;122(6):301-16.
- Molfino AM, Pertegato F. L'arazzo di Ester e Assuero le ragioni e I problemi di un restauro in Museo (Poldi Pezzoli). *Tecniche di conservazione degli arazzi: tre giornate di studio Firenze 18-20 Settembre 1981*; Firenze: Leo S. Olschki; 1986. p. 87-91.
- Mouri C, Laursen R. Identification of anthraquinone markers for distinguishing Rubia species in madder-dyed textiles by HPLC. *Microchimica Acta*. 2012;179(1):105-13.
- Murugesh Babu K. *Silk: processing, properties and applications*. Cambridge: Woodhead Publishing in association with the Textile Institute; 2013. 264 p.
- N. Hulme A, McNab H, Peggie D, Quye A, Vanden Berghe I, Wouters J. Analytical characterisation of the main component found in logwood dyed textile samples after extraction with hydrochloric acid. *ICOM 14th Triennial Meeting Preprints*. 22005. p. 783-8.

Najjar W, Pupin C, Legrand X, Boude S, Soulat D, Dal Santo P. Analysis of frictional behaviour of carbon dry woven reinforcement. *Journal of Reinforced Plastics and Composites*. 2014;33(11):1037-47.

Negri AP, Cornell HJ, Rivett DE. A Model for the Surface of Keratin Fibers. *Textile Research Journal*. 1993;63(2):109-15.

Nilsson J, Naturvetenskapliga f, Department of C, Faculty of S, Göteborgs u, Gothenburg U, et al. Evaluation of stitched support methods for the remedial conservation of historic silk costumes. *e-conservation Journal*. 2015(3).

Nilsson J, Vilaplana F, Karlsson S, Bjurman J, Iversen T. The Validation of Artificial Ageing Methods for Silk Textiles Using Markers for Chemical and Physical Properties of Seventeenth-Century Silk. *Stud Conserv*. 2010;55(1):55-65.

Nilsson J. Ageing and conservation of silk: University of Gothenburg; 2015.

Odlyha M, Theodorakopoulos C, Campana R. Studies on woollen threads from historical tapestries. *Autex Research Journal*. 2007;7(1):9-18.

Odlyha M, Wang Q, Foster GM, de Groot J, Horton M, Bozec L. Thermal Analysis of Model and Historic Tapestries. *Journal of Thermal Analysis and Calorimetry*. 2005;82:627-46.

Ortega Saez N, Vanden Berghe I, Schalm O, De Munck B, Caen J. Material analysis versus historical dye recipes: ingredients found in black dyed wool from five Belgian archives (1650-1850). *Conservar Património*. 2019;31:116-32.

Otłowska O, Ślebioda M, Kot-Wasik A, Karczewski J, Śliwka-Kaszyńska M. Chromatographic and Spectroscopic Identification and Recognition of Natural Dyes, Uncommon Dyestuff Components, and Mordants: Case Study of a 16th Century Carpet with Chintamani Motifs. *Molecules* 2018;23(2):339.

Paggie DA. The development and application of analytical methods for the identification of dyes on historical textiles: University of Edinburgh; 2006.

Pan B, Qian K, Xie H, Asundi A. Two-dimensional digital image correlation for in-plane displacement and strain measurement: a review. *Measurement Science and Technology*. 2009;20(6):062001.

Pan B, Wu D, Xia Y. An active imaging digital image correlation method for deformation measurement insensitive to ambient light. *Optics & Laser Technology*. 2012;44(1):204-9.

Pan B, Xie H, Wang Z. Equivalence of digital image correlation criteria for pattern matching. *Appl Opt*. 2010;49(28):5501-9.

Pan B, Yu L, Wu D. High-Accuracy 2D Digital Image Correlation Measurements with Bilateral Telecentric Lenses: Error Analysis and Experimental Verification. *Experimental Mechanics*. 2013;53(9):1719-33.

Pan B. Digital image correlation for surface deformation measurement: historical developments, recent advances and future goals. *Measurement Science and Technology*. 2018;29(8):082001.

Peggie DA, Hulme AN, McNab H, Quye A. Towards the identification of characteristic minor components from textiles dyed with weld (*Reseda luteola* L.) and those dyed with Mexican cochineal (*Dactylopius coccus* Costa). *Microchimica Acta*. 2008;162(3):371-80.

Peggie DA, Kirby J, Poulin J, Genuit W, Romanuka J, Wills DF, et al. Historical mystery solved: a multi-analytical approach to the identification of a key marker for the historical use of brazilwood (*Caesalpinia* spp.) in paintings and textiles. *Analytical Methods*. 2018;10(6):617-23.

Pertegato F. Painting in tapestry conservation: is it heresy? In: Barnett J, Cok S, editors. 'The Misled Eye...' Reconstruction and Camouflage Techniques in Tapestry Conservation; Amsterdam: TRON; 1996. p. 97-109.

Petroviciu I, Crețu I, Vanden Berghe I, Wouters J, Medvedovici A, Albu F, et al. A discussion on the red anthraquinone dyes detected in historic textiles from Romanian collections. *e-Preservation Science*. 2012;9:90-6.

Petroviciu I, Crețu I, Vanden Berghe I, Wouters J, Medvedovici A, Albu F. Flavonoid dyes detected in historical textiles from Romanian collections. *e-Preservation Science*. 2014;11:84-90.

Petroviciu I, Teodorescu I, Albu F, Vîrgolici M, Nagoda E, Medvedovici A. Dyes and biological sources in nineteenth to twentieth century ethnographic textiles from Transylvania, Romania. *Heritage Science*. 2019;7.

Phipps E. Looking at textiles: a guide to technical terms. Los Angeles: J. Paul Getty Museum; 2011. 94 p.

Pinna D, Galeotti M, Rizzo A. Brownish alterations on the marble statues in the church of Orsanmichele in Florence: what is their origin? *Heritage Science*. 2015;3(7).

Popov VL. Contact mechanics and friction: physical principles and applications. Berlin: Springer; 2010. 362 p.

Pow CV. The Conservation of Tapestries for Museum Display. *Stud Conserv*. 1970;15(2):134-53.

Quye A, Cardon D, Paul JB. The Crutchley Archive: Red Colours on Wool Fabrics from Master Dyers, London 1716-1744. *Textile History*. 2020;1-48.

Quye A, Hallett K, Herrero Carretero C, Monitoring of Damage in Historic Tapestries (Project). 'Wroughte in gold and silk' : preserving the art of historic tapestries. Edinburgh: NMS Enterprises Limited-Publishing; 2009. viii, 134 p.

Ramkumar S, Leaf G, Harlock S. A Study of the Frictional Properties of 1×1 Rib-knitted Cotton Fabrics. *Journal of the Textile Institute*. 2000;91:374-82.

Ramos T, Furtado A, Eslami S, Alves S, Rodrigues H, Arêde A, et al. 2D and 3D digital image correlation in civil engineering-measurements in a masonry wall. *Procedia Engineering*. 2015;114:215-22.

Rampazzi L. Calcium oxalate films on works of art: A review. *Journal of Cultural Heritage*. 2019;40:195-214.

Reeves P. Alternate Methods of Hanging Tapestries. *Bulletin of the American Institute for Conservation of Historic and Artistic Works*. 1973;13(2):83-98.

Reu P. All about Speckles: Aliasing. *Experimental Techniques*. 2014;38(5):1-3.

Reu P. All about Speckles: Contrast. *Experimental Techniques*. 2015;39(1):1-2.

Reu P. All about Speckles: Edge Sharpness. *Experimental Techniques*. 2015;39(2):1-2.

Reu P. All about Speckles: Speckle Density. *Experimental Techniques*. 2015;39(3):1-2.

Reu P. All about speckles: Speckle Size Measurement. *Experimental Techniques*. 2014;38(6):1-2.

Rippon JA. The Structure of Wool. In: Lewis DM, Rippon JA, editors. The Coloration of Wool and other Keratin Fibres. Bradford: John Wiley & Sons in association with the Society of Dyers and Colourists 2013. p. 1-42.

Rodriguez-Arias HA. Low-cost automatic device for obtaining the coefficient of static friction. *IOP Conference Series: Materials Science and Engineering*. 2019;519:012018.

Rodríguez-Vera R, Kujawinska M, Díaz-Urbe R, Malesa M, Malowany K, Piekarczyk A, et al. Digital image correlation method: a versatile tool for engineering and art structures investigations. *Proceedings of the Optics for Arts, Architecture, and Archaeology III*; Munich2011. p. 80119R.

Sabatini F, Nacci T, Degano I, Colombini MP. Investigating the composition and degradation of wool through EGA/MS and Py-GC/MS. *Journal of Analytical and Applied Pyrolysis*. 2018;135:111-21.

Salmanpour AH, Mojsilovic N. Application of Digital Image Correlation for strain measurements of large masonry walls. *The 5th Asia Pacific congress on computational mechanics*; Singapore2013.

Schäfer K, Goddinger D, Höcker H. Photodegradation of tryptophan in wool. *Journal of the Society of Dyers and Colourists*. 1997;113(12):350-5.

Schön M. *The Mechanical and Supporting effect of stitches in Textile Conservation*: Göteborgs Universitet; 2017.

Schreier HW, Sutton MA. Systematic errors in digital image correlation due to undermatched subset shape functions. *Experimental Mechanics*. 2002;42(3):303-10.

Seminaire international la restauration et la conservation des tapisseries, Paris 18, 19, 20 juin 1984. Paris: Centre national des arts plastiques; 1984. 162 p.

Serrano A, Sousa M, Hallett J, Simmonds MS, Nesbitt M, Lopes JA. Identification of *Dactylopius cochineal* species with high-performance liquid chromatography and multivariate data analysis. *Analyst*. 2013;138(20):6081-90.

Serrano A, Sousa MM, Hallett J, Lopes JA, Oliveira MC. Analysis of natural red dyes (cochineal) in textiles of historical importance using HPLC and multivariate data analysis. *Analytical and Bioanalytical Chemistry*. 2011;401(2):735-43.

Serrano A, van den Doel A, van Bommel M, Hallett J, Joosten I, van den Berg KJ. Investigation of crimson-dyed fibres for a new approach on the characterization of cochineal and kermes dyes in historical textiles. *Analytica Chimica Acta*. 2015;897:116-27.

Shahid M, Wertz J, Degano I, Aceto M, Khan MI, Quye A. Analytical methods for determination of anthraquinone dyes in historical textiles: A review. *Analytica Chimica Acta*. 2019;1083:58-87.

Shepard L. Changing approaches to tapestry conservation: the conservation of a set of seven eighteenth-century tapestries. In: Lennard F, Hayward M, editors. *Tapestry Conservation: Principles and Practice*. Oxford: Butterworth-Heinemann; 2006. p. 28-36.

Skoog DA, West DM, Holler FJ, Crouch SR. *Fondamenti di Chimica Analitica*. Città di Castello: EdiSES; 2009. 1051 p.

Smith GJ, Miller IJ, Daniels V. Phototendering of wool sensitized by naturally occurring polyphenolic dyes. *Journal of Photochemistry and Photobiology A: Chemistry*. 2005;169(2):147-52.

Smith GJ. New Trends in Photobiology (Invited Review): Photodegradation of keratin and other structural proteins. *Journal of Photochemistry and Photobiology B*. 1995;27:187-98.

Smith M, Thompson K, Lennard F. A literature review of analytical techniques for materials characterisation of painted textiles-Part 2: spectroscopic and chromatographic analytical instrumentation. *Journal of the Institute of Conservation*. 2017;40(3):252-66.

Smith MJ, Flowers TH, Lennard FJ. Mechanical properties of wool and cotton yarns used in twenty-first century tapestry: Preparing for the future by understanding the present. *Stud Conserv*. 2015;60(6):375-83.

Standard B. BS EN 14882:2005. 2005.

Standard B. BS EN ISO 13934-1:2013. 2013.

Strlič M, Thickett D, Taylor J, Cassar, M. Damage functions in heritage science. *Stud Conserv.* 2013;58(2):80-87.

Sun Z, Lyons JS, McNeill SR. Measuring Microscopic Deformations with Digital Image Correlation. *Optics and Lasers in Engineering.* 1997;27(4):409-28.

Surowiec I, Quye A, Trojanowicz M. Liquid chromatography determination of natural dyes in extracts from historical Scottish textiles excavated from peat bogs. *Journal of Chromatography A.* 2006;1112(1):209-17.

Sutherland H, editor A low tech approach to high tech analysis. *New Perspectives: Contemporary Conservation Thinking and Practice Icon 2019 Conference*; 2019; Belfast: Icon.

Sutherland H, Lennard F. "Each to their own"? An investigation into the spacing of laid-thread couching as used in textile conservation. *Newsletter of the ICOM Committee for Conservation, Working Group of Textiles.* 2017;39.

Sutton MA, Schreier HW, Orteu J-J. *Image Correlation for Shape, Motion and Deformation Measurements.* New York: Springer Science+Business Media; 2009. 321 p.

Sutton MA, Yan JH, Tiwari V, Schreier HW, Orteu JJ. The effect of out-of-plane motion on 2D and 3D digital image correlation measurements. *Optics and Lasers in Engineering.* 2008;46(10):746-57.

Swift JA, Smith JR. Microscopical investigations on the epicuticle of mammalian keratin fibres. *Journal of Microscopy.* 2001;204(3):203-11.

Szostek B, Orska-Gawrys J, Surowiec I, Trojanowicz M. Investigation of natural dyes occurring in historical Coptic textiles by high-performance liquid chromatography with UV-Vis and mass spectrometric detection. *Journal of Chromatography A.* 2003;1012(2):179-92.

Tamburini D, Cartwright CR, Melchiorre Di Crescenzo M, Rayner G. Scientific characterisation of the dyes, pigments, fibres and wood used in the production of barkcloth from Pacific islands. *Archaeological and Anthropological Sciences.* 2019;11(7):3121-41.

Tapestry Conservation: Principles and Practice. Lennard F, Hayward M editors. Oxford: Butterworth-Heinemann; 2006. xxv, 247 p.

Tapestry in the Baroque: threads of splendor. Campbell TP, editor. New York: Metropolitan Museum of Art.; 2007. 563 p.

Tecniche di conservazione degli arazzi: tre giornate di studio Firenze 18-20 Settembre 1981. Convegno Internazionale di Studi sull'Ars Nova Italiana del Trecento; 1986; Firenze: Leo S. Olschki.

The Conservation of Tapestries and Embroideries: Proceedings of Meetings at the Institut Royal du Patrimoine Artistique Brussels, Belgium September 21-24, 1987. Grimstad K, editor. Marina del Rey: The Getty Conservation Institute; 1989. 117 p.

'The Misled Eye...' *Reconstruction and Camouflage Techniques in Tapestry Conservation.* Barnett J, Cok S, editors. Amsterdam: Textiel Restauratoren Overleg Nederland (TRON); 1996. 142 p.

Thickett D, Luxford N, Lankester P, *Environmental Management Challenges and Strategies in Historic Houses.* Proceedings of the artifact, its context and their narrative: multidisciplinary conservation in historic house museums; Los Angeles: ICOM-CC; 2012.

Thickett D, Pretzel B. FTIR surface analysis for conservation. *Heritage Science.* 2020;8(1):5.

Thomson FP. *Tapestry: mirror of history.* Newton Abbot: David & Charles; 1980. 224 p.

- Thomson WG. A history of tapestry from the earliest times until the present day. London: Hodder and Stoughton; 1906. xvi, 506 p.
- Thorndike GH, Varley L. Measurement of the Coefficient of Friction between Samples of the Same Cloth. *Journal of the Textile Institute Proceedings*. 1961;52(6):P255-P71.
- Thurman CM. Tapestry: the purposes, form, and function of the medium from its inception until today. In: Bennett A, editor. *Acts of the Tapestry Symposium*; San Francisco: Fine Arts Museums of San Francisco; 1979. p. 5-19.
- Timár-Balázsy Ag, Eastop D. Chemical principles of textile conservation. London: Routledge; 1998. 480 p. p.
- Tong W. An Evaluation of Digital Image Correlation Criteria for Strain Mapping Applications. *Strain*. 2005;41(4):167-75.
- Troalen LG, Phillips AS, Pegg DA, Barran PE, Hulme AN. Historical textile dyeing with *Genista tinctoria* L.: a comprehensive study by UPLC-MS/MS analysis. *Analytical Methods*. 2014;6(22):8915-23.
- Troalen LG. *Historic Dye Analysis: Method Development and New Applications In Cultural Heritage*: University Of Edinburgh; 2013.
- Trosbach G. *Physikalische Untersuchungen an historischen Tapisserien*: Technische Universitat Munchen; 2002.
- van Loon A, Gambardella AA, Gonzalez V, Cotte M, De Nolf W, Keune K, et al. Out of the blue: Vermeer's use of ultramarine in *Girl with a Pearl Earring*. *Heritage Science*. 2020;8(25).
- Vanden Berghe I, Wouters J. Identification and condition evaluation of deteriorated protein fibres at the sub-microgram level by calibrated amino acid analysis. *Scientific Analysis of Ancient and Historic Textiles: Postprints*. London: Archetype Publications Ltd.; 2005. p. 151-8.
- Vanden Berghe I. Towards an early warning system for oxidative degradation of protein fibres in historical tapestries by means of calibrated amino acid analysis. *Journal of Archaeological Science*. 2012;39(5):1349-59.
- Varoli-Piazza R, Rosicarello R, Giorgi M. The use of photogrammetry in determining the correct method of displaying a textile artefact: the cowl of St. Francis of Assisi. In: Bridgland J, editor. *ICOM committee for conservation, 11th triennial meeting in Edinburgh, Scotland, 1996: Preprints*. London: James & James; 1996. p. 726-31.
- Vilaplana F, Nilsson J, Sommer DVP, Karlsson S. Analytical markers for silk degradation: comparing historic silk and silk artificially aged in different environments. *Analytical and Bioanalytical Chemistry*. 2015;407:1433-49.
- Vilde V, Thickett D, Hollis D, Grau-Bové J, Richardson E. Digital image correlation for condition monitoring of lined painting. In: Bridgland J, editor. *ICOM Committee for Conservation Triennial meeting, 18th, Copenhagen, Denmark, 2017: Preprints*. Paris: International Council of Museums; 2017.
- Wang Z, Zhao J, Fei L, Jin Y, Zhao D. Deformation Monitoring System Based on 2D-DIC for Cultural Relics Protection in Museum Environment with Low and Varying Illumination. *Mathematical Problems in Engineering*. 2018;2018.
- Ward S, Ewer P. Tapestry Conservation at Biltmore House. *The International Journal of Museum Management and Curatorship* 1988;7:381-8.
- Wertz J. *Turkey red dyeing in late-19th century Glasgow: Interpreting the historical process through re-creation and chemical analysis for heritage research and conservation*: University of Glasgow; 2017.

Wertz JH, Quye A, France D. Turkey red prints: identification of lead chromate, Prussian blue and logwood on Turkey red calico. *Conservar Património: Studies in Historical Textiles*. 2019;31:31-9.

Wiegerink JG. The Moisture Relations of Textile Fibres at Elevated Temperatures. *Textile Research*. 1940;10(9):357-71.

Wild C, Brutillot A. The conservation of tapestries in Bavaria. In: Lennard F, Hayward M, editors. *Tapestry Conservation: Principles and Practice*. Oxford: Butterworth-Heinemann; 2006. p. 177-84.

Williams HR, Lennard F, Eastop D, Dulieu-Barton JM, Chambers AR. Application of digital image correlation to tapestry & textile condition assessment. *Proceedings of AIC Textile Specialty Group*. 192009. p. 156-70.

Wilson D. A Study of Fabric-on-Fabric Dynamic Friction. *Journal of the Textile Institute Transactions*. 1963;54(4):T143-T55.

Wilson H, Carr C, Hacke M. Production and validation of model iron-tannate dyed textiles for use as historic textile substitutes in stabilisation treatment studies. *Chemistry Central Journal*. 2012;6(1):44.

Wood J, Gauvin C, Young C, Taylor A, Balint D, Charalambides M, Reconstruction of historical temperature and relative humidity cycles within Knole House, Kent. *Journal of Cultural Heritage*, 2019 (39).

Wouters J, Grzywacz CM, Claro A. Markers for Identification of Faded Safflower (*Carthamus tinctorius* L.) Colorants by HPLC-PDA-MS - Ancient Fibres, Pigments, Paints and Cosmetics Derived from Antique Recipes. *Stud Conserv*. 2010;55(3):186-203.

Wouters J, Verhecken A. The scale insect dyes (Homoptera: Coccoidea). Species recognition by HPLC and diode-array analysis of the dyestuffs. *Annales de la Société entomologique de France (NS)*. 1989;25:393-410.

www.royalcollection.org.uk

Yazawa K, Ishida K, Masunaga H, Hikima T, Numata K. Influence of Water Content on the B-Sheet Formation, Thermal Stability, Water Removal, and Mechanical Properties of Silk Materials. *Biomacromolecules*. 2016;17(3):1057-66.

Ye CC, Dulieu-Barton JM, Chambers AR, Lennard FJ, Eastop DD. Condition monitoring of textiles using optical techniques. *Key Engineering Materials*. 2009;413-414:447-54.

Ye CC, Dulieu-Barton JM, Webb DJ, Zhang C, Peng GD, Chambers AR, et al. Applications of polymer optical fibre grating sensors to condition monitoring of textiles. *Journal of Physics: Conference Series* 2009;178:012020.

Young C, Hibberd R, Ackroyd P. An investigation into the adhesive bond and transfer of tension in lined canvas paintings. ICOM Committee for Conservation Triennial meeting, 13th, Rio de Janeiro, Brazil, 2002: Preprints. I. London: James & James; 2002. p. 370-8.

Young C. Using DIC to develop an Experimental Methodology for Measuring Moisture Induced Fatigue in Panel Paintings. 2015.

Young CRT. Measurement of the Biaxial Tensile Properties of Paintings on Canvas: Imperial College, University of London; 1996.

Yu L, Pan B. In-plane displacement and strain measurements using a camera phone and digital image correlation. *Optical Engineering* 2014;53(5):054107.

Zaffino C, Bedini GD, Mazzola G, Guglielmi V, Bruni S. Online coupling of high-performance liquid chromatography with surface-enhanced Raman spectroscopy for the identification of historical dyes. *Journal of Raman Spectroscopy*. 2016;47(5):607-15.

Zaffino C, Bertagna M, Guglielmi V, Dozzi MV, Bruni S. In-situ spectrofluorimetric identification of natural red dyestuffs in ancient tapestries. *Microchemical Journal*. 2017;132:77-82.

Zeng Y, Liu Y, Liu J, Zheng H, Zhou Y, Peng Z, et al. Application of electron paramagnetic resonance spectroscopy, Fourier transform infrared spectroscopy-attenuated total reflectance and scanning electron microscopy to the study of the photo-oxidation of wool fiber. *Analytical Methods*. 2015;7(24):10403-8.

Zhang X, Vanden Berghe I, Wyeth P. Heat and moisture promoted deterioration of raw silk estimated by amino acid analysis. *Journal of Cultural Heritage*. 2011;12(4):408-11.

Zhao X, Wen Y, Zhao J, Zhao D. Study of the quality of wood texture patterns in digital image correlation. *Optik*. 2018;171:370-6.

Publications and presentations

Peer-reviewed articles

Lennard, F., Costantini, R. and Harrison, P. (2021) Understanding the Role of Friction and Adhesion in the Display of Tapestries on Slanted Supports. *Studies in Conservation*, 66(1), 32-43. (doi: 10.1080/00393630.2020.1761184)

Costantini, R., Lennard, F., Alsayednoor, J. and Harrison, P. (2020) Investigating mechanical damage mechanisms of tapestries displayed at different angles using 2D DIC. *European Physical Journal Plus*, 135, 515. (doi: 10.1140/epjp/s13360-020-00520-7)

Alsayednoor, J., Harrison, P., Dobbie, M., Costantini, R. and Lennard, F. (2019) Evaluating the use of digital image correlation for strain measurement in historic tapestries using representative deformation fields. *Strain*, 55(2), e12308. (doi: 10.1111/str.12308)

International conferences

Costantini, R., Lennard, F., and Harrison, P. (2020) Mechanical damage in historic tapestries: results from a scientific investigation on causes and remedies [oral presentation]. 48th Annual Meeting of the American Institute for Conservation, online, summer 2020

Lennard F., Costantini R., Alsayednoor, J., Harrison, P. (2019) Taking the strain: using Digital Image Correlation to monitor strain in tapestries displayed on slanted supports [oral presentation]. Icon Conference 2019, Belfast, UK, 12-14 June 2019